2018

Assessment of the neuroprotective efficacy of poly-arginine-18 (R18) peptides in a pre-clinical model of perinatal hypoxic-ischaemic encephalopathy (HIE)

Adam Edwards
The University of Notre Dame Australia

Assessment of the neuroprotective efficacy of poly-arginine-18 (R18) peptides in a pre-clinical model of perinatal hypoxic-ischaemic encephalopathy (HIE)

by

Mr Adam B. Edwards, BBioMedSc (Honours)

Thesis presented for the degree of Doctor of Philosophy

The University of Notre Dame Australia

School of Health Sciences

2018

ABSTRACT

Hypoxic-ischaemic encephalopathy (HIE) is one of the leading causes of mortality and morbidity in infants, globally. This disorder eventuates following a reduction in oxygenated cerebral blood flow to the foetus *in utero*, leading to excitotoxic-mediated brain cell (e.g. neuron, glia and glial progenitor cell) death. Currently, there is no clinically appropriate neuroprotective treatment to reduce acute brain injury following HIE. Recent studies have demonstrated that poly-arginine and cationic arginine-rich peptides (CARPs; e.g. R18: R = arginine residues) exhibit potent neuroprotective properties in both *in vitro* and adult animal models of ischaemia, and therefore have the potential to be developed into a neuroprotective treatment to reduce brain injury following HIE. Therefore, the aim of this thesis was to assess the neuroprotective efficacy of CARPs in a model of perinatal HIE in the rat.

To elucidate the neuroprotective efficacy of CARPs, a novel surgical modification to the original *in vivo* Rice-Vannucci model of perinatal HIE was developed. Using 7-day old Sprague-Dawley rats, brain injury was induced following the permanent ligation of the common and external carotid arteries, followed by a period of transient hypoxia (8% O_2/92% N_2). Results from this experiment demonstrated that the occlusion of common and external carotid arteries reduced cerebral communicational and/or anastomotic blood flow, reducing variability and improving the reliability in the presence of a cerebral infarct. The demonstration and termination of cerebral communicational and/or anastomotic blood flow improved the pre-clinical assessment of neuroprotective therapies to treat HIE.

The CARPs, R18, R18D (D-enantiomer) and JNKI-1-TATD, were assessed in the modified Rice-Vannucci model of HIE when administered intraperitoneally, immediately after the cessation of hypoxia-ischaemia (HI; 8% O_2/92% N_2 for 2.5 h). Treatment with R18 and R18D significantly reduced infarct volume and improved behavioural assessments in this model. Surprisingly, the well-characterised neuroprotective peptide JNKI-1-1TATD, used as a positive control and benchmark, did not exhibit any significant neuroprotection. Succeeding positive results obtained following R18D administration immediately after HI, its therapeutic window was further assessed. R18D significantly decreased infarct volume and improved behavioural assessments when administered intraperitoneally up to 1 hour after the cessation of HI; correlating to 3.5 hours since HI onset. To confirm the neuroprotective mechanism of action of CARPs in HIE, an established *in vitro* primary cortical neuronal excitotoxic injury model was used. Results from this experiment demonstrate that CARPs reduce excitotoxic intracellular calcium influx in a dose-dependent fashion, providing evidence for a role in the reduction of several calcium-dependent pro-cell death cascades. The demonstration of significant neuroprotection following R18 peptide administration provides evidence for a novel therapeutic, which has the potential to reduce brain injury in infants who suffer HIE.

In summary, this thesis has identified a novel surgical modification to improve the reliability and reproducibility of the original Rice-Vannucci model of HIE. In addition, the administration of the R18 and R18D peptides following perinatal HIE, significantly reduces brain injury and improves behavioural assessments when administered up to 3.5 hours after the onset of HI. These findings demonstrate that CARPs provide an exciting and novel approach to reduce brain injury following HIE.

ACKNOWLEDGEMENTS

Firstly, I would like to express my sincere thanks and appreciation to my supervisors, Bruno Meloni, Ryan Anderton and Neville Knuckey, for without them, the work within this thesis would not have been possible. A special mention to Bruno Meloni, whose patience, wisdom and support extended far beyond my PhD, and for that, I cannot thank him enough.

To the staff and students of the Perron Institute, in particular the Stroke Research Group, the past 3.5 years have been incredibly enjoyable and everyone, in one way or another, has assisted me throughout my journey. A special mention to Frank Mastaglia whose poignant advice and knowledge was critical to my professional development.

To my two families, the Edwards' and the Frzop's, without your ears, your shoulders or your food, the journey throughout my PhD would have been a very different affair. In particular, to my parents, you gave me the opportunity of an education and taught me the importance of a strong work ethic, both of which were, and will continue to be paramount in my achievements within my PhD and beyond.

An extra special mention goes to my partner, Melissa. At every point along the winding road, you were there by my side. At times, it felt you knew more about my projects than I did. Thank you for being my grounding support and my tether to reality. Thank you for being you.

DECLARATION

I hereby declare that:

- This thesis is submitted as part of the requirement for a Doctor of Philosophy degree as a result of my own work and research. All other sources have been indicated and acknowledged.
- Permission has been granted by co-authors for any work that has been co-published to be included in this thesis.
- This thesis has been substantially completed during the course of enrolment and its content has not previously been submitted or accepted for any other degree in this or any other institution.
- I understand that this work may be electronically scanned for detection of plagiarism.

Signed.....

Adam B. Edwards

Signed.....

Coordinating Supervisor: Bruno Meloni

Approval of final thesis

PUBLICATIONS ARISING FROM THIS THESIS

Edwards A., Anderton R., Knuckey N., Meloni B. 2018. Review: Perinatal hypoxic-ischaemic encephalopathy and neuroprotective peptide therapies: a case for cationic arginine-rich peptides (CARPs). *Brain Sciences*, 7; 8 (8). doi: 10.3390/brainsci8080147.

Edwards A., Anderton R., Knuckey N., Meloni B. 2018. Assessment of therapeutic window for poly-arginine-18D (R18D) in a P7 rat model of perinatal hypoxic ischaemic encephalopathy. *Journal of Neuroscience Research*, 96 (11): 1816-1826. doi: 10.1002/jnr.24315.

Edwards A., Cross J., Anderton R., Knuckey N., Meloni B. 2018. Poly-arginine R18 and R18D (D-enantiomer) peptides reduce infarct volume and improves behavioural outcomes following perinatal hypoxic-ischaemic encephalopathy in the P7 rat. *Molecular Brain*, 11 (1): 8. doi: 10.1186/s13041-018-0352-0.

Edwards A., Feindel K., Cross J., Anderton R., Clark V., Knuckey N., Meloni B. 2017. Modification to the Rive-Vannucci perinatal hypoxic-ischaemic encephalopathy model in the P7 rat improves the reliability of cerebral infarct development after 48 hours. *Journal of Neuroscience Methods*, 288. doi: 10.1016/j.jneumeth.2017.06.016.

CONFERENCE PROCEEDINGS ARISING FROM THIS THESIS

Edwards A., Anderton S., Knuckey N., Meloni B. 2017. *The poly-arginine-18 (R18) peptide is neuroprotective in a modified model of perinatal hypoxic-ischaemic encephalopathy; a dose-response and therapeutic window study*. Oral presentation at: Combined Biological Sciences Meeting; Perth, Australia.

Edwards A., Feindel K., Cross J., Anderton R., Clark V., Knuckey N., Meloni B. 2017. Neuroprotective efficacy of poly-arginine-18 (R18) peptides using an *in vivo* model of perinatal hypoxic-ishcaemic encephalopathy. *Journal of Cerebral Blood Flow and Metabolism*, 37 (IS) 1-97. doi: 10.1177/0271678X17695978.

Edwards A., Feindel K., Cross J., Anderton R., Clark V., Knuckey N., Meloni B. 2017. Neuroprotective efficacy of poly-arginine-18 (R18) peptides using an *in vivo* model of perinatal hypoxic-ishcaemic encephalopathy. Oral presentation at: Berlin Brain, 28th Symposium of Cerebral Blood Flow, Metabolism and Function; Berlin, Germany.

Edwards A., Anderton R., Knuckey N., Meloni B. 2016. *Babies' brains matter too*. Oral presentation: 3-minute thesis, 10th Federation of European Neurosciences Societies (FENS) Forum of Neuroscience; Copenhagen, Denmark.

Edwards A., Anderton R., Knuckey N., Meloni B. 2016. *Neuroprotective efficacy of poly-arginine peptides using an in vitro excitotoxicity model; implications for therapeutics*. Poster presentation at: 10th Federation of European Neurosciences Societies (FENS) Forum of Neuroscience; Copenhagen, Denmark.

Edwards A., Cross J., Anderton R., Knuckey N., Meloni B. 2016. *Neuroprotective efficacy of poly-arginine peptides using an in vitro model of neonatal hypoxic-ischaemic encephalopathy*. Poster presentation at: Combined Biological Sciences Meeting; Perth, Australia.

AWARDS ARISING FROM THIS THESIS

Fee Remission Postgraduate Scholarship

The University of Notre Dame Australia;

Fremantle, Australia (2015 – 2018).

University Postgraduate Award

The University of Notre Dame Australia;

Fremantle, Australia (2015 – 2018).

Young Investigator Travel Programme Award

10th Federation of European Neurosciences Societies (FENS) Forum of Neuroscience;

Copenhagen, Denmark (2016).

Student Oral Presentation Prize

Combined Biological Sciences Meeting (CBSM);

Perth, Australia (2017).

Berlin Brain Travel Bursary

Berlin Brain and Brain Positron Emission Tomography Conference;

Berlin, Germany (2017)

Student Poster Prize

Science on the Swan;

Fremantle, Australia (2018).

Student Oral Presentation Prize

Science on the Swan;

Fremantle, Australia (2018).

TABLE OF CONTENTS

LIST OF ABBREVIATIONS

AMPA	α-amino-3-hydroxy-5-methyl-4-isoxazolepropionic acid
ANOVA	Analysis of variance
ATP	Adenosine triphosphate
AUC	Area under the curve
BSS	Balanced salt solution
CARP	Cationic arginine-rich peptide
CBF	Cerebral blood flow
CCA	Common carotid artery
CCAO	Common carotid artery occlusion
CPP	Cell penetrating peptide
DNA	Deoxyribonucleic acid
ECA	External carotid artery
ECAO	External carotid artery occlusion
EPO	Erythropoietin
FAIR	Fluid attenuation inversion recovery
GABA	γ-aminobutyric acid
HI	Hypoxic-ischaemic or hypoxia-ischaemia
HIE	Hypoxic-ischaemic encephalopathy
ICA	Internal carotid artery

ICV	Intracerebroventricular
IL	Interleukin
IP	Intraperitoneal
IV	Intravenous
LPS	Lipopolysaccharide
MCAO	Middle cerebral artery occlusion
MEM	Minimum essential medium
$MgSO_4$	Magnesium sulfate
MMP	Matrix metalloproteinase
MPTP	Mitochondrial permeability transition pore
MRA	Magnetic resonance angiography
MRI	Magnetic resonance imaging
MTS	3-(4, 5, dimethyliazol-2-yl)-5-(3-carboxymethoxy-phenyl)-2-(4-sulfophenyl)-2H–tetrazolium salt
NMDA	N-methyl-$_D$-aspartic acid
P7	7-day-old
PASL	Pulsed arterial spin labelling
ROS	Reactive oxygen species
SD	Sprague-Dawley
SE-EPI	Spin-echo echo-planar imaging

TOF	Time of flight
TTC	Triphenyl tetrazolium chloride

LIST OF FIGURES

LIST OF TABLES

Chapter 1

General Introduction

1.1 INTRODUCTION

Perinatal hypoxic-ischaemic encephalopathy (HIE; also referred to as perinatal asphyxia) is a devastating condition, which affects the brain of term (> 36 weeks gestation) and pre-term (≤ 36 weeks gestation) infants. Brain injury associated with HIE is a leading cause of mortality among infants, while survivors are often left with lifelong disabilities such as cerebral palsy, epilepsy, intellectual disability and autism spectrum disorders (Kolevzon, Gross, & Reichenberg, 2007; O'Shea, 2008; Perlman, 1997; Pisani et al., 2009). There are currently no clinically available pharmacological neuroprotective treatments to reduce brain injury following HIE. For this reason, there is an urgent need for the development of a safe and widely applicable neuroprotective agent for infants who suffer HIE. Current clinical interventions to minimise HIE are limited to the use of hypothermia in term infants. However, the availability of a neuroprotective agent that can be administered soon after hypoxia-ischaemia (HI), to both pre-term and term infants, either in combination with hypothermia or alone (e.g. when hypothermia therapy is not an available treatment option), would provide the best opportunity to preserve brain tissue and thereby reduce mortality, improve patient quality of life and lessen the social and economic impact of this devastating condition.

Recent studies in A/Prof Meloni's laboratory have demonstrated that cationic arginine-rich peptides and poly-arginine peptides (hereafter referred to as CARPs, unless otherwise stated) have potent neuroprotective properties in *in vitro* and animal injury models that mimic the effects of brain ischaemia (Meloni, Brookes, et al., 2015; Meloni et al., 2014, 2017; Meloni, Milani, et al., 2015; Milani et al., 2018, 2017; Milani, Clark, et al., 2016; Milani, Knuckey, Anderton, Cross, & Meloni, 2016). To

determine the neuroprotective potential of CARPs as a neuroprotective therapy for HIE, initial pre-clinical studies using *in vitro* and a small animal model of HIE are required. Consequently, the focus of this thesis was to examine the efficacy of the poly-arginine peptide R18 in HIE by using an *in vitro* neuronal cell excitotoxicity model and in an *in vivo* model of HIE in the P7 rat.

1.2 PERINATAL HYPOXIC-ISCHAEMIC ENCEPHALOPATHY (HIE)

1.2.1 Epidemiology

Perinatal HIE remains a leading cause of infant mortality and morbidity, accounting for 23% of infant mortality worldwide (Lawn, Shibuya, & Stein, 2005), with an incidence in developed countries of 2 – 6 per 1,000 live term births and 7 per 1,000 live pre-term births (Chalak et al., 2012; de Haan et al., 2006; Hankins & Speer, 2003; Wall et al., 2010). In developing countries, the incidence drastically increases to 30 – 100 per 1,000 live births overall (Simiyu, Mchaile, Katsongeri, Philemon, & Msuya, 2017). Of infants surviving HIE, 10% demonstrate persistent motor abnormalities and 50% demonstrate sensory and/or cognitive abnormalities (Hack et al., 1992; Lee et al., 2013). The frequency of motor and cognitive disorders associated with HIE has remained stable since the 1990s (Vincer et al., 2006; Wilson-Costello et al., 2007).

1.2.2 Aetiology

The aetiology associated with HIE represents the complexity of this neurological condition. Risk factors associated with HIE are summarised in Table 1.1 and include

intrapartum insults (e.g. nuchal cord, umbilical cord knotting, umbilical haemorrhage, placental abruption, pre-eclampsia and shoulder dystocia) and demographic factors (e.g. nulliparity and gestational age of foetus).

Table 1.1 Risk factors associated with HIE

Risk factor	Evidence	References
Nuchal cord	Nuchal cord increases the risk of HIE due to the reduction of cerebral blood flow through the compression of arterial and venous flow in the fetal neck	Peesay, 2017
Umbilical cord knotting	Umbilical cord knotting increases the risk of HIE due to the reduction in perfusion of blood to the foetus via the impairment of arterial and venous flow in the umbilical cord.	Peesay, 2017
Umbilical haemorrhage	Umbilical haemorrhage increases the risk of HIE due to the reduction in perfusion of blood through the foetus	Scutiero et al., 2018
Placental abruption	Detachment of the placenta from the uterus increases the risk of HIE due to the reduction in the perfusion of blood to the placenta and foetus	Downes, Grantz, & Shenassa, 2017
Pre-eclampsia	Disorders of maternal hypertension increase the risk of HIE due to the development of placental lesions, leading to a reduction in the perfusion of blood to the foetus	Martinello, Hart, Yap, Mitra, & Robertson, 2017
Shoulder dystocia	Shoulder dystocia is known to increase the risk of HIE	Politi, D'Emidio, Cignini, Giorlandino, & Giorlandino, 2010
Maternal infection	Maternal infections are known to increase the risk of HIE	Jenster et al., 2014
Nulliparity	An increased risk of HIE is associated with first time pregnancies	Liljestrom, Wikstrom, Agren, & Jonsson, 2018
Gestational age	An increased risk of HIE is associated with lower gestational age	(Ong et al., 2015)

1.2.3 Clinical aspects

The clinical presentation of symptoms following HIE is complex, with no early definitive diagnostic modality available to the clinician. Every infant born at 1 and 5 minutes of age is subjected to an Apgar assessment (inclusion criteria for therapeutic hypothermia, which is discussed below), which includes the assignment of a numerical score from 0 - 2 following examination of each of an infant's appearance, pulse, grimace, activity and respiration; with a low score indicating potential infant demise. If HIE is suspected within the first hours of birth, a neurological examination of the infant is performed and scored using the Sarnat grading scale; 1 = mild HIE, 2 = moderate HIE and 3 = severe HIE (see Table 1.2). A diagnosis of HIE occurs through the combination of Apgar and Sarnat scores, and when possible magnetic resonance imaging and amplitude integrated/conventional electroencephalography. Generally, between the age of 18 – 24 months, confirmatory diagnostic tests are performed for infants who have suffered HIE. The Bayley Scales of Infant and Toddler Development assessment is a common confirmatory diagnostic test examining a child's cognitive score, language score, motor score, cognitive delay, language delay and motor delay. Often it is not until later in life can an individual be definitively diagnosed with neurological sequelae associated with HIE (e.g. cerebral palsy, epilepsy, intellectual disability and autism spectrum disorders) (Driscoll, Felice, Kenny, Boylan, & O'Keeffe, 2018; Glass et al., 2009; Perlman, 1997; Robertson & Finer, 1993).

Table 1.2 Sarnat staging for diagnosis of HIE severity

Severity	Stage 1 (Mild)	Stage 2 (Moderate)	Stage 3 (Severe)
Level of consciousness	Hyperalert	Lethargic or obtuned	Stupor or coma
Activity	Normal	Decreased	Absent
Muscle tone	Normal	Mild hypertonia	Flaccid
Posture	Mild distal flexion	Strong distal flexion	Intermittent decerebration
Stretch reflexes	Overactive	Overactive	Decreased or absent
Suck	Weak	Weak or absent	Absent
Moro (startle)	Strong	Weak	Absent
Tonic neck	Slight	Strong	Absent
Pupils	Mydriasis	Miosis	Variable
Heart rate	Tachycardia	Bradycardia	Variable
Seizures	None	Common	Uncommon

1.3 PATHOPHYSIOLOGY

HIE occurs following an impediment of oxygenated cerebral blood flow (CBF), resulting in a pathophysiological cascade eventuating in programmed cell death. The fetal brain is particularly sensitive to a HI environment, due to the requirement of a constant supply of energy in the form of adenosine triphosphate (ATP). When this energy supply is interrupted, excitotoxicity occurs through the uncontrolled release of excitatory neurotransmitters such as glutamic acid; marking the beginning of the ischaemic cascade (Johnston, 1995). An in-depth assessment of pathophysiological cascades following HI is presented below and in Chapter 2.

1.3.1 Necrosis

Cellular necrosis is the primary cell death pathway initiated following severe HI (Northington, Chavez-Valdez, & Martin, 2011) and is defined by cellular swelling, karyolysis and lysis. Necrosis occurs following the failure of homeostasis due to an

excitotoxic influx of calcium and sodium, resulting in mitochondrial dysfunction and reactive oxygen species (ROS) production.

1.3.2 Apoptosis

Cellular apoptosis is the primary cell death pathway initiated following moderate HI (Northington et al., 2011) and is defined by cellular shrinkage, fragmentation into apoptotic bodies and rapid phagocytosis. Multiple apoptotic pathways have been demonstrated to be involved in HI, generally, apoptosis is ATP- and caspase-dependent. Following ATP depletion, calcium influx and the activation of calcium-dependent caspases, several pro-apoptotic proteins are released into the cytosol.

1.3.3 Excitotoxicity

Following prolonged HI, cellular homeostasis is disrupted and results in the failure of the cell (e.g. neurons, glia and glial precursor cells) to maintain ionic gradients, resulting in uncontrolled cellular depolarisation and release of glutamic acid into the synaptic cleft (Olney, Price, Samson, & Labruyere, 1986). High extracellular levels of glutamic acid cause cellular excitotoxicity, producing cytotoxic cellular influx of calcium ions. Increased intracellular levels of calcium activates calcium-dependent proteases, ROS production, cytotoxic oedema, mitochondrial dysfunction and the stimulation of pro-cell death pathways (Arai, Vanderklish, Kessler, Lee, & Lynch, 1991; Castilho, Ward, & Nicholls, 1999; O'Hare et al., 2005; Stout, Raphael, Kanterewicz, Klann, & Reynolds, 1998; Zhang, Dawson, Dawson, & Snyder, 1994).

1.3.4 Oxidative stress

As the developing brain is comprised of high levels of unsaturated fatty acids which are susceptible to lipid peroxidation, metals catalysing free radical reactions and low concentrations of antioxidants, the developing brain is highly susceptible to oxidative stress (Ikonomidou & Kaindl, 2011). Following HI, resident microglia produce excess inflammatory cytokines (IL-1β, TNF-α, etc.), glutamic acid, nitric oxide and ROS (Kaur, Rathnasamy, & Ling, 2013; Lai et al., 2017). Rapid increases in these levels of cytokines within cerebral tissue induces apoptosis, inhibits neurogenesis and contributes to immune cell migration to the site of HI injury.

1.3.5 Mitochondrial dysfunction

In cells affected by HI, several processes result in the activation of pro-apoptotic Bcl-2 proteins (e.g. Bid, Bax, etc.), resulting in mitochondrial membrane permeability transition (MPT) (Bernardi et al., 2006; Wang et al., 2009). In addition, oxidative stress caused by ROS plays a critical role in mitochondrial dysfunction including ischaemic starvation, reperfusion-induced hyper activation and delayed neuronal death (Sanderson, Reynolds, Kumar, Przyklenk, & Hüttemann, 2013), prompting MPT and mitochondrial release of cytochrome-c. Cytosolic cytochrome-c, along with deoxyadenosine triphosphate, interact with apoptotic protease activating factor-1 (Apaf-1) to form the apoptosome, contributing to pro-apoptotic cell death via the activation of pro-caspase-9 (Thornton et al., 2012). Further alterations to mitochondria, such as mitochondrial outer membrane permeabalisation, results in the release of other pro-apoptotic factors, including apoptosis-inducing factor, endonuclease-G and second mitochondria-derived activator of caspases

(smac)/DIABLO (Blomgren & Hagberg, 2006; Zhu et al., 2007), all of which mediate chromatin fragmentation and increase the activation of pro-apoptotic caspases, leading to cell death.

1.3.6 Inflammation

Following HI, resident microglia become activated in the cerebral parenchyma and develop macrophage-like attributes (e.g. phagocytic properties, cytokine production, matrix metalloproteinase release and antigen presentation) (Iadecola & Anrather, 2011). Specifically, the release of matrix metalloproteinases compromises blood brain barrier integrity, promoting the invasion of peripheral leukocytes into the cerebral parenchyma; exacerbating cerebral injury (Kaur, Sivakumar, Yip, & Ling, 2009). Like macrophages, astrocytes also become activated due to the release of pro-inflammatory cytokines, and ROS. Activated astrocytes subsequently release pro-inflammatory cytokines [interleukin (IL)-6, tumour necrosis factor (TNF)α, IL1α/β and interferon (INF)γ]; further exacerbating pro-cell death pathways (e.g. apoptosis) (Liu & Mccullough, 2013; Tuttolomondo, Di Raimondo, di Sciacca, Pinto, & Licata, 2008).

1.4 CURRENT ACUTE CLINICAL NEUROPROTECTIVE TREATMENT

Hypothermia

The use of hypothermia for the clinical treatment of HIE is presented in Chapter 2. Briefly, moderate hypothermia (33.5°C for 72 h) applied within 6 hours of birth improves the survival and neurodevelopmental outcomes in infants suffering from

moderate and severe HIE. While hypothermia is considered standard care in the treatment of infants with HIE and is well tolerated in term infants (Azzopardi et al., 2009; Gluckman et al., 2005; Jacobs et al., 2011; Shankaran et al., 2005), it does not provide complete protection. Of those term infants who have moderate or severe encephalopathy, therapeutic hypothermia was shown to decrease mortality from 40% to 28%, while in surviving infants, neurological morbidity was reduced from 31% to 19% of infants receiving hypothermia (Jacobs et al., 2013). The use of hypothermia is widely associated with increased risks of adverse events such as bradycardia and thrombocytopenia (Jacobs et al., 2013); although it is widely accepted that the risk of adverse events is outweighed by the neuroprotective outcomes demonstrated by a significant reduction in mortality or major neurodevelopmental disability 18 months after HIE (Jacobs et al., 2013).

Importantly, whilst hypothermia is safe in pre-term infants suffering necrotising enterocolitis (Hall et al., 2010), it has not been adequately evaluated for use in pre-term infants suffering HIE. Information regarding the safety and efficacy of hypothermia to treat pre-term infants suffering HIE is lacking, although information may be available in the near future (NCT1793129). In one study, hypothermia in pre-term infants was associated with higher mortality and increased clinical complications when compared to term infants, although the study did not include a normothermic pre-term control group (Rao et al., 2017).

1.5 OTHER CLINICAL NEUROPROTECTIVE APPROACHES UNDER CONSIDERATION

The following outlines neuroprotective approaches to treat HIE, that are currently, or have been assessed in human clinical trials.

1.5.1 Xenon

The noble gas xenon is an approved anaesthetic drug (Stoppe et al., 2013) with organoprotective and neuroprotective properties when administered alone or in combination with hypothermia in pre-clinical models of HIE (Banks, Franks, & Dickinson, 2010; David et al., 2003; Faulkner et al., 2011; Hobbs et al., 2008; Thoresen, Hobbs, Wood, Chakkarapani, & Dingley, 2009). Whilst the mechanism of action of xenon neuroprotection has not been elucidated, xenon is known to prevent N-methyl-$_{D}$-aspartic acid (NMDA) receptor over activation via competitive inhibition at the glycine site of the NMDA receptor (Dickinson et al., 2007).

Two clinical studies have assessed the safety of xenon in term infants with HIE and treated with hypothermia (33.5°C for 72 h). In one study, treatment with xenon (50% for 18 h; inhaled) and hypothermia was demonstrated to be safe (Dingley et al., 2014; ISRCTN75602528). The second study also demonstrated that xenon (30% for 24 h; inhaled) and hypothermia treatment was safe (Azzopardi et al., 2016; NCT00934700 and ISRCTN08886155), but concluded that adjunct xenon therapy is unlikely to improve the neuroprotective effect of hypothermia.

1.5.2 Topiramate

Topiramate is an anti-epileptic drug approved for partial and generalised seizures in adults and children. It has neuroprotective properties in pre-clinical models of HIE when administered alone or in combination with hypothermia (Cowell, Xu, Galasso, & Silverstein, 2002). Topiramate has been demonstrated to confer neuroprotection through the reduction in sodium- and calcium-dependent action potentials (DeLorenzo, Sombati, & Coulter, 2000), enhancement of γ-aminobutyric acid-mediated neuronal chloride influx (White, Brown, Woodhead, Skeen, & Wolf, 1997) and the inhibition of α-amino-3-hydroxy-5-methyl-4-isoxazolepropionic acid and kainate type glutamic acid receptors (Koh & Jensen, 2001).

One clinical study has assessed the safety of topiramate in term infants with HIE and treated with hypothermia (33.5°C for 72 h) (Filippi et al., 2010; NCT01241019). Topiramate administration (10mg/kg once daily for 3 days; orally) was demonstrated to be safe; although hypothermia did slow the rate of clearance of topiramate from the body. A second clinical study has been completed, but the results have not been published to date (NCT01765218).

1.5.3 Pre-term therapeutic hypothermia

One clinical study has assessed the safety of hypothermia (33.5°C for 72 h) in pre-term neonates (34 – 35 weeks gestation) suffering HIE (Rao et al., 2017; NCT00620711). The study demonstrated that the use of hypothermia was feasible, but cautioned its use for future application due to the increased risk of mortality and side effects. Additional, clinical studies are currently recruiting patients for the investigation of safety and efficacy of hypothermia in pre-term infants

(NCT01793129; 33.5°C for 72 h; 33 – 35 weeks gestation; expected completion October 2022 and NCT02676063; 33.5°C for 72 h; ≥ 34 weeks gestation; expected completion February 2021).

1.5.4 Antenatal magnesium sulfate ($MgSO_4$)

Magnesium is a non-competitive NMDA receptor antagonist and following HI-mediated excitotoxicity, magnesium is thought to prevent excitotoxic neuronal calcium influx (Kang et al., 2011) as well as reduce pro-inflammatory cytokines IL-6 and TNFα (Aryana, Rajaei, Bagheri, Karimi, & Dabbagh, 2014). For decades, $MgSO_4$ has been administered antenatally for the prevention of seizures in women with pre-eclampsia and eclampsia. Through antenatal administration, foetuses are passively exposed to $MgSO_4$; with fetal $MgSO_4$ levels almost half of the maternal blood levels (Sherwin et al., 2014).

Five clinical studies have assessed the safety and/or efficacy of $MgSO_4$ in pre-term infants suffering HIE when administered to the mother in the antepartum period. Three studies demonstrated that $MgSO_4$ administration 4g within 24 h of birth (Crowther et al., 2003; ACTRN12606000252516; Marret et al., 2006) or 4g bolus followed by 1 g/h for 24 h was safe, but did not appear to improve infant outcomes (The Magpie Trial Collective Group, 2002; ISRCTN86938761). One study (Rouse et al., 2008; NCT00014989), demonstrated $MgSO_4$ (6g bolus followed by 2g/h maintenance for 12 h) was safe and reduced the rates of cerebral palsy at 1 year of age. Another study (Mittendorf et al., 1997) was prematurely terminated due to high mortality rates in

infants born to mothers administrated $MgSO_4$ (4 g bolus, then 2 – 3 g/h infusion). A clinical study is currently recruiting patients (ACTRN12611000491965; 4g $MgSO_4$ within 24 h of birth).

1.5.5 Erythropoietin (EPO) and darbepoetin adjuvant to hypothermia

EPO is commonly used clinically for its erythropoietic properties to treat anaemia. Recombinant human EPO has been examined as a potential neuroprotective agent both *in vitro* and animal studies of HIE. Current dose regimens to elicit erythropoiesis are administered subcutaneously at 400 IU/kg, three times a week, or intravenously at 200 IU/kg, daily (Robertson et al., 2012). EPO is known to increase neural stem cell proliferation (Zhang et al., 2017) and encourage cerebrovascular remodelling (Keogh, Yu, & Wei, 2007). EPO has also been demonstrated to be neuroprotective in animal models of ischaemic stroke, traumatic brain injury, chronic hypoxia and HIE as well as improve neurodevelopmental outcomes in pre-term infants (discussed below). Despite EPO's neuroprotective properties, an appropriate clinical therapeutic dose and confirmation of efficacy in HIE has not yet been ascertained. Assessment of EPO in rodent models of HIE has demonstrated that doses ranging from 1,000 to 5,000 IU/kg are neuroprotective (Gonzalez et al., 2009; Chung, Kong, Goldberg, Stowe, & Raman, 2015; Fan, van Bel, van der Kooij, Heijnen, & Groenendaal, 2013).

Clinical studies have assessed the safety of EPO and darbepoetin (a modified form of EPO), in term infants suffering HIE and treated with hypothermia (33.5°C for 72 h). These studies demonstrated that EPO or darbepoetin in combination with hypothermia was safe (Wu et al., 2012; NCT00719407; Baserga et al., 2015; NCT01471015). A

clinical study further assessing the efficacy of EPO with hypothermia in term infants is currently recruiting patients (NCT03079167; estimated completion December 2020).

1.6 CARPS AND NEUROPROTECTION

As previously outlined, this project aims to extend the previous findings that initially identified that CARPs, including poly-arginine peptides, possess intrinsic neuroprotective properties. Neuroprotective CARPs typically range in size from 6 – 30 amino acids and are cationic due to the presence of arginine, lysine and to a lesser extent histidine residues. CARPs have the capacity to cross the plasma membrane and enter cells, and for this reason they are also referred to as cell penetrating peptides (CPPs). CARPs can also cross the blood brain barrier and enter the brain. Due to their membrane traversing properties, CARPs (i.e. cationic CPPs) have been extensively used for the intracellular delivery of agents in experimental *in vitro* and animal studies (Meloni, Milani, et al., 2015), as well as for the delivery of agents into the brain. A review summarising the application of CARPs as a neuroprotective therapeutic treatment for HIE is presented in Chapter 2.

1.7 AIMS OF THE THESIS

The overall goal of this thesis is to examine the neuroprotective efficacy of CARPs, namely the poly-arginine peptide R18, in a rat model of HIE. In order to accomplish this goal, a P7 rat model of HIE was established and characterised. Using different treatment regimens (e.g. $_{L}$- and $_{D}$-enantiomer R18, different peptide doses and

administration time points post-HI) the HIE model was subsequently used to examine the efficacy of R18 to reduce brain injury and improve functional outcomes.

Specific aims of the project are:

Aim 1: To establish and characterise a more reliable and reproducible P7 rat model of HIE.

Hypothesis: Occlusion of the common and external carotid arteries (as opposed to occlusion of the common carotid artery only), followed by transient hypoxia will generate a more consistent brain lesion.

Aim 2: To examine the dose response neuroprotective efficacy of R18 ($_{L}$- and $_{D}$-enantiomers; R18 and R18D, respectively) using the newly established P7 rat model of HI (as described in Aim 1).

Hypothesis: R18 peptides are neuroprotective following HIE.

Aim 3: To examine the therapeutic time window and dose responsiveness of R18 (as identified in Aim 2) using the P7 rat model of HIE.

Hypothesis: R18 will be effective when administered several hours after the commencement of hypoxia.

1.8 REFERENCES

Arai, A., Vanderklish, P., Kessler, M., Lee, K., & Lynch, G. (1991). A brief period of hypoxia causes proteolysis of cytoskeletal proteins in hippocampal slices. *Brain Research*, *555*(2), 276–280. https://doi.org/10.1016/0006-8993(91)90352-V

Aryana, P., Rajaei, S., Bagheri, A., Karimi, F., & Dabbagh, A. (2014). Acute Effect of Intravenous Administration of Magnesium Sulfate on Serum Levels of Interleukin-6 and Tumor Necrosis Factor-α in Patients Undergoing Elective Coronary Bypass Graft With Cardiopulmonary Bypass. *Anesthesiology and Pain Medicine*, *4*(3). https://doi.org/10.5812/aapm.16316

Azzopardi, D., Robertson, N. J., Bainbridge, A., Cady, E., Charles-Edwards, G., Deierl, A., … Edwards, A. D. (2016). Moderate hypothermia within 6 h of birth plus inhaled xenon versus moderate hypothermia alone after birth asphyxia (TOBY-Xe): a proof-of-concept, open-label, randomised controlled trial. *The Lancet Neurology*, *15*(2), 145–153. https://doi.org/10.1016/S1474-4422(15)00347-6

Azzopardi, D. V., Strohm, B., Edwards, A. D., Dyet, L., Halliday, H. L., Juszczak, E., … Brocklehurst, P. (2009). Moderate Hypothermia to Treat Perinatal Asphyxial Encephalopathy. *New England Journal of Medicine*, *361*(14), 1349–1358. https://doi.org/10.1056/NEJMoa0900854

Banks, P., Franks, N. P., & Dickinson, R. (2010). Competitive Inhibition at the Glycine Site of the N-Methyl-d-Aspartate Receptor Mediates Xenon Neuroprotection against Hypoxia–Ischemia. *Anesthesiology*, *112*(3), 614–622. https://doi.org/10.1097/ALN.0b013e3181cea398

Baserga, M. C., Beachy, J. C., Roberts, J. K., Ward, R. M., DiGeronimo, R. J., Walsh, W. F., … Yoder, B. A. (2015). Darbepoetin administration to neonates undergoing cooling for encephalopathy: a safety and pharmacokinetic trial. *Pediatric Research*, *78*(3), 315–322. https://doi.org/10.1038/pr.2015.101

Bernardi, P., Krauskopf, A., Basso, E., Petronilli, V., Blalchy-Dyson, E., Di Lisa, F., … Forte, M. A. (2006). The mitochondrial permeability transition from in vitro artifact to disease target. *FEBS Journal*, *273*(10), 2077–2099. https://doi.org/10.1111/j.1742-4658.2006.05213.x

Blomgren, K., & Hagberg, H. (2006). Free radicals, mitochondria, and hypoxia–ischemia in the developing brain. *Free Radical Biology and Medicine*, *40*(3), 388–397. https://doi.org/10.1016/j.freeradbiomed.2005.08.040

Castilho, R. F., Ward, M. W., & Nicholls, D. G. (1999). Oxidative stress, mitochondrial function, and acute glutamate excitotoxicity in cultured cerebellar granule cells. *J Neurochem*, *72*(4), 1394–1401.

Chalak, L. F., Rollins, N., Morriss, M. C., Brion, L. P., Heyne, R., & Sánchez, P. J. (2012). Perinatal acidosis and hypoxic-ischemic encephalopathy in preterm infants of 33 to 35 weeks' gestation. *The Journal of Pediatrics*, *160*(3), 388–394. https://doi.org/10.1016/j.jpeds.2011.09.001

Chung, E., Kong, X., Goldberg, M. P., Stowe, A. M., & Raman, L. (2015). Erythropoietin-mediated neuroprotection in a pediatric mouse model of chronic hypoxia. *Neuroscience Letters*, *597*, 54–59. https://doi.org/10.1016/j.neulet.2015.04.026

Cowell, R. M., Xu, H., Galasso, J. M., & Silverstein, F. S. (2002). Hypoxic-ischemic injury induces macrophage inflammatory protein-1alpha expression in immature

rat brain. *Stroke*, *33*(3), 795–801. https://doi.org/10.1161/hs0302.103740

Crowther, C. A., Hiller, J. E., Doyle, L. W., Haslam, R. R., & Group, for the A. C. T. of M. S. (ACTOMgSO4) C. (2003). Effect of Magnesium Sulfate Given for Neuroprotection Before Preterm Birth<SUBTITLE>A Randomized Controlled Trial</SUBTITLE> *JAMA*, *290*(20), 2669. https://doi.org/10.1001/jama.290.20.2669

David, H. N., Leveille, F., Chazalviel, L., MacKenzie, E. T., Buisson, A., Lemaire, M., & Abraini, J. H. (2003). Reduction of Ischemic Brain Damage by Nitrous Oxide and Xenon. *Journal of Cerebral Blood Flow & Metabolism*, *23*(10), 1168–1173. https://doi.org/10.1097/01.WCB.0000087342.31689.18

de Haan, M., Wyatt, J. S., Roth, S., Vargha-Khadem, F., Gadian, D., & Mishkin, M. (2006). Brain and cognitive-behavioural development after asphyxia at term birth. *Developmental Science*, *9*(4), 350–358. https://doi.org/10.1111/j.1467-7687.2006.00499.x

DeLorenzo, R. J., Sombati, S., & Coulter, D. A. (2000). Effects of Topiramate on Sustained Repetitive Firing and Spontaneous Recurrent Seizure Discharges in Cultured Hippocampal Neurons. *Epilepsia*, *41*(s1), 40–44. https://doi.org/10.1111/j.1528-1157.2000.tb02170.x

Dickinson, R., Peterson, B. K., Banks, P., Simillis, C., Martin, J. C. S., Valenzuela, C. A., … Franks, N. P. (2007). Competitive Inhibition at the Glycine Site of the N-Methyl-d-aspartate Receptor by the Anesthetics Xenon and Isoflurane. *Anesthesiology*, *107*(5), 756–767. https://doi.org/10.1097/01.anes.0000287061.77674.71

Dingley, J., Tooley, J., Liu, X., Scull-Brown, E., Elstad, M., Chakkarapani, E., …

Thoresen, M. (2014). Xenon ventilation during therapeutic hypothermia in neonatal encephalopathy: a feasibility study. *Pediatrics*, *133*(5), 809–818. https://doi.org/10.1542/peds.2013-0787

Do women with pre-eclampsia, and their babies, benefit from magnesium sulphate? The Magpie Trial: a randomised placebo-controlled trial. (2002). *The Lancet*, *359*(9321), 1877–1890. https://doi.org/10.1016/S0140-6736(02)08778-0

Downes, K. L., Grantz, K. L., & Shenassa, E. D. (2017). Maternal, Labor, Delivery, and Perinatal Outcomes Associated with Placental Abruption: A Systematic Review. *American Journal of Perinatology*, *34*(10), 935–957. https://doi.org/10.1055/s-0037-1599149

Driscoll, D. J. O. ., Felice, V. D., Kenny, L. C., Boylan, G. B., & O'Keeffe, G. W. (2018). Mild prenatal hypoxia-ischemia leads to social deficits and central and peripheral inflammation in exposed offspring. *Brain, Behavior, and Immunity*. https://doi.org/10.1016/J.BBI.2018.01.001

Fan, X., van Bel, F., van der Kooij, M. A., Heijnen, C. J., & Groenendaal, F. (2013). Hypothermia and erythropoietin for neuroprotection after neonatal brain damage. *Pediatric Research*, *73*(1), 18–23. https://doi.org/10.1038/pr.2012.139

Faulkner, S., Bainbridge, A., Kato, T., Chandrasekaran, M., Kapetanakis, A. B., Hristova, M., … Robertson, N. J. (2011). Xenon augmented hypothermia reduces early lactate/N-acetylaspartate and cell death in perinatal asphyxia. *Annals of Neurology*, *70*(1), 133–150. https://doi.org/10.1002/ana.22387

Filippi, L., Poggi, C., la Marca, G., Furlanetto, S., Fiorini, P., Cavallaro, G., … Guerrini, R. (2010). Oral Topiramate in Neonates with Hypoxic Ischemic Encephalopathy Treated with Hypothermia: A Safety Study. *The Journal of*

Pediatrics, *157*(3), 361–366. https://doi.org/10.1016/J.JPEDS.2010.04.019

Glass, H. C., Glidden, D., Jeremy, R. J., Barkovich, A. J., Ferriero, D. M., & Miller, S. P. (2009). Clinical Neonatal Seizures are Independently Associated with Outcome in Infants at Risk for Hypoxic-Ischemic Brain Injury. *The Journal of Pediatrics*, *155*(3), 318–323. https://doi.org/10.1016/J.JPEDS.2009.03.040

Gluckman, P. D., Wyatt, J. S., Azzopardi, D., Ballard, R., Edwards, A. D., Ferriero, D. M., … Gunn, A. J. (2005). Selective head cooling with mild systemic hypothermia after neonatal encephalopathy: multicentre randomised trial. *The Lancet*, *365*(9460), 663–670. https://doi.org/10.1016/S0140-6736(05)17946-X

Gonzalez, F. F., Abel, R., Almli, C. R., Mu, D., Wendland, M., & Ferriero, D. M. (2009). Erythropoietin sustains cognitive function and brain volume after neonatal stroke. *Developmental Neuroscience*, *31*(5), 403–411. https://doi.org/10.1159/000232558

Hack, M., Breslau, N., Aram, D., Weissman, B., Klein, N., & Borawski-Clark, E. (1992). The effect of very low birth weight and social risk on neurocognitive abilities at school age. *Journal of Developmental and Behavioral Pediatrics : JDBP*, *13*(6), 412–420. Retrieved from http://www.ncbi.nlm.nih.gov/pubmed/1469109

Hall, N. J., Eaton, S., Peters, M. J., Hiorns, M. P., Alexander, N., Azzopardi, D. V, & Pierro, A. (2010). Mild controlled hypothermia in preterm neonates with advanced necrotizing enterocolitis. *Pediatrics*, *125*(2), e300-8. https://doi.org/10.1542/peds.2008-3211

Hankins, G. D. V, & Speer, M. (2003). Defining the pathogenesis and pathophysiology of neonatal encephalopathy and cerebral palsy. *Obstetrics and Gynecology*,

102(3), 628–636. Retrieved from http://www.ncbi.nlm.nih.gov/pubmed/12962954

Hobbs, C., Thoresen, M., Tucker, A., Aquilina, K., Chakkarapani, E., & Dingley, J. (2008). Xenon and Hypothermia Combine Additively, Offering Long-Term Functional and Histopathologic Neuroprotection After Neonatal Hypoxia/Ischemia. *Stroke*, *39*(4), 1307–1313. https://doi.org/10.1161/STROKEAHA.107.499822

Iadecola, C., & Anrather, J. (2011). The immunology of stroke: from mechanisms to translation. *Nature Medicine*, *17*(7), 796–808. https://doi.org/10.1038/nm.2399

Ikonomidou, C., & Kaindl, A. M. (2011). Neuronal Death and Oxidative Stress in the Developing Brain. *Antioxidants & Redox Signaling*, *14*(8), 1535–1550. https://doi.org/10.1089/ars.2010.3581

Jacobs, S. E., Berg, M., Hunt, R., Tarnow-Mordi, W. O., Inder, T. E., & Davis, P. G. (2013). Cooling for newborns with hypoxic ischaemic encephalopathy. *Cochrane Database of Systematic Reviews*. https://doi.org/10.1002/14651858.CD003311.pub3

Jacobs, S. E., Morley, C. J., Inder, T. E., Stewart, M. J., Smith, K. R., McNamara, P. J., … Infant Cooling Evaluation Collaboration. (2011). Whole-Body Hypothermia for Term and Near-Term Newborns With Hypoxic-Ischemic Encephalopathy. *Archives of Pediatrics & Adolescent Medicine*, *165*(8), 692. https://doi.org/10.1001/archpediatrics.2011.43

Jenster, M., Bonifacio, S. L., Ruel, T., Rogers, E. E., Tam, E. W., Partridge, J. C., … Glass, H. C. (2014). Maternal or neonatal infection: association with neonatal encephalopathy outcomes. *Pediatric Research*, *76*(1), 93–99.

https://doi.org/10.1038/pr.2014.47

Johnston, M. V. (1995). Neurotransmitters and vulnerability of the developing brain. *Brain & Development*, *17*(5), 301–306. Retrieved from http://www.ncbi.nlm.nih.gov/pubmed/8579213

Kang, S. W., Choi, S.-K., Park, E., Chae, S.-J., Choi, S., Jin Joo, H., … Park, H.-K. (2011). Neuroprotective effects of magnesium-sulfate on ischemic injury mediated by modulating the release of glutamate and reduced of hyperreperfusion. *Brain Research*, *1371*, 121–128. https://doi.org/10.1016/j.brainres.2010.11.057

Kaur, C., Rathnasamy, G., & Ling, E.-A. (2013). Roles of Activated Microglia in Hypoxia Induced Neuroinflammation in the Developing Brain and the Retina. *Journal of Neuroimmune Pharmacology*, *8*(1), 66–78. https://doi.org/10.1007/s11481-012-9347-2

Kaur, C., Sivakumar, V., Yip, G. W., & Ling, E. A. (2009). Expression of syndecan-2 in the amoeboid microglial cells and its involvement in inflammation in the hypoxic developing brain. *Glia*, *57*(3), 336–349. https://doi.org/10.1002/glia.20764

Keogh, C. L., Yu, S. P., & Wei, L. (2007). The effect of recombinant human erythropoietin on neurovasculature repair after focal ischemic stroke in neonatal rats. *The Journal of Pharmacology and Experimental Therapeutics*, *322*(2), 521–528. https://doi.org/10.1124/jpet.107.121392

Koh, S., & Jensen, F. E. (2001). Topiramate blocks perinatal hypoxia-induced seizures in rat pups. *Annals of Neurology*, *50*(3), 366–372. https://doi.org/10.1002/ana.1122

Kolevzon, A., Gross, R., & Reichenberg, A. (2007). Prenatal and Perinatal Risk Factors for Autism. *Archives of Pediatrics & Adolescent Medicine*, *161*(4), 326. https://doi.org/10.1001/archpedi.161.4.326

Lai, J. C. Y., Rocha-Ferreira, E., Ek, C. J., Wang, X., Hagberg, H., & Mallard, C. (2017). Immune responses in perinatal brain injury. *Brain, Behavior, and Immunity*, *63*, 210–223. https://doi.org/10.1016/j.bbi.2016.10.022

Lawn, J., Shibuya, K., & Stein, C. (2005). No cry at birth: global estimates of intrapartum stillbirths and intrapartum-related neonatal deaths. *Bulletin of the World Health Organization*, *83*(6), 409–417. https://doi.org//S0042-96862005000600008

Lee, A. C. C., Kozuki, N., Blencowe, H., Vos, T., Bahalim, A., Darmstadt, G. L., … Lawn, J. E. (2013). Intrapartum-related neonatal encephalopathy incidence and impairment at regional and global levels for 2010 with trends from 1990. *Pediatric Research*, *74 Suppl 1*, 50–72. https://doi.org/10.1038/pr.2013.206

Liljestrom, L., Wikstrom, A.-K., Agren, J., & Jonsson, M. (2018). Antepartum risk factors for moderate to severe neonatal hypoxic ischemic encephalopathy: a Swedish national cohort study. *Acta Obstetricia et Gynecologica Scandinavica*, *97*(5), 615–623. https://doi.org/10.1111/aogs.13316

Liu, F., & Mccullough, L. D. (2013). Inflammatory responses in hypoxic ischemic encephalopathy. *Acta Pharmacologica Sinica*, *34*(9), 1121–1130. https://doi.org/10.1038/aps.2013.89

Marret, S., Marpeau, L., Zupan-Simunek, V., Eurin, D., Lévêque, C., Hellot, M.-F., … PREMAG trial group. (2006). Magnesium sulphate given before very-preterm birth to protect infant brain: the randomised controlled PREMAG trial*. *BJOG:*

An International Journal of Obstetrics & Gynaecology, *114*(3), 310–318. https://doi.org/10.1111/j.1471-0528.2006.01162.x

Martinello, K., Hart, A. R., Yap, S., Mitra, S., & Robertson, N. J. (2017). Management and investigation of neonatal encephalopathy: 2017 update. *Archives of Disease in Childhood. Fetal and Neonatal Edition*, *102*(4), F346. https://doi.org/10.1136/ARCHDISCHILD-2015-309639

Meloni, B., Brookes, L., Clark, V., Cross, J., Edwards, A., Anderton, R., … Knuckey, N. (2015). Poly-arginine and arginine-rich peptides are neuroprotective in stroke models. *J Cereb Blood Flow Metab*. https://doi.org/10.1038/jcbfm.2015.11

Meloni, B., Craig, A., Milech, N., Hopkins, R., Watt, P., & Knuckey, N. (2014). The neuroprotective efficacy of cell-penetrating peptides TAT, penetratin, Arg-9, and Pep-1 in glutamic acid, kainic acid, and in vitro ischemia injury models using primary cortical neuronal cultures. *Cell Mol Neurobiol*, *34*(2), 173–181. https://doi.org/10.1007/s10571-013-9999-3

Meloni, B., Milani, D., Cross, J., Clark, V., Edwards, A., Anderton, R., … Knuckey, N. (2017). Assessment of the Neuroprotective Effects of Arginine-Rich Protamine Peptides, Poly-Arginine Peptides (R12-Cyclic, R22) and Arginine–Tryptophan-Containing Peptides Following In Vitro Excitotoxicity and/or Permanent Middle Cerebral Artery Occlusion in Rats. *NeuroMolecular Medicine*, *19*(2–3), 271–285. https://doi.org/10.1007/s12017-017-8441-2

Meloni, B., Milani, D., Edwards, A., Anderton, R., O'Hare Doig, R., Fitzgerald, M., … Knuckey, N. (2015). Neuroprotective peptides fused to arginine-rich cell penetrating peptides: Neuroprotective mechanism likely mediated by peptide endocytic properties. *Pharmacology & Therapeutics*, *153*, 36–54.

https://doi.org/10.1016/j.pharmthera.2015.06.002

Milani, D., Bakeberg, M. C., Cross, J. L., Clark, V. W., Anderton, R. S., Blacker, D. J., … Meloni, B. P. (2018). Comparison of neuroprotective efficacy of poly-arginine R18 and R18D (D-enantiomer) peptides following permanent middle cerebral artery occlusion in the Wistar rat and in vitro toxicity studies. *PLoS ONE*, *13*(3), e0193884. https://doi.org/10.1371/journal.pone.0193884

Milani, D., Clark, V., Cross, J., Anderton, R., Knuckey, N., & Meloni, B. (2016). Poly-arginine peptides reduce infarct volume in a permanent middle cerebral artery rat stroke model. *BMC Neuroscience*, *17*(1), 19. https://doi.org/10.1186/s12868-016-0253-z

Milani, D., Cross, J., Anderton, R., Blacker, D., Knuckey, N., & Meloni, B. (2017). Neuroprotective efficacy of poly-arginine R18 and NA-1 (TAT-NR2B9c) peptides following transient middle cerebral artery occlusion in the rat. *Neuroscience Research*, *114*, 9–15. https://doi.org/10.1016/j.neures.2016.09.002

Milani, D., Knuckey, N., Anderton, R., Cross, J., & Meloni, B. (2016). The R18 Polyarginine Peptide Is More Effective Than the TAT-NR2B9c (NA-1) Peptide When Administered 60 Minutes after Permanent Middle Cerebral Artery Occlusion in the Rat. *Stroke Research and Treatment*, *2016*, 1–9. https://doi.org/10.1155/2016/2372710

Mittendorf, R., Covert, R., Boinan, J., Khoshnood, B., Lee, K.-S., & Siegler, M. (1997). Is tocolytic magnesium sulphate associated with increased total paediatric mortality? *The Lancet*, *350*(9090), 1517–1518. https://doi.org/10.1016/S0140-6736(97)24047-X

Northington, F. J., Chavez-Valdez, R., & Martin, L. J. (2011). Neuronal cell death in

neonatal hypoxia-ischemia. *Annals of Neurology*, *69*(5), 743–758. https://doi.org/10.1002/ana.22419

O'Hare, M. J., Kushwaha, N., Zhang, Y., Aleyasin, H., Callaghan, S. M., Slack, R. S., … Park, D. S. (2005). Differential roles of nuclear and cytoplasmic cyclin-dependent kinase 5 in apoptotic and excitotoxic neuronal death. *The Journal of Neuroscience : The Official Journal of the Society for Neuroscience*, *25*(39), 8954–8966. https://doi.org/10.1523/JNEUROSCI.2899-05.2005

O'Shea, T. M. (2008). Diagnosis, treatment, and prevention of cerebral palsy. *Clinical Obstetrics and Gynecology*, *51*(4), 816–828. https://doi.org/10.1097/GRF.0b013e3181870ba7

Olney, J. W., Price, M. T., Samson, L., & Labruyere, J. (1986). The role of specific ions in glutamate neurotoxicity. *Neuroscience Letters*, *65*(1), 65–71. https://doi.org/10.1016/0304-3940(86)90121-7

Ong, K. K., Kennedy, K., Castañeda-Gutiérrez, E., Forsyth, S., Godfrey, K. M., Koletzko, B., … Fewtrell, M. (2015). Postnatal growth in preterm infants and later health outcomes: a systematic review. *Acta Paediatrica (Oslo, Norway : 1992)*, *104*(10), 974–986. https://doi.org/10.1111/apa.13128

Peesay, M. (2017). Nuchal cord and its implications. *Maternal Health, Neonatology and Perinatology*, *3*, 28. https://doi.org/10.1186/s40748-017-0068-7

Perlman, J. M. (1997). Intrapartum hypoxic-ischemic cerebral injury and subsequent cerebral palsy: medicolegal issues. *Pediatrics*, *99*(6), 851–859. https://doi.org/10.1542/PEDS.99.6.851

Pisani, F., Orsini, M., Braibanti, S., Copioli, C., Sisti, L., & Turco, E. C. (2009).

Development of epilepsy in newborns with moderate hypoxic-ischemic encephalopathy and neonatal seizures. *Brain & Development*, *31*(1), 64–68. https://doi.org/10.1016/j.braindev.2008.04.001

Politi, S., D'Emidio, L., Cignini, P., Giorlandino, M., & Giorlandino, C. (2010). Shoulder dystocia: an Evidence-Based approach. *Journal of Prenatal Medicine*, *4*(3), 35. Retrieved from https://www.ncbi.nlm.nih.gov/pmc/articles/PMC3279180/

Rao, R., Trivedi, S., Vesoulis, Z., Liao, S. M., Smyser, C. D., & Mathur, A. M. (2017). Safety and Short-Term Outcomes of Therapeutic Hypothermia in Preterm Neonates 34-35 Weeks Gestational Age with Hypoxic-Ischemic Encephalopathy. *The Journal of Pediatrics*, *183*, 37–42. https://doi.org/10.1016/j.jpeds.2016.11.019

Robertson, C., & Finer, N. (1993). Long-Term Follow-Up of Term Neonates with Perinatal Asphyxia. *Clinics in Perinatology*, *20*(2), 483–499. https://doi.org/10.1016/S0095-5108(18)30405-6

Robertson, N. J., Tan, S., Groenendaal, F., van Bel, F., Juul, S. E., Bennet, L., … Mallard, C. (2012). Which neuroprotective agents are ready for bench to bedside translation in the newborn infant? *The Journal of Pediatrics*, *160*(4), 544–552.e4. https://doi.org/10.1016/j.jpeds.2011.12.052

Rouse, D. J., Hirtz, D. G., Thom, E., Varner, M. W., Spong, C. Y., Mercer, B. M., … Roberts, J. M. (2008). A Randomized, Controlled Trial of Magnesium Sulfate for the Prevention of Cerebral Palsy. *New England Journal of Medicine*, *359*(9), 895–905. https://doi.org/10.1056/NEJMoa0801187

Sanderson, T. H., Reynolds, C. A., Kumar, R., Przyklenk, K., & Hüttemann, M.

(2013). Molecular Mechanisms of Ischemia–Reperfusion Injury in Brain: Pivotal Role of the Mitochondrial Membrane Potential in Reactive Oxygen Species Generation. *Molecular Neurobiology*, *47*(1), 9–23. https://doi.org/10.1007/s12035-012-8344-z

Scutiero, G., Giulia, B., Iannone, P., Nappi, L., Morano, D., & Greco, P. (2018). Umbilical Cord Hematoma: A Case Report and Review of the Literature. *Obstetrics and Gynecology International*, *2018*, 2610980. https://doi.org/10.1155/2018/2610980

Shankaran, S., Laptook, A. R., Ehrenkranz, R. A., Tyson, J. E., McDonald, S. A., Donovan, E. F., … National Institute of Child Health and Human Development Neonatal Research Network. (2005). Whole-Body Hypothermia for Neonates with Hypoxic–Ischemic Encephalopathy. *New England Journal of Medicine*, *353*(15), 1574–1584. https://doi.org/10.1056/NEJMcps050929

Sherwin, C. M. T., Balch, A., Campbell, S. C., Fredrickson, J., Clark, E. A. S., Varner, M., … Spigarelli, M. G. (2014). Maternal Magnesium Sulphate Exposure Predicts Neonatal Magnesium Blood Concentrations. *Basic & Clinical Pharmacology & Toxicology*, *114*(4), 318–322. https://doi.org/10.1111/bcpt.12166

Simiyu, I. N., Mchaile, D. N., Katsongeri, K., Philemon, R. N., & Msuya, S. E. (2017). Prevalence, severity and early outcomes of hypoxic ischemic encephalopathy among newborns at a tertiary hospital, in northern Tanzania. *BMC Pediatrics*, *17*(1), 131. https://doi.org/10.1186/s12887-017-0876-y

Stoppe, C., Rimek, A., Rossaint, R., Rex, S., Stevanovic, A., Schälte, G., … Coburn, M. (2013). Xenon consumption during general surgery: a retrospective

observational study. *Medical Gas Research*, *3*(1), 12. https://doi.org/10.1186/2045-9912-3-12

Stout, A. K., Raphael, H. M., Kanterewicz, B. I., Klann, E., & Reynolds, I. J. (1998). Glutamate-induced neuron death requires mitochondrial calcium uptake. *Nat Neurosci*, *1*(5), 366–373. https://doi.org/10.1038/1577

Thoresen, M., Hobbs, C. E., Wood, T., Chakkarapani, E., & Dingley, J. (2009). Cooling Combined with Immediate or Delayed Xenon Inhalation Provides Equivalent Long-Term Neuroprotection after Neonatal Hypoxia—Ischemia. *Journal of Cerebral Blood Flow & Metabolism*, *29*(4), 707–714. https://doi.org/10.1038/jcbfm.2008.163

Thornton, C., Rousset, C. I., Kichev, A., Miyakuni, Y., Vontell, R., Baburamani, A. A., … Hagberg, H. (2012). Molecular Mechanisms of Neonatal Brain Injury. *Neurology Research International*, *2012*, 1–16. https://doi.org/10.1155/2012/506320

Tuttolomondo, A., Di Raimondo, D., di Sciacca, R., Pinto, A., & Licata, G. (2008). Inflammatory cytokines in acute ischemic stroke. *Current Pharmaceutical Design*, *14*(33), 3574–3589. Retrieved from http://www.ncbi.nlm.nih.gov/pubmed/19075734

Vincer, M. J., Allen, A. C., Joseph, K. S., Stinson, D. A., Scott, H., & Wood, E. (2006). Increasing Prevalence of Cerebral Palsy Among Very Preterm Infants: A Population-Based Study. *PEDIATRICS*, *118*(6), e1621–e1626. https://doi.org/10.1542/peds.2006-1522

Wall, S. N., Lee, A. C. C., Carlo, W., Goldenberg, R., Niermeyer, S., Darmstadt, G. L., … Lawn, J. E. (2010). Reducing intrapartum-related neonatal deaths in low-

and middle-income countries-what works? *Seminars in Perinatology*, *34*(6), 395–407. https://doi.org/10.1053/j.semperi.2010.09.009

Wang, X., Carlsson, Y., Basso, E., Zhu, C., Rousset, C. I., Rasola, A., … Hagberg, H. (2009). Developmental Shift of Cyclophilin D Contribution to Hypoxic-Ischemic Brain Injury. *Journal of Neuroscience*, *29*(8), 2588–2596. https://doi.org/10.1523/JNEUROSCI.5832-08.2009

White, H. S., Brown, S. D., Woodhead, J. H., Skeen, G. A., & Wolf, H. H. (1997). Topiramate enhances GABA-mediated chloride flux and GABA-evoked chloride currents in murine brain neurons and increases seizure threshold. *Epilepsy Research*, *28*(3), 167–179. Retrieved from http://www.ncbi.nlm.nih.gov/pubmed/9332882

Wilson-Costello, D., Friedman, H., Minich, N., Siner, B., Taylor, G., Schluchter, M., & Hack, M. (2007). Improved Neurodevelopmental Outcomes for Extremely Low Birth Weight Infants in 2000-2002. *PEDIATRICS*, *119*(1), 37–45. https://doi.org/10.1542/peds.2006-1416

Wu, Y. W., Bauer, L. A., Ballard, R. A., Ferriero, D. M., Glidden, D. V, Mayock, D. E., … Juul, S. E. (2012). Erythropoietin for neuroprotection in neonatal encephalopathy: safety and pharmacokinetics. *Pediatrics*, *130*(4), 683–691. https://doi.org/10.1542/peds.2012-0498

Zhang, H., Fang, X., Huang, D., Luo, Q., Zheng, M., Wang, K., … Yin, Z. (2017). Erythropoietin signaling increases neurogenesis and oligodendrogenesis of endogenous neural stem cells following spinal cord injury both in vivo and in vitro. *Molecular Medicine Reports*, *17*(1), 264–272. https://doi.org/10.3892/mmr.2017.7873

Zhang, J., Dawson, V., Dawson, T., & Snyder, S. (1994). Nitric oxide activation of poly(ADP-ribose) synthetase in neurotoxicity. *Science*, *263*(5147), 687–689. https://doi.org/10.1126/science.8080500

Zhu, C., Wang, X., Deinum, J., Huang, Z., Gao, J., Modjtahedi, N., … Blomgren, K. (2007). Cyclophilin A participates in the nuclear translocation of apoptosis-inducing factor in neurons after cerebral hypoxia-ischemia. *The Journal of Experimental Medicine*, *204*(8), 1741–1748. https://doi.org/10.1084/jem.20070193

Chapter 2

Perinatal hypoxic-ischaemic encephalopathy and neuroprotective peptide therapies: a case for cationic arginine rich peptides (CARPs)

Published: Brain Sciences

Review: Perinatal hypoxic-ischaemic encephalopathy and neuroprotective peptide therapies: a case for cationic arginine-rich peptides (CARPs).

Adam B. Edwards [1,2,3], Ryan S. Anderton [1,2,4], Neville W. Knuckey [1,3,4], Bruno P. Meloni [1,3,4]

[1] Perron Institute for Neurological and Translational Science, Nedlands, Western Australia

[2] School of Health Sciences, The University of Notre Dame Australia, Fremantle, Western Australia

[3] Department of Neurosurgery, Sir Charles Gardiner Hospital, Nedlands, Western Australia

[4] Centre for Neuromuscular and Neurological Disorders, The University of Western Australia, Nedlands, Western Australia

Author contributions

Adam Edwards: 85%

Ryan Anderton: 3%

Neville Knuckey: 2%

Bruno Meloni: 10%

Signed..... Signed.....

Adam Edwards Bruno Meloni (coordinating supervisor)

brain sciences

MDPI

Review

Perinatal Hypoxic-Ischemic Encephalopathy and Neuroprotective Peptide Therapies: A Case for Cationic Arginine-Rich Peptides (CARPs)

Adam B. Edwards [1,2,3,*], Ryan S. Anderton [1,2,4], Neville W. Knuckey [1,3,4] and Bruno P. Meloni [1,3,4]

1 Perron Institute for Neurological and Translational Science, Nedlands, WA 6009, Australia; ryan.anderton@nd.edu.au (R.S.A.); neville.knuckey@health.wa.gov.au (N.W.K.); bruno.meloni@perron.uwa.edu.au (B.P.M.)
2 School of Health Sciences and Institute for Health Research, The University of Notre Dame Australia, Fremantle, WA 6160, Australia
3 Department of Neurosurgery, Sir Charles Gairdner Hospital, QEII Medical Centre, Nedlands, WA 6009, Australia
4 Centre for Neuromuscular and Neurological Disorders, The University of Western Australia, Nedlands, WA 6009, Australia
* Correspondence: adam.edwards1@my.nd.edu.au; Tel.: +61-08-6457-0316

Received: 28 June 2018; Accepted: 1 August 2018; Published: 7 August 2018

Abstract: Perinatal hypoxic-ischemic encephalopathy (HIE) is the leading cause of mortality and morbidity in neonates, with survivors suffering significant neurological sequelae including cerebral palsy, epilepsy, intellectual disability and autism spectrum disorders. While hypothermia is used clinically to reduce neurological injury following HIE, it is only used for term infants (>36 weeks gestation) in tertiary hospitals and improves outcomes in only 30% of patients. For these reasons, a more effective and easily administrable pharmacological therapeutic agent, that can be used in combination with hypothermia or alone when hypothermia cannot be applied, is urgently needed to treat pre-term (≤36 weeks gestation) and term infants suffering HIE. Several recent studies have demonstrated that cationic arginine-rich peptides (CARPs), which include many cell-penetrating peptides [CPPs; e.g., transactivator of transcription (TAT) and poly-arginine-9 (R9; 9-mer of arginine)], possess intrinsic neuroprotective properties. For example, we have demonstrated that poly-arginine-18 (R18; 18-mer of arginine) and its D-enantiomer (R18D) are neuroprotective in vitro following neuronal excitotoxicity, and in vivo following perinatal hypoxia-ischemia (HI). In this paper, we review studies that have used CARPs and other peptides, including putative neuroprotective peptides fused to TAT, in animal models of perinatal HIE. We critically evaluate the evidence that supports our hypothesis that CARP neuroprotection is mediated by peptide arginine content and positive charge and that CARPs represent a novel potential therapeutic for HIE.

Keywords: hypoxic-ischemic encephalopathy; hypoxia-ischemia; birth asphyxia; neuroprotection; cationic arginine-rich peptides; animal models

1. Introduction

Perinatal hypoxic-ischemic encephalopathy (HIE; also referred to as birth asphyxia) remains the leading cause of neonatal mortality and morbidity, with an incidence in developed nations of 2–6 and 7 in every 1000 live term (>36 weeks gestation) and pre-term (≤36 weeks gestation) births, respectively [1,2]. The incidence is even higher in developing countries, with rates of up to 30 per 1000 live full-term births [3,4]. Of the individuals affected by HIE, 15–20% will die in the

postnatal period, and an additional 25% will develop severe and permanent neurological sequela. Each year, HIE accounts for up to 1.2 million deaths [5] and some form of central nervous system (CNS) dysfunction in an estimated 1.15 million neonates [6] such as cerebral palsy, epilepsy, global developmental delay, intellectual disability, behavioral disorders and autism spectrum disorders [7–11]. While hypothermia is used as a therapeutic intervention to minimize brain injury in neonates suffering HIE, it only provides beneficial outcomes in approximately 30% of patients and has several limitations (reviewed below). Therefore, an effective and easily administrable pharmacological therapeutic agent to improve patient outcomes when used as an adjunct to hypothermia, on its own or when hypothermia cannot be applied is urgently needed.

In recent years, there has been an increased application of putative neuroprotective peptides designed to target cyto-damaging or cyto-protective pathways to reduce injury in acute brain disorders such as HIE. One reason for this interest is the discovery of cell-penetrating peptides (CPPs), allowing for the delivery of neuroprotective peptides and other molecular cargos (e.g., proteins, nucleic acids and nanoparticles) across the blood brain barrier (BBB) and into cells within the CNS. Most studies assessing neuroprotective peptides in animal models of HIE use the cationic arginine-rich CPP, transactivator of transcription ($TAT_{47–57}$ YGRKKRRQRRR), as the 'carrier' molecule. However, several years ago, our and other laboratories demonstrated that the TAT peptide has modest intrinsic neuroprotective properties in its own right [12–17]. We subsequently demonstrated that other cationic arginine-rich peptides [CARPs; e.g., penetratin, protamine, sodium calcium exchanger inhibitory peptide (XIP), poly-arginine peptides (e.g., R9, R12 and R18; R indicates amino acid arginine and number indicates mer)], possess potent neuroprotective properties in both in vitro and animal models of cerebral ischemia and/or hypoxia [12,18–29], and demonstrated that the arginine content and peptide positive charge are critical determinants of neuroprotection [19,27,28].

Based on the recent application of cationic CPPs for the delivery of putative neuroprotective peptides in animal models of HIE and the recent discovery of the intrinsic neuroprotective properties of CARPs, the objectives of this review are: (i) catalogue studies that have used peptides as neuroprotective agents in HIE, especially those employing a CPP delivery system; and (ii) to evaluate the potential neuroprotective effects of both CPP and cargo molecules in terms of their arginine content and cationic charge, as well as the content of other potentially neuroprotective amino acids such as tryptophan [29]. We will propose that the neuroprotective properties of most, if not all putative neuroprotective peptides fused to cationic CPPs are likely to be mediated in a large part by the actions of the carrier CPP (e.g., TAT) rather than the cargo molecule itself, with potency being further enhanced according to the amino acid content of the cargo (e.g., number of arginine residues) [19]. In addition, we will also review the evidence that CARPs have multiple cellular modes of action that underlie their neuroprotective properties.

First, we provide a brief overview of the major underlying pathophysiological mechanisms associated with HIE and the application of hypothermia as an acute therapy for the disorder.

2. Pathophysiology of Perinatal Hypoxia-Ischemic Brain Injury

2.1. Initiation of the Pathophysiological Cascade in HIE

The etiology of HIE is associated with a variety of maternal, placental and fetal conditions; all of which have variable clinical manifestations. These conditions include, but are not limited to, chronic maternal hypoxia (e.g., chronic utero-placental hypoxia, cardiopulmonary arrest, acute hypotension, pulmonary embolism or vascular disease), pre-eclampsia, nuchal cord, umbilical cord knotting, umbilical cord prolapse, shoulder dystocia and premature placental detachment [30]. Perinatal hypoxia is initiated following an impairment of oxygenated cerebral blood flow (CBF) to the fetus, triggering responses at both the systemic and cellular levels. The fetal brain is particularly sensitive to a HI environment, as there is a requirement of a constant supply of energy in the form of ATP, and when interrupted, excitotoxicity occurs through the uncontrolled release of excitatory neurotransmitters

such as glutamate; marking the beginning of the ischemic cascade. The acute and downstream consequences of the ischemic cascade are damaging to neurons and other cells (e.g., glial progenitor cells and astrocytes) at the cytoplasmic and mitochondrial levels, as well as causing disruption to the BBB and the activation of inflammatory responses.

2.2. Excitotoxicity

The metabolic rate of the fetal brain is largely determined by the stage of gestational development [30]. To meet metabolic demands, developing neural tissue metabolizes lactate, ketone bodies and glucose. When compared to the developed brain, the fetal brain is more adaptable with respect to energy utilization, thereby increasing its capacity to tolerate hypoxia-ischemia (HI) [31]. However, in the event of a critical depletion of ATP due to prolonged HI, the fetal brain eventually becomes susceptible to injury.

Following prolonged HI, cellular homeostasis is disrupted due to the depletion of ATP and failure to maintain ionic gradients, and as a result, neurons depolarize and release glutamate into the synaptic cleft [32]. High extracellular levels of glutamate cause excitotoxicity in neurons and other cells, namely glial progenitor cells, that express glutamate receptors (NMDA; *N*-methyl-D-asparate, AMPA; α-amino-3-hydroxy-5-methy-4-isoxazolepropionic acid, kainic acid and metabotropic glutamate receptors), producing a cytotoxic cellular influx of calcium ions [33]. The increased levels of intracellular calcium in neurons and glial progenitor cells in turn results in the activation of calcium-dependent proteases, lipases and deoxyribonuclease (DNase), reactive oxygen species (ROS) production, oxidative stress, cytotoxic edema, mitochondrial dysfunction and the stimulation of pro-cell death pathways [34–38].

2.3. Oxidative Stress

Oxidative stress plays an important role in the pathophysiology of HIE, as the developing brain comprises high levels of unsaturated fatty acids susceptible to lipid peroxidation, metals catalyzing free radical reactions and low concentrations of antioxidants [39]. The resulting heightened sensitivity to oxidative stress and ROS production following HI causes significant damage to lipids (lipid oxidation), nucleic acids (DNA degeneration) and proteins (protein oxidation). Sources of ROS following HI include, the mitochondrial electron transport chain (ETC), NADPH oxidases (NOX), xanthine oxidase (XO), arachidonic acid (12/15 lipoxygenase), and nitric oxide synthase (NOS). In particular, NOS has been targeted in HIE, with strategies to ablate or inhibit NOS activity invariably being neuroprotective in animal models of HIE [40].

2.4. Mitochondrial Dysfunction

Mitochondria have diverse functions, including ATP generation, intracellular calcium regulation, ROS production, biosynthesis of amino acids, lipids and nucleotides and pro-cell death signaling. The role of mitochondria in HIE has been extensively reviewed [41–43]. Here we focus on the role of mitochondria in potentiating secondary pathophysiological cascades contributing to HI. Mitochondria contribute to secondary brain injury following HI via the regulation of cell death pathways, namely apoptosis. Cellular apoptosis following HI is activated via both intrinsic (e.g., in response to mitochondrial dysfunction and damaged DNA) and extrinsic [e.g., in response to cell death receptors such as Fas and tissue necrosis factor-α (TNF-α)] pathways and involve the release of pro-cell death proteins from mitochondria.

In cells affected by HI, several processes such as excitotoxicity, ROS production, activation of p53, DNA damage and altered mitochondrial function can influence the activity of pro-apoptotic Bcl-2 proteins (e.g., Bid and Bax), resulting in Bax-dependent mitochondrial membrane permeability transition (MPT) [44,45]. In addition, excessive mitochondrial ROS generation, due to leakage from the ETC, can oxidize the inner mitochondrial membrane phospholipid, cardiolipin, promoting mitochondrial membrane permeability transition pore (MPTP) opening and subsequent release of

cytochrome-c. Cytosolic cytochrome-c, along with deoxyadenosine triphosphate (dATP), interact with apoptotic protease activating factor-1 (Apaf-1) to form the apoptosome, which cleaves and activates pro-caspase-9 [46]. Activated caspase-9 in turn activates caspase-3, which is a major proteolytic enzyme responsible for the ultimate dismantling of cells during apoptotic cell death.

Further alterations to mitochondria, such as mitochondrial outer membrane permeabilization (MOMP), results in the release other pro-apoptotic factors into the cytosol, including apoptosis-inducing factor (AIF), endonuclease G (Endo-G), and Smac/DIABLO [47,48]. Translocation of AIF and Endo-G to the nucleus mediates chromatin fragmentation and Smac/DIABLO interacts with inhibitors of apoptosis to reduce their actions on activated caspases.

TNF cell death receptor signaling mainly stimulates the extrinsic pathway by activating caspase-8, which activates other caspases, including caspase-3. While beyond the scope of this review, it is also important to note that other cell death pathways associated with necrosis, necroptosis, ferroptosis and autophagy may also be activated in response to HI. These pathways can be activated in response to one or more cellular disturbances such as calcium influx, mitochondrial dysfunction, cellular energy depletion, ROS production, TNF receptors cell signaling and other cellular cell signaling pathways (e.g., adenosine monophosphate-activated protein kinase).

2.5. Inflammation

The inflammatory response following HIE has been extensively reviewed by [49,50] and is therefore briefly discussed. In the immature brain following HI, an innate immune response occurs within minutes of the injury [51]. Initially, microglia become activated within the cerebral parenchyma, followed by a systemic inflammatory response, mediated by the infiltration of circulating monocytes, neutrophils and T-cells into the brain. Activated microglia develop macrophage-like attributes, such as phagocytic properties, cytokine production, antigen presentation and matrix metalloproteinase (MMP) release. The release and activation of MMPs by microglia can compromise BBB integrity, further promoting the invasion of peripheral leukocytes into the cerebral parenchyma; exacerbating ensuing cerebral injury. A hallmark of HIE is the aggregation of amoeboid microglia within the periventricular white matter, resulting in the production of inflammatory cytokines (TNF-α and IL1-β), NO and other ROS [52]; collectively potentiating the toxic effects of the ischemic cascade in neurons, glial progenitor cells and the cerebral vasculature.

While astrocytes attempt to provide neuroprotective support to neurons and glia via the release of glutathione, superoxide dismutase (SOD), extra-synaptic uptake of glutamate and the maintenance of ion channel gradients, these protective mechanisms can be quickly overrun. As with microglia, astrocytes become hyper-activated due to the effects of pro-inflammatory cytokines, ROS, and dying neurons and glia. Activated astrocytes also release pro-inflammatory cytokines (IL-6, TNF-α, IL-1α/β and INF-γ), further exacerbating HI-induced cell death pathways (e.g., apoptosis). In addition, astrocytes secrete chemokines that attracts systemic immune cells to infiltrate affected tissue, further aggravating tissue injury.

3. Current Clinical Treatments: Hypothermia

Hypothermia is considered one of the most effective neuroprotective treatment interventions in both experimental and clinical settings. While the exact beneficial effects of hypothermia are yet to be elucidated in HIE, it is known to suppress many of the neuro-damaging events associated with HI including excitotoxicity, apoptosis, inflammation, oxidative stress and BBB disruption [53].

In HIE, moderate hypothermia (33.5 °C for 72 h), applied within 6 h of birth, improves the survival and neurodevelopmental outcomes in infants suffering from moderate and severe HIE. While hypothermia is now considered standard care in the treatment of HIE and is well tolerated in term infants [54–57], it does not provide complete protection. Of the infants who have moderate or severe encephalopathy, therapeutic hypothermia was shown to decrease mortality from 40% to 28%,

while in surviving infants neurological morbidity was reduced from 31% to 19% of infants receiving therapeutic hypothermia [58].

Importantly, while hypothermia is safe in pre-term infants with necrotising enterocolitis [59], it has not been adequately evaluated for use in pre-term infants suffering HIE. Information regarding the safety and efficacy of hypothermia to treat pre-term infants suffering HIE is lacking, although information may be available in the near future (NCT1793129). In one study, hypothermia in pre-term infants was associated with higher mortality and increased clinical complications when compared to term infants [60], although the study did not include a normothermic pre-term control group. The inadequate application of hypothermia in the pre-term neonate highlights the need for the development of safer therapeutic interventions in these patients following HI.

In addition, the induction of hypothermia requires specialized equipment, intensive care monitoring and trained staff, limiting its use to centers that have the facilities and medical personnel to undertake the procedure. This develops uncertainty regarding the timing, safety and efficacy of initiating hypothermia in infants before transfer to a centre equipped to deliver hypothermia. For example, the transfer of infants suffering HIE to a medical centre to provide hypothermia can exceed 6 h from the time of birth and that attempts of passive cooling during transport can result in excessive cooling [61]. In light of this, there is an urgent need for the application of an acute neuroprotective therapy for infants who suffer HIE when hypothermia cannot be applied immediately, or is not available. In addition, as the incidences of mortality and morbidity are still relatively high following hypothermia, there is a requirement for additional therapeutic agents, adjuvant to hypothermia, to further improve outcomes in infants suffering HIE.

4. Neuroprotective Peptides and Their Therapeutic Application in HIE

4.1. Peptide Therapeutics

Peptides represent an important and increasingly popular class of therapeutic agent. To date, over 60 general peptide drugs have been approved in the United States, Europe, and Japan, approximately 140 are in active clinical development and more than 500 peptides are being examined in preclinical therapeutic studies [62]. Peptides have several beneficial properties over traditional drugs such as high biological and structural diversity, less toxicity and accumulation in tissue and reduced propensity to cause drug-drug interactions. The main disadvantage of most peptides is their inability to cross the BBB and enter cells, which is an important issue if the peptide has an intracellular target and/or is targeting a CNS disorder. However, as outlined above, the delivery of peptides into the CNS and into cells can be achieved by using CPPs. For this reason, CPPs have been widely utilized as a carrier molecule for the delivery of neuroactive compounds into the CNS, including putative neuroprotective peptides. Below we review experimental studies that have used neuroprotective peptides in HIE models, including putative neuroprotective peptides fused to a CPP. First, we summarize findings from our own and other laboratories highlighting the intrinsic neuroprotective properties of CARPs.

4.2. CARPs Are Intrinsically Neuroprotective

An early study by Ferrer-Montiel et al. [63], demonstrated that cationic arginine-rich hexapeptides (i.e. containing 2–6 arginine residues; net charge +3–+7; e.g., RRRRRR-NH_2) were neuroprotective in an in vitro hippocampal neuronal NMDA excitotoxic model. These findings were in line with subsequent studies in our and other laboratories, demonstrating that the CPP TAT (YGRKKRRQRRR; net charge +8) possesses intrinsic neuroprotective properties following in vitro glutamic acid excitotoxicity and oxygen glucose deprivation (OGD), as well as in vivo following excitotoxicity and cerebral ischemia in rats [13–16,64,65]. We subsequently demonstrated that in an in vitro cortical neuronal excitotoxic model, the CPPs poly-arginine-9 (RRRRRRRRR-NH_2; net charge +10) and penetratin (RQIKIWFQNRRMKWKK-NH_2; net charge +8) were even more potent than TAT [12]. The high potency of R9 led us to explore other poly-arginine peptides (e.g., R1, R3, R6–R15, R18, R22),

as well as several other CARPs, including protamine in the in vitro excitotoxic and OGD neuronal injury models [27–29]. These studies confirmed that CARPs are highly neuroprotective, with efficacy increasing with arginine content and peptide positive charge; peaking at R15 to R18 for poly-arginine peptides [27,29] [Note arginine and lysine (K) are the only positively charged amino acids, while histidine has a low positive charge].

Our laboratory has also demonstrated that CARPs and in particular the poly-arginine peptide R18 are neuroprotective in in vivo experimental brain ischemic and/or hypoxic injury models [18,20–22,24,26,27,29], and that CARPs can reduce neuronal cell surface glutamate receptor levels and excitotoxic calcium influx [19,22,23,25,27,28]. As highlighted previously [19], based on our findings, we have proposed that the neuroprotective properties of most, if not all, putative neuroprotective peptides fused to cationic CPPs (e.g., TAT, R9 and penetratin), as well as other CARPs, are determined by the arginine content and positive charge of the peptide, with potency also influenced by other amino acid residues (e.g., lysine, tryptophan and phenylalanine) [19,29]. Importantly, an arginine and cationic charge mediated neuroprotective mechanism of action of CARPs, including CPP-fused to putative neuroprotective peptides (e.g., TAT-NR2B9c and TAT-NR2Bct), is supported in studies by Marshall et al. [65] and more recently McQueen et al. [66]. Based on studies from our own and other laboratories, we believe that the mechanism of action of putative neuroprotective peptides fused to a CPP need to be critically re-evaluated. In light of the potentially confounding effects of CPPs and/or peptide arginine content and positive charge, we will review studies using neuroprotective peptides in HIE models. First, we provide a summary of the known and potential neuroprotective actions of CARPs.

4.3. Cationic Arginine-Rich Cell-Penetrating Peptide Neuroprotective Mechanisms of Actions

While the exact mechanisms of the neuroprotective effects are still being explored, we and others have demonstrated that CARPs have multiple, potentially simultaneous mechanisms of action. CARPs and putative neuroprotective peptides fused to cationic arginine-rich CPPs (i.e., TAT or R9; e.g., JNKI-1-TATD, TAT-NR2B9c/NA-1, TAT-CBD3/R9-CBD3-A6K and TAT-3.2-III-IV) can mitigate excitotoxic or potassium evoked neuronal intracellular calcium influx [19,27,67–69]. One mechanism whereby CARPs have the capacity to reduce intracellular calcium influx is the reduction of neuronal cell surface ion channels and receptors; thereby reducing excitotoxic calcium influx. To this end, CARPs have been demonstrated to reduce the cell surface expression or function of neuronal NMDA receptors [23,63,70–73], voltage gated calcium channels (CaV2.2 and CaV3.3) [68,70,74,75], a voltage gated sodium channel (NaV1.7) [76] and the sodium calcium exchanger 3 (NCX3) [70]. Given their effects on different receptors, and the positive charge of CARPs, they may also be antagonizing ion channel receptor function directly and/or by affecting calcium or sodium ion influx via an electrostatic mechanism.

In addition to neuronal cell surface receptor interactions, CARPs may also exert pleiotropic neuroprotective effects by targeting mitochondria and maintaining mitochondrial integrity by reducing calcium influx into the organelle [65,77–83]. CARPs have the capacity to inhibit proteolytic enzymes including the proteasome [84,85], as well as pro-protein convertases [86–88] that activate MMPs [89]. Inhibition of the proteasome is known to be beneficial following cerebral ischemia [90–92]; a mechanism that could be mediated by increased activity of hypoxia-inducible factor 1-α (HIF1α) and decreased activity of nuclear factor κ-light-chain-enhancer of B cells (NFκB). Similarly, MMP activation in the brain is known to be detrimental following cerebral ischemia and inhibiting MMP activation is neuroprotective (see review Cunningham et al. [93]).

Furthermore, there is also evidence that CARPs activate pro-survival signaling pathways [67,94], modulate immune responses [95–97] and act as anti-oxidant molecules in their own right due to their guanidine group in arginine residues [65,83,98–101].

Interestingly, the neuroprotective potency of CARPs appears to correlate with the same characteristic that improve the ability of cationic CPPs to target and transverse cellular membranes [19,29].

This suggests that CARP-mediated neuroprotection is associated with cellular membrane interactions (e.g., plasma and mitochondrial), anionic structures (phospholipids/cardiolipin, heparan sulfate proteoglycans, chondroitin sulfate proteoglycans, sialic acid resides, anionic regions of surface receptors) and/or increased levels of cellular uptake, which enable the peptides to interact with membrane (e.g., ion channel receptors) and intracellular targets (e.g., proteins, ROS and mitochondria).

4.4. Studies Using CARPs in Animal Models of HIE

All descriptive details of the studies discussed below are presented in chronological order of publication (Table 1).

4.4.1. TAT-NEMO Binding Domain (NBD)

NEMO binding domain (NBD) is an 11-amino acid peptide (NBD: $TALDWSWLQTE_{735–745;}$ net charge −2) derived from the Nuclear Factor-κβ (NF-κβ) Essential Modulator (NEMO)/IKK-γ-Binding Domain. The NBD peptide was designed to inhibit the activation of NFκB, a transcription factor involved in many stress responses. For example, NBD was originally developed to suppress inflammatory responses (e.g., IL-6, iNOS, MMP-9 and COX-2) and the regulation of apoptotic Bcl proteins (e.g., Bcl-2 and Bcl-x) following cytokine stimulation in several disorders including inflammatory bowel disease, arthritis, type I diabetes, multiple sclerosis and Parkinson's disease [102]. Activation of NF-κB requires upstream kinase complex formation (IκB-kinase; IKK) composed of the IKKα, IKKβ and NEMO proteins. For NF-κB activation, NEMO interacts with a carboxyl terminal sequence within both IKK-α and IKK-β, known as the NBD. The NBD peptide inhibits NF-κB activation by blocking NEMO/IKK complex formation [103].

The first study examining the neuroprotective efficacy of the NBD peptide in a model of HIE (P12 rat) administered the peptide [(14,820 nmol/kg: intraperitoneally (IP)] immediately, 6 and 12 h after hypoxia and did not demonstrate any neuroprotection; instead NBD appeared to increase brain injury [104]. To improve delivery to the brain, the NBD peptide was fused to TAT (TAT-NBD: YGRKKRRQRRR-TALDWSWLQTE; net charge +6) and assessed in a P7 rat model of HIE [105], where administration (6917 nmol/kg: IP) immediately and 3 h, or as a single injection at 0, 3 or 6 h, after hypoxia was neuroprotective up to 6 weeks post-HI. When TAT-NBD was administered immediately and 3 h after hypoxia it prevented up-regulation of p53 and activation of caspase-3 24 h post-HI. TAT-NBD treatment also prevented the activation of IKK in the brain 3 h post-HI. Despite TAT-NBD inhibiting IKK and NF-κB activation, it had no effect on HI-induced increases in cytokines (e.g., IL-1β, TNF-α, IL-4, IL-10 and IL-1-RA). The study also assessed a TAT-NBD control peptide, where two tryptophan residues were substituted for two alanine residues (YGRKKKRRQRRR-TALD**A**S**A**LQTE; net charge +6) and was shown not to be neuroprotective. Further assessment of TAT-NBD (6817 nmol/kg: IP) involving administration immediately and 3 h, immediately, 3, 6 and 12 h, immediately, 6 and 12 h, as well as 18 and 21 h after hypoxia [106], revealed long-term neuroprotection only in animals treated immediately and 3 h post-HI. Concomitantly, TAT-NBD treatment immediately and 3 h after hypoxia significantly reduced HI-mediated cytokine levels, whereas immediate, 3, 6 and 12-h treatment did not reduce cytokines. In a subsequent study, TAT-NBD treatment (6818 nmol/kg: IP) immediately and 3 h after hypoxia demonstrated significant improvements in behavioral outcomes up to 14 weeks post-HI [107].

Since intrauterine infections can be associated with HIE, TAT-NBD was assessed in a lipopolysaccharide (LPS)-sensitized (IP injection) HIE model in the P7 rat [108]. Animals were administered with TAT-NBD (477 nmol/kg) intranasally (IN) 10 min after hypoxia, using three HI injury conditions; HI only, 4-h LPS-pre-treatment + HI or 72-h LPS-pre-treatment + HI. Treatment with TAT-NBD significantly reduced brain injury only in the LPS-sensitized HI models, when assessed 7 days post-HI. While it was surprising that TAT-NBD did not reduce brain injury following HI only, its neuroprotective actions in LPS-sensitized HI models may be due to the ability of the cationic TAT-NBD peptide to electrostatically bind and neutralize anionic LPS molecules or by reducing the

effects of inflammatory cytokines. Neutralizing LPS would have the effect of suppressing the molecules capacity to evoke an immune response and inflammatory response. In support of this mechanism, previous studies using in vitro cell and in vivo tissue injury models have demonstrated that CARPs (e.g., HBD-2, HNP-1 and indolicidin) can bind to LPS and reduce its inflammatory effects [109]. Furthermore, it is possible that the IN delivery of TAT-NBD was enough to reduce the detrimental effects of LPS, but not ischemic injury associated with HI.

4.4.2. TAT-mGluR1

mGluR1 is a 14-amino acid peptide (mGluR1: VIKPLTKSYQGSGK$_{929–942}$; net charge +3), corresponding to an intracellular region of the metabotropic glutamate receptor-1α (mGluR1α) protein that is cleaved by calpain in neurons following excitotoxicity [110]. It is proposed that TAT-mGluR1 (YGRKKRRQRRR-VIKPLTKSYQGSGK, net charge +11) blocks the ability of calpain to cleave mGluR1α and thus maintain the receptors ability to stimulate the neuroprotective phosphoinositide 3-kinase/protein kinase B (PI3K-Akt) signaling pathway and protect neurons from the toxic effects of excitotoxic calcium influx [110]. In a neuronal model of kainic acid mediated excitotoxicity, TAT-mGluR1 prevented mGluR1α truncation and reduced neuronal cell death [110]. In a P7 rat model of HIE [111] TAT-mGluR1 (58,590 nmol/kg; IP) administered 1 h before hypoxia significantly reduced cerebral infarction at 24 h post-HI.

4.4.3. c-Jun N-Terminal Kinase (JNK) Inhibitors

JNKI-1 is a 20-amino acid peptide (also referred to as JBD: RPKRPTTLNLFPQVPRSQDT$_{157–176}$; net charge +3), derived from the signaling adaptor protein c-Jun N-terminal kinase protein-1 (JNKI-1) [112]. JNKs are a member of the mitogen-activated protein kinases (MAPK) family, encoded by the *Jnk1*, *Jnk2* and *Jnk3* genes, with high expression levels in neurons, especially after pathological injury (e.g., excitotoxicity, stroke, epilepsy and HI) [113]. The JNKI-1 peptide can inhibit JNK interaction with JNK-interacting protein-1 (JIP-1), blocking JNK phosphorylation and activation, thereby inhibiting downstream pro-death cellular signaling pathways [112]. JNK has emerged as a central mediator of excitotoxic damage in the developing [114,115] and developed CNS [116,117]. The JNKI-1 peptide derivatives bound to TAT, such as TAT-JNKI-1L (YGRKKRRQRRR-PP-RPKRPTTLNLFPQVPRSQDT-NH_2, net charge +12) and its retro inverso D-enantiomer JNKI-1-TATD (tdqsrpvqpflnlttprkpr-pp-rrrqrrkkrgy-NH_2; net charge +12, lower case indicates D-isoform amino acids) have demonstrated in vitro and/or in vivo neuroprotective properties. Studies using the JNKI-1 peptide alone (D-JNKI-1) or when fused to TAT (TAT-JNKI-1L and JNKI-1-TATD) have been assessed in neonatal HIE models.

The initial study examining the efficacy of D-JNKI-1 (tdqsrpvqpflnlttprkpr-NH_2; net charge +4) in a P7 rat model of HIE when administered (76 nmol/kg: IP) 30 min before and 3, 5, 8, 12 and 20 h after hypoxia did not reveal any reduction in cerebral infarction at 24 h [115], although there was evidence for reduced calpain, caspase-3 and autophagic activation.

A subsequent study demonstrated that the TAT-fused peptide JNKI-1-TATL administered (2446 nmol/kg; IP) immediately and 3 h or 3 h after hypoxia, significantly reduced cerebral infarction at 48 h, while administration 6 h after hypoxia was ineffective [118]. When administered immediately and 3 h after hypoxia, functional benefits were observed 14 weeks post-HI. Despite improvements in cerebral infarct and functional outcomes, JNKI-1-TATL failed to prevent caspase-8-mediated cleavage of Bid, which was unexpected, as activated JNK is known to induce caspase-8 cleavage of Bid and promote mitochondrial pro-apoptotic cell death pathways; this suggests JNKI-1-TATL-mediated neuroprotection was occurring via mechanism independent of JNK suppression.

In a second study, the $_D$-isoform peptide JNKI-1-TATD (2616 nmol/kg: IP) significantly reduced cerebral infarct volume when administered immediately, 3 or 6 h after hypoxia, but not when administered immediately and 3 h after hypoxia [119]. JNKI-1-TATD treatment also provided long-term functional improvements. It was also demonstrated that treatment with JNKI-1-TATD reduced

mitochondrial levels of phosphorylated JNK, preserved mitochondrial integrity, and up-regulated anti-apoptotic proteins 24 h post-HI. The study also assessed a mitochondrial JNK scaffold inhibiting peptide, Sab_{KIM1} (gfeslsvpspldlsgprvva-pp-rrrqrrkkrg; net charge +7) and a scrambled control (lpsvfgdvgapsrlpevsls-pp-rrrqrrkkrg; net charge +7); Sab (SH3 domain-binding protein 5) is a mitochondrial scaffold protein required for JNK kinase activity. Administration of Sab_{KIM1} (2700 and 5555 nmol/kg: IP) immediately after hypoxia was neuroprotective, whereas the scrambled peptide (2700 nmol/kg: IP) was ineffective.

In our laboratory, administration of JNKI-1-TATD (1000 nmol/kg; IP) immediately after hypoxia resulted in a positive trend in reduced total infarct volume (15% reduction) although it did not improve behavioral outcomes 48 h post-HI [22]. It was also demonstrated that in cultured cortical neurons JNKI-1-TATD dose-dependently reduced glutamic acid mediated excitotoxic intracellular calcium influx.

While it was surprising that the Sab_{KIM1} scrambled control peptide did not display any neuroprotection, it is possible that the amino acid sequence of the cargo peptide may have influenced neuroprotective potency. Importantly, we and others have confirmed that TAT-fused scrambled peptides such as TAT-p53DMs and TAT-NR2cts [29,66] still retain neuroprotective properties, again pointing to an active role of the TAT carrier and peptide arginine content mediated neuroprotective action.

4.4.4. TAT-BH4

BH4 is a 25-amino acid peptide derived from the Bcl-x(L) protein BH4 homology domain region ($RTGYDNREIVMKYIHYKLSQRGYEW_{6–30}$, net charge +2.1). The BH4 domain is required by Bcl-x(L) to block cytochrome-c release from mitochondria and prevent MPTP opening [120], as well as inhibiting endoplasmic reticulum (ER) calcium release into the cytosol by binding to a regulatory domain of the inositol triphosphate-3 (IP3) receptor [121]; highlighting potential mechanisms whereby the BH4 peptide could exert a neuroprotective action after HI.

The TAT-BH4 (YGRKKRRQRRR-RTGYDNREIVMKYIHYKLSQRGYEW, net charge +10.1) peptide was demonstrated to reduce cerebral tissue damage and caspase-3 activation when administered intracerebroventricularlly (ICV; 5 µL/20 ng) 30 min before hypoxia in a P7 rat model of HI [122]. Interestingly, exposure of cultured adult neural stem cells to TAT-BH4 promoted axonal remodeling, suggesting the peptide exerts other effects that may be beneficial in improving recovery following HI.

4.4.5. Osteopontin (OPN) and TAT-Fused OPN Peptide (TAT-OPN)

Osteopontin (OPN) is a secreted acidic glycoprotein containing an arginine-glycine-aspartate (RGD) motif and possesses multiple cellular functions including chemotactic and cytokine-like actions. The OPN protein is expressed in various tissues including bone, placenta, pancreas and the CNS [123]. Following cerebral ischemia, OPN deficient mice demonstrate increased neurodegeneration [124] and when administered ICV, the protein is neuroprotective in several adult rodent cerebral ischemia and hemorrhagic stroke models [125–128].

Mechanisms thought to be associated with OPN-mediated neuroprotection include binding to the cell surface αvβ3 integrin receptor to stimulate pro-survival signaling (i.e., PI3K/Akt pathway), anti-inflammatory effects [126,129–131], inhibition of inducible NOS [132,133] STAT1 ubiquitination/degradation and by reducing MMP-9 and NF-κβ activation. Despite OPN's demonstrated neuroprotective effects, in one study OPN deficient mice demonstrated no change in susceptibility to ischemic brain injury [126].

The first study to examine the neuroprotective efficacy of OPN in HIE used full length recombinant OPN protein (rOPN) in a P7 rat model of HI [134]. Animals treated with rOPN (0.03 or 0.1 µg per animal: ICV) 60 min after hypoxia, displayed a reduction in infarct volume at 48 h and significant improvements in behavioral outcomes at 7 weeks post-HI. In contrast, treatment with rOPN (0.05 µg/animal: ICV or 1.2 µg/animal: IN) or thrombin cleaved rOPN (1.2 µg/animal: IN) was not neuroprotective in

a P5 mouse model of HI [135]. To improve cerebral delivery of OPN, a shorter peptide containing the RGD motif (IVPTVDVPNGRGDSLAYGLR$_{134–153}$; net charge 0) was developed. However, the shorter peptide was not neuroprotective when administered ICV (0.2 µg/animal) or IN (30 µg/animal) before hypoxia in P5 mice [135]. In a subsequent study the OPN$_{134–153}$ peptide was fused to TAT (TAT-OPN; YGRKKRRQRRR-IVPTVDVPNGRGDSLAYGLR, net charge +8) and assessed in a P9 mouse model of HI [136] using several peptide treatment regimens consisting of multiple dosing using IN, IP or ICV administration (see Table 1 for details). No treatment regimen reduced infarct volume or improved functional assessments up to 35 days post-HI. Taken together, current evidence indicates that at the dosing schedules examined for the TAT-OPN peptide, it is not neuroprotective in HIE rodent models.

4.4.6. P5-TAT

P5 is a 24-amino acid peptide derived from the C-terminal region of the p35 protein (KEAFWDRCLSVINLMSSKMLQINA$_{254–277}$, net charge +0.9). Following cleavage of p35 by calpain, a cleavage fragment known as p25 can bind to cyclin-dependent kinase 5 (Cdk5) and alter its cellular location and stimulate its activity [137], which is known to be associated with neuronal cell death [138–140]. Administration (3,660, 7,320 and 9,761 nmol/kg: IP) of a modified P5 peptide (TFP5: KEAFWDRCLSVINLMSSKMLQINAYARAARRAARR; net charge +5.9) can improve outcomes in Parkinson's disease, Alzheimer's disease, and adult ischemic stroke models in rodents [140–142].

A dose-response assessment (0.23, 2.30, 5.76 and 11.5 nmol/kg; IP) of P5-TAT (KEAFWDRCLSVINLMSSKMLQINA-YGRKKRRQRRR, net charge +8.9) when administered 30 min before hypoxia in P7 rats demonstrated that all doses, except 0.23 nmol/kg, significantly reduced cerebral infarct volume at 48 h [143]. In addition, P5-TAT, when administered (11.5 nmol/kg; IP) 24 h after hypoxia, significantly improved behavioral outcomes up to 3 weeks post-HI. However, P5-TAT treatment following HI did not have any effect on the levels of Cdk5 activators, p35, p25 or p29, despite suppressing cleavage of caspase-3.

4.4.7. D-TAT-GESV

GESV is a 4-amino acid peptide (GESV, net charge −1) derived from the carboxyterminal PDZ motif (PDZ-G(D/E)XV; net charge −1) of nNOS. Proteins containing PDZ domains play a key role in anchoring receptor proteins in the membrane to intracellular cytoskeletal structures (e.g., actin and microtubules) and cytosolic proteins. Following NMDA receptor stimulation, nitric oxide synthase-1 adaptor protein (NOS1AP) via its PDZ binding domain, binds nNOS and recruits the protein to the cell membrane where it generates nitric oxide (NO). The D-TAT-GESV peptide (ygrkkrrqrrr-GESV, net charge +7) inhibits NOS1AP/nNOS binding, and is believed to confer neuroprotection by reducing NO production and activation of the p38 MAPK stress pathway [144]. In a P7 rat model of HIE, D-TAT-GESV (100 ng: ICV), administered before hypoxia reduced cerebral infarction at 7 days post-HI [145]. In comparison, the control peptide D-TAT-GASA (100 ng: ICV) was ineffective [145], which is not surprising since alanine residues can reduce CARP neuroprotective efficacy [19].

4.4.8. TAT-NR2B9c/NA-1

The development of NR2B9c as a neuroprotective agent has recently been discussed in detail [146]. Briefly, NR2B9c is a 9 amino acid peptide (KLSSIESDV$_{1479–1487}$) derived from the intracellular terminal carboxyl region of the NMDA receptor NR2B subunit protein, a site that binds the adaptor protein postsynaptic density-95 (PSD-95). PSD-95 couples nNOS to the NR2B subunit and following NMDA receptor activation stimulates NO generation. The NR2B9c peptide was developed on the basis that it blocks NR2B subunit and PSD-95 binding and thereby inhibiting NO production following NMDA receptor stimulation.

TAT-NR2B9c (YGRKKRRQRRR-KLSSIESDV; net charge +7) administered (19,850 nmol/kg; IP) either 110 min or 20 min before hypoxia in mice reduced brain injury at 24 h post-HI [147]. In addition, TAT-NR2B9c treatment significantly improved behavioral outcomes up to 7 days after HI. Interestingly, a 3000 nmol/kg dose (IP), administered 20 min before hypoxia was ineffective.

4.4.9. Poly-Arginine-18 (R18 and R18D)

R18 (RRRRRRRRRRRRRRRRRR; net charge +18) and its D-enantiomer (rrrrrrrrrrrrrrrrrr; net charge +18) is an 18-amino acid peptide and has been demonstrated to have potent neuroprotective properties in various in vitro and in vivo stroke related injury models [18,24,26,29]. Moreover, we have recently demonstrated for the first time that R18 and R18D (30, 100, 300 and 1000 nmol/kg; IP), administered immediately after hypoxia, reduced cerebral infarct volume and improved behavioral outcomes at 48 h post-HI [22]. In an additional study, administration of R18D 30 (10, 30, 300 and 1000 nmol/kg; IP) and 60 min (30 nmol/kg; IP) after hypoxia, reduced cerebral infarct volume and improved behavioral outcomes at 48 h post-HI [21].

4.5. Other Peptides Examined in Animal Models of HIE

Several other peptides, not fused to a CPP, have also been examined in animal models of HIE. All descriptive details of the studies discussed below are presented in chronological order of publication and in Table 1.

4.5.1. COG133

COG133 is a 20-amino acid peptide (TEELRVRLASHLRKLRKRLL$_{133–152}$, net charge +5.1) derived from the apolipoprotein E (apoE) protein. COG133 has been demonstrated to be neuroprotective in several acute brain injury models and demonstrated to possess anti-oxidant, anti-excitotoxic and anti-inflammatory properties [148–152]. Exactly how the COG133 peptide imparts its anti-oxidant, anti-excitotoxic and anti-inflammatory properties is not known, but the positive charge of the peptide has been considered as a critical factor [19,148]. When examined in a P7 rat model of HIE, COG133 administration (40, 200, 300, 400 and 2000 nmol/kg: ICV) immediately before hypoxia displayed a neuroprotective dose-response effect [151].

4.5.2. Connexin 43 (Cx43) Derived Peptides

Astrocytic gap junction hemichannels play an essential role in the regulation of electrolytes and metabolites between the cytosol and extracellular space. Under physiological conditions, hemichannels are usually in a closed state. Specifically, connexin 43 (Cx43) hemichannel opening occurs following hypoxia, ischemia and OGD [153–156], resulting in a disruption to cellular homeostasis and an exacerbation of excitotoxicity [157]. The non-specific blocking of gap junction hemichannels with octanol and carbenoxolone demonstrates neuroprotective effects in in vitro models of hippocampal hypoxic-hypoglycemic injury [158,159]. To overcome the non-specific blocking of gap junction hemichannels, small mimetic peptides that bind to the extracellular loop of Cx43 hemichannels, blocking hemichannel opening have been developed [160].

Several studies have assessed the administration of a Cx43 mimetic peptide (Peptide 5: VDKFLSRPTEKT, net charge +1) in fetal sheep models of HIE. Administration of Peptide 5 continuously for either 1 (50,000 nmol/kg/h; ICV) or 25 h (50,000 nmol/kg over 1 h and then over 24 h; ICV), beginning 90 min after hypoxia, improved electroencephalographic (EEG) recovery, reduced seizure activity and improved the return of sleep state cycling. In addition, the 25-h infusion of Peptide 5 improved oligodendrocyte survival at 7 days post-HI [161]. Another study demonstrated Peptide 5 administration immediately after hypoxia (50,000 nmol/kg over 1 h and then over 24 h; ICV) improved neuronal and oligodendrocyte cell survival, whereas peptide administration beginning during hypoxia (50,000 nmol/kg for 1 h and then for 24 h; ICV) was not neuroprotective [162]. In contrast, a continuous high dose infusion of Peptide 5 (50,000 nmol/kg/h over 25 h: ICV) immediately after hypoxia did not improve neurological outcome and contributed to cerebral edema in the fetal sheep 7 days post-HI [163]. In a pre-term (103 days gestation) fetal sheep model of HI, Peptide 5 administration (50,000 nmol/kg for 1 h and then for 24 h; ICV) commencing 90 min after hypoxia improved EEG recovery, reduced neuronal death and increased oligodendrocyte cell survival 7 days post-HI [164]. A study using

term fetal sheep assessed Peptide 5 and hypothermia (32 ± 1 °C; 72 h), as individual treatments and when combined. Peptide 5 administration 3 h after hypoxia (50,000 nmol/kg for 1 h and then for 24 h; ICV) and hypothermia treatments alone, improved EEG power, neuronal and oligodendrocyte cell survival at 7 days post-HI. However, combined Peptide 5 and hypothermia treatment did not result in any additional improvement in EEG power or histological outcomes [165]. This suggests that neuroprotective targets, other than hemichannels, may be more appropriate to improve the therapeutic effects of hypothermia for HIE.

Other Cx43 mimetic peptides (Gap 26: VCYDKSFPISHVR; net charge +1 and Gap 27: SRPTEKTIFII; net charge +1) have demonstrated neuroprotective efficacy in a P7 rat model of HIE [166]. Gap 26 (0.64, 3.22, 6.44, 16.1 and 32.2 nmol/kg; IP) and Gap 27 (16.1 nmol/kg; IP) administered 1 h before hypoxia, reduced infarct volume at 48 h post-HI; however, the two lower doses of Gap 26 were ineffective. In addition, multiple administrations of Gap 26 (32.2 nmol/kg: IP) every day for 7 days, beginning 24 h after hypoxia reduced brain injury and improved neurological function, up to 3 weeks post-HI.

Since Cx43 mimetic peptides Peptide 5, Gap26 and Gap 27 have only one arginine residue and low cationic charge, it would seem unlikely the peptides are operating via a CARP mechanism of action.

4.5.3. Apelin-36

Apelin is an endogenous ligand of the apelin receptor, a G protein-coupled receptor, which is widely expressed throughout the body, including neurons and oligodendrocytes [167]. The human *APELIN* gene encodes a 77 amino acid pre-protein, that is cleaved into at least three biologically active fragments, Apelin-$13_{(65–77)}$, Apelin-$17_{(61–77)}$ and Apelin-$36_{(42–77)}$. The active apelin fragments are widely expressed in the body including the CNS [168]. Apelin peptides have been demonstrated to reduce neuronal excitotoxicity and activate extracellular signal-regulated kinase 1/2 ERK-1/2 and PI3K/Akt cell survival pathways in cultured neurons [169–171]. Apelin-36 (LVQPRGSRNGPGPWQGGRRKFRRQRPRLSHKGPMPF$_{42–77}$; net charge +10.1) has been assessed in a P7 rat model of HIE [172] with administration (1000 ng: IP) 1 h before hypoxia reduced infarct volume at 48 h post-HI, and improving neurological function up to 14 days post-HI.

4.5.4. Innate Defense Regulator (IDR) Peptide IDR-1018

Innate defense regulator (IDR) peptides are endogenous cationic host defense peptides [173,174]. IDRs modulate inflammatory responses by increasing the recruitment of immune cells to sites of infection and inflammation; increasing wound-healing properties. It is believed that IDRs reduce cerebral injury following HI by reducing the impact of damaging inflammatory responses. IDR-1018 (VRLIVAVRIWRR-NH_2; net charge +5) is a synthetic host defense peptide examined in an LPS-sensitized model of HIE in P9 mice [175]. IDR-1018 administered (5208 nmol/kg: IP) 4 h before hypoxia reduced brain injury-related gene pathways that include p53 activation and calcium signaling. In addition, IDR-1018 administered (5208 nmol/kg: IP) 3 h after hypoxia, reduced infarct and inflammatory mediators (e.g., TNF-α, IL-1β, IL-4, IL-6, IL-10, IL-17, keratinocyte chemoattractant, INF-γ and granulocyte-macrophage colony stimulating factor) 8 days post-HI.

Table 1. Studies using CARPs and other peptides examined in animal models of HIE.

Peptide/Protein Name; Net Charge [a]	Proposed Target [b]	Peptide Sequence [c]	Injury Model [d]	Route & Time before/after HI Agent Administered [e]	Dose	NP [f]	Study
TAT-NBD; +6	NFκB	TAT-TALDWSWLQTE	P7 (W): CCAO/8% O2; 120 min	IP: 0 & 3 h, or 0, 3, 6, 9 or 12 h	6917 nmol/kg	Yes, up to 6 h	[105]
				IP: 0 & 3 h, or 0, 9 & 12 h, or 18 & 21 h	6817 nmol/kg	Yes, only for 0 & 3 h	[106]
				IP: 0 & 3 h	6818 nmol.kg	Yes	[107]
			P7 (W): CCAO/10% O2; 90 min + LPS 4 or 72 h before hypoxia	IN; 10 min	477 nmol/kg	Yes, only for LPS	[108]
TAT-mGluR1; +3	Calpain	TAT-VIKPLTKSYQGSGK	P7 (SD): CCAO/8% O2; 150 min	IP: −1 h	58,590 nmol/kg	Yes	[111]
D-JNKI-1; +4	JIP	tdqsrpvqpflnlttprkpr-NH_2	P7 (SD): CCAO/8% O2; 120 min	IP, −0.5, 3, 5, 8, 12 and 20 h	76 nmol/kg	No	[115]
JNKI-1-TATL; +12		TAT-PPRPKRPTTLNLFPQVPRSQDT-NH_2	P7 (W): CCAO/8% O2; 120 min	IP: 0 and 3 h, or 3 h or 6 h	2446 nmol/kg	Yes, except 6 h	[118]
JNKI-1-TATD; +12		tdqsrpvqpflnlttprkpr-pp-tat-NH_2	P7 (W): CCAO/8% O2; 120 min	IP: 0, 3 or 6 h, or 0 & 3 h	2616 nmol/kg	Yes except 0 & 3 h	[119]
Sab_{KIM1} +7		lpsvfgdvgapsrlpevsls-pp-tat		IP: 0 h	2777 or 5555 nmol/kg	Yes	
JNKI-1-TATD; +12		tdqsrpvqpflnlttprkpr-pp-tat-NH_2	P7 (SD): ECA/CCAO/8% O2; 150 min	IP: 0 min	1000 nmol/kg	No	[22]
TAT-BH4; +2.1	Apoptosis	TAT-RTGYDNREIVMKYIHYKLSQRGYEW	P7 (SD♂): CCAO/8% O2; 150 min	ICV: −0.5 h	5 µL/20 ng	Yes	[122]
T-OPN	$\alpha_v\beta_3$ integrin receptor	Thrombin cleaved OPN	P5 (C57B6/6J): CCAO/10% O2; 70 min	IN: −70 min	1.2 µg	No	[135]
$OPN_{134–153}$; 0		IVPTVDVPNGRGDSLAYR		IN or ICV: −70 min	IN: 30 µg/ICV: 0.2 µg		
$OPN_{154–198}$; −4.9		SKSRSFQVSDEQYPDATDEDLTSHMKSGES KESLDVIPVAQLLSM		ICV: −70 min	0.5 µg		
TAT-OPN; +8		TAT-IVPTVDVPNGRGDSLAYGLR	P9 (C57BL/6N): CCAO/10% O2; 50 min	IN: 0 h or 0 & 3 h, or 0, 3 h, 1, 2 & 3 d IP: 0 h, or 5, 7, 9, 11, 13, 15 d, or 0, 1, 3, 5, 7, 9, 11, 13, 15 d ICV: 1 h	350 or 2100 ng 2746 nmol/kg 100 ng	No	[136]
P5-TAT; +8.9	P35	KEAFWDRCLSVINLMSSKMLQINA-TAT	P7 (SD): CCAO/8% O2; 150 min	IP: −1 h IP: 24 h	0.23, 2.3, 5.76, or 11.5 nmol/kg 11.5 nmol/kg	Yes, except 0.23 nmol/kg	[143]
D-TAT-GESV; +7	NOS	ygrkkrrqrrr-GESV	P7 (SD♂); CCAO/8% O2; 120 min	ICV: −120 min	100 ng/animal	Yes	[145]
TAT-NR2B9c; +7	PSD-95	TAT-KLSSIESDV	P7 (CD1): CCAO/7.5%; 60 min	IP: −110 or −20 min	3000 nmol/kg	Yes	[147]
R18; +18	Multiple	RRRRRRRRRRRRRRRRR	P7 (SD): ECA/CCAO/8% O2; 150 min	IP: 0 h	30, 100, 300 or 1000 nmol/kg	Yes	[22]
R18D; +18		rrrrrrrrrrrrrrrr					
R18D; +18		rrrrrrrrrrrrrrrr		IP: +0.5 h IP: +1 h IP: +1.5 h	10, 30, 100, 300 or 1000 nmol/kg 30 or 300 nmol/kg 30 or 300 nmol/kg	Yes, except 100 nmol/kg Yes, except 300 nmol/kg No	[21]
COG133; 5.1	LDLR	Ac-TEELRVRLASHLRKLRKRLL-NH_2	P7 (W): CCAO/8% O2; 150 min	ICV: −0 h	40, 200, 300, 400, or 2000 nmol/kg	Yes, except 300 nmol/kg	[151]

Table 1. *Cont.*

Peptide/Protein Name; Net Charge [a]	Proposed Target [b]	Peptide Sequence [c]	Injury Model [d]	Route & Time before/after HI Agent Administered [e]	Dose	NP [f]	Study
Peptide 5; +1	Cx43 astrocytic hemichannel	VDKFLSRPTEKT	GD128 (Romney/Suffolk sheep): bilateral tCCAO; 30 min	ICV: 1.5 h	50,000 nmol/kg/h for 1 h ± 50,000 nmol/kg/24 h for 24 h	Yes	[161]
				ICV: −1 h or 0 h	50,000 nmol/kg/h: 1 h + 50,000 nmol/kg/24 h for 24 h	Yes, except −1 h	[162]
				ICV: 0 h	50,000 nmol/kg/h: 1 h + 50,000 nmol/kg/24 h for 24 h 50,000 nmol/kg/h for 25 h	Yes, except high continuous dose	[163]
				ICV: 3 h ± Hypothermia: 32 °C for 72 h; 3 h after tCCAO	50,000 nmol/kg/h for 1 h + 50,000 nmol/kg/24 h for 24 h	Yes, no additive effect	[165]
			GD103 (Romney/Suffolk sheep): bilateral tCCAO for 25 min	ICV: 1.5 h	50,000 nmol/kg/h for 1 h + 50,000 nmol/kg/24 h for 24 h	Yes	[164]
Gap 26; +1		VCYDKSFPISHVR	P7 (SD): CCAO/8% O2; 150 min	IP: −1 h IP: daily for 1 to 7 d	0.64, 3.22, 6.44, 16.1, or 32.2 nmol/kg 32.2 nmol/kg	Yes, except 0.64 and 3.22 nmol/kg	[166]
Gap 27; +1		SRPTEKTIFII		IP: −1 h	16.1 nmol/kg	Yes	
Apelin-36; +10.1	Apelin receptor	LVQPRGSRNGPGPWQGGRRKFRRQRPRLSHKGPMPF	P7 (SD): CCAO8% O2; 150 min	IP: −1 h	240 nmol/kg	Yes	[172]
IDR-1018; +5	Immune modulation	VRLIVAVRIWRR-NH_2	P9 (C57BL/6J): CCAO/10% O2; 20 min + LPS 14 h before hypoxia	IP: −4 h or 3 h	5208 nmol/kg	Yes	[175]

Bold data indicates peptides used in studies. [a] Net charge at pH 7, MUT: mutant peptide, SCR: scrambled peptide. [b] NFκB: nuclear factor kappa-light-chain-enhancer of activated B cells, JIP: c-Jun N-terminal kinase-interacting protein, NOS: nitric oxide synthase, PSD-95: postsynaptic density-95, LDLR: low-density lipoprotein receptor. [c] Peptides synthesized using D-amino acids are represented in lowercase, TAT = GRKKRRQRRR. [d] W: Wistar, SD: Sprague-Dawley, C57B/6: C57 black 6, CD1: cluster of differentiation 1, CCAO: common carotid artery occlusion, ECA: external carotid artery occlusion, tCCAO: transient common carotid artery occlusion, ♂= male, GD = gestational day. [e] IP: intraperitoneal, IN: intranasal, ICV: intracerebroventricular, h: hours, min: minutes; negative (−) = treatment before hypoxia. [f] Neuroprotection and or positive effects.

5. Do All CARPs Including TAT-Fused Peptides Share a Common Neuroprotective Mechanism of Action?

Based on previous studies in our and other laboratories, examining the neuroprotective properties of various CARPs, we view it highly likely that the neuroprotection demonstrated by the CARPs described above (i.e., TAT-NBD, TAT-mGluR1, JNKI-1-TATL, JNKI-1-TATD, Sab_{KIM1}, TAT-BH4, P5-TAT, D-TAT-GESV, TAT-NR2B9c, R18, R18D, COG133, Apelin-36 and IDR-1018) is largely mediated by peptide arginine content and positive charge [19,27,29,65,66]. There are several lines of evidence that support this hypothesis, which we provide below. In addition, we previously provided an explanation why we believe a CARP-mediated neuroprotective mechanism of action is operating for the TAT-NR2B9c and JNKI-1-TATD peptides, rather than the mechanism of action in which they were originally developed [27].

It has been demonstrated that CARPs inhibit neuronal excitotoxic calcium [19,22,23,25,27,28] and potassium [64,75] influx and in doing so inhibit many of the pathophysiological processes downstream from the ischemic excitotoxic cascade (e.g., calpain activation, mitochondrial dysfunction and ROS production, calcium induced cell signaling and lipase and DNase activation). Therefore, given that the vast majority of the proposed mechanisms of action of developed TAT-fused and other neuroprotective CARPs are molecular targets downstream from excitotoxicity (e.g., NF-κB, JNK and Cdk5), it is not surprising that they are effective and appear to be inhibiting their intended targets.

Interestingly, in addition to the inhibition of excitotoxic cationic ion influx, CARPs also have the capacity to modulate other cellular processes that are neuroprotective following HI such as proteolytic enzyme activation (e.g., proteasome and MMPs), ERK-1/2 and Akt phosphorylation and the modulation of immune responses. For example, in the case of TAT-NBD, which was developed to block NF-κB activation, the ability of CARPs to inhibit the proteasome [84,85,176,177] would have the effect of preventing NF-κB activation by preventing proteasomal degradation of the NF-κB inhibitor protein i-κB.

In the case of Apelin-36, other CARPs, such as protamine and R9 (ALX40-4C) can also bind to the apelin receptor [178,179]. Therefore, it is possible that CARPs, in addition to Apelin-36, may also be able to stimulate pro-cell survival ERK-1/2 and Akt pathways [180]. Although it should be mentioned that not surprisingly, Apelin-36 can also reduce excitotoxic calcium influx [169–171]. In the case of CARP-mediated immune modulation, mR18L (Ac-GFRRFLGSWARIYRAFVG-NH_2; net charge +4) is known to reduce LPS-induced systemic infection [181], dRK6 (RRKRRR; net charge +6) inhibits TNFα and IL-6 production by monocytes [182] and hBD3-3 (GKCSTRGRKCCRRKK; net charge +8) downregulates NF-κB induced inflammation [183]. Thus, CARPs have the potential to suppress many of the toxic inflammatory responses associated with HIE.

Future studies examining the efficacy of putative neuroprotective peptides fused to TAT would benefit with respect to confirming neuroprotective mechanisms of action by fusing the peptide to a non-cationic CPP (e.g., MTS; AAVALLPAVLLALLP) and/or replacing any negatively charged aspartate (D) and glutamate (E) residues within the peptide sequence with arginine residues; we predict these two manipulations will decrease and increase neuroprotective efficacy, respectively. It is also advisable to confirm if the TAT-fused peptide has the capacity to reduce excitotoxic calcium influx.

6. Conclusions

There is now a large body of data from various sources demonstrating that CARPs comprise a class of peptide with significant neuroprotective potential for development as an adjuvant to hypothermia, or when hypothermia cannot be applied, for the treatment of HIE. While further studies are required to elucidate neuroprotective mechanisms, available evidence indicates that CARP neuroprotection is determined by the peptide's arginine content and cationic charge and more specifically by the guanidine head group in the arginine residues. Interestingly, CARP neuroprotective potency appears to correlate with the same characteristics that improves the ability of the cationic CPPs to target and traverse cellular membranes [19,29]. Taken together it is clear that CARPs possess many properties

enabling them to target both intracellular and extracellular damaging and protective pathways that are likely to be beneficial following HIE, not to mention their ability to cross the BBB and enter cells. In conclusion, CARPs, including poly-arginine peptides, offer an exciting therapeutic approach for HIE with the potential to reduce the severity of brain injury via potentially several neuroprotective mechanisms of action.

7. Future Directions

There are several further considerations to be addressed before translation of CARPs as a therapeutic for HIE in the clinic. It will be important to firstly identify a CARP that has high efficacy and the greatest potential to be effective in HIE, in both pre-term and term infants. In addition, preclinical studies will need to examine CARP treatment in combination with hypothermia to ensure safety, and to identify any synergistic effects in terms of improving patient outcomes. It is also important that beneficial results obtained in rodent models of HI, especially with combining CARPs and hypothermia, are confirmed in a large animal model (e.g., piglet or lamb), allowing for assessment in a gyrencephalic brain with greater comparability to the human and that the efficacy of IV administration should be established prior to clinical trials.

Author Contributions: Conceptualization, A.B.E. & B.P.M.; Methodology, A.B.E. & B.P.M.; Writing—Original Draft Preparation, A.B.E. & B.P.M.; Writing—Review and Editing, A.B.E., R.S.A., N.W.K. & B.P.M. Visualization, A.B.E., R.S.A., N.W.K. & B.P.M.; Supervision, R.S.A, N.W.K. & B.P.M.

Funding: This research received no external funding.

Acknowledgments: The authors acknowledge the feedback on the manuscript provided by Frank Mastaglia.

Conflicts of Interest: B.P.M. and N.W.K. are named inventors of several patent applications regarding the use of arginine-rich peptides as neuroprotective agents. The other authors declare no conflict of interest.

References

1. Chalak, L.F.; Rollins, N.; Morriss, M.C.; Brion, L.P.; Heyne, R.; Sánchez, P.J. Perinatal acidosis and hypoxic-ischemic encephalopathy in preterm infants of 33 to 35 weeks' gestation. *J. Pediatr.* **2012**, *160*, 388–394. [CrossRef] [PubMed]
2. Wall, S.N.; Lee, A.C.; Carlo, W.; Goldenberg, R.; Niermeyer, S.; Darmstadt, G.L.; Keenan, W.; Bhutta, Z.A.; Perlman, J.; Lawn, J.E. Reducing intrapartum-related neonatal deaths in low- and middle-income countries-what works? *Semin. Perinatol.* **2010**, *34*, 395–407. [CrossRef] [PubMed]
3. Chowdhury, H.R.; Thompson, S.; Ali, M.; Alam, N.; Yunus, M.; Streatfield, P.K. Causes of neonatal deaths in a rural subdistrict of Bangladesh: Implications for intervention. *J. Health Popul. Nutr.* **2010**, *28*, 375–382. [CrossRef] [PubMed]
4. Simiyu, I.N.; Mchaile, D.N.; Katsongeri, K.; Philemon, R.N.; Msuya, S.E. Prevalence, severity and early outcomes of hypoxic ischemic encephalopathy among newborns at a tertiary hospital, in northern Tanzania. *BMC Pediatr.* **2017**, *17*, 131. [CrossRef] [PubMed]
5. Lawn, J.; Shibuya, K.; Stein, C. No cry at birth: Global estimates of intrapartum stillbirths and intrapartum-related neonatal deaths. *Bull. World Health Organ.* **2005**, *83*, 409–417. [PubMed]
6. Lee, A.C.; Kozuki, N.; Blencowe, H.; Vos, T.; Bahalim, A.; Darmstadt, G.L.; Niermeyer, S.; Ellis, M.; Robertson, N.J.; Cousens, S.; et al. Intrapartum-related neonatal encephalopathy incidence and impairment at regional and global levels for 2010 with trends from 1990. *Pediatr. Res.* **2013**, *74* (Suppl. 1), 50–72. [CrossRef] [PubMed]
7. Perlman, J.M. Intrapartum hypoxic-ischemic cerebral injury and subsequent cerebral palsy: Medicolegal issues. *Pediatrics* **1997**, *99*, 851–859. [CrossRef] [PubMed]
8. Kolevzon, A.; Gross, R.; Reichenberg, A. Prenatal and Perinatal Risk Factors for Autism. *Arch. Pediatr. Adolesc. Med.* **2007**, *161*, 326–333. [CrossRef] [PubMed]
9. O'Shea, T.M. Diagnosis, treatment, and prevention of cerebral palsy. *Clin. Obstet. Gynecol.* **2008**, *51*, 816–828. [CrossRef] [PubMed]

10. Pisani, F.; Orsini, M.; Braibanti, S.; Copioli, C.; Sisti, L.; Turco, E.C. Development of epilepsy in newborns with moderate hypoxic-ischemic encephalopathy and neonatal seizures. *Brain Dev.* **2009**, *31*, 64–68. [CrossRef] [PubMed]
11. De Haan, M.; Wyatt, J.S.; Roth, S.; Vargha-Khadem, F.; Gadian, D.; Mishkin, M. Brain and cognitive-behavioural development after asphyxia at term birth. *Dev. Sci.* **2006**, *9*, 350–358. [CrossRef] [PubMed]
12. Meloni, B.; Craig, A.; Milech, N.; Hopkins, R.; Watt, P.; Knuckey, N. The neuroprotective efficacy of cell-penetrating peptides TAT, penetratin, Arg-9, and Pep-1 in glutamic acid, kainic acid, and in vitro ischemia injury models using primary cortical neuronal cultures. *Cell. Mol. Neurobiol.* **2014**, *34*, 173–181. [CrossRef] [PubMed]
13. Vaslin, A.; Rummel, C.; Clarke, P.G.H. Unconjugated TAT carrier peptide protects against excitotoxicity. *Neurotox. Res.* **2009**, *15*, 123–126. [CrossRef] [PubMed]
14. Craig, A.J.; Meloni, B.P.; Watt, P.; Knuckey, N.W. Attenuation of Neuronal Death by Peptide Inhibitors of AP-1 Activation in Acute and Delayed In Vitro Ischaemia (Oxygen/Glucose Deprivation) Models. *Int. J. Pept. Res. Ther.* **2010**, *17*, 1–6. [CrossRef]
15. Meade, A.J.; Meloni, B.P.; Mastaglia, F.L.; Watt, P.M.; Knuckey, N.W. AP-1 inhibitory peptides attenuate in vitro cortical neuronal cell death induced by kainic acid. *Brain Res.* **2010**, *1360*, 8–16. [CrossRef] [PubMed]
16. Meade, A.J.; Meloni, B.P.; Cross, J.; Bakker, A.J.; Fear, M.W.; Mastaglia, F.L.; Watt, P.M.; Knuckey, N.W. AP-1 inhibitory peptides are neuroprotective following acute glutamate excitotoxicity in primary cortical neuronal cultures. *J. Neurochem.* **2010**, *112*, 258–270. [CrossRef] [PubMed]
17. Xu, W.; Zhou, M.; Baudry, M. Neuroprotection by cell permeable TAT-mGluR1 peptide in ischemia: Synergy between carrier and cargo sequences. *Neuroscientist* **2008**, *14*, 409–414. [CrossRef] [PubMed]
18. Milani, D.; Knuckey, N.; Anderton, R.; Cross, J.; Meloni, B. The R18 Polyarginine Peptide Is More Effective Than the TAT-NR2B9c (NA-1) Peptide When Administered 60 min after Permanent Middle Cerebral Artery Occlusion in the Rat. *Stroke Res. Treat.* **2016**, *2016*, 2372710. [PubMed]
19. Meloni, B.P.; Milani, D.; Edwards, A.B.; Amderton, R.S.; O'Hare Doig, R.L.; Fitzgerald, M.; Palmer, T.N.; Kunckey, N.W. Neuroprotective peptides fused to arginine-rich cell penetrating peptides: Neuroprotective mechanism likely mediated by peptide endocytic properties. *Pharmacol. Ther.* **2015**, *153*, 36–54. [CrossRef] [PubMed]
20. Milani, D.; Bakeberg, M.C.; Cross, J.L.; Clark, V.W.; Anderton, R.S.; Blacker, D.J.; Knuckey, N.W.; Meloni, B.P. Comparison of neuroprotective efficacy of poly-arginine R18 and R18D (D-enantiomer) peptides following permanent middle cerebral artery occlusion in the Wistar rat and in vitro toxicity studies. *PLoS ONE* **2018**, *13*, e0193884. [CrossRef] [PubMed]
21. Edwards, A.B.; Anderton, R.S.; Knuckey, N.W.; Meloni, B.P. Assessment of therapeutic window for poly-arginine-18D (R18D) in a P7 rat model of perinatal hypoxic-ischaemic encephalopathy. *In Press. J. Neurosci. Res.* **2018**.
22. Edwards, A.B.; Cross, J.L.; Anderton, R.S.; Knuckey, N.W.; Meloni, B.P. Poly-arginine R18 and R18D (D-enantiomer) peptides reduce infarct volume and improves behavioural outcomes following perinatal hypoxic-ischaemic encephalopathy in the P7 rat. *Mol. Brain* **2018**, *11*, 8. [CrossRef] [PubMed]
23. MacDougall, G.; Anderton, R.S.; Edwards, A.B.; Knuckey, N.W.; Meloni, B.P. The Neuroprotective Peptide Poly-Arginine-12 (R12) Reduces Cell Surface Levels of NMDA NR2B Receptor Subunit in Cortical Neurons; Investigation into the Involvement of Endocytic Mechanisms. *J. Mol. Neurosci.* **2016**, *61*, 235–246. [CrossRef] [PubMed]
24. Milani, D.; Clark, V.; Cross, J.; Anderton, R.; Knuckey, N.; Meloni, B. Poly-arginine peptides reduce infarct volume in a permanent middle cerebral artery rat stroke model. *BMC Neurosci.* **2016**, *17*, 19. [CrossRef] [PubMed]
25. Chiu, L.S.; Anderton, R.S.; Cross, J.L.; Clark, V.W.; Edwards, A.B.; Knuckey, N.W.; Meloni, B.P. Assessment of R18, COG1410, and APP96-110 in excitotoxicity and traumatic brain injury. *Transl. Neurosci.* **2017**, *8*, 147–157. [CrossRef] [PubMed]
26. Milani, D.; Cross, J.; Anderton, R.; Blacker, D.; Knuckey, N.; Meloni, B. Neuroprotective efficacy of poly-arginine R18 and NA-1 (TAT-NR2B9c) peptides following transient middle cerebral artery occlusion in the rat. *Neurosci. Res.* **2017**, *114*, 9–15. [CrossRef] [PubMed]

27. Meloni, B.P.; Brookes, L.M.; Clark, V.W.; Cross, J.L.; Edwards, A.B.; Anderton, R.S.; Hopkins, R.M.; Hoffmann, K.; Knuckey, N.W. Poly-arginine and arginine-rich peptides are neuroprotective in stroke models. *J. Cereb. Blood Flow Metab.* **2015**, *35*, 993–1004. [CrossRef] [PubMed]
28. Edwards, A.B.; Anderton, R.S.; Knuckey, N.W.; Meloni, B.P. Characterisation of neuroprotective efficacy of modified poly-arginine-9 (R9) peptides using a neuronal glutamic acid excitotoxicity model. *Mol. Cell. Biochem.* **2016**, *426*, 75–85. [CrossRef] [PubMed]
29. Meloni, B.P.; Milani, D.; Cross, J.L.; Clark, V.W.; Edwards, A.B.; Anderton, R.S.; Blacker, D.J.; Knuckey, N.W. Assessment of the Neuroprotective Effects of Arginine-Rich Protamine Peptides, Poly-Arginine Peptides (R12-Cyclic, R22) and Arginine–Tryptophan-Containing Peptides Following In Vitro Excitotoxicity and/or Permanent Middle Cerebral Artery Occlusion in Rats. *Neuromol. Med.* **2017**, *19*, 271–285. [CrossRef] [PubMed]
30. Novak, C.M.; Ozen, M.; Burd, I. Perinatal Brain Injury: Mechanisms, Prevention, and Outcomes. *Clin. Perinatol.* **2018**, *45*, 357–375. [CrossRef] [PubMed]
31. Giussani, D.A. The fetal brain sparing response to hypoxia: Physiological mechanisms. *J. Physiol.* **2016**, *594*, 1215–1230. [CrossRef] [PubMed]
32. Olney, J.W.; Price, M.T.; Samson, L.; Labruyere, J. The role of specific ions in glutamate neurotoxicity. *Neurosci. Lett.* **1986**, *65*, 65–71. [CrossRef]
33. Choi, D.W. Excitotoxic cell death. *J. Neurobiol.* **1992**, *23*, 1261–1276. [CrossRef] [PubMed]
34. Arai, A.; Vanderklish, P.; Kessler, M.; Lee, K.; Lynch, G. A brief period of hypoxia causes proteolysis of cytoskeletal proteins in hippocampal slices. *Brain Res.* **1991**, *555*, 276–280. [CrossRef]
35. Zhang, J.; Dawson, V.; Dawson, T.; Snyder, S. Nitric oxide activation of poly(ADP-ribose) synthetase in neurotoxicity. *Science* **1994**, *263*, 687–689. [CrossRef] [PubMed]
36. Stout, A.K.; Raphael, H.M.; Kanterewicz, B.I.; Klann, E.; Reynolds, I.J. Glutamate-induced neuron death requires mitochondrial calcium uptake. *Nat. Neurosci.* **1998**, *1*, 366–373. [CrossRef] [PubMed]
37. Castilho, R.F.; Ward, M.W.; Nicholls, D.G. Oxidative stress, mitochondrial function, and acute glutamate excitotoxicity in cultured cerebellar granule cells. *J. Neurochem.* **1999**, *72*, 1394–1401. [CrossRef] [PubMed]
38. O'Hare, M.J.; Kushwaha, N.; Zhang, Y.; Aleyasin, H.; Callaghan, S.M.; Slack, R.S.; Albert, P.R.; Vincent, I.; Park, D.S. Differential roles of nuclear and cytoplasmic cyclin-dependent kinase 5 in apoptotic and excitotoxic neuronal death. *J. Neurosci.* **2005**, *25*, 8954–8966. [CrossRef] [PubMed]
39. Ikonomidou, C.; Kaindl, A.M. Neuronal Death and Oxidative Stress in the Developing Brain. *Antioxid. Redox Signal.* **2011**, *14*, 1535–1550. [CrossRef] [PubMed]
40. Favié, L.M.A.; Cox, A.R.; van den Hoogen, A.; Nijboer, C.H.A.; Peeters-Scholte, C.M.P.C.D.; van Bel, F.; Egberts, T.C.G.; Rademaker, C.M.A.; Groenendaal, F. Nitric Oxide Synthase Inhibition as a Neuroprotective Strategy Following Hypoxic–Ischemic Encephalopathy: Evidence From Animal Studies. *Front. Neurol.* **2018**, *9*, 258. [CrossRef] [PubMed]
41. Rousset, C.I.; Baburamani, A.A.; Thornton, C.; Hagberg, H. Mitochondria and perinatal brain injury. *J. Matern. Fetal Neonatal Med.* **2012**, *25* (Suppl. 1), 35–38. [CrossRef] [PubMed]
42. Thornton, C.; Hagberg, H. Role of mitochondria in apoptotic and necroptotic cell death in the developing brain. *Clin. Chim. Acta.* **2015**, *451 Pt A*, 35–38. [CrossRef]
43. Lu, Y.; Tucker, D.; Dong, Y.; Zhao, N.; Zhuo, X.; Zhang, Q. Role of Mitochondria in Neonatal Hypoxic-Ischemic Brain Injury. *J. Neurosci. Rehabil.* **2015**, *2*, 1–14. [PubMed]
44. Wang, X.; Carlsson, Y.; Basso, E.; Zhu, C.; Rousset, C.I.; Rasola, A.; Johansson, B.R.; Blomgren, K.; Mallard, C.; Bernardi, P.; et al. Developmental Shift of Cyclophilin D Contribution to Hypoxic-Ischemic Brain Injury. *J. Neurosci.* **2009**, *29*, 2588–2596. [CrossRef] [PubMed]
45. Bernardi, P.; Krauskopf, A.; Basso, E.; Petronilli, V.; Blachly-Dyson, E.; Di Lisa, F.; Forte, M.A. The mitochondrial permeability transition from in vitro artifact to disease target. *FEBS J.* **2006**, *273*, 2077–2099. [CrossRef] [PubMed]
46. Thornton, C.; Rousset, C.I.; Kichev, A.; Miyakuni, Y.; Vontell, R.; Baburamani, A.A.; Fleiss, B.; Gressens, P.; Hagberg, H. Molecular Mechanisms of Neonatal Brain Injury. *Neurol. Res. Int.* **2012**, *2012*, 1–16. [CrossRef] [PubMed]
47. Blomgren, K.; Hagberg, H. Free radicals, mitochondria, and hypoxia–ischemia in the developing brain. *Free Radic. Biol. Med.* **2006**, *40*, 388–397. [CrossRef] [PubMed]

48. Zhu, C.; Wang, X.; Deinum, J.; Huang, Z.; Gao, J.; Modjtahedi, N.; Neagu, M.R.; Nilsson, M.; Eriksson, P.S.; Hagberg, H.; et al. Cyclophilin A participates in the nuclear translocation of apoptosis-inducing factor in neurons after cerebral hypoxia-ischemia. *J. Exp. Med.* **2007**, *204*, 1741–1748. [CrossRef] [PubMed]
49. Hagberg, H.; Mallard, C.; Ferriero, D.M.; Vannucci, S.J.; Levison, S.W.; Vexler, Z.S.; Gressens, P. The role of inflammation in perinatal brain injury. *Nat. Rev. Neurol.* **2015**, *11*, 192–208. [CrossRef] [PubMed]
50. Liu, F.; McCullough, L.D. Inflammatory responses in hypoxic ischemic encephalopathy. *Acta Pharmacol. Sin.* **2013**, *34*, 1121–1130. [CrossRef] [PubMed]
51. Algra, S.O.; Groeneveld, K.M.; Schadenberg, A.W.; Haas, F.; Evens, F.C.; Meerding, J.; Koenderman, L.; Jansen, N.J.; Prakken, B.J. Cerebral ischemia initiates an immediate innate immune response in neonates during cardiac surgery. *J. Neuroinflamm.* **2013**, *10*, 796. [CrossRef] [PubMed]
52. Kaur, C.; Sivakumar, V.; Yip, G.W.; Ling, E.A. Expression of syndecan-2 in the amoeboid microglial cells and its involvement in inflammation in the hypoxic developing brain. *Glia* **2009**, *57*, 336–349. [CrossRef] [PubMed]
53. Ma, H.; Sinha, B.; Pandya, R.S.; Lin, N.; Popp, A.J.; Li, J.; Tao, J.; Wang, X. Therapeutic hypothermia as a neuroprotective strategy in neonatal hypoxic-ischemic brain injury and traumatic brain injury. *Curr. Mol. Med.* **2012**, *12*, 1282–1296. [CrossRef] [PubMed]
54. Gluckman, P.D.; Wyatt, J.S.; Azzopardi, D.; Ballard, R.; Edwards, A.D.; Ferriero, D.M.; Polin, R.A.; Robertson, C.M.; Thoresen, M.; Whitelaw, A.; et al. Selective head cooling with mild systemic hypothermia after neonatal encephalopathy: Multicentre randomised trial. *Lancet* **2005**, *365*, 663–670. [CrossRef]
55. Shankaran, S.; Laptook, A.R.; Ehrenkranz, R.A.; Tyson, J.E.; McDonald, S.A.; Donovan, E.F.; Fanaroff, A.A.; Poole, W.K.; Wright, L.L.; Higgins, R.D.; et al. Whole-body hypothermia for neonates with hypoxic-ischemic encephalopathy. *N. Engl. J. Med.* **2005**, *353*, 1574–1584. [CrossRef] [PubMed]
56. Azzopardi, D.V.; Strohm, B.; Edwards, A.D.; Dyet, L.; Halliday, H.L.; Juszczak, E.; Kapellou, O.; Levene, M.; Marlow, N.; Porter, E.; et al. Moderate Hypothermia to Treat Perinatal Asphyxial Encephalopathy. *N. Engl. J. Med.* **2009**, *361*, 1349–1358. [CrossRef] [PubMed]
57. Jacobs, S.E.; Morley, C.J.; Inder, T.E.; Stewart, M.J.; Smith, K.R.; McNamara, P.J.; Wright, I.M.; Kirpalani, H.M.; Darlow, B.A.; Doyle, L.W.; et al. Whole-Body Hypothermia for Term and Near-Term Newborns With Hypoxic-Ischemic Encephalopathy. *Arch. Pediatr. Adolesc. Med.* **2011**, *165*, 692–700. [CrossRef] [PubMed]
58. Jacobs, S.E.; Berg, M.; Hunt, R.; Tarnow-Mordi, W.O.; Inder, T.E.; Davis, P.G. Cooling for newborns with hypoxic ischaemic encephalopathy. *Cochrane Database Syst. Rev.* **2013**. [CrossRef] [PubMed]
59. Hall, N.J.; Eaton, S.; Peters, M.J.; Hiorns, M.P.; Alexander, N.; Azzopardi, D.V.; Pierro, A. Mild controlled hypothermia in preterm neonates with advanced necrotizing enterocolitis. *Pediatrics* **2010**, *125*, e300–e308. [CrossRef] [PubMed]
60. Rao, R.; Trivedi, S.; Vesoulis, Z.; Liao, S.M.; Smyser, C.D.; Mathur, A.M. Safety and Short-Term Outcomes of Therapeutic Hypothermia in Preterm Neonates 34–35 Weeks Gestational Age with Hypoxic-Ischemic Encephalopathy. *J. Pediatr.* **2016**. [CrossRef] [PubMed]
61. Committee on Fetus and Newborn; Papile, L.A.; Baley, J.E.; Benitz, W.; Cummings, J.; Carlo, W.A.; Eichenwald, E.; Kumar, P.; Polin, R.A.; Tan, R.C. Hypothermia and neonatal encephalopathy. *Pediatrics* **2014**, *133*, 1146–1150. [PubMed]
62. Fosgerau, K.; Hoffmann, T. Peptide therapeutics: Current status and future directions. *Drug Discov. Today* **2015**, *20*, 122–128. [CrossRef] [PubMed]
63. Ferrer-Montiel, A.V.; Merino, J.M.; Blondelle, S.E.; Perez-Paya, E.; Houghten, R.A.; Montal, M. Selected peptides targeted to the NMDA receptor channel protect neurons from excitotoxic death. *Nat. Biotechnol.* **1998**, *16*, 286–291. [CrossRef] [PubMed]
64. Xu, W.W.; Zhou, M.M.; Baudry, M. Neuroprotection by Cell Permeable TAT-mGluR1 Peptide in Ischemia: Synergy between Carrier and Cargo Sequences. *Neuroscientist* **2008**, *14*, 409–414. [CrossRef] [PubMed]
65. Marshall, J.; Wong, K.Y.; Rupasinghe, C.N.; Tiwari, R.; Zhao, X.; Berberoglu, E.D.; Sinkler, C.; Liu, J.; Lee, I.; Parang, K.; et al. Inhibition of *N*-Methyl-D-aspartate-induced Retinal Neuronal Death by Polyarginine Peptides Is Linked to the Attenuation of Stress-induced Hyperpolarization of the Inner Mitochondrial Membrane Potential. *J. Biol. Chem.* **2015**, *290*, 22030–22048. [CrossRef] [PubMed]
66. McQueen, J.; Ryan, T.J.; McKay, S.; Marwick, K.; Baxter, P.; Carpanini, S.M.; Wishart, T.M.; Gillingwater, T.H.; Manson, J.C.; Wylie, D.J.A.; et al. Pro-death NMDA receptor signaling is promoted by the GluN2B C-terminus independently of Dapk1. *Elife* **2017**, *6*, e17161. [CrossRef] [PubMed]

67. Cook, D.R.; Gleichman, A.J.; Cross, S.A.; Doshi, S.; Ho, W.; Jordan-Sciutto, K.L.; Lynch, D.R.; Kolson, D.L. NMDA receptor modulation by the neuropeptide apelin: Implications for excitotoxic injury. *J. Neurochem.* **2011**, *118*, 1113–1123. [CrossRef] [PubMed]
68. García-Caballero, A.; Gadotti, V.M.; Stemkowski, P.; Weiss, N.; Souza, I.A.; Hodgkinson, V.; Bladen, C.; Chen, L.; Hamid, J.; Pizzoccaro, A.; et al. The deubiquitinating enzyme USP5 modulates neuropathic and inflammatory pain by enhancing Cav3.2 channel activity. *Neuron* **2014**, *83*, 1144–1158. [CrossRef] [PubMed]
69. Xie, J.Y.; Chew, L.A.; Yang, X.; Wang, Y.; Qu, C.; Wang, Y.; Federici, L.M.; Fitz, S.D.; Ripsch, M.S.; Due, M.R.; et al. Sustained relief of ongoing experimental neuropathic pain by a CRMP2 peptide aptamer with low abuse potential. *Pain* **2016**, *157*, 2124–2140. [CrossRef] [PubMed]
70. Brustovetsky, T.; Pellman, J.J.; Yang, X.-F.F.; Khanna, R.; Brustovetsky, N. Collapsin response mediator protein 2 (CRMP2) interacts with N-methyl-D-aspartate (NMDA) receptor and Na^+/Ca^{2+} exchanger and regulates their functional activity. *J. Biol. Chem.* **2014**, *289*, 7470–7482. [CrossRef] [PubMed]
71. Sinai, L.; Duffy, S.; Roder, J.C. Src inhibition reduces NR2B surface expression and synaptic plasticity in the amygdala. *Learn. Mem.* **2010**, *17*, 364–371. [CrossRef] [PubMed]
72. Tu, W.; Xu, X.; Peng, L.; Zhong, X.; Zhang, W.; Soundarapandian, M.M.; Balel, C.; Wang, M.; Jia, N.; Zhang, W.; et al. DAPK1 interaction with NMDA receptor NR2B subunits mediates brain damage in stroke. *Cell* **2010**, *140*, 222–234. [CrossRef] [PubMed]
73. Fan, J.; Cowan, C.M.; Zhang, L.Y.J.; Hayden, M.R.; Raymond, L.A. Interaction of postsynaptic density protein-95 with NMDA receptors influences excitotoxicity in the yeast artificial chromosome mouse model of Huntington's disease. *J. Neurosci.* **2009**, *29*, 10928–10938. [CrossRef] [PubMed]
74. Brittain, J.M.; Chen, L.; Wilson, S.M.; Brustovetsky, T.; Gao, X.; Ashpole, N.M.; Molosh, A.I.; You, H.; Hudmon, A.; Shekhar, A.; et al. Neuroprotection against traumatic brain injury by a peptide derived from the collapsin response mediator protein 2 (CRMP2). *J. Biol. Chem.* **2011**, *286*, 37778–37792. [CrossRef] [PubMed]
75. Feldman, P.; Khanna, R. Challenging the catechism of therapeutics for chronic neuropathic pain: Targeting CaV2.2 interactions with CRMP2 peptides. *Neurosci. Lett.* **2013**, *557 Pt A*, 27–36. [CrossRef]
76. François-Moutal, L.; Dustrude, E.T.; Wang, Y.; Brustovetsky, T.; Dorame, A.; Ju, W.; Moutal, A.; Perez-Miller, S.; Brustovetsky, N.; Gokhale, V.; et al. Inhibition of the Ubc9 E2 SUMO conjugating enzyme–CRMP2 interaction decreases NaV1.7 currents and reverses experimental neuropathic pain. *Pain* **2018**, *1*. [CrossRef] [PubMed]
77. Birk, A.V.; Chao, W.M.; Liu, S.; Soong, Y.; Szeto, H.H. Disruption of cytochrome c heme coordination is responsible for mitochondrial injury during ischemia. *Biochim. Biophys. Acta* **2015**, *1847*, 1075–1084. [CrossRef] [PubMed]
78. Ferré, C.A.; Davezac, N.; Thouard, A.; Peyrin, J.M.; Belenguer, P.; Miguel, M.C.; Gonzalez-Dunia, D.; Szelechowski, M. Manipulation of the N-terminal sequence of the Borna disease virus X protein improves its mitochondrial targeting and neuroprotective potential. *FASEB J.* **2016**, *30*, 1523–1533. [CrossRef] [PubMed]
79. Rigobello, M.P.; Barzon, E.; Marin, O.; Bindoli, A. Effect of polycation peptides on mitochondrial permeability transition. *Biochem. Biophys. Res. Commun.* **1995**, *217*, 144–149. [CrossRef] [PubMed]
80. Szelechowski, M.; Betourne, A.; Monnet, Y.; Ferre, C.A.; Thouard, A.; Foret, C.; Peyrin, J.M.; Hunot, S.; Gonzalez-Dunia, D. A viral peptide that targets mitochondria protects against neuronal degeneration in models of Parkinson's disease. *Nat. Commun.* **2014**, *5*, 5181. [CrossRef] [PubMed]
81. Szeto, H.H.; Liu, S.; Soong, Y.; Wu, D.; Darrah, S.F.; Cheng, F.Y.; Zhao, Z.; Ganger, M.; Tow, C.Y.; Seshan, S.V. Mitochondria-targeted peptide accelerates ATP recovery and reduces ischemic kidney injury. *J. Am. Soc. Nephrol.* **2011**, *22*, 1041–1052. [CrossRef] [PubMed]
82. Zhao, K.; Zhao, G.M.; Wu, D.; Soong, Y.; Birk, A.V.; Schiller, P.W.; Szeto, H.H. Cell-permeable peptide antioxidants targeted to inner mitochondrial membrane inhibit mitochondrial swelling, oxidative cell death, and reperfusion injury. *J. Biol. Chem.* **2004**, *279*, 34682–34690. [CrossRef] [PubMed]
83. Cerrato, C.P.; Pirisinu, M.; Vlachos, E.N.; Langel, Ü. Novel cell-penetrating peptide targeting mitochondria. *FASEB J.* **2015**, *29*, 4589–4599. [CrossRef] [PubMed]
84. Anbanandam, A.; Albarado, D.C.; Tirziu, D.C.; Simons, M.; Veeraraghavan, S. Molecular basis for proline- and arginine-rich peptide inhibition of proteasome. *J. Mol. Biol.* **2008**, *384*, 219–227. [CrossRef] [PubMed]
85. Gaczynska, M.; Osmulski, P.A.; Gao, Y.; Post, M.J.; Simons, M. Proline- and arginine-rich peptides constitute a novel class of allosteric inhibitors of proteasome activity. *Biochemistry* **2003**, *42*, 8663–8670. [CrossRef] [PubMed]

86. Cameron, A.; Appel, J.; Houghten, R.A.; Lindberg, I. Polyarginines Are Potent Furin Inhibitors. *J. Biol. Chem.* **2000**, *275*, 36741–36749. [CrossRef] [PubMed]
87. Fugere, M.; Appel, J.; Houghten, R.A.; Lindberg, I.; Day, R. Short polybasic peptide sequences are potent inhibitors of PC5/6 and PC7: Use of positional scanning-synthetic peptide combinatorial libraries as a tool for the optimization of inhibitory sequences. *Mol. Pharmacol.* **2007**, *71*, 323–332. [CrossRef] [PubMed]
88. Kacprzak, M.M.; Peinado, J.R.; Than, M.E.; Appel, J.; Hanrich, S.; Lipkind, G.; Houghten, R.A.; Bode, W.; Lindberg, I. Inhibition of furin by polyarginine-containing peptides: Nanomolar inhibition by nona-D-arginine. *J. Biol. Chem.* **2004**, *279*, 36788–36794. [CrossRef] [PubMed]
89. Tian, S.; Huang, Q.; Fang, Y.; Wu, J. FurinDB: A database of 20-residue furin cleavage site motifs, substrates and their associated drugs. *Int. J. Mol. Sci.* **2011**, *12*, 1060–1065. [CrossRef] [PubMed]
90. Doeppner, T.R.; Kaltwasser, B.; Kuckelkorn, U.; Henkelein, P.; Bretschneider, E.; Kilic, E.; Hermann, D.M. Systemic Proteasome Inhibition Induces Sustained Post-stroke Neurological Recovery and Neuroprotection via Mechanisms Involving Reversal of Peripheral Immunosuppression and Preservation of Blood-Brain-Barrier Integrity. *Mol. Neurobiol.* **2016**, *53*, 6332–6341. [CrossRef] [PubMed]
91. Wojcik, C.; di Napoli, M. Ubiquitin-proteasome system and proteasome inhibition: New strategies in stroke therapy. *Stroke* **2004**, *35*, 1506–1518. [CrossRef] [PubMed]
92. Chen, W.; Hartman, R.; Ayer, R.; Maracantionio, S.; Kamper, J.; Tang, J.; Zhang, J.H. Matrix metalloproteinases inhibition provides neuroprotection against hypoxia-ischemia in the developing brain. *J. Neurochem.* **2009**, *111*, 726–736. [CrossRef] [PubMed]
93. Cunningham, L.A.; Wetzel, M.; Rosenberg, G.A. Multiple roles for MMPs and TIMPs in cerebral ischemia. *Glia* **2005**, *50*, 329–339. [CrossRef] [PubMed]
94. Yang, Y.; Zhang, X.; Cui, H.; Zhang, C.; Zhu, C.; Li, L. Apelin-13 protects the brain against ischemia/reperfusion injury through activating PI3K/Akt and ERK1/2 signaling pathways. *Neurosci. Lett.* **2014**, *568*, 44–49. [CrossRef] [PubMed]
95. Hilchie, A.L.; Wuerth, K.; Hancock, R.E.W. Immune modulation by multifaceted cationic host defense (antimicrobial) peptides. *Nat. Chem. Biol.* **2013**, *9*, 761–768. [CrossRef] [PubMed]
96. Kellett, D.N. On the Anti-Inflammatory Activity of Protamine Sulphate and of Hexadimethrine Bromide, Inhibitors of Plasma Kinin Formation. *Br. J. Pharmacol. Chemother.* **1965**, *24*, 705–713. [CrossRef] [PubMed]
97. Li, L.H.; Ju, T.C.; Hsieh, C.Y.; Dong, W.C.; Chen, W.T.; Hua, K.F.; Chen, W.J. A synthetic cationic antimicrobial peptide inhibits inflammatory response and the NLRP3 inflammasome by neutralizing LPS and ATP. *PLoS ONE* **2017**, *12*, e0182057. [CrossRef] [PubMed]
98. Courderot-Masuyer, C.; Dalloz, F.; Maupoil, V.; Rochette, L. Antioxidant properties of aminoguanidine. *Fundam. Clin. Pharmacol.* **1999**, *13*, 535–540. [CrossRef] [PubMed]
99. Yildiz, G.; Demiryürek, A.T.; Sahin-Erdemli, I.; Kanzik, I. Comparison of antioxidant activities of aminoguanidine, methylguanidine and guanidine by luminol-enhanced chemiluminescence. *Br. J. Pharmacol.* **1998**, *124*, 905–910. [CrossRef] [PubMed]
100. Lass, A.; Suessenbacher, A.; Wölkart, G.; Mayer, B.; Brunner, F. Functional and analytical evidence for scavenging of oxygen radicals by L-arginine. *Mol. Pharmacol.* **2002**, *61*, 1081–1088. [CrossRef] [PubMed]
101. Mandal, S.M.; Bharti, R.; Porto, W.F.; Guari, S.S.; Mandal, M.; Franco, O.L.; Ghosh, A.K. Identification of multifunctional peptides from human milk. *Peptides* **2014**, *56*, 84–93. [CrossRef] [PubMed]
102. Harari, O.A.; Liao, J.K. NF-κB and innate immunity in ischemic stroke. *Ann. N. Y. Acad. Sci.* **2010**, *1207*, 32–40. [CrossRef] [PubMed]
103. May, M.J.; Marienfeld, R.B.; Ghosh, S. Characterization of the Ikappa B-kinase NEMO binding domain. *J. Biol. Chem.* **2002**, *277*, 45992–46000. [CrossRef] [PubMed]
104. Van den Tweel, E.R.; Kavelaars, A.; Lombardi, M.S.; Groenendaal, F.; May, M.; Heijnen, C.J.; van Bel, F. Selective inhibition of nuclear factor-kappaB activation after hypoxia/ischemia in neonatal rats is not neuroprotective. *Pediatr. Res.* **2006**, *59*, 232–236. [CrossRef] [PubMed]
105. Nijboer, C.H.A.; Heijnen, C.J.; Groenendaal, F.; May, M.J.; van Bel, F.; Kavelaars, A. Strong neuroprotection by inhibition of NF-kappaB after neonatal hypoxia-ischemia involves apoptotic mechanisms but is independent of cytokines. *Stroke* **2008**, *39*, 2129–2137. [CrossRef] [PubMed]
106. Nijboer, C.H.; Heijnen, C.J.; Groenendaal, F.; May, M.J.; van Bel, F.; Kavelaars, A. A dual role of the NF-kappaB pathway in neonatal hypoxic-ischemic brain damage. *Stroke* **2008**, *39*, 2578–2586. [CrossRef] [PubMed]

107. Van der Kooij, M.A.; Nijboer, C.H.; Ohl, F.; Groenendaal, F.; Heijnen, C.J.; ven Bel, F.; Kavelaars, A. NF-kappaB inhibition after neonatal cerebral hypoxia-ischemia improves long-term motor and cognitive outcome in rats. *Neurobiol. Dis.* **2010**, *38*, 266–272. [CrossRef] [PubMed]
108. Yang, D.; Syn, Y.Y.; Lin, X.; Baumann, J.M.; Dunn, R.S.; Lindquist, D.M.; Kaun, C.Y. Intranasal delivery of cell-penetrating anti-NF-κB peptides (Tat-NBD) alleviates infection-sensitized hypoxic-ischemic brain injury. *Exp. Neurol.* **2013**, *247*, 447–455. [CrossRef] [PubMed]
109. Le Roy, D.; Di Padova, F.; Tees, R.; Lengacher, S.; Landmann, R.; Glauser, M.P.; Calandra, T.; Heumann, D. Monoclonal antibodies to murine lipopolysaccharide (LPS)-binding protein (LBP) protect mice from lethal endotoxemia by blocking either the binding of LPS to LBP or the presentation of LPS/LBP complexes to CD14. *J. Immunol.* **1999**, *162*, 7454–7460. [PubMed]
110. Xu, W.; Wong, T.P.; Chery, N.; Gaertner, T.; Wang, Y.T.; Baudry, M. Calpain-Mediated mGluR1α Truncation: A Key Step in Excitotoxicity. *Neuron* **2007**, *53*, 399–412. [CrossRef] [PubMed]
111. Zhou, M.; Xu, W.; Liao, G.; Bi, X.; Baudry, M. Neuroprotection against neonatal hypoxia/ischemia-induced cerebral cell death by prevention of calpain-mediated mGluR1alpha truncation. *Exp. Neurol.* **2009**, *218*, 75–82. [CrossRef] [PubMed]
112. Borsello, T.; Croquelois, K.; Hornung, J.P.; Clarke, P.G. N-methyl-d-aspartate-triggered neuronal death in organotypic hippocampal cultures is endocytic, autophagic and mediated by the c-Jun N-terminal kinase pathway. *Eur. J. Neurosci.* **2003**, *18*, 473–485. [CrossRef] [PubMed]
113. Gupta, S.; Barrett, T.; Whitmarch, A.J.; Cavanagh, J.; Sluss, H.K.; Derijard, B.; Davis, R.J. Selective interaction of JNK protein kinase isoforms with transcription factors. *EMBO J.* **1996**, *15*, 2760–2770. [PubMed]
114. Wang, L.W.; Chang, Y.C.; Chen, S.J.; Tseng, C.H.; Tu, Y.F.; Liao, N.S.; Huang, C.C.; Ho, C.J. TNFR1-JNK signaling is the shared pathway of neuroinflammation and neurovascular damage after LPS-sensitized hypoxic-ischemic injury in the immature brain. *J. Neuroinflamm.* **2014**, *11*, 215. [CrossRef] [PubMed]
115. Ginet, V.; Puyal, J.; Magnin, G.; Clarke, P.G.H.; Truttmann, A.C. Limited role of the c-Jun N-terminal kinase pathway in a neonatal rat model of cerebral hypoxia-ischemia. *J. Neurochem.* **2009**, *108*, 552–562. [CrossRef] [PubMed]
116. Yang, D.D.; Kuan, C.Y.; Whitmarch, A.J.; Rincon, M.; Zheng, T.S.; Davis, R.J.; Rakic, P.; Flavell, R.A. Absence of excitotoxicity-induced apoptosis in the hippocampus of mice lacking the Jnk3 gene. *Nature* **1997**, *389*, 865–870. [CrossRef] [PubMed]
117. Centeno, C.; Repici, M.; Chatton, J.Y.; Riederer, B.M.; Bonny, C.; Nicod, P.; Price, M.; Clarke, P.G.; Papa, S.; Franzoso, G.; Borsello, T. Role of the JNK pathway in NMDA-mediated excitotoxicity of cortical neurons. *Cell Death Differ.* **2007**, *14*, 240–253. [CrossRef] [PubMed]
118. Nijboer, C.H.; van der Kooij, M.A.; van Bel, F.; Ohl, F.; Heijnen, C.J.; Kavelaars, A. Inhibition of the JNK/AP-1 pathway reduces neuronal death and improves behavioral outcome after neonatal hypoxic-ischemic brain injury. *Brain. Behav. Immun.* **2010**, *24*, 812–821. [CrossRef] [PubMed]
119. Nijboer, C.H.; Bonestroo, H.J.C.; Zijlstra, J.; Kavelaars, A.; Heijnen, C.J. Mitochondrial JNK phosphorylation as a novel therapeutic target to inhibit neuroinflammation and apoptosis after neonatal ischemic brain damage. *Neurobiol. Dis.* **2013**, *54*, 432–444. [CrossRef] [PubMed]
120. Shimizu, S.; Konishi, A.; Kodama, T.; Tsujimoto, Y. BH4 domain of antiapoptotic Bcl-2 family members closes voltage-dependent anion channel and inhibits apoptotic mitochondrial changes and cell death. *Proc. Natl. Acad. Sci. USA* **2000**, *97*, 3100–3105. [CrossRef] [PubMed]
121. Rong, Y.P.; Bultynck, G.; Aromolaran, A.S.; Zhong, F.; Parys, J.B.; De Smedt, H.; Mignery, G.A.; Roderick, H.L.; Bootman, M.D.; Distelhorst, C.W. The BH4 domain of Bcl-2 inhibits ER calcium release and apoptosis by binding the regulatory and coupling domain of the IP3 receptor. *Proc. Natl. Acad. Sci. USA* **2009**, *106*, 14397–14402. [CrossRef] [PubMed]
122. Donnini, S.; Solito, R.; Monti, M.; Balduini, W.; Carloni, S.; Cimino, M.; Bampton, E.T.; Pinon, L.G.; Nicotera, P.; Thorpe, P.E.; Ziche, M. Prevention of ischemic brain injury by treatment with the membrane penetrating apoptosis inhibitor, TAT-BH4. *Cell Cycle* **2009**, *8*, 1271–1278. [CrossRef] [PubMed]
123. Denhardt, D.T.; Guo, X. Osteopontin: A protein with diverse functions. *FASEB J.* **1993**, *7*, 1475–1482. [CrossRef] [PubMed]
124. Schroeter, M.; Zickler, P.; Denhardt, D.T.; Hartung, H.-P.; Jander, S. Increased thalamic neurodegeneration following ischaemic cortical stroke in osteopontin-deficient mice. *Brain* **2006**, *129*, 1426–1437. [CrossRef] [PubMed]

125. Doyle, K.P.; Yang, T.; Lessov, N.S.; Ciesielski, T.M.; Stevens, S.L.; Simon, R.P.; King, J.S.; Stenzel-Poore, M.P. Nasal administration of osteopontin peptide mimetics confers neuroprotection in stroke. *J. Cereb. Blood Flow Metab.* **2008**, *28*, 1235–1248. [CrossRef] [PubMed]
126. Meller, R.; Stevens, S.L.; Minami, M.; Cameron, J.A.; King, S.; Rosenzweif, H.; Doyle, K.; Lessov, N.S.; Simon, R.P.; Stenzel-Poore, M.P. Neuroprotection by osteopontin in stroke. *J. Cereb. Blood Flow Metab.* **2005**, *25*, 217–225. [CrossRef] [PubMed]
127. Jin, Y.; Kim, I.Y.; Kim, I.D.; Lee, H.K.; Park, J.Y.; Han, P.L.; Kim, K.K.; Choi, H.; Lee, J.K. Biodegradable gelatin microspheres enhance the neuroprotective potency of osteopontin via quick and sustained release in the post-ischemic brain. *Acta Biomater.* **2014**, *10*, 3126–3135. [CrossRef] [PubMed]
128. Wu, B.; Ma, Q.; Suzuki, H.; Chen, C.; Liu, W.; Tang, J.; Zhang, J. Recombinant Osteopontin Attenuates Brain Injury after Intracerebral Hemorrhage in Mice. *Neurocrit. Care* **2011**, *14*, 109–117. [CrossRef] [PubMed]
129. Jin, Y.C.; Lee, H.; Kim, S.W.; Kim, I.D.; Lee, H.K.; Lee, Y.; Han, P.L.; Lee, J.K. Intranasal Delivery of RGD Motif-Containing Osteopontin Icosamer Confers Neuroprotection in the Postischemic Brain via $\alpha_v\beta_3$ Integrin Binding. *Mol. Neurobiol.* **2016**, *53*, 5652–5663. [CrossRef] [PubMed]
130. Das, R.; Mahabeleshwar, G.H.; Kundu, G.C. Osteopontin Stimulates Cell Motility and Nuclear Factor κB-mediated Secretion of Urokinase Type Plasminogen Activator through Phosphatidylinositol 3-Kinase/Akt Signaling Pathways in Breast Cancer Cells. *J. Biol. Chem.* **2003**, *278*, 28593–28606. [CrossRef] [PubMed]
131. Gary, D.S.; Milhavet, O.; Camandola, S.; Mattson, M.P. Essential role for integrin linked kinase in Akt-mediated integrin survival signaling in hippocampal neurons. *J. Neurochem.* **2003**, *84*, 878–890. [CrossRef] [PubMed]
132. Hwang, S.M.; Lopez, C.A.; Heck, D.E.; Gardner, C.R.; Laskin, D.L.; Laskin, J.D.; Denhardt, D.T. Osteopontin inhibits induction of nitric oxide synthase gene expression by inflammatory mediators in mouse kidney epithelial cells. *J. Biol. Chem.* **1994**, *269*, 711–715. [PubMed]
133. Rollo, E.E.; Laskin, D.L.; Denhardt, D.T. Osteopontin inhibits nitric oxide production and cytotoxicity by activated RAW264.7 macrophages. *J. Leukoc. Biol.* **1996**, *60*, 397–404. [CrossRef] [PubMed]
134. Chen, W.; Ma, Q.; Suzuki, H.; Hartman, R.; Tang, J.; Zhang, J.H. Osteopontin reduced hypoxia-ischemia neonatal brain injury by suppression of apoptosis in a rat pup model. *Stroke* **2011**, *42*, 764–769. [CrossRef] [PubMed]
135. Albertsson, A.M.; Zhang, X.; Leavenworth, J.; Bi, D.; Nair, S.; Qiao, L.; Hagberg, H.; Mallard, C.; Cantor, H.; Wang, X. The effect of osteopontin and osteopontin-derived peptides on preterm brain injury. *J. Neuroinflamm.* **2014**, *11*, 197. [CrossRef] [PubMed]
136. Bonestroo, H.J.C.C.; Nijboer, C.H.; van Velthoven, C.T.J.J.; van Bel, F.; Heijnen, C.J. The Neonatal Brain Is Not Protected by Osteopontin Peptide Treatment after Hypoxia-Ischemia. *Dev. Neurosci.* **2015**, *37*, 142–152. [CrossRef] [PubMed]
137. Zheng, Y.L.; Amin, N.D.; Hu, Y.F.; Rudrabhatla, P.; Shukla, V.; Kanungo, J.; Kesavapany, S.; Grant, P.; Albers, W.; Pant, H.C. A 24-Residue Peptide (p5), Derived from p35, the Cdk5 Neuronal Activator, Specifically Inhibits Cdk5-p25 Hyperactivity and Tau Hyperphosphorylation. *J. Biol. Chem.* **2010**, *285*, 34202–34212. [CrossRef] [PubMed]
138. Su, S.C.; Tsai, L.-H. Cyclin-Dependent Kinases in Brain Development and Disease. *Annu. Rev. Cell Dev. Biol.* **2011**, *27*, 465–491. [CrossRef] [PubMed]
139. Fischer, A.; Sananbenesi, F.; Pang, P.T.; Lu, B.; Tsai, L.-H. Opposing Roles of Transient and Prolonged Expression of p25 in Synaptic Plasticity and Hippocampus-Dependent Memory. *Neuron* **2005**, *48*, 825–838. [CrossRef] [PubMed]
140. Ji, Y.B.; Zhuang, P.P.; Ji, Z.; Wu, Y.M.; Gu, Y.; Gao, X.Y.; Pan, S.Y.; Hu, Y.F. TFP5 peptide, derived from CDK5-activating cofactor p35, provides neuroprotection in early-stage of adult ischemic stroke. *Sci. Rep.* **2017**, *7*, 40013. [CrossRef] [PubMed]
141. Shukla, V.; Zheng, Y.L.; Mishra, S.K.; Amin, N.D.; Steiner, J.; Grant, P.; Kesavapany, S.; Pant, H.C. A truncated peptide from p35, a Cdk5 activator, prevents Alzheimer's disease phenotypes in model mice. *FASEB J.* **2013**, *27*, 174–186. [CrossRef] [PubMed]
142. Binukumar, B.K.; Shukla, V.; Amin, N.D.; Grant, P.; Bhaskar, M.; Skuntz, S.; Steiner, J.; Pant, H.C. Peptide TFP5/TP5 derived from Cdk5 activator P35 provides neuroprotection in the MPTP model of Parkinson's disease. *Mol. Biol. Cell* **2015**, *26*, 4478–4491. [CrossRef] [PubMed]

143. Tan, X.; Chen, Y.; Li, J.; Li, X.; Miao, Z.; Xin, N.; Zhu, J.; Ge, W.; Feng, Y.; Xu, X. The inhibition of Cdk5 activity after hypoxia/ischemia injury reduces infarct size and promotes functional recovery in neonatal rats. *Neuroscience* **2015**, *290*, 552–560. [CrossRef] [PubMed]
144. Soriano, F.X.; Martel, M.A.; Papadia, S.; Vaslin, A.; Baxter, P.; Rickman, C.; Forder, J.; Tymianski, M.; Duncan, R.; Aarts, M.; et al. Specific targeting of pro-death NMDA receptor signals with differing reliance on the NR2B PDZ ligand. *J. Neurosci.* **2008**, *28*, 10696–10710. [CrossRef] [PubMed]
145. Li, L.L.; Ginet, V.; Liu, X.; Vergun, O.; Tuittila, M.; Mathieu, M.; Bonny, C.; Puyal, J.; Truttmann, A.C.; Courtney, M.J. The nNOS-p38MAPK Pathway Is Mediated by NOS1AP during Neuronal Death. *J. Neurosci.* **2013**, *33*, 8185–8201. [CrossRef] [PubMed]
146. Ballarin, B.; Tymianski, M. Discovery and development of NA-1 for the treatment of acute ischemic stroke. *Acta Pharmacol. Sin.* **2018**, *39*, 661–668. [CrossRef] [PubMed]
147. Xu, B.; Xiao, A.J.; Chen, W.; Turlova, E.; Liu, R.; Barszcyk, A.; Sun, C.L.F.; Liu, L.; Tymianski, M.; Feng, Z.P.; et al. Neuroprotective Effects of a PSD-95 Inhibitor in Neonatal Hypoxic-Ischemic Brain Injury. *Mol. Neurobiol.* **2016**, *53*, 5962–5970. [CrossRef] [PubMed]
148. Aono, M.; Bennett, E.R.; Kim, K.S.; Lynch, J.R.; Myers, J.; Pearlstein, R.D.; Warner, D.S.; Laskowitz, D.T. Protective effect of apolipoprotein E-mimetic peptides on N-methyl-D-aspartate excitotoxicity in primary rat neuronal-glial cell cultures. *Neuroscience* **2003**, *116*, 437–445. [CrossRef]
149. Laskowitz, D.T.; Thekdi, A.D.; Thekdi, S.D.; Han, S.K.; Myers, J.K.; Pizzo, S.V.; Bennett, E.R. Downregulation of Microglial Activation by Apolipoprotein E and ApoE-Mimetic Peptides. *Exp. Neurol.* **2001**, *167*, 74–85. [CrossRef] [PubMed]
150. Lynch, J.R.; Tang, W.; Wang, H.; Vitek, M.P.; Bennett, E.R.; Sullivan, P.M.; Warner, D.S.; Laskowitz, D.T. APOE Genotype and an ApoE-mimetic Peptide Modify the Systemic and Central Nervous System Inflammatory Response. *J. Biol. Chem.* **2003**, *278*, 48529–48533. [CrossRef] [PubMed]
151. McAdoo, J.D.; Warner, D.S.; Goldberg, R.N.; Vitek, M.P.; Pearlstein, R.; Laskowitz, D.T. Intrathecal administration of a novel apoE-derived therapeutic peptide improves outcome following perinatal hypoxic-ischemic injury. *Neurosci. Lett.* **2005**, *381*, 305–308. [CrossRef] [PubMed]
152. Misra, U.K.; Adlakha, C.L.; Gawdi, G.; McMillian, M.K.; Pizzo, S.V.; Laskowitz, D.T. Apolipoprotein E and mimetic peptide initiate a calcium-dependent signaling response in macrophages. *J. Leukoc. Biol.* **2001**, *70*, 677–683. [PubMed]
153. Krysko, D.V.; Leybaert, L.; Vandenabeele, P.; D'Herde, K. Gap junctions and the propagation of cell survival and cell death signals. *Apoptosis* **2005**, *10*, 459–469. [CrossRef] [PubMed]
154. Kondo, R.P.; Wang, S.-Y.; John, S.A.; Weiss, J.N.; Goldhaber, J.I. Metabolic Inhibition Activates a Non-selective Current Through Connexin Hemichannels in Isolated Ventricular Myocytes. *J. Mol. Cell. Cardiol.* **2000**, *32*, 1859–1872. [CrossRef] [PubMed]
155. Decrock, E.; De Vuyst, E.; Vinken, M.; Van Moorhem, M.; Vranckx, K.; Wang, N.; Van Laeken, L.; De Brock, M.; D'Herde, K.; Lai, C.P.; et al. Connexin 43 hemichannels contribute to the propagation of apoptotic cell death in a rat C6 glioma cell model. *Cell Death Differ.* **2009**, *16*, 151–163. [CrossRef] [PubMed]
156. Orellana, J.A.; Hernandez, D.E.; Ezan, P.; Velarde, V.; Bennett, M.V.; Giaume, C.; Saez, J.C. Hypoxia in high glucose followed by reoxygenation in normal glucose reduces the viability of cortical astrocytes through increased permeability of connexin 43 hemichannels. *Glia* **2010**, *58*, 329–343. [CrossRef] [PubMed]
157. Ye, Z.-C.; Wyeth, M.S.; Baltan-Tekkok, S.; Ransom, B.R. Functional hemichannels in astrocytes: A novel mechanism of glutamate release. *J. Neurosci.* **2003**, *23*, 3588–3596. [CrossRef] [PubMed]
158. Frantseva, M.V.; Kokarovtseva, L.; Naus, C.G.; Carlen, P.L.; MacFabe, D.; Velazquez, J.L.P. Specific gap junctions enhance the neuronal vulnerability to brain traumatic injury. *J. Neurosci.* **2002**, *22*, 644–653. [CrossRef] [PubMed]
159. Frantseva, M.V.; Kokarovtseva, L.; Velazquez, J.L.P. Ischemia-Induced Brain Damage Depends on Specific Gap-Junctional Coupling. *J. Cereb. Blood Flow Metab.* **2002**, *22*, 453–462. [CrossRef] [PubMed]
160. O'Carroll, S.J.; Alkadhi, M.; Nicholson, L.F.B.; Green, C.R. Connexin43 Mimetic Peptides Reduce Swelling, Astrogliosis, and Neuronal Cell Death after Spinal Cord Injury. *Cell Commun. Adhes.* **2008**, *15*, 27–42. [CrossRef] [PubMed]
161. Davidson, J.O.; Green, C.R.; Nicholson, L.F.; O'Carroll, S.J.; Fraser, M.; Bennet, L.; Gunn, A.J. Connexin hemichannel blockade improves outcomes in a model of fetal ischemia. *Ann. Neurol.* **2012**, *71*, 121–132. [CrossRef] [PubMed]

162. Davidson, J.O.; Green, C.R.; Nicholson, L.F.B.; Bennet, L.; Gunn, A.J. Connexin hemichannel blockade is neuroprotective after, but not during, global cerebral ischemia in near-term fetal sheep. *Exp. Neurol.* **2013**, *248*, 301–308. [CrossRef] [PubMed]
163. Davidson, J.O.; Green, C.R.; Nicholson, L.F.B.; Bennet, L.; Gunn, A.J. Deleterious Effects of High Dose Connexin 43 Mimetic Peptide Infusion After Cerebral Ischaemia in Near-Term Fetal Sheep. *Int. J. Mol. Sci.* **2012**, *13*, 6303–6319. [CrossRef] [PubMed]
164. Davidson, J.O.; Drury, P.P.; Green, C.R.; Nicholson, L.F.; Bennet, L.; Gunn, A.J. Connexin hemichannel blockade is neuroprotective after asphyxia in preterm fetal sheep. *PLoS ONE* **2014**, *9*, e96558. [CrossRef] [PubMed]
165. Davidson, J.O.; Rout, A.L.; Wassink, G.; Yuill, C.A.; Zhang, F.G.; Green, C.R.; Benent, L.; Gunn, A.J. Non-Additive Effects of Delayed Connexin Hemichannel Blockade and Hypothermia after Cerebral Ischemia in Near-Term Fetal Sheep. *J. Cereb. Blood Flow Metab.* **2015**, *35*, 2052–2061. [CrossRef] [PubMed]
166. Li, X.; Zhao, H.; Tan, X.; Kostrzewa, R.M.; Du, G.; Chen, Y.; Zhu, J.; Miao, Z.; Yu, H.; Kong, J.; et al. Inhibition of connexin43 improves functional recovery after ischemic brain injury in neonatal rats. *Glia* **2015**, *63*, 1553–1567. [CrossRef] [PubMed]
167. Choe, W.; Albright, A.; Sulcove, J.; Jaffer, S.; Hesselgesser, J.; Lavi, E.; Crino, P.; Kolson, D.L. Functional expression of the seven-transmembrane HIV-1 co-receptor APJ in neural cells. *J. Neurovirol.* **2000**, *6* (Suppl. 1), S61–S69. [PubMed]
168. O'Carroll, A.-M.; Selby, T.L.; Palkovits, M.; Lolait, S.J. Distribution of mRNA encoding B78/apj, the rat homologue of the human APJ receptor, and its endogenous ligand apelin in brain and peripheral tissues. *Biochim. Biophys. Acta Gene Struct. Expr.* **2000**, *1492*, 72–80. [CrossRef]
169. Zeng, X.J.; Yu, S.P.; Zhang, L.; Wei, L. Neuroprotective effect of the endogenous neural peptide apelin in cultured mouse cortical neurons. *Exp. Cell Res.* **2010**, *316*, 1773–1783. [CrossRef] [PubMed]
170. Cheng, B.; Chen, J.; Bai, B.; Xin, Q. Neuroprotection of apelin and its signaling pathway. *Peptides* **2012**, *37*, 171–173. [CrossRef] [PubMed]
171. Ishimaru, Y.; Sumino, A.; Kajioka, D.; Shibagaki, F.; Yamamuro, A.; Yoshioka, Y.; Maeda, S. Apelin protects against NMDA-induced retinal neuronal death via an APJ receptor by activating Akt and ERK1/2, and suppressing TNF-α expression in mice. *J. Pharmacol. Sci.* **2017**, *133*, 34–41. [CrossRef] [PubMed]
172. Gu, Q.; Zhai, L.; Feng, X.; Chen, J.; Miao, Z.; Ren, L.; Qian, X.; Yu, J.; Li, Y.; Xu, X.; et al. Apelin-36, a potent peptide, protects against ischemic brain injury by activating the PI3K/Akt pathway. *Neurochem. Int.* **2013**, *63*, 535–540. [CrossRef] [PubMed]
173. Nijnik, A.; Madera, L.; Ma, S.; Waldbrook, M.; Elliott, M.R.; Easton, D.M.; Mayer, M.L.; Mullaly, S.C.; Kindrachuk, J.; Jenssen, H.; et al. Synthetic Cationic Peptide IDR-1002 Provides Protection against Bacterial Infections through Chemokine Induction and Enhanced Leukocyte Recruitment. *J. Immunol.* **2010**, *184*, 2539–2550. [CrossRef] [PubMed]
174. Wuerth, K.C.; Falsafi, R.; Hancock, R.E.W. Synthetic host defense peptide IDR-1002 reduces inflammation in Pseudomonas aeruginosa lung infection. *PLoS ONE* **2017**, *12*, e0187565. [CrossRef] [PubMed]
175. Bolouri, H.; Savman, K.; Wang, W.; Thomas, A.; Maurer, N.; Dullaghan, E.; Fjell, C.D.; Ek, C.J.; Hagberg, H.; Hancock, R.E.; et al. Innate defense regulator peptide 1018 protects against perinatal brain injury. *Ann. Neurol.* **2014**, *75*, 395–410. [CrossRef] [PubMed]
176. Bao, J.; Sato, K.; Li, M.; Gao, Y.; Abid, R.; Aird, W.; Simons, M.; Post, M.J. PR-39 and PR-11 peptides inhibit ischemia-reperfusion injury by blocking proteasome-mediated IκBα degradation. *Am. J. Physiol. Circ. Physiol.* **2001**, *281*, H2612–H2618. [CrossRef] [PubMed]
177. Kloss, A.; Henklein, P.; Siele, D.; Schmolke, M.; Apcher, S.; Kuehn, L.; Sheppard, P.W.; Dahlmann, B. The cell-penetrating peptide octa-arginine is a potent inhibitor of proteasome activities. *Eur. J. Pharm. Biopharm.* **2009**, *72*, 219–225. [CrossRef] [PubMed]
178. Zhou, N.; Fang, J.; Acheampong, E.; Mukhtar, M.; Pomerantz, R.J. Binding of ALX40-4C to APJ, a CNS-based receptor, inhibits its utilization as a co-receptor by HIV-1. *Virology* **2003**, *312*, 196–203. [CrossRef]
179. le Gonidec, S.; Chaves-Almagro, C.; Bai, Y.; Kang, H.J.; Smith, A.; Wangecg, E.; Huang, X.P.; Prats, H.; Knibiehler, B.; Roth, B.L.; et al. Protamine is an antagonist of apelin receptor, and its activity is reversed by heparin. *FASEB J.* **2017**, *31*, 2507–2519. [CrossRef] [PubMed]

180. Masri, B.; Morin, N.; Pedebernade, L.; Knibiehler, B.; Audigier, Y. The apelin receptor is coupled to Gi1 or Gi2 protein and is differentially desensitized by apelin fragments. *J. Biol. Chem.* **2006**, *281*, 18317–18326. [CrossRef] [PubMed]
181. Sharifov, O.F.; Nayyar, G.; Ternovoy, V.V.; Mishra, V.K.; Litovsky, S.H.; Palgunachari, M.N.; Gerber, D.W.; Anantharamaiah, G.M.; Gupta, H. Cationic peptide mR18L with lipid lowering properties inhibits LPS-induced systemic and liver inflammation in rats. *Biochem. Biophys. Res. Commun.* **2013**, *436*, 705–710. [CrossRef] [PubMed]
182. Yoo, S.A.; Bae, D.G.; Ryoo, J.W.; Kim, H.R.; Park, G.S.; Cho, C.S.; Chae, C.B.; Kim, W.U. Arginine-rich anti-vascular endothelial growth factor (anti-VEGF) hexapeptide inhibits collagen-induced arthritis and VEGF-stimulated productions of TNF-alpha and IL-6 by human monocytes. *J. Immunol.* **2005**, *174*, 5846–5855. [CrossRef] [PubMed]
183. Lee, J.Y.; Suh, J.S.; Kim, J.M.; Kim, J.H.; Park, H.J.; Park, Y.J.; Chung, C.P. Identification of a cell-penetrating peptide domain from human beta-defensin 3 and characterization of its anti-inflammatory activity. *Int. J. Nanomed.* **2015**, *10*, 5423–5434.

Chapter 3

General Materials and Methods

3.1 MATERIALS AND METHODS

In addition to information provided in Chapters 4 - 6, many of the materials and methods used in this thesis are provided in this chapter.

3.2 PEPTIDES USED IN THIS THESIS

The peptides used for *in vitro* and animal studies are summarised in Table 3.1. All peptides were purified using high performance liquid chromatography and were subjected to hydrolysis and amino acid liquid chromatography analysis to obtain a precise measurement of peptide content (Mimotopes, Melbourne, Australia). For animal studies, all peptides were prepared in 0.9% sodium chloride for injection (Pfizer, Perth, Australia), aliquoted into a 50 µl volume within 300 µl syringes and stored at -20°C until use.

Table 3.1 Summary of the peptides used in this thesis

Peptide	Sequence*	Arginine residues	Charge at pH 7
R18	H-RRRRRRRRRRRRRRRRRR-OH	18	+18
R18D	H-rrrrrrrrrrrrrrrrr-OH	18	+18
JNKI-1-TATD	H-tdqsrpvqpflnlttprkprpp-rrrqrrkkrg-NH_2	9	+12

*T = threonine, D = aspartic acid, Q = glutamine, S = serine, R = arginine, P = proline, V = valine, F = phenylalanine, L = leucine, N = asparagine, K = lysine. Lowercase letters signifies $_D$-enantiomer amino acid.

3.3 P7 RAT MODELS OF HYPOXIC-ISCHAEMIC ENCEPHALOPATHY

3.3.1 Animal ethics approval

All animal surgical procedures and behavioural studies were approved by the University of Western Australia's Animal Ethics Committee (RA/3/100/1329 and RA/3/100/1569), in accordance with the Policies and Guidelines of the National Health and Medical Research Council, Australia. In the design of these studies, every effort was made to minimise the amount of animal suffering and follow Animal Research: Reporting of *In Vivo* Experiments (ARRIVE) guidelines (Kilkenny, Browne, Cuthill, Emerson, & Altman, 2010), where appropriate. All animal surgical procedures and behavioural studies were conducted in an Association for Assessment and Accreditation of Laboratory Animal Care International (AAALAC) accredited animal research facility.

3.3.2 Animals numbers used in experimentation

Pregnant nulliparous Sprague-Dawley rats (dam; Animal Resource Centre, Murdoch, Australia) were used for experiments presented in this thesis. For determining a pup's age, day of birth was considered P0. At P2, all litters were counted and where appropriate were culled to 10 – 12 pups per dam; this is to facilitate uniform growth of the pups without littermate competition for feeding. Animals with a weight range of 14.5 ± 1.5 grams were used for studies, with animals falling outside this weight range on day P7 excluded. In addition, while animals were sexed, both male and female pups were used in studies, in a random and blinded fashion. Prior to any surgical procedure, the dam and pups were housed in ventilated cages (Techniplast, Paola, Malta) which were placed in an animal holding room maintained at 25 ± 1°C.

3.3.3 Behavioural assessments

For all behavioural assessments, each animal was given three attempts to complete each behavioural assessment per day, with 5 minutes between each attempt and assessment. All of the assessments used in this thesis are considered highly reproducible throughout the murine pre-weaning period (< P30) and are strain- and sex-independent (Heyser, 2004). In between all behavioural assessments, all animals were placed on a heating pad (37°C) to prevent hypothermia. Forty-eight hours after hypoxia-ischaemia (HI) pups' responses in all 3 behavioural assessments were recorded 3 times.

3.3.3.1 Righting reflex

For the righting reflex, pups were placed on a flat surface covered with a tightly stretched close-knit fabric, to ensure adequate friction. Pups were placed in a supine position and the time recorded for them to rotate to a prone position recorded (in seconds).

The righting reflex required behavioural sensitisation (i.e. pre-training). For three consecutive days before surgery (P4 – 6; inclusive), pups were accustomed to the righting reflex with a mean target inclusion range of ≤ 2 seconds by the day of surgery (P7; behavioural baseline recording measurement). Any animal that did not meet the inclusion criteria was excluded from the study.

3.3.3.2 Negative geotactic response

For the negative geotactic response, animals were placed on a board covered with tightly stretched close-knit fabric, to ensure adequate friction. The board was positioned on a 45° slope

and at the start of assessment, pups were placed facing downslope. The time for the pups to rotate 150° up the 45° slope recorded (in seconds).

The negative geotactic response required behavioural sensitisation. For three consecutive days before surgery (P4 – 6; inclusive), pups were accustomed to the negative geotactic response with a mean target inclusion range of ≤ 30 seconds by the day of surgery (P7; behavioural baseline recording measurement). Any animal that did not meet the inclusion criteria was excluded from the study.

3.3.3.3 Wire-hang assessment

The wire-hang assessment involved suspending pups by their forelimbs on a 2 mm diameter steel wire, suspended 20 cm above a soft foam surface and recording the time taken (in seconds) for the animal to fall to the foam surface.

The wire-hang assessment did not require any behavioural sensitisation and pups' performance was assessed on the day of surgery (P7; behavioural baseline recording measurement) and did not have any study inclusion criteria.

3.3.4 Original Rice-Vannucci HI surgical procedure

Anaesthesia was induced using a facemask with 5% isoflurane in 100% O_2, and once the animal was anaesthetised, the isoflurane concentration was reduced and maintained at 1.5 ± 0.5%; the duration of anaesthesia from induction to beginning of recovery did not exceed 10 minutes.

Through a 1 cm mid-line ventral incision, the right common carotid artery (CCA) was exposed and carefully dissected from the vagus nerve, venous circulation and carotid body. The CCA was permanently ligated using a 6-0 silk suture. A diagrammatic description of this surgical procedure is presented in Chapter 3, Figure 1. The wound was closed using Vetbond (3M, Maplewood, USA) and the animals recovered on 100% O_2 for 5 minutes. Sham-operated animals underwent the same operative procedure, except the exposed CCA was not ligated.

Following surgical recovery, pups were returned to their dam for approximately 1 hour prior to hypoxia, which consisted of placing between 4 and 6 pups into an airtight container (approximate volume: 4 litres) and gassing the container with warm humidified gas (8% O_2/92 % N_2; 3 litres/minute) for 2.5 hours. During the gassing procedure, the container was housed in an incubator maintained at 35°C. Following hypoxia, pups were removed from the container and immediately administered peptide or saline (IP bolus; 50 µL), then placed back with the dam. For delayed post-hypoxia treatment administration, following hypoxia, pups were immediately returned to their dam and at the appropriate time injected with peptide or saline. Sham-operated animals remained with the dam at all times after the surgical procedure.

3.3.5 Modified Rice-Vannucci HI surgical procedure

For the modified Rice-Vannucci model, the surgical procedure was the same as described above for the original Rice-Vannucci model, except both the CCA and external carotid artery (ECA) were permanently occluded using a 6-0 silk suture. A diagrammatic description of this surgical procedure is presented in Chapter 3, Figure 1.

3.3.6 Post-surgical analgesia, animal body temperature monitoring and housing

All animals were administered pethidine analgesia (5 mg/kg; intraperitoneally) immediately before the cessation of anaesthesia. Animal surface body temperature was monitored periodically throughout the surgical and hypoxia procedures and immediately post-hypoxia using an infrared thermometer. To avoid animals becoming hypothermic during the surgical procedure and when separated from the dam during behavioural assessments, animals were placed on a heating pad maintained at 37°C. During the surgical procedure, if the animal's body temperature decreased (< 36.5°C) a heating fan would be used to maintain a surface body temperature of 37°C. In addition, from the conclusion of surgical anaesthesia to the experimental endpoint, all animals (pups and dam) are housed at 27 ± 1°C in a Ventilated Warming Cabinet (Techniplast, Paola, Malta).

3.4 *EX VIVO* ASSESSMENT OF BRAIN INJURY

3.4.1 Tissue sectioning and triphenyl tetrazolium chloride (TTC) staining

Forty-eight hours after HI, animals were euthanised by lethal intraperitoneal injection of pentobarbitone (50 mg/kg; intraperitoneally). Infarct volume measurement was performed using coronal brain slices stained with TTC. The brain was carefully removed from the skull and placed in 0.9% sodium chloride and cooled for 15 minutes at -80°C before being placed in an adult mouse brain matrix (Note: the adult mouse brain matrix is a suitable size for a P9 rat brain). Razor blades were inserted into the matrix to generate 2 mm coronal slices. The brain slices were incubated for 20 minutes at 37°C in a 3% TTC (w/v; in 0.9% sodium chloride) to stain viable non-infarcted tissue, then fixed by placing in 4% formalin for at least 24 hours.

3.4.2 Measurement of infarct volume from TTC stained coronal slices

Digital images of coronal brain slices (not including cerebellum) were acquired with a colour scanner and analysed using ImageJ software (National Institute of Health, Maryland, United States of America) to calculate an infarct volume. The calculation accounts for changes in hemisphere size due to oedema and is presented below and in Chapter 3:

$$Corrected\ infarct\ volume = \left(\frac{Contralateral\ hemisphere\ volume}{Ipsilateral\ hemisphere\ volume}\right)(Infarct\ volume)$$

Once the infarct area for all sections was defined, the total infarct volume was presented as a percentage of total brain volume.

3.5 STATISTICAL ANALYSIS

Data from mean total infarct volume measurements were evaluated by analysis of variance (ANOVA) followed by Fisher's *post hoc* analysis. Data for behavioural assessments were analysed as described in Chapters 4 - 6.

3.6 REFERENCES

Heyser, C. J. (2004). Assessment of Developmental Milestones in Rodents. In *Current Protocols in Neuroscience* (Vol. Chapter 8, p. Unit 8.18). Hoboken, NJ, USA: John Wiley & Sons, Inc. https://doi.org/10.1002/0471142301.ns0818s25

Kilkenny, C., Browne, W. J., Cuthill, I. C., Emerson, M., & Altman, D. G. (2010). Improving bioscience research reporting: the ARRIVE guidelines for reporting animal research. *PLoS Biology*, *8*(6), e1000412. https://doi.org/10.1371/journal.pbio.1000412

Chapter 4

Modification to the Rice-Vannucci perinatal hypoxic-ischaemic encephalopathy model in the P7 rat improves the reliability of cerebral infarct development after 48 hours

Published: Journal of Neuroscience Methods

Modification to the Rice-Vannucci perinatal hypoxic-ischaemic encephalopathy model in the P7 rat improves the reliability of cerebral infarct development after 48 hours

Adam B. Edwards [1,2,3], Kirk W. Feindel [4], Jane L. Cross [1,3,5], Ryan S. Anderton [1,2,5], Vincent W. Clark [1], Neville W. Knuckey [1,3,5], Bruno P. Meloni [1,3,5]

[1] Perron Institute for Neurological and Translational Science, Nedlands, Western Australia

[2] School of Health Sciences, The University of Notre Dame Australia, Fremantle, Western Australia

3 Department of Neurosurgery, Sir Charles Gardiner Hospital, Nedlands, Western Australia

[4] Centre for Microscopy Characterisation and Analysis, The University of Western Australia, Nedlands, Western Australia

[5] Centre for Neuromuscular and Neurological Disorders, The University of Western Australia, Nedlands, Western Australia

Author contributions

Adam Edwards: 76%

Kirk Feindel: 5%

Jane Cross: 3%

Ryan Anderton: 3%

Vincent Clark: 3%

Neville Knuckey: 5%

Bruno Meloni: 5%

Signed..... Signed.....

Adam Edwards Bruno Meloni (coordinating supervisor)

Journal of Neuroscience Methods 288 (2017) 62–71

Contents lists available at ScienceDirect

Journal of Neuroscience Methods

journal homepage: www.elsevier.com/locate/jneumeth

Modification to the Rice-Vannucci perinatal hypoxic-ischaemic encephalopathy model in the P7 rat improves the reliability of cerebral infarct development after 48 hours

Adam B. Edwards[a,b,c,*], Kirk W. Feindel[d], Jane L. Cross[a,c,e], Ryan S. Anderton[a,b,e], Vincent W. Clark[a], Neville W. Knuckey[a,c,e], Bruno P. Meloni[a,c,e]

[a] Perron Institute for Neurological and Translational Science, Nedlands, 6009, Western Australia, Australia
[b] School of Health Sciences, The University of Notre Dame Australia, Fremantle, 6160, Western Australia, Australia
[c] Department of Neurosurgery, Sir Charles Gardiner Hospital, QEII Medical Centre, Nedlands, 6009, Western Australia, Australia
[d] Centre for Microscopy, Characterisation and Analysis, The University of Western Australia, Nedlands, 6009, Western Australia, Australia
[e] Centre for Neuromuscular and Neurological Disorders, The University of Western Australia, Nedlands, 6009, Western Australia, Australia

HIGHLIGHTS

- An improved surgical procedure to reduce infarct volume variability.
- Procedure involves ligation of the common and external carotid arteries (CCA/ECA).
- The method abolishes communicational blood flow through internal carotid artery.
- CCA/ECA occlusion plus hypoxia improves infarct volume standard deviation.
- CCA/ECA occlusion plus hypoxia improves functional assessment reliability.

ARTICLE INFO

Article history:
Received 3 February 2017
Received in revised form 19 June 2017
Accepted 20 June 2017
Available online 23 June 2017

Keywords:
Neonatal ischaemia
Brain ischaemia
Perinatal hypoxia
Cerebral blood flow
Angiography
Arterial spin labelling
Animal models

ABSTRACT

Background: The Rice-Vannucci model of hypoxic-ischaemic encephalopathy (HIE) has been associated with a high degree of variability with respect to the development of cerebral infarction and infarct lesion volume. For this reason, we examined the occurrence of communicational blood flow within the common carotid (CCA), internal (ICA), and external (ECA) carotid arteries following CCA occlusion as a source of variability in the model.
New method: We propose a novel modification to the Rice-Vannucci model, whereby both the CCA and ECA are permanently ligated; mitigating communicational blood flow.
Results: Using magnetic resonance angiography, phase-contrast velocity encoding, and pulsed arterial spin labelling, the modified Rice-Vannucci model (CCA/ECA occlusion) was demonstrated to mitigate communicational blood flow, whilst significantly reducing ipsilateral hemispherical cerebral blood flow (CBF). Comparatively, the original Rice-Vannucci model (CCA occlusion) demonstrated anterograde and retrograde blood flow within the ICA and CCA, respectively, with a non-significant reduction in ipsilateral CBF. Furthermore, CCA/ECA occlusion plus hypoxia (8% O_2/92% N_2; 2.5 h) resulted in 100% of animals presenting with an infarct (vs 87%), significantly larger infarct volume at 48 h (18.5% versus 10.0%; $p < 0.01$), reduced standard deviation (± 10% versus ± 15%), and significantly worsened functional outcomes when compared to CCA occlusion plus hypoxia.
Comparison with existing method: We compared a modified Rice-Vannucci model (CCA/ECA occlusion ± hypoxia) to the commonly used Rice-Vannucci model (CCA occlusion ± hypoxia).
Conclusion: This study demonstrates that CCA/ECA occlusion in the Rice-Vannucci model of HIE reduces infarct volume variability by limiting communicational blood flow.

1. Introduction

Perinatal hypoxic-ischaemic encephalopathy (HIE) occurs at a rate of 1–3 per 1000 live births, with the resulting brain injury

* Corresponding author at: Perron Institute for Neurological and Translational Science, QEII Medical Centre, 8 Verdun St, Nedlands, Western Australia, 6009, Australia.
E-mail address: adam.edwards1@my.nd.edu.au (A.B. Edwards).

http://dx.doi.org/10.1016/j.jneumeth.2017.06.016
0165-0270/

causing death or neurological sequelae such as cerebral palsy, epilepsy, cognitive/behavioural disorders, and mental retardation (Graham et al., 2008; Kurinczuk et al., 2010; Vannucci and Perlman, 1997). Currently, while neonatal hypothermia can improve outcomes in the term infant (≥37 weeks gestation), there is an urgent need for the development of a safe and effective pharmacological neuroprotective and/or neuroregenerative agent that can be easily applied following HIE. The development of any new therapies for HIE requires a reliable and reproducible animal model that can be used for the assessment of potential neuroprotective or neuroregenerative agents, as well as pathophysiological cascades.

The HIE model in the 7-day-old (P7) rat first described by Rice et al. (1981), commonly referred to as the Rice-Vannucci model, is by far the most commonly used model for perinatal neuroprotection, neuroregenerative, and pathophysiological studies (Rice et al., 1981; Ditelberg et al., 1996; Sheldon et al., 1996; McQuillen et al., 2003). Reliable and reproducible injury development is imperative for any ischaemic brain injury model, including HIE. In this regard the Rice-Vannucci model is widely reported to be associated with variable outcomes in terms of infarct presence, infarct volume size, and by extension, functional outcomes (Rice et al., 1981; Ota et al., 1997; Palmer et al., 1990, 1993; Silverstein et al., 2016; Hagberg et al., 1994; Ashwal et al., 2007; Okusa et al., 2014).

Whilst a number of potential sources of variability within the Rice-Vannucci model have been reported (Table 1), one additional source of variability in both neonatal and adult ischaemic brain injury models can be attributed to cerebral collateral circulation via the circle of Willis and cerebral anastomoses. Cerebral collateral circulation can stabilise cerebral blood flow following vessel occlusion and/or haemodynamic compromise. For example, following common carotid artery (CCA) occlusion, compensatory blood flow is redistributed to the affected brain region through the circle of Willis. Similarly, in the Rice-Vannucci model, while permanent CCA occlusion is thought to impede blood flow through the internal carotid artery (ICA) and the external carotid artery (ECA) branches, retrograde perfusion is reported to occur from the ECA to the ICA, thereby reperfusing cerebral tissue supplied by the ICA (Bates et al., 2003). This retrograde perfusion occurs through two routes: firstly, via facial, orbital, and meningeal branches, originating from the ECA providing retrograde collateral connections between the ECA and the ICA (Fig. 1) (Cuccione et al., 2016); and secondly, via collateral blood flow through the ECA by anastomotic branches with the superior and inferior thyroidal, or occipital arteries (Fig. 1) (Nikanfar et al., 2004).

Against this background and in light of the variability seen in infarct development associated with the Rice-Vannucci model, the aim of this study was to investigate the presence of retrograde and anterograde blood flow through the CCA and ICA respectively, following CCA occlusion and CCA/ECA occlusion in P7 Sprague-Dawley rats. To investigate collateral circulation we performed magnetic resonance imaging (MRI) experiments to examine CBF following the standard Rice-Vannucci CCA occlusion. To improve infarct development reproducibility in the Rice-Vannucci model we modified the procedure by occluding the CCA in addition to the ECA (hereafter referred to as CCA/ECA occlusion; Fig. 1).

2. Materials and methods

All experimental procedures in this study adhered to the guidelines approved and specified by the Animal Ethics Committee of the University of Western Australia, in accordance with the Policies and Guidelines of the National Health and Medical Research Council, Australia.

2.1. Rice-Vannucci and modified HIE surgical models

Unsexed, P7 Sprague-Dawley rat pups (Animal Resource Centre, Murdoch, Australia) with a body weight of 13–16 g were used. Litters were culled to a maximum of 10 pups per litter to facilitate uniform growth without littermate competition. Rat pups were anaesthetised using isoflurane (5% induction, 1–2% maintenance) in 100% oxygen, while on a heating pad (37 °C); the duration of anaesthesia from induction to beginning of recovery did not exceed 10 min. Through a 1 cm mid-line ventral incision, the right common, internal, and external carotid arteries were exposed and isolated from the vagus nerve, venous circulation, and carotid body. For the Rice-Vannucci CCA occlusion model, the right CCA was permanently ligated using 6–0 silk sutures, while for the CCA/ECA occlusion model, the right CCA and ECA were permanently ligated using 6-0 silk sutures. The wound was closed using Vetbond (3 M, Maplewood, USA) and the animals allowed to recover on 100% oxygen for 5 min on a heating pad. Animals were provided with analgaesia (pethidine, 5 mg/kg; intraperitoneally) immediately before cessation of anaesthesia. Sham-operated animals underwent the same operative procedure except the exposed carotid arteries were not ligated.

Rat pups were returned to their dam for 1 h before the commencement of hypoxia. Hypoxia consisted of placing up to 5 pups in an airtight container (approximate volume: 4 L) and exposing them to humidified and warmed hypoxic gas (8% O_2/92% N_2; 3 L/min) for 2.5 h. The container was placed inside an incubator with an ambient air temperature of 35 °C, ensuring a core body temperature of 36–37 °C, periodically monitored using an infrared thermometer.

To avoid any bias in outcomes of animals undergoing the different surgical procedures for HIE, each batch of animals exposed to hypoxia consisted of 2–3 animals with CCA occlusion and 2–3 animals with CCA/ECA occlusion. Additionally, operator was blinded to surgical procedure groups for infarct volume analysis and functional assessment.

Following hypoxia-ischaemia, animals were placed on a heating pad (37 °C) for 5 min in a normoxic environment before being placed back with the dam. To avoid hypothermia, rat cages were housed at 26–28 °C during the study.

2.2. Infarct volume assessment

Forty-eight hours after hypoxia-ischaemia, animals were euthanased by pentobarbital overdose (50 mg/kg; intraperitoneally) and infarct volume determined by preparing 2 mm thick coronal brain slices, and incubating in 3% 2,3,5-triphenyltetrazolium chloride (TTC; Sigma Aldrich, St. Louis, USA) at 37 °C for 20 min, followed by fixation in 4% formalin at room temperature overnight. Digital images of coronal sections were acquired using a colour scanner and analysed, using ImageJ software (3rd edition, NIH, Bethesda, USA). Total infarct volume was determined by measuring areas of infarcted tissue on both sides of the 2 mm sections. Infarct measurements were corrected for oedema using the formula:

$$\text{Corrected infarct volume} = \left(\frac{\text{Contralateral hemisphere volume}}{\text{Ipsilateral hemisphere volume}}\right)\left(\text{Infarct volume}\right)$$

Where ipsilateral hemisphere indicates hemisphere with observable infarct and contralateral hemisphere indicates hemisphere with no observable infarct. Final infarct data is expressed as

Table 1
Proposed sources of infarct variability within Rice-Vannucci HIE model.

Proposed variability	Animal	Model	HI parameters	Results	Refs.
Strain	C57BL/6, 129SVJ, BALB/c, CD1, and FVB	LPS – HIE	8% O_2/92% N_2; 30 min	Varied ischaemic lesion development. Small infarct (129SVJ & C57BL/6), moderate infarct (BALB/c), and severe infarct (CD1 & FVB).	Rocha-Ferreira et al. (2015)
Litter size	Sprague-Dawley; P7, P8, and P9	HIE	8% O_2/92% N_2; 135 min	Varied ischaemic lesion development. Non-culled litters reported uneven distribution of infarct lesions (absent, mild, moderate, and severe infarct). Culled litters reported severe and moderate infarcts. Weight of pups had no influence on ischaemic lesion.	Oakden et al. (2002)
Resuscitation	Wistar; P10	HIE	8% O_2/92% N_2; 75 min	Resuscitation of pups in 100% oxygen did not affect short term neuropathological outcomes.	Wood et al. (2016a)
Isoflurane	Sprague-Dawley; P7 and P10	HIE	8% O_2/92% N_2; 150 min	Exposure time of <9 min to isoflurane improves development of ischaemic lesion, whilst isoflurane exposure time of >9 min reduces ischaemic injury.	Chen et al. (2011)
Blood sugar	Wistar; P7	HIE	8% O_2/92% N_2; 60 min. Bilateral CCA occlusion	Increased blood glucose levels after HI reduces ischaemic injury	Hattori and Wasterlain, (1990)
Hypothermia	Wistar; P7	HIE	8% O_2/92% N_2; 100 min	Lower temperature (30–33.5 °C) after HI reduced ischaemic injury	Wood et al. (2016b)
Maternal diet	Wistar; P7	HIE	8% O2/92% N2; 90 min	Maternal diet does not affect development of ischaemic lesion. Maternal diet pre- and postnatally influenced functional recovery after hypoxia-ischaemia.	Barks et al. (2017)

All hypoxic-ischaemic (HI) parameters indicate unilateral occlusion of the CCA, unless otherwise stated. O_2 = oxygen, N_2 = nitrogen, and min = minutes, Refs = references.

percentage infarct volume compared to whole brain (minus cerebellum).

2.3. Functional testing

To determine if the development of brain infarct was associated with reduced sensorimotor function, three neurological tests (righting reflex, negative geotactic response, and rope-hang) were performed at 48 h after hypoxia-ischaemia. For three consecutive days before surgery (P4 – 6; inclusive), pups were accustomed to behavioural assessments with a target inclusion range of ≤2 s for the righting reflex and ≤30 s for the negative geotactic response. Any animal that did not record responses within these parameters at P7 (day of surgery) were excluded from the experiment. All of these reflexes are highly reproducible throughout the murine pre-weaning period (<P30) and are strain- and gender-independent (Heyser, 2004). Each animal was given three attempts to complete each sensorimotor task, with 5 min between each attempt. Testing of all reflexes was performed on a board covered with a tightly-stretched close knit-fabric, to ensure adequate friction.

The righting reflex involved placing pups in a supine position, and measuring the time (in sec) required to flip to the prone position. The negative geotactic response involved placing pups facing down-slope, on a 45° angled surface, and measuring the time required (in sec) for the animal to turn 150° upslope. Rope-hang was performed by suspending pups by their forelimbs on a 2 mm diameter steel wire suspended 20 cm above a foam surface, and recording the time taken (in sec) for the animal to fall to the foam surface.

2.4. Magnetic resonance imaging

Animals were placed into three groups for imaging studies: (i) sham-operated, (ii) CCA occlusion, and (iii) CCA/ECA occlusion. Animals assigned to MRI were not exposed to hypoxic conditions (carotid vessel occlusion only). Imaging occurred on the day of surgery (P7). Each animal was anaesthetised with isoflurane (5% induction, 0.5–1.5% maintenance) in 100% oxygen; the duration of anaesthesia from induction to euthanasia did not exceed 60 min.

MRI scans were performed with a Bruker BioSpec 94/30 US/R magnet (B_0 = 9.4 T), Avance III HD console, BGA-6SHP gradients, ParaVision 6.0.1 software, 35 mm inner diameter H-1 quadrature transmit-receive volume coil, and mouse cradle. To determine the position of the brain in the magnet, a FLASH based scout scan was performed over a field-of-view (FOV) = 50 mm × 50 mm, with repetition time (TR) = 200 msec, echo time (TE) = 3.8 msec, and five interlaced 1.5 mm slices with a 1.0 mm gap, in three orthogonal directions. A 2D multi-slice multi-echo sequence was used to obtain a series of T2-weighted images in the sagittal plane, with a FOV = 36 mm × 27 mm, in-plane pixel size = 150 μm × 150 μm, from 700 μm thick interlaced slices, with TR = 2400 msec, echo spacing (ESP) = 8 msec, at TE = 12 msec and 60 msec, and fat suppression. Time-of-flight (TOF) angiography (Reese et al., 1999; Beckmann, 2000) was completed using a 3D FLASH scan with coronal orientation, FOV = 24 mm × 22 mm × 18 mm, voxel size = 80 μm × 80 μm × 150 μm, TR = 12 msec, TE = 2 msec, flip angle (α) = 20°, and fat suppression. Velocity mapping was completed with phase-contrast angiography (Dumoulin and Turski, 2000) using the FLOWMAP sequence, with coronal slices positioned to cover the CCA, ICA, and ECA, with FOV = 20 mm × 20 mm, in-plane pixel size = 80 μm × 80 μm, from 10 interleaved 700 μm thick slices with a gap of 250 μm, and a velocity encoding range of +/−35 cm/sec. Lastly, a pulsed arterial spin labelling (PASL) (Detre et al., 1992) perfusion scan was completed with a fluid attenuation inversion recovery (FAIR) (Kim, 1995), single-shot, spin-echo echo-planar imaging (SE-EPI) sequence. Prior to the EPI scan B_0 field shimming was completed using the Bruker MAPSHIM routine according to standard procedures. The PASL scan was completed for a single 1 mm coronal slice positioned over the cerebral territory of the middle cerebral artery (Supplementary Fig. 1), with FOV = 22 mm × 22 mm, in-plane pixel size = 200 μm × 200 μm, with fixed recovery time = 12 s, TE = 12.5 msec, α = 90°, a set of eight inversion times (Xie et al., 2008) (30, 350, 700, 1050, 1400, 1750, 2100, and 2450 msec), and fat suppression.

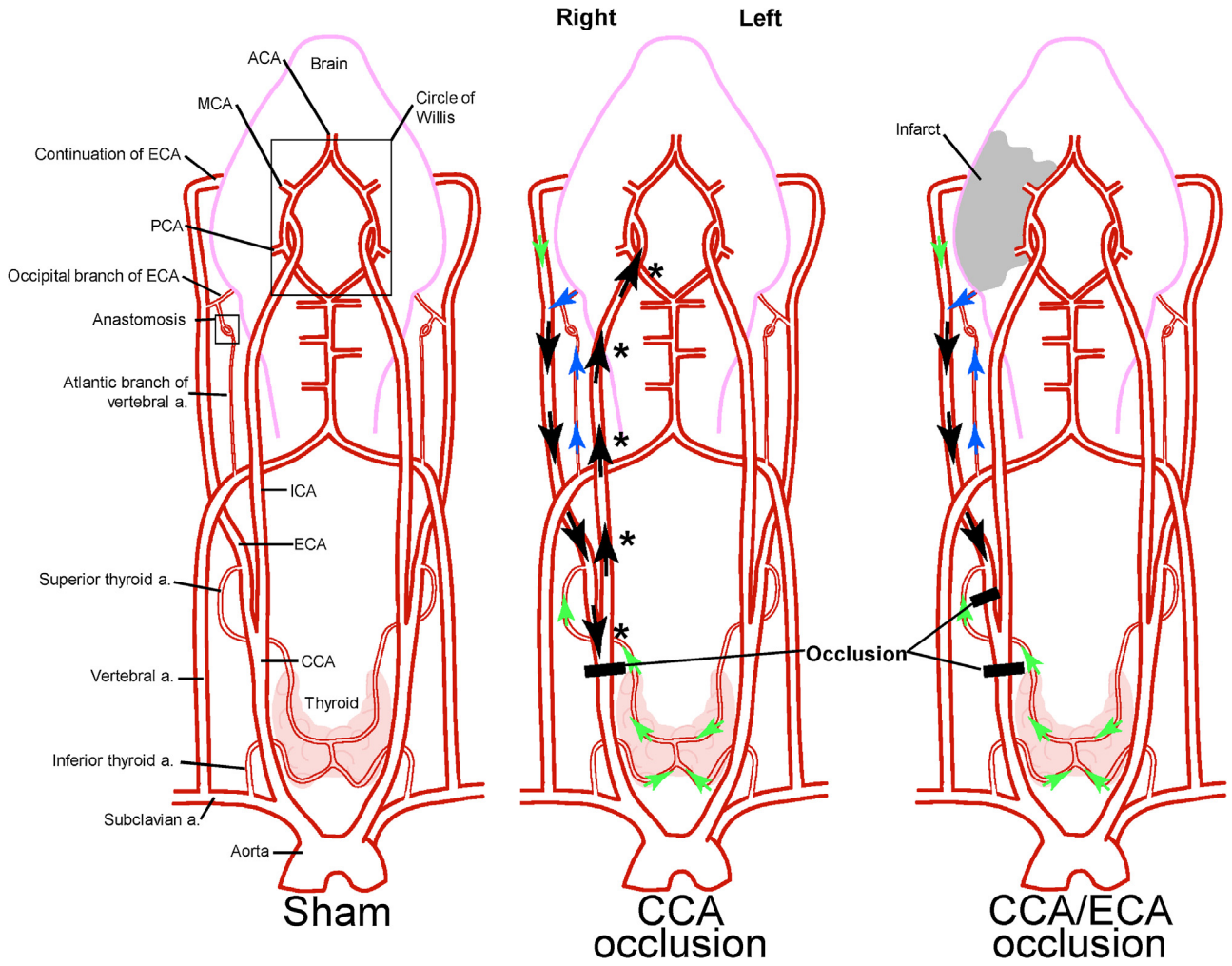

Fig. 1. Diagrammatic representation of communicational and anastomotic blood flow for CCA occlusion and CCA/ECA occlusive surgical procedures (image not to scale). Green arrows (in colour image) indicate path of communicational blood flow. Blue arrows (in colour image) indicate path of anastomotic blood flow. Black arrows indicate path of net blood flow (combined communicational and anastomotic flow; * indicates blood flow within ICA). a. = artery. Continuation of the ECA includes facial, orbital, and meningeal arteries. (For interpretation of the references to colour in this figure legend, the reader is referred to the web version of this article.)

Further imaging parameters are provided in the Supplementary Information.

During MRI procedures the temperature and respiration of the animal was monitored using a Model 1030 Monitoring System (Small Animal Instruments Inc, New York, USA) and animal temperature was maintained using a heating blanket connected to a recirculating water bath (ThermoFisher, Massachusetts, USA).

2.5. Processing of FAIR-EPI data

Analysis and evaluation of the regional CBF was completed within ParaVision 6.0.1 using the manufacturer provided macro 'ASL Perfusion Processing' that calculates perfusion based on the T_1 difference method according to (Herscovitch and Raichle, 1985; Kober et al., 2004):

$$rCBF = \lambda \left(\frac{T_{1nonsel}}{T_{1blood}}\right)\left(\frac{1}{T_{1sel}} - \frac{1}{T_{1nonsel}}\right)$$

where λ is the blood partition coefficient assumed to be 0.89 mL g^{-1} for mice (Leithner et al., 2010), $T_{1nonsel}$ and T_{1sel} are the longitudinal relaxation times of blood calculated from the images with non-selective or slab-selective inversions, and T_{1blood} = 2.4 s at a magnetic field strength of 9.4 T (Dobre et al., 2007). The rCBF values are expressed in mL of blood per 100 g of tissue per minute, and mean values and standard deviations for specific regions were evaluated using manually defined regions-of-interest using T1-weighted images as an anatomical guide (Supplementary Fig. 2).

2.6. Statistical analysis

Mean percentage infarct volume measurement and data from functional tests were evaluated by non-paired t-test. Values of $p < 0.05$ were considered statistically significant. CBF data were evaluated within groups using paired t-test. Value of $p < 0.05$ were considered statistically significant. Additionally, functional assessment and CBF data were evaluated between groups using a pairwise comparison analysis of variance (ANOVA) followed by Bonferroni post hoc analysis. Values of $p < 0.05$ were considered as significant.

3. Results

3.1. Time-of-flight magnetic resonance angiography (TOF-MRA)

Time-of-flight magnetic resonance angiography was performed in animals 3–6 h following surgery for CCA occlusion, CCA/ECA

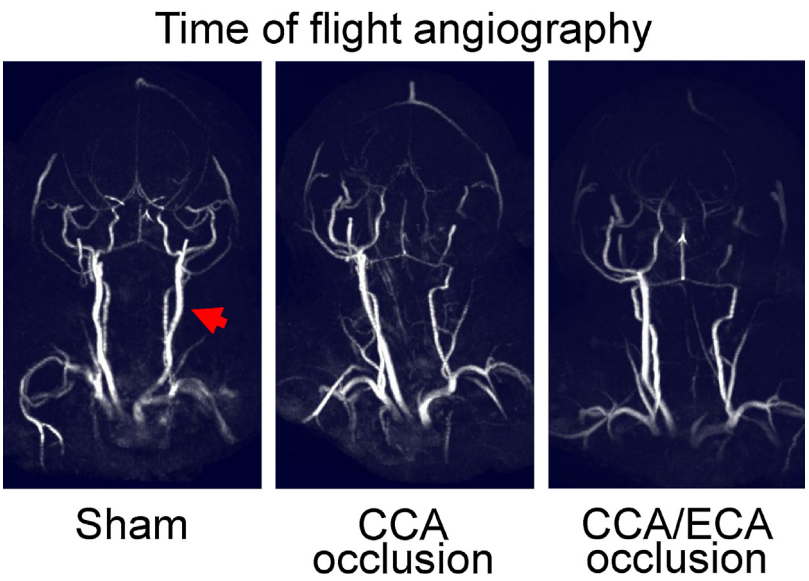

Fig. 2. Maximum intensity projections of time-of-flight magnetic resonance angiography depicting arterial flow from caudal to rostral direction in sham, CCA occlusion, or CCA/ECA occlusion animals. Arrow represents the presence of the common carotid artery.

occlusion, or sham procedures (animals were not exposed to hypoxia) to qualitatively visualise blood flow within vessels of the neck and caudal brain. Representative images are presented in Fig. 2. Despite the aforementioned significant differences between the two surgical artery occlusion models, animals undergoing CCA occlusion or CCA/ECA occlusion procedures demonstrated the absence of a magnetic resonance signal in the right CCA; confirming successful surgical occlusion of the CCA or CCA/ECA when compared to the sham group.

3.2. Phase-contrast velocity encoding

Phase-contrast velocity encoding was performed in animals 3–6 h following surgery for CCA occlusion, CCA/ECA occlusion, or sham procedures (animals were not exposed to hypoxia) to quantitatively measure blood flow velocities (cm/sec) within the CCA, ICA, and ECA. In sham animals, the flow of blood within the CCA occurs in an anterograde direction (from caudal to rostral) and continues into the ICA and ECA. In animals receiving either CCA or CCA/ECA occlusion, cessation of anterograde flow should occur due to artery occlusion. Data and representative images are presented in Fig. 3b and c . Despite the occlusion of the right CCA, one animal that underwent the CCA occlusion procedure demonstrated blood flow velocities within the right CCA (Fig. 3b and c), and right ICA (Fig. 3b). In comparison, all animals that underwent the CCA/ECA occlusion procedure reported no blood flow within the CCA (Fig. 3c).

The aforementioned animal within the CCA occlusion group recorded a retrograde blood flow (-6.363 ± 2.54 cm/sec; Fig. 3b and c) within the right CCA and anterograde blood flow (4.543 ± 0 cm/sec; Fig. 3c) within the right ICA. Between CCA occlusion, CCA/ECA occlusion, and sham animal groups, no statistical difference was observed in the distribution of blood flow velocities within the non-occluded left CCA (19.87 ± 9.45 cm/sec, 22.8 ± 9.09 cm/sec, and 20.52 ± 9.49 cm/sec respectively; Fig. 3c). Additionally, there was no significant difference between right and left CCA velocities within the sham animal group (Fig. 3c).

Variability in mean velocities in the left CCA (non-occluded) following CCA occlusion, CCA/ECA occlusion, and sham procedures, whilst uniform across all groups, is likely to reflect the angle of the velocity encoding slice and/or depth of anaesthesia of the animals.

3.3. Pulsed arterial spin labelling (PASL)

Pulsed arterial spin labelling was performed in animals 3–6 h following surgery for CCA occlusion, CCA/ECA occlusion, or sham procedures (animals were not exposed to hypoxia) to quantitatively measure the cerebral blood flow (CBF) (ml/100 g/min) within a coronal slice at the level of the middle cerebral artery (determined using TOF-MRA). Representative images and data are presented in Fig. 4a and b. The occlusion of the right CCA or CCA/ECA resulted in reduced CBF in the ipsilateral (right) hemisphere when compared to the non-occluded (left) hemisphere (12.7 mL/100 g/min; $p = 0.02$ and 21.6 mL/100 g/min; $p = 0.002$, respectively; Fig. 4a and b).

The CCA/ECA occlusion demonstrated a significant reduction in right hemispherical CBF when compared to the sham ($p = 0.03$). Comparatively, the CCA occlusion did not demonstrate a significant reduction in right hemispherical CBF when compared to the sham. Additionally, there was no significant difference in left CBF between groups. When comparing total CBF (combined left and right hemispheres) there is a trend that depicts a reduction in CBF between surgical occlusion groups when compared to the sham group (Fig. 4b).

3.4. Infarct volume measurements after HIE

Data on infarct volume for animals undergoing CCA occlusion or CCA/ECA occlusion combined with hypoxia are presented in Fig. 5a and b. These results demonstrate that the CCA/ECA occlusion HIE model, when compared to the CCA occlusion HIE model, results in 100% of animals presenting with an observable infarct (versus 87%), a significantly larger infarct volume (18.5% versus 10.0%; $p < 0.01$) and a reduced standard deviation ($\pm 10\%$ versus $\pm 15\%$).

Data on infarct volume for animals undergoing CCA or CCA/ECA occlusion alone, and CCA/ECA occlusion plus hypoxia (2.5 h) are presented in Fig. 6a and b. These results demonstrate that vessel occlusion in combination with hypoxia (HIE) is required to generate an observable cerebral infarct. Animals with CCA/ECA occlusion plus hypoxia produced a significant infarct volume compared with animals undergoing CCA or CCA/ECA occlusion only (13.9% versus 0% and 0% respectively; $p < 0.01$).

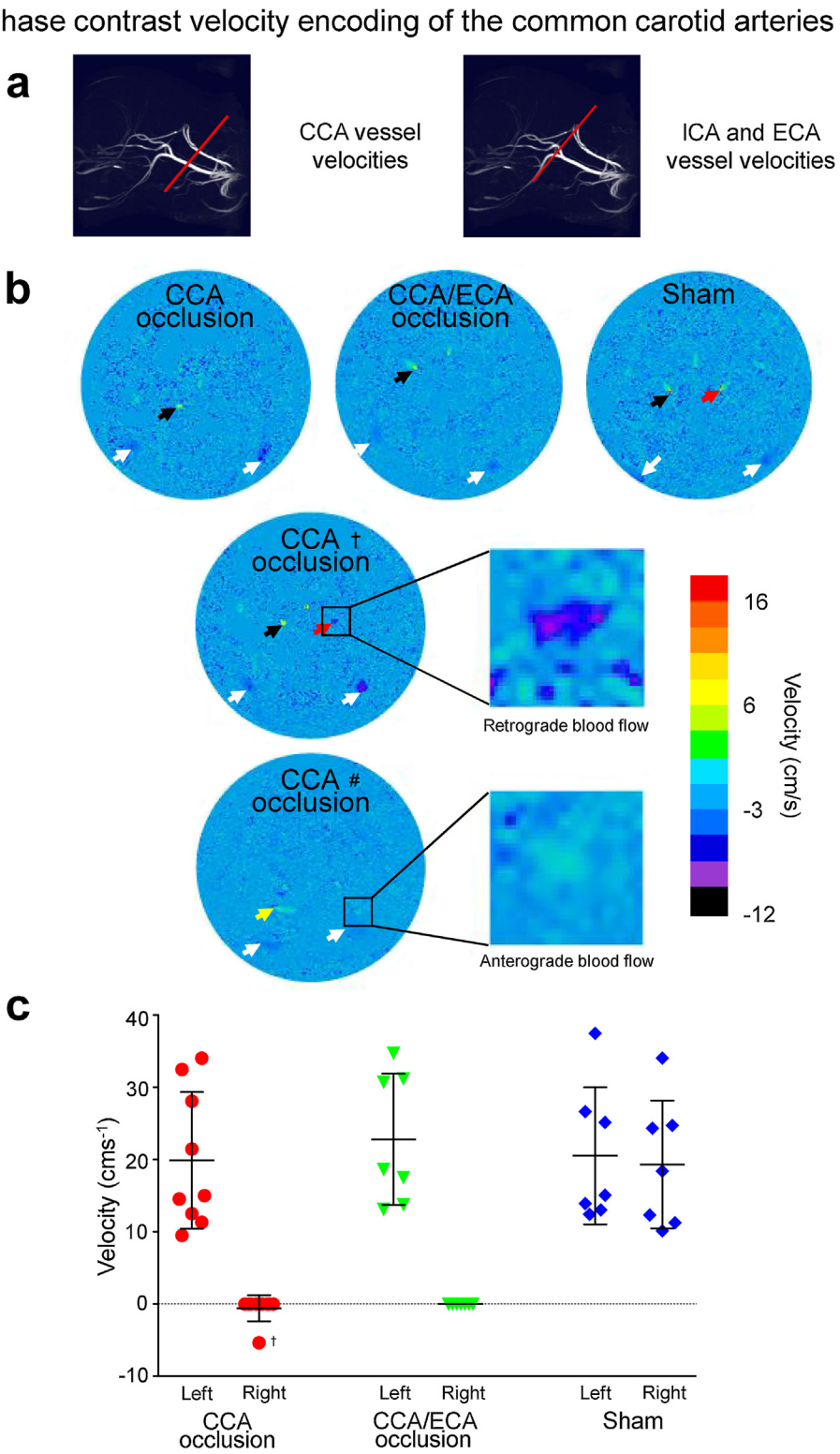

Fig. 3. Velocity analysis of blood through the pre- and post-bifurcated left and right CCA. (a) Grayscale time-of-flight angiography demonstrating coronal slice positioning of phase-contrast velocity encoding FLOWMAP sequence. Coronal slice positioning of CCA, ICA, and ECA mean vessel velocities (b) representative coronal section using 2D phase-contrast velocity encoding of the CCA. (c) Individual blood velocities through the left and right CCA represented as mean ± SD. † Denotes animal with observable reversal of blood within the CCA. # Denotes animal with observable blood flow within the ICA. Black arrow indicates left CCA, white arrow indicates venous jugular flow, and yellow arrow indicates left ICA. (For interpretation of the references to colour in this figure legend, the reader is referred to the web version of this article.)

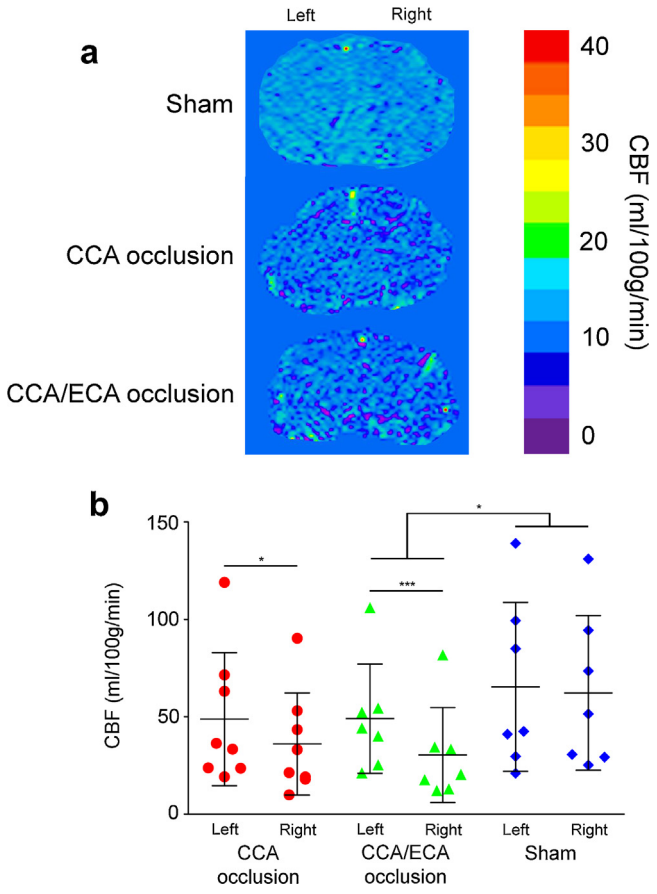

Fig. 4. Cerebral blood flow (CBF) (mL/100 g/min) measured by PASL. Coronal CBF maps obtained at the level of the middle cerebral artery (bregma 1.32). (a) Representative CBF maps in CCA occlusion, CCA/ECA occlusion, and sham animals. (b) Individual CBF values of left and right hemispheres; CBF values are mean ± SD. $^{*}p < 0.05$ and $^{***}p < 0.01$.

3.5. Functional outcomes after HIE

Data on functional outcomes for animals undergoing CCA or CCA/ECA occlusion combined with hypoxia are presented in Fig. 5c. Animals undergoing the CCA or CCA/ECA occlusion HIE model procedure displayed a significant level of reduced sensorimotor function as assessed with the rope-hang test ($p < 0.01$ and $p < 0.001$ respectively; Fig. 5c) compared to sham animals. In addition, animals subjected to the CCA or CCA/ECA occlusion HIE model displayed reduced sensorimotor coordination in the negative geotactic response, and increased reaction times for righting reflex ($p < 0.05$ and $p < 0.001$, respectively; Fig. 5c) when compared to sham. Animals subjected to the CCA/ECA occlusion HIE model displayed a significant increase in negative geotactic response time ($p < 0.05$; Fig. 5c) when compared to sham. Conversely, animals subjected to the CCA occlusion HIE model did not display a significant increase in negative geotactic response when compared to sham (Fig. 5c).

In addition, functional parameters for animals undergoing CCA or CCA/ECA occlusion alone, and CCA/ECA occlusion plus hypoxia are presented in Fig. 6c. Animals undergoing CCA or CCA/ECA occlusion only did not display any significant deviation in functional outcomes compared to sham animals. In contrast, animals subjected to CCA/ECA occlusion plus hypoxia displayed reduced rope-hang times ($p < 0.02$; Fig. 6c) and trends for negative responses in righting reflex and negative geotactic response when compared to sham animals.

4. Discussion

The Rice-Vannucci HIE model, which is arguably the most commonly used pre-clinical model to replicate perinatal HIE, has long been recognised as being affected by high variability with respect to cerebral infarct volume, with infarcts often graded as absent, mild, moderate, or severe (Ota et al., 1997; Okusa et al., 2014; Cuccione et al., 2016; Liu et al., 2009; Noh et al., 2006). In the present study, we have demonstrated that the permanent occlusion of the CCA and ECA and exposure to hypoxia in P7 rats induces a more reproducible and larger cerebral infarct compared to rats subjected to CCA occlusion and hypoxia (i.e. the original Rice-Vannucci model). In addition, histological outcomes in the CCA/ECA occlusion and hypoxia HIE model corroborated functional outcomes. Furthermore, we have confirmed that CCA occlusion or CCA/ECA occlusion alone does not elicit an observable cerebral infarct.

While many explanations have been proposed to account for the inconsistencies associated with the Rice-Vannucci procedure (Table 1), we were able to confirm, using MRI studies, that collateral blood supply to the affected hemisphere is a significant source of variability in the model. For example, using MRA phase-contrast velocity encoding, retrograde blood flow within the CCA and anterograde blood flow within the ICA were demonstrated to exist following CCA occlusion in some cases. The source of retrograde CCA and anterograde ICA flow is from collateral and/or anastomotic flow from the ECA. In support of this, MRI studies using the CCA/ECA occlusion procedure demonstrated a more reliable disruption in cerebral haemodynamics, through the absence of blood flow within the right CCA, ECA, and ICA.

To date, the collateral and/or anastomotic blood flow within the immature rodent has not been robustly characterised. There are significant similarities between human and murine extracranial and cerebral vessel anatomy (Cuccione et al., 2016; Yamasaki, 1990), which are used to determine the source of collateral and/or anastomotic blood flow within the Rice-Vannucci model (Fig. 1). Specifically, following CCA occlusion, the patency of the ipsilateral hemisphere can be maintained through extracranial collateral vessels, supplying blood flow into the ECA in a retrograde manner, maintaining the anterograde flow within the ICA (Nikanfar et al., 2004; Kaspera et al., 2005; Bajkó et al., 2013). In humans, extracranial collateral blood flow originates from the ipsilateral thyrocervical trunk (via subclavian artery), vertebral artery, occipital artery, from the contralateral ECA (via facial occipital, and maxilla branches), and from occipital artery anastomosis to the vertebral artery (Bajkó et al., 2013; Tsai et al., 2005; Parthenis et al., 2008; Levine and Welch, 1989; Alexander et al., 2014; Suwanwela and Suwanwela, 1998). The commonly demonstrated collateral flow supplied by the leptomeningeal artery is not observed in the rat (Coyle and Jokelainen, 1982). In various animal models, the presence of collateral blood flow preserving the patency of the ICA has been reported. For example, in swine, occlusion of the CCA and ECA depletes anterograde blood flow within the ICA (Bates et al., 2003). Additionally, the presence of collateral blood supply preserving the patency of the ICA in P7 rodents has been reported following middle cerebral artery occlusion (Bonnin et al., 2011) and CCA occlusion (Choy et al., 2006).

With regards to the surgical approach taken in this study, the findings indicate that the occlusion of the ICA alone would have similar effects to occlusion of the CCA and ECA. Notwithstanding, the ICA is anatomically placed under the sternocleidomastoid muscle, which would require the muscle to be manipulated surgically to gain access to the ICA. Such surgical manipulation would predispose the sternocleidomastoid muscle to injury, potentially affecting the performance of the animal in motor functional tests and the ability to feed. Therefore, in our studies, occlusion of the CCA and ECA was chosen over occlusion of the ICA alone, which reduces

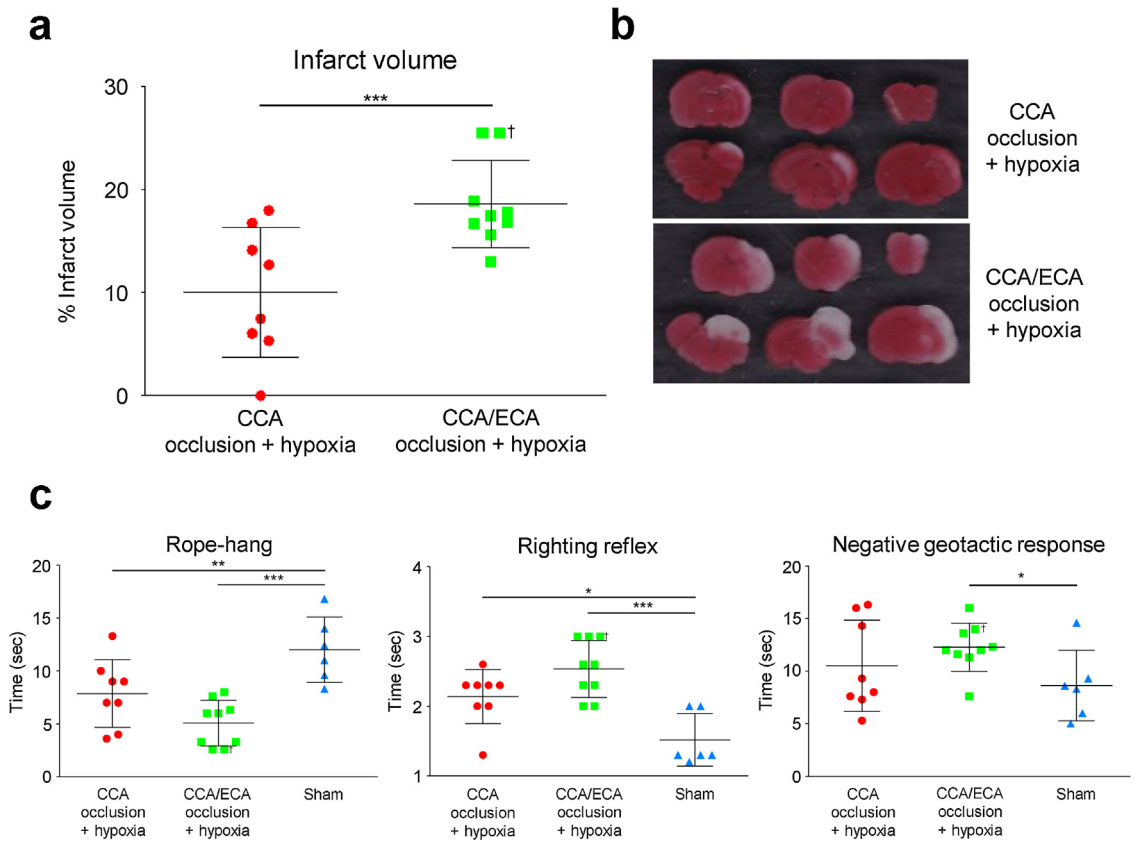

Fig. 5. Infarct volume analysis, representative images of coronal brain slices, and behavioural assessment 48 h after hypoxic-ischaemic insult. (a) Infarct volume analysis, represented as a percentage (%) infarct volume in relation to whole brain volume as determined 48 h after hypoxic-ischaemic insult. Values are mean ± SD. (b) Representative images of TTC stained coronal brain slices. (c) Functional assessments using rope-hang, righting reflex, and negative geotactic response tests 48 h after hypoxic-ischaemic insult. All animals received a combination of surgical occlusion and hypoxia. Rope-hang, time (sec = s) for animal to hold onto a rope. Righting reflex, Time (sec) for animal to rotate from supine to prone position. Negative geotactic response, time (sec) for animal to rotate 150° up a 45° slope. † Denotes animal that was assigned the largest infarct due to hemisphere liquefaction, which did not permit coronal brain slicing and infarct volume analysis. Time values are mean ± SD. $^{*}p < 0.05$, $^{**}p < 0.02$, and $^{***}p < 0.01$.

surgical time while depleting the anterograde or retrograde flow within the ICA.

To our knowledge, this is the first report that defines CBF using PASL following extracranial vessel occlusion in immature rats. The use of PASL is a non-invasive technique for the assessment of CBF in various rat stroke models (Baskerville et al., 2012). In line with previous studies (Buckley et al., 2015), using PASL we demonstrated that there is a bilateral reduction in CBF following CCA or CCA/ECA occlusion compared to sham surgical animals. Additionally, CCA or CCA/ECA occlusion results in a significant reduction in blood flow in the affected right hemisphere when compared to the unaffected left hemisphere. Furthermore, the CCA/ECA occlusion procedure resulted in a statistically significant ($p = 0.03$) reduction in CBF in the affected hemisphere when compared to the CBF of the sham.

The primary aim of this study was to confirm the superiority of the CCA/ECA occlusion HIE model through the mitigation of ICA patency, which was conclusively demonstrated by a significant reduction of CBF in the ipsilateral hemisphere. Despite the significant reduction in CBF of the CCA/ECA occlusion procedure, establishment of an ischaemic infarct lesion is unlikely, as CBF must fall below 18 mL/100 g/min to elicit ischaemia (Bouma and Muizelaar, 1995). In agreement with this, and in line with a previous study (Buckley et al., 2015), we have demonstrated that CCA/ECA occlusion in combination with hypoxia is required to elicit a cerebral infarct.

A limitation of this study is anaesthetisation using isoflurane, which can reduce mean arterial pressure and heart rate below conscious baselines at concentrations greater than 1.5% (Constantinides et al., 2011). With this in mind, animals assigned to PASL groups were not exposed to concentrations of isoflurane above 1.5%. Furthermore, mean arterial pressure is known to be independent of changes in CBF in sham animals (Manole et al., 2009). In addition, whilst the 48-h endpoint used in the present study is commonly used in neuroprotective, neuroregenerative and pathophysiological investigations, we acknowledge that additional characterization of the CCA/ECA occlusion HIE model at extended end points is required if the model is to be used for long-term studies.

5. Conclusion

The modification to the Rice-Vannucci surgical procedure through the ligation of the CCA and ECA is shown to improve model reproducibility in terms of mitigation of cerebral and communicational blood flow and improving reliability in infarct presence, infarct size, and behavioural outcomes.

Author's contributions

AE and JC contributed to animal procedures, post-surgical monitoring, functional assessment, infarct volume analysis, and statistical analysis. AE, KF, and VC contributed to magnetic resonance imaging procedures and results analysis. AE, RA, NK, and BM contributed to experimental design and manuscript preparation. All authors read and approved the final manuscript.

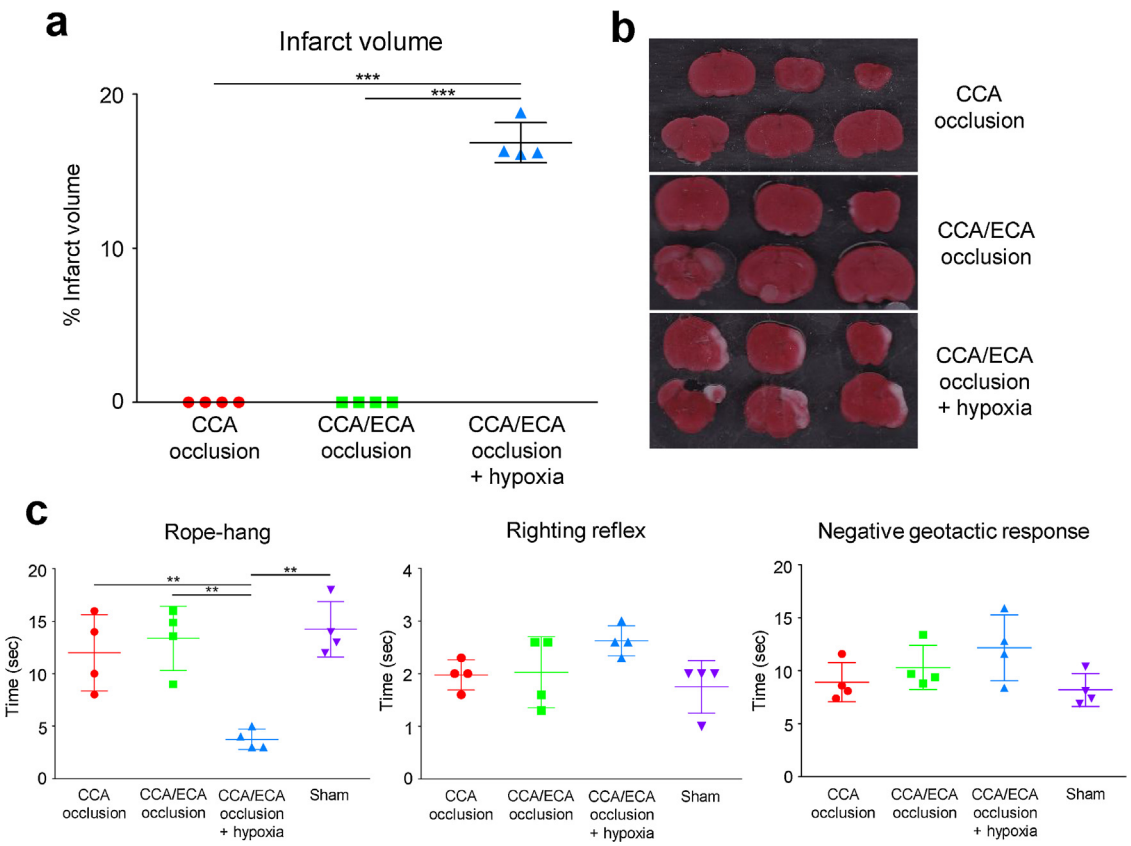

Fig. 6. Infarct volume analysis, representative images of coronal brain slices, and behavioural assessment of ischaemic (CCA or CCA/ECA occlusion) or hypoxic-ischaemic (CCA/ECA occlusion and hypoxia) injury 48 h after insult. (a) Infarct volume analysis, represented as a percentage (%) infarct volume in relation to whole brain volume as determined 48 h after ischaemic or hypoxic-ischaemic insult. Values are mean ± SD, $^{*}p < 0.01$ when compared between groups. (b) Representative images of TTC stained coronal brain slices from CCA occlusion only, CCA/ECA occlusion only, and CCA/ECA occlusion and hypoxia groups. (c) Functional assessments using rope-hang, righting reflex, and negative geotactic response tests 48 h after ischaemic or hypoxic-ischaemic insult. Rope-hang: time (sec = s) for the animal to hold onto a rope. Righting reflex: time (sec = s) for the animal to rotate from supine to prone position. Negative geotactic response: time (sec = s) for the animal to rotate 150° up a 45° slope. Time values are mean ± SD, $^{**}p < 0.02$, and $^{***}p < 0.01$.

Competing interests

The authors declare no competing interests with respect to the research, authorship, and/or publication of this article.

Acknowledgments

This study in part was supported by the Department of Neurosurgery, Sir Charles Gairdner Hospital, and a University of Notre Dame Australia RIS grant, and a Neurotrauma Research Program of Western Australia grant. The authors acknowledge the facilities and the scientific and technical assistance of the National Imaging Facility at the Centre for Microscopy, Characterisation and Analysis, The University of Western Australia, a facility funded by the University, State, and Commonwealth Governments. The authors thank Prof Norman Palmer for comments and suggestions regarding the manuscript.

Appendix A. Supplementary data

Supplementary data associated with this article can be found, in the online version, at http://dx.doi.org/10.1016/j.jneumeth.2017.06.016.

References

Alexander, M.D., English, J., Hetts, S.W., 2014. Occipital artery anastomosis to vertebral artery causing pulsatile tinnitus. J. Neurointerv. Surg. 6 (March (2)), e15.

Ashwal, S., Tone, B., Tian, H.R., Chong, S., Obenaus, A., 2007. Comparison of two neonatal ischemic injury models using magnetic resonance imaging. Pediatr. Res. 61 (January (1)), 9–14.

Bajkó, Z., Bălaşa, R., Moţăţăianu, A., Maier, S., Chebuţ, O.C., Szatmári, S., 2013. Common carotid artery occlusion: a case series. ISRN Neurol. 2013, 198595.

Barks, J.D., Liu, Y., Shangguan, Y., Djuric, Z., Ren, J., Silverstein, F.S., 2017. Maternal high-fat diet influences outcomes after neonatal hypoxic-ischemic brain injury in rodents. J. Cereb. Blood Flow Metab. 37 (January (1)), 307–318.

Baskerville, T.A., Mccabe, C., Weir, C.J., Macrae, I.M., Holmes, W.M., 2012. Noninvasive MRI measurement of CBF: evaluating an arterial spin labelling sequence with 99 m Tc- HMPAO CBF autoradiography in a rat stroke model. J. Cereb. Blood Flow Metab. 32 (10), 973–977.

Bates, M.C., Dorros, G., Parodi, J., Ohki, T., 2003. Reversal of the direction of internal carotid artery blood flow by occlusion of the common and external carotid arteries in a swine model. Catheter. Cardiovasc. Interv. 60 (October (2)), 270–275.

Beckmann, N., 2000. High resolution magnetic resonance angiography non-invasively reveals mouse strain differences in the cerebrovascular anatomy in vivo. Magn. Reson. Med. 44 (August (4)), 252–258.

Bonnin, P., Leger, P.-L., Deroide, N., Fau, S., Baud, O., Pocard, M., Charriaut-Marlangue, C., Renolleau, S., 2011. Impact of intracranial blood-flow redistribution on stroke size during ischemia-reperfusion in 7-day-old rats. J. Neurosci. Methods 198 (May (1)), 103–109.

Bouma, G.J., Muizelaar, J.P., 1995. Cerebral blood flow in severe clinical head injury. New Horiz. 3 (August (3)), 384–394.

Buckley, E.M., Patel, S.D., Miller, B.F., Franceschini, M.A., Vannucci, S.J., 2015. In vivo monitoring of cerebral hemodynamics in the immature rat: effects of hypoxia-ischemia and hypothermia. Dev. Neurosci. 37 (May (4–5)), 407–416.

Chen, H., Burris, M., Fajilan, A., Spagnoli, F., Tang, J., Zhang, J.H., 2011. Prolonged exposure to isoflurane ameliorates infarction severity in the rat pup model of neonatal hypoxia-ischemia. Transl. Stroke Res. 2 (September (3)), 382–390.

Choy, M., Ganesan, V., Thomas, D.L., Thornton, J.S., Proctor, E., King, M.D., van der Weerd, L., Gadian, D.G., Lythgoe, M.F., 2006. The chronic vascular and haemodynamic response after permanent bilateral common carotid occlusion in newborn and adult rats. J. Cereb. Blood Flow Metab. 26 (August (8)), 1066–1075.

Constantinides, C., Mean, R., Janssen, B.J., 2011. Effects of isoflurane anesthesia on the cardiovascular function of the C57BL/6 mouse. ILAR J. 52 (3), e21–e31.
Coyle, P., Jokelainen, P.T., 1982. Dorsal cerebral arterial collaterals of the rat. Anat. Rec. 203 (July (3)), 397–404.
Cuccione, E., Padovano, G., Versace, A., Ferrarese, C., Beretta, S., Campbell, B., et al., 2016. Cerebral collateral circulation in experimental ischemic stroke. Exp. Transl. Stroke Med. 8 (December (1)), 2.
Detre, J.A., Leigh, J.S., Williams, D.S., Koretsky, A.P., 1992. Perfusion imaging. Magn. Reson. Med. 23 (January (1)), 37–45.
Ditelberg, J.S., Sheldon, R.A., Epstein, C.J., Ferriero, D.M., 1996. Brain injury after perinatal hypoxia-ischemia is exacerbated in copper/zinc superoxide dismutase transgenic mice. Pediatr. Res. 39 (February (2)), 204–208.
Dobre, M.C., Uğurbil, K., Marjanska, M., 2007. Determination of blood longitudinal relaxation time (T1) at high magnetic field strengths. Magn. Reson. Imaging 25 (June (5)), 733–735.
Dumoulin, C., Turski, P., 2000. Methods in Biomedical Magnetic Resonance Imaging and Spectroscioy, 1st ed. Wiley.
Graham, E.M., Ruis, K.A., Hartman, A.L., Northington, F.J., Fox, H.E., 2008. A systematic review of the role of intrapartum hypoxia-ischemia in the causation of neonatal encephalopathy. Am. J. Obstet. Gynecol. 199 (December (6)), 587–595.
Hagberg, H., Gilland, E., Diemer, N.H., Andiné, P., 1994. Hypoxia-ischemia in the neonatal rat brain: histopathology after post-treatment with NMDA and non-NMDA receptor antagonists. Biol. Neonate 66 (4), 205–213.
Hattori, H., Wasterlain, C.G., 1990. Posthypoxic glucose supplement reduces hypoxic-ischemic brain damage in the neonatal rat. Ann. Neurol. 28 (August (2)), 122–128.
Herscovitch, P., Raichle, M.E., 1985. What is the correct value for the brain-blood partition coefficient for water? J. Cereb. Blood Flow Metab. 5 (March (1)), 65–69.
Heyser, C.J., 2004. Assessment of developmental milestones in rodents. In: Current Protocols in Neuroscience, Vol. Chapter 8. John Wiley & Sons, Inc., Hoboken, NJ, USA, p. Unit 8.18.
Kaspera, W., Majchrzak, H., Ładziński, P., Tomalski, W., 2005. Color doppler sonographic evaluation of collateral circulation in patients with cerebral aneurysms and the occlusion of the brachiocephalic vessels. Neurosurgery 57 (December (6)), 1117–1126.
Kim, S.G., 1995. Quantification of relative cerebral blood flow change by flow-sensitive alternating inversion recovery (FAIR) technique: application to functional mapping. Magn. Reson. Med. 34 (September (3)), 293–301.
Kober, F., Iltis, I., Izquierdo, M., Desrois, M., Ibarrola, D., Cozzone, P.J., Bernard, M., 2004. High-resolution myocardial perfusion mapping in small animals in vivo by spin-labeling gradient-echo imaging. Magn. Reson. Med. 51 (January (1)), 62–67.
Kurinczuk, J.J., White-Koning, M., Badawi, N., 2010. Epidemiology of neonatal encephalopathy and hypoxic-ischaemic encephalopathy. Early Hum. Dev. 86 (June (6)), 329–338.
Leithner, C., Müller, S., Füchtemeier, M., Lindauer, U., Dirnagl, U., Royl, G., 2010. Determination of the brain–blood partition coefficient for water in mice using MRI. J. Cereb. Blood Flow Metab. 30 (November (11)), 1821–1824.
Levine, S.R., Welch, K.M., 1989. Common carotid artery occlusion. Neurology 39 (February (2) Pt. 1), 178–186.
Liu, C., Lin, N., Wu, B., Qiu, Y., 2009. Neuroprotective effect of memantine combined with topiramate in hypoxic?ischemic brain injury. Brain Res. 1282, 173–182.
Manole, M.D., Foley, L.M., Hitchens, T.K., Kochanek, P.M., Hickey, R.W., Bayir, H., Alexander, H., Ho, C., Clark, R.S.B., 2009. Magnetic resonance imaging assessment of regional cerebral blood flow after asphyxial cardiac arrest in immature rats. J. Cereb. Blood Flow Metab. 29 (January (1)), 197–205.
McQuillen, P.S., Sheldon, R.A., Shatz, C.J., Ferriero, D.M., 2003. Selective vulnerability of subplate neurons after early neonatal hypoxia-ischemia. J. Neurosci. 23 (April (8)), 3308–3315.
Nikanfar, M., Farhoudi, M., Tarzamni, M.K., Mansoorizadeh, R., 2004. Contralateral external carotid artery as collateral to internal carotid artery in a patient with common carotid artery occlusion. Internet J. Neurol. Internet J. Neurol. 5 (1).
Noh, M.-R., Kim, S.K., Sun, W., Park, S.K., Choi, H.C., Lim, J.H., Kim, I.H., Kim, H.-J., Kim, H., Eun, B.-L., 2006. Neuroprotective effect of topiramate on hypoxic ischemic brain injury in neonatal rats. Exp. Neurol. 201 (2), 470–478.
Oakden, E., Chiswick, M., Rothwell, N., Loddick, S., 2002. The influence of litter size on brain damage caused by hypoxic-ischemic injury in the neonatal rat. Pediatr. Res. 52 (November (5)), 692–696.
Okusa, C., Oeschger, F., Ginet, V., Wang, W.-Z., Hoerder-Suabedissen, A., Matsuyama, T., Truttmann, A.C., Molnár, Z., 2014. Subplate in a rat model of preterm hypoxia-ischemia. Ann. Clin. Transl. Neurol. 1 (September (9)), 679–691.
Ota, A., Ikeda, T., Ikenoue, T., Toshimori, K., 1997. Sequence of neuronal responses assessed by immunohistochemistry in the newborn rat brain after hypoxia-ischemia. Am. J. Obstet. Gynecol. 177 (3), 519–526.
Palmer, C., Vannucci, R.C., Towfighi, J., 1990. Reduction of perinatal hypoxic-ischemic brain damage with allopurinol. Pediatr. Res. 27 (April (4) Pt. 1), 332–336.
Palmer, C., Towfighi, J., Roberts, R.L., Heitjan, D.F., 1993. Allopurinol administered after inducing hypoxia-ischemia reduces brain injury in 7-day-old rats. Pediatr. Res. 33 (no. Pt 1), 405–411.
Parthenis, D.G., Kardoulas, D.G., Ioannou, C.V., Antoniadis, P.N., Kafetzakis, A., Angelidou, K.I., Katsamouris, A.N., 2008. Total occlusion of the common carotid artery: a modified classification and its relation to clinical status. Ultrasound Med. Biol. 34 (June (6)), 867–873.
Reese, T., Bochelen, D., Sauter, A., Beckmann, N., Rudin, M., 1999. Magnetic resonance angiography of the rat cerebrovascular system without the use of contrast agents. NMR Biomed. 12 (June (4)), 189–196.
Rice, J.E., Vannucci, R.C., Brierley, J.B., 1981. The influence of immaturity on hypoxic-ischemic brain damage in the rat. Ann. Neurol. 9 (February (2)), 131–141.
Rocha-Ferreira, E., Phillips, E., Francesch-Domenech, E., Thei, L., Peebles, D.M., Raivich, G., Hristova, M., 2015. The role of different strain backgrounds in bacterial endotoxin-mediated sensitization to neonatal hypoxic–ischemic brain damage. Neuroscience 311 (December), 292–307.
Sheldon, R.A., Chuai, J., Ferriero, D.M., 1996. A rat model for hypoxic-ischemic brain damage in very premature infants. Biol. Neonate 69 (5), 327–341.
Silverstein, F.S., Buchanan, K., Hudson, C., Johnston, M.V., 2016. Flunarizine limits hypoxia-ischemia induced morphologic injury in immature rat brain. Stroke 17 (3), 477–482.
Suwanwela, N.C., Suwanwela, N., 1998. Takayasu arteritis: ultrasonographic evaluation of the cervico-cerebral arteries. Int. J. Cardiol. 66 (October (Suppl. 1)), S163–S173.
Tsai, C.-F., Jeng, J.-S., Lu, C.-J., Yip, P.-K., 2005. Clinical and ultrasonographic manifestations in major causes of common carotid artery occlusion. J. Neuroimaging 15 (January (1)), 50–56.
Vannucci, R.C., Perlman, J.M., 1997. Interventions for perinatal hypoxic-ischemic encephalopathy. Pediatrics 100 (December (6)), 1004–1014.
Wood, T., Smit, E., Maes, E., Osredkar, D., Falck, M., Elstad, M., Thoresen, M., 2016a. Monitoring of cerebral blood flow during hypoxia-ischemia and resuscitation in the neonatal rat using laser speckle imaging. Physiol. Rep. 4 (April (7)), e12749.
Wood, T., Osredkar, D., Puchades, M., Maes, E., Falck, M., Flatebø, T., Walløe, L., Sabir, H., Thoresen, M., 2016b. Treatment temperature and insult severity influence the neuroprotective effects of therapeutic hypothermia. Sci. Rep. 6 (March), 23430.
Xie, J., Gallichan, D., Gunn, R.N., Jezzard, P., 2008. Optimal design of pulsed arterial spin labeling MRI experiments. Magn. Reson. Med. 59 (April (4)), 826–834.
Yamasaki, M., 1990. Comparative anatomical studies of thyroid and thymic arteries: I. Rat (Rattus norvegicus albinus). Am. J. Anat. 188 (July (3)), 249–259.

Supplementary Table 1. All RF pulses were automatically calculated within ParaVision 6.0.1 based on the Shinnar-Le Roux (SLR) algorithm.

Sequence	Orientation	NA	TR (ms)	TE (ms)	Flip (°)	ESP (ms)	RARE factor	BW (Hz)	FOV (mm × mm)	MTX_{acq} (R × PE)	PF	MTX_{reco} (R × PE)	PIX (□m × □m)	NS	THK (□m)	Gap (□m)	Time (ms)
2D FLASH	tri-plane	2	60	3.0	30	-	-	75000	50 × 50	250 × 167	0.67 PE	250 × 250	200 × 200	5	1000	1000	0:20
2D MSME	sagittal	1	2400	12, 60	90	8	-	75000	36 × 27	240 × 112	0.62 PE	240 × 180	150 × 150	20	700	50	4:28
3D TOF FLASH	coronal*	1	12	2	20	-	-	89285.7	24 × 22 x 18	208 × 206 × 133	0.69 R	300 × 276 × 120	80 × 80 × 150	-	-	-	5:29
2D FLOWMAP	coronal*	12	100	4	20	-	-	59523.8	20 × 20	188 × 250	0.75 R	250 × 250	80 × 80	10	700	250	10:00
2D FAIR-SE-EPI	coronal*	1	12000	12.5	90	-	-	340909.1	22 × 22	110 × 69	0.63 PE	110 × 110	200 × 200	1	1000	-	3:32
2D RARE	coronal*	4	3900	36	90	12	8	59523.8	24 × 20	320 × 176	0.66 PE	320 × 266	75 × 75	34	500	20	5:43
2D RARE	sagittal	4	3900	36	90	12	8	59523.8	24 × 20	320 × 176	0.66 PE	320 × 266	75 × 75	27	500	20	5:43
2D RARE	axial*	4	3900	36	90	12	8	59523.8	24 × 20	320 × 176	0.66 PE	320 × 266	75 × 75	20	500	20	5:43

*relative to rat brain anatomy, NA = number of averages, TR = repeat time, TE = echo time, ESP = echo spacing, ETL = RARE echo train length, BW = receiver bandwidth, FOV = field-of-view, MTX_{acq} = image acquisition matrix size, PF = partial Fourier acquisition in phase-encode (PE) or read (R) direction, MTX_{reco} = image reconstruction matrix size, PIX = in-plane pixel size, NS = number of slices, THK = slice thickness, Gap = inter-slice gap.

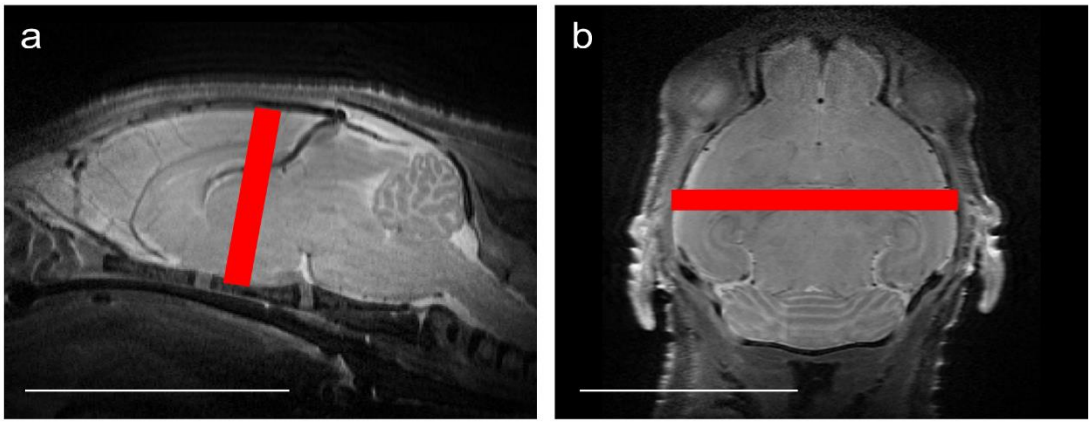

Supplementary Figure 1. Grayscale 2D, T2-weighted RARE slices in the (a) sagittal and (b) coronal plane demonstrating the 1 mm ASL slice positioning in Figure 4 (red bar; to scale). White bar = 1 cm.

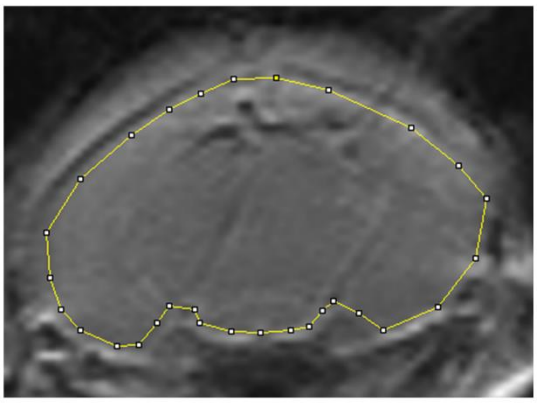

Supplementary Figure 2. Grayscale T1-weighted slice in the coronal plane. Region of interest (ROI) indicated for ASL values represented in Figure 3.

Chapter 5

Poly-arginine R18 and R18D (D-enantiomer) peptides reduce infarct volume and improves behavioural outcomes following perinatal hypoxic-ischaemic encephalopathy in the P7 rat

Published: Molecular Brain

Poly-arginine R18 and R18D (D-enantiomer) peptides reduce infarct volume and improves behavioural outcomes following perinatal hypoxic ischaemic encephalopathy in the P7 rat

Adam B. Edwards [1,2,3], Jane L. Cross [1,3,4], Ryan S. Anderton [1,2,4], Neville W. Knuckey [1,3,4], Bruno P. Meloni [1,3,4]

[1] Perron Institute for Neurological and Translational Science, Nedlands, Western Australia

[2] School of Health Sciences, The University of Notre Dame Australia, Fremantle, Western Australia

[3] Department of Neurosurgery, Sir Charles Gardiner Hospital, Nedlands, Western Australia

[4] Centre for Neuromuscular and Neurological Disorders, The University of Western Australia, Nedlands, Western Australia

Author contributions

Adam Edwards: 85%

Jane Cross: 2%

Ryan Anderton: 5%

Neville Knuckey: 3%

Bruno Meloni: 5%

Signed..... Signed.....

Adam Edwards Bruno Meloni (coordinating supervisor)

Edwards et al. Molecular Brain (2018) 11:8
https://doi.org/10.1186/s13041-018-0352-0

Molecular Brain

RESEARCH Open Access

Poly-arginine R18 and R18D (D-enantiomer) peptides reduce infarct volume and improves behavioural outcomes following perinatal hypoxic-ischaemic encephalopathy in the P7 rat

Adam B. Edwards[1,2,3], Jane L. Cross[1,3,4], Ryan S. Anderton[1,2,4], Neville W. Knuckey[1,3,4] and Bruno P. Meloni[1,3,4*]

Abstract

We examined the neuroprotective efficacy of the poly-arginine peptide R18 and its D-enantiomer R18D in a perinatal hypoxic-ischaemic (HI) model in P7 Sprague-Dawley rats. R18 and R18D peptides were administered intraperitoneally at doses of 30, 100, 300 or 1000 nmol/kg immediately after HI (8% O_2/92%N_2 for 2.5 h). The previously characterised neuroprotective JNKI-1-TATD peptide at a dose of 1000 nmol/kg was used as a control. Infarct volume and behavioural outcomes were measured 48 h after HI. For the R18 and R18D doses examined, total infarct volume was reduced by 25.93% to 43.80% ($P = 0.038$ to < 0.001). By comparison, the JNKI-1-TATD reduced lesion volume by 25.27% ($P = 0.073$). Moreover, R18 and R18D treatment resulted in significant improvements in behavioural outcomes, while with JNKI-1-TATD there was a trend towards improvement. As an insight into the likely mechanism underlying the effects of R18, R18D and JNKI-1-TATD, the peptides were added to cortical neuronal cultures exposed to glutamic acid excitotoxicity, resulting in up to 89, 100 and 71% neuroprotection, respectively, and a dose dependent inhibition of neuronal calcium influx. The study further confirms the neuroprotective properties of poly-arginine peptides, and suggests a potential therapeutic role for R18 and R18D in the treatment of HIE.

Keywords: Hypoxic-ischaemic encephalopathy, Hypoxia-ischaemia, Neuroprotection, Poly-arginine peptides, R18, Cationic arginine-rich peptides (CARPs)

Introduction

In the human neonate, hypoxic-ischaemic encephalopathy (HIE) remains the leading cause of neonatal mortality and morbidity, with a reported incidence of 1–3 per 1000 live term births [1], [2]. Neurological sequelae associated with HIE include cerebral palsy, epilepsy, mental retardation and learning disabilities [3]. Clinically, treatment to reduce brain injury for HIE is extremely limited, consisting of moderate hypothermia (32–34 °C), maintained for up to 72 h. While hypothermia appears to be well tolerated, its safety has only been assessed in full-term infants (37–40 weeks gestation), hence no treatments are available for preterm neonates with HIE born before 37 weeks gestation. In addition, while hypothermia has been shown to improve outcomes in clinical trials, 31–55% of infants do not benefit from the therapy and suffer severe neurological sequelae [4]. Furthermore, hypothermia can only be used in hospital settings that have the necessary equipment and trained staff to induce and monitor hypothermia following HIE, and thus is not available in non-tertiary hospitals or hospitals located in remote locations and in many developing countries.

Due to the need for additional neuroprotective strategies for HIE, research has focused on the development of a pharmacological neuroprotective agent that can be

* Correspondence: bruno.meloni@perron.uwa.edu.au
[1]Perron Institute for Neurological and Translational Sciences, QEII Medical Centre, RR Block, Ground Floor, 8 Verdun St, Nedlands, WA 6009, Australia
[3]Department of Neurosurgery, Sir Charles Gardiner Hospital, QEII Medical Centre, Western Nedlands 6009, Australia
Full list of author information is available at the end of the article

administered alone and/or in combination with current hypothermia treatment to improve neonatal outcomes in HIE. An added advantage of a pharmacological neuroprotective agent is the possibility it can be used in remote locations, is effective in preterm infants, and/or can improve neuroprotective outcomes for hypothermia. We and others have recently demonstrated that cationic arginine-rich and poly-arginine peptides (hereafter referred to as CARPs) have potent neuroprotective properties in in vitro excitotoxicity neuronal injury models [5–13], as well as in animal stroke models [10, 11, 14–16]. In particular, we have demonstrated that the poly-arginine peptide, R18, is highly neuroprotective in permanent and transient middle cerebral artery occlusion (MCAO) stroke models [11, 14–16].

While the exact mechanisms of the neuroprotective effects are still being explored, we and others have demonstrated that CARPs, including "putative" neuroprotective peptides fused to cationic arginine-rich cell penetrating peptides (i.e. TAT or R9; e.g. JNKI-1-TATD, TAT-NR2B9c/NA-1, TAT-CBD3/R9-CBD3-A6K and TAT-3.2-III-IV) have the ability to mitigate excitotoxic or potassium evoked neuronal intracellular calcium influx [7, 8, 17–19], and in doing so, likely suppress damaging down-stream signaling and cell death pathways. Beyond this, we have demonstrated that the poly-arginine R12 and TAT-NR2B9c/NA-1 peptides reduce neuronal cell surface expression of the glutamate receptor subunit NR2B [20]. The ability of CARPs to reduce neuronal cell surface levels of NR2B (due to internalization during endocytic uptake) is at least one mechanism whereby the peptides reduce the damaging effects of glutamate-induced calcium influx and excitotoxicity. Additionally, other "putative" neuroprotective peptides bound to TAT or R9 have been shown to reduce neuronal surface expression or activity of NMDA receptors [5, 21–23], as well as voltage gated calcium channels CaV2.2 [21, 24, 25] and CaV3.3 [18], and the sodium calcium exchanger 3 (NCX3) [21]. Given their effects on different receptors, presently, it cannot be ruled out that CARPs, due to their cationic charge, are also antagonizing ion channel receptor function directly and/or affecting calcium ion influx via an electrostatic mechanism [7, 9].

In addition to CARPs reducing the effects of excitotoxicity, based on other properties of this class of peptide, they may exert more pleiotropic neuroprotective effects by targeting mitochondria and maintaining mitochondrial integrity [6, 26–32], thereby reducing reactive oxygen species (ROS) production and release of pro-cell death proteins such as cytochrome-c. Furthermore, CARPs have the capacity to inhibit proteolytic enzymes including the proteasome [33, 34], as well as proprotein convertases [35–37] that activate matrix metalloproteinases (MMPs) [38]. Inhibition of the proteasome is known to be beneficial following cerebral ischaemia [39, 40], a mechanism that could be mediated by increased activity of hypoxia-inducible factor 1-α (HIF1α) and decreased activity of nuclear factor κ-light-chain-enhancer of B cells (NFκB). Similarly, due to the damaging effects of MMPs on the neurovascular unit and blood brain barrier, any down-regulation of their proteolytic activity is likely to be beneficial following brain HI. In addition, there is also evidence that CARPs can activate pro-survival signaling pathways [17, 41] and modulate immune responses [42–44], as well as act as anti-oxidant molecules in their own right due to their guanidino group containing arginine residues [32, 45–49].

Since HIE and stroke are thought to share many pathophysiological processes (e.g. excitotoxicity and oxidative stress) it is likely that R18 will also be effective in reducing HI brain injury. To this end, several CARPs, including "putative" neuroprotective peptides fused to TAT such as JNKI-1-TATD [50], P5-TAT [51], TAT-NDB [52], TAT-mGluR1 [53], TAT-NR2B9c/NA-1 [53], IDR-1018 [54], and COG133 [55], have demonstrated efficacy in perinatal HI models. Importantly, CARPs like the TAT peptide also have cell penetrating properties and can cross the blood brain barrier and enter the brain [56–58].

Therefore, given the demonstrated efficacy of the R18 poly-arginine peptide in a number of experimental stroke studies [11, 14–16], the present study examined the neuroprotective efficacy and dose responsiveness of R18, as well as its D-amino acid enantiomer (R18D) in a perinatal HI model in the P7 Sprague-Dawley rat, and their effects on neuronal calcium influx in an in vitro glutamic acid excitotoxicity model. In addition, as a control, the study also examined the effects of the cationic arginine-rich JNKI-1-TATD peptide, which has previously been shown to be neuroprotective in various rodent brain injury models, including perinatal HI [50, 59].

Methods

Animal ethics and study design

All experimental procedures in this study adhered to the guidelines approved and specified by the Animal Ethics Committee of the University of Western Australia (RA/3/100/1329), in accordance with the Policies and Guidelines of the National Health and Medical Research Council, Australia. Treatments were randomised and all procedures (e.g. peptide administration, behavioural testing and infarct volume analysis) were performed while being blinded to treatments.

Peptides used in the study

Peptides used in the study are shown in Table 1. R18, R18D and JNKI-1-TATD used were synthesised by Mimotopes (Melbourne, Australia). Peptides were purified

Table 1 Peptides used in study

Peptide	Sequence[a]	Arginine/AA residues	% Arginine residues	Net charge
R18	H-RRRRRRRRRRRRRRRRRR-OH	18/18	100	+ 18
R18D	H-rrrrrrrrrrrrrrrrrr-OH	18/18	100	+ 18
JNKD	H-tdqsrpvqpflnlttprkprpp-rrrqrrkkrg-NH_2	9/32	28	+ 12

[a]At the N-terminus, H indicates free amine. At the C-terminus, OH indicates free acid, and NH_2 indicates amide. AA = amino acids. Lowercase single letter code indicates D-isoform of the amino acid. JNKD = JNKI-1-TATD

using high performance liquid chromatography to at least 98% purity, and were subject to peptide hydrolysis and amino acid liquid chromatography analysis to obtain a precise measure of peptide content.

For the in vitro and animal studies, peptides were prepared as a 500 μM stock solution in water for irrigation (Baxter, Australia), and in 0.9% sodium chloride for injection (Pfizer, Australia), respectively. Reconstituted peptides were stored at − 20 °C until use.

Surgical procedure for modified Rice-Vannucci model

We used a modified Rice-Vannucci HI model. This involved occluding the right common, as well as the right external carotid artery, a procedure that we have previously demonstrated to lead to the generation of a highly reliable infarct [60]. Briefly, unsexed, Sprague-Dawley P7 rat pups (Animal Resource Centre, Murdoch, Australia; P0 = day of birth) with a body weight of 13–16 g were used. Litters were culled to a maximum of 12 pups per litter to facilitate uniform growth without littermate competition. Rat pups were anaesthetised using isoflurane (5% induction, 1–2% maintenance) in 100% oxygen, while on a heating pad (37 °C). Through a 1 cm mid-line ventral incision, the right common, internal and external carotid arteries were exposed and isolated from the vagus nerve, venous circulation and carotid body. The right common carotid and external carotid arteries were permanently ligated using 6–0 silk sutures. The wound was closed using Vetbond (3M, Maplewood, USA) and the animals were recovered on 100% oxygen for 5 min on a heating pad. The duration of anaesthesia from induction to beginning of recovery was between 5 and 8 min. Animals were provided with analgaesia (pethidine, 5 mg/kg; intraperitoneally) immediately before cessation of anaesthesia. Sham-operated animals underwent the same operative procedure, except the exposed carotid arteries were not ligated.

Rat pups were returned to their dam for 1 h before the commencement of hypoxia which consisted of placing 4 to 6 pups in an airtight container (approximate volume: 4 L) and exposing them to humidified and warmed hypoxic gas (8% O_2/92% N_2; 3 L/min) for 2.5 h. The container was placed inside an incubator with an ambient air temperature of 35 °C, ensuring a body temperature of 36–37 °C, which was periodically monitored using an infrared thermometer. Following hypoxia, animals were placed on a heating pad for 5 min in a normoxic environment before being placed back with the dam. Sham-operated animals remained with the dam at all times.

Peptide administration

Immediately after hypoxia, treatments were administered intraperitoneally (50 μl bolus) and consisted of either the vehicle (saline; 0.9% sodium chloride), or R18 or R18D at four different doses (30, 100, 300 or 1000 nmol/kg) or JNKI-1-TATD at a single dose (1000 nmol/kg).

Animals used and sample size

One hundred and thirty-three Sprague-Dawley P7 pups housed under controlled conditions on a 12-h light-dark cycle underwent surgery for HI or the sham procedure (i.e. anesthesia, neck incision, wound closure and analgesia). Twenty-seven animals were excluded from the study; a list of animal exclusions is provided in Table 2. The saline treatment group consisted of 19 animals and the sham group 6 animals. All other treatment groups consisted of between 7 and 11 animals (see Fig. 1a and Table 3). Additional vehicle treated animals were included in the study to ensure that each batch of animals subjected to HI contained a vehicle control and to increase the statistical power of the study.

Infarct volume assessment

Forty-eight hours after HI, animals were euthanised by pentobarbital overdose (50 mg/kg; intraperitoneally). Infarct volume was determined by preparing 2 mm thick coronal brain slices, and incubating in 3% 2,3,5-triphenyltetrazolium chloride (TTC; Sigma Aldrich, St. Louis, USA) at 37 °C for 20 min, followed by fixation in 4% formalin at room temperature overnight. Digital images of coronal slices were acquired using a colour scanner and analysed, using ImageJ software (3rd edition, NIH, Bethesda, USA). Total infarct volume was determined by measuring areas of infarcted tissue on both sides of the 2 mm slices. Infarct volume measurements were corrected for a degree of hemisphere volume changes [60]. Final infarct data is expressed as percentage infarct volume compared to whole brain (minus cerebellum). For analysis of infarct volumes in male and female animals,

Table 2 Animals excluded in the study

Exclusion rationale	Number of exclusions	Peptide	Dose	Total number of exclusions
No detectable infarct	3	Saline	–	15
	1	R18	300	
	3	R18	100	
	2	R18	300	
	1	R18	1000	
	2	R18D	30	
	1	R18D	300	
	1	R18D	1000	
	1	JNKD	1000	
Hyperthermia[a]	1	R18	1000	1
Failure to complete behavioural assessment	3	–	–	3
Surgical haemorrhage[b]	5	–	–	5
Premature death[c]	3	–	–	3

All peptide doses are in nmol/kg. [a]Hyperthermia is a recorded body temperature > 37.5. [b]Surgical haemorrhage is defined as any animal which had an abnormal bleed (arterial rupture) during the surgical parameter. [c]Premature deaths occurred during hypoxia. JNKD = JNKI-1-TATD

due to low numbers of each gender per group, data for the different doses of R18 and R18D were combined.

Behavioural assessment

To determine if the development of cerebral infarct was associated with reduced sensorimotor outcomes, three neurological tests (righting reflex, negative geotactic response and wire-hang) were performed at 48 h after HI, as previously reported [60]. Briefly, for three consecutive days before surgery (P4 to P6 inclusive), pups were accustomed to behavioural assessments with a target inclusion range of ≤2 s for the righting reflex and ≤30 s for the negative geotactic response. Any animal that did not record responses within these parameters at P7 (day of surgery) were excluded from the experiment. All of these reflexes are highly reproducible throughout the murine pre-weaning period (< P30) and are strain- and gender-independent [61]. Each animal was given three attempts to complete each sensorimotor task, with 5 min between each attempt. Testing of all reflexes was performed on a board covered with a tightly-stretched close knit-fabric, to ensure adequate friction.

The righting reflex involved placing pups in a supine position, and measuring the time required to rotate to the prone position. The negative geotactic response involved placing pups facing down-slope, on a 45° angled surface, and measuring the time required for the animal to turn 150° upslope. Wire-hang test was performed by suspending pups by their forelimbs on a 2 mm diameter steel wire suspended 20 cm above a foam surface, and recording the time taken for the animal to fall to the foam surface.

Cortical neuronal cultures

Establishment of rat primary cortical neuronal cultures was performed as previously described [8, 10]. Briefly, cortical tissue was obtained directly from E18-day old embryos. Dissociated neurons were seeded into 96-well-sized glass wells (7 mm diameter, Grace, Melbourne, Australia), 96-well plastic plates (Nunc, Thermo Fisher Scientific, Melbourne, Australia) in Neurobasal/2% B27 supplement (Life Technologies, Melbourne, Australia) and maintained in a CO_2 incubator (5% CO_2, 95% air balance, 98% humidity) at 37 °C until use on day in vitro 10 to 14. Under these conditions, cultures routinely consist of > 97% neurons and 1–3% astrocytes.

Glutamic acid excitotoxicity

A dose response experiment was performed as previously described [8]. Briefly, peptides in a 50 μl volume in Minimum Essential Medium (Life Technologies)/2% B27 supplement (MEM/B27) were added to culture wells for 10 min at 37 °C in the CO_2 incubator before the addition of 50 μl MEM/B27 containing glutamic acid ($_L$-glutamic acid; Sigma-Aldrich: 200 μM; final concentration 100 μM). Following a 5 min incubation at 37 °C in the CO_2 incubator (note: peptide concentration reduced by half during this step), media was replaced with 100 μL MEM/B27 and cultures wells were incubated for a further 24 h at 37 °C in the CO_2 incubator. Untreated controls with or without glutamic acid treatment underwent the same incubation steps and media additions.

At different times after treatment (e.g. 0.5 to 4 h and 18–24 h), cultures were examined by light microscopy for qualitative assessment of neuronal cell viability. Neuronal viability was quantitatively measured by MTS

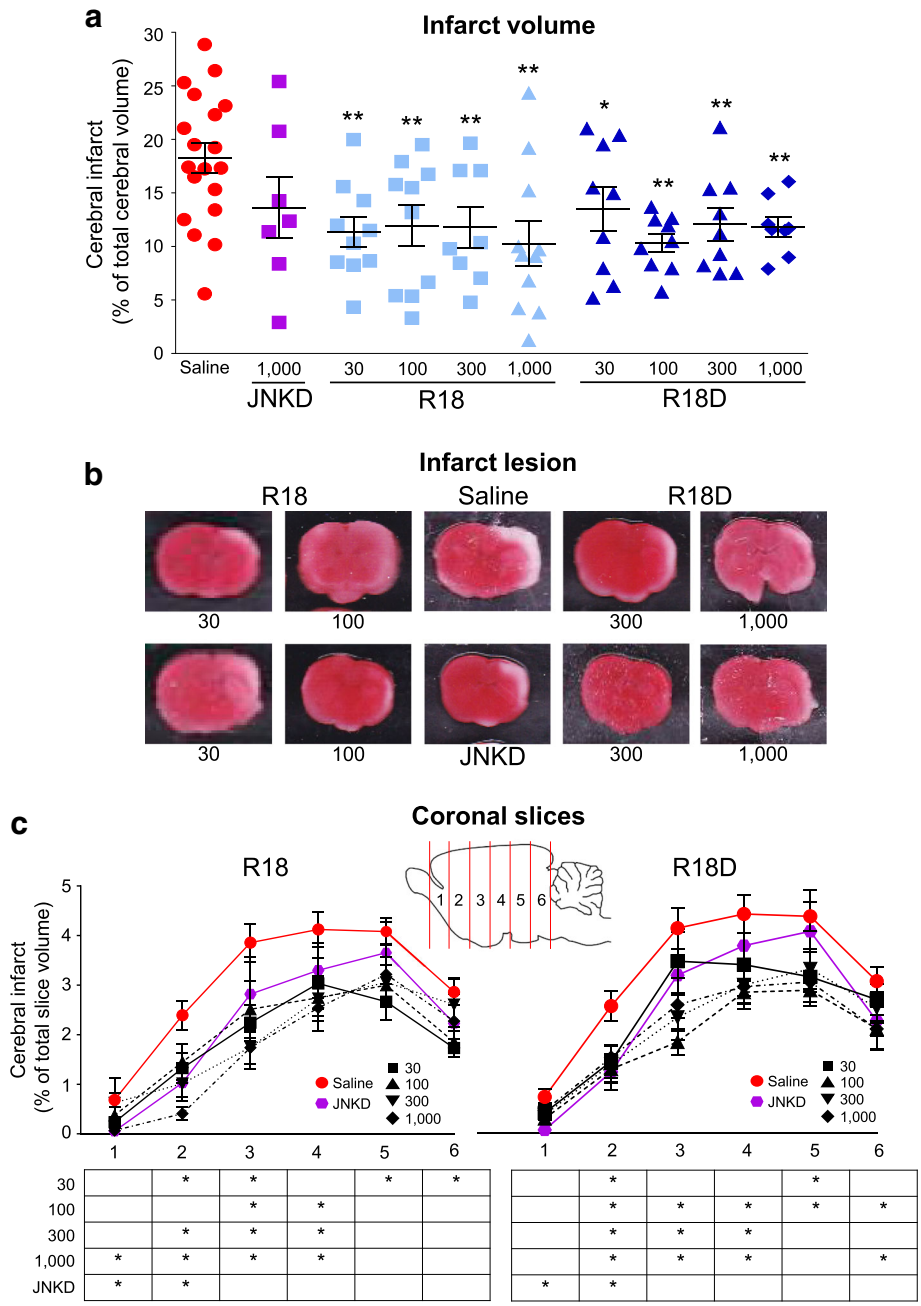

Fig. 1 Percentage infarct volume; percentage infarct volume, representative images of coronal brain slices and percentage infarct volume in brain slices for the different treatment groups as determined 48 h after HI. Treatments were administered intraperitoneally (saline or R18, R18D and JNKI-1-TATD; doses in nmol/kg) immediately after hypoxia. **a** Percentage of infarct volume when compared to total brain volume. **b** Representative TTC coronal brain slice 2, from saline and peptide treated animals. Minor adjustments to brightness and contrast has been made to improve digital images. **c** Infarct volume analysis in 2 mm coronal brain slices (slices numbered 1–6 from rostral to caudal) from saline and peptide treated animals. Statistical significance is expressed in the table. Values are mean ± SE; $^{*}P < 0.05$, $^{**}P < 0.01$ when compared to saline. JNKD = JNKI-1-TATD

(3-(4,5,dimethyliazol-2-yl)-5-(3-carboxymethoxy-phenyl)-2-(4-sulfophenyl)-2H–tetrazolium salt) assay (Promega, Sydney, Australia). The MTS absorbance data were converted to reflect proportional cell viability relative to both the untreated (no insult; 100% viability) and treated (glutamic acid; 5% viability) controls. At least four wells were used in assays, repeated a minimum of three to four times independently.

Intracellular calcium kinetics

Intracellular calcium influx was monitored as previously described [8]. Briefly, primary cortical neuronal cultures

Table 3 Cerebral infarct. Percentage of total cerebral volume

Treatment	Dose	N	Mean of total infarct volume (%)	SE (%)	Reduction in total infarct volume (%)	*P*
Saline	–	19	18.24	1.393	–	–
JNKD	1000	7	13.63	2.843	25.27	0.073
R18	30	10	11.34	1.401	37.82	**0.002**
	100	10	11.93	1.924	34.59	**0.004**
	300	8	11.78	1.921	35.42	**0.007**
	1000	11	10.25	2.082	43.80	**< 0.001**
R18D	30	9	13.51	2.058	25.93	**0.038**
	100	9	10.33	0.874	43.36	**< 0.001**
	300	9	12.07	1.540	33.82	**0.007**
	1000	8	11.83	0.957	35.14	**0.007**

N number of animals, *SE* standard error of mean, *P* calculated compared to saline vehicle control. All doses are in nmol/kg. Mean and SE expressed as percentage of total cerebral volume. JNKD = JNKI-1-TATD. Percentage reduction is mean percentage reduction compared to saline. All values $P < 0.05$ are in bold

were loaded with the fluorescent calcium ion indicator Fura-2 AM (5 μM; Sigma Aldrich) in 50 μL MEM/B27, 0.1% pluronic F-127 (Sigma Aldrich), for 20 min at 37 °C in the CO_2 incubator. Fura-2 AM solution was removed from wells, replaced with 50 μL MEM/B27 containing peptides (R18 and R18D; 0.2, 2 and 5 μM) or NMDA and AMPA receptor blockers (MK801/CNQX; 5 μM/5 μM; Tocris Bioscience, Bristol, United Kingdom) and incubated for 10 min at 37 °C in the CO_2 incubator. Control cultures received 50 μL of MEM/B27 only. After the 10 min incubation period, media in wells was replaced with 50 μL of balanced salt solution (BSS: mM: 116 NaCl, 5.4 KCl, 1.8 $CaCl_2$, 0.8 $MgSO_4$, 1 NaH_2PO_4; pH 7.2) and wells transferred to a spectrophotometer (BMG Labtec, CLARIOstar, Mornington, Australia) while maintaining temperature at 37 °C. Fifty microliters of BSS containing glutamic acid (200 μM; 100 μM final concentration) was added to wells, and every 5 s, starting 30 s before and for 90 s after glutamic acid addition, spectrophotometer measurements (excitation: 355 nm/emission 495 nm) were recorded. Experiments were performed in triplicate. Area under the curve (AUC) for calcium kinetics data was calculated by trapezoidal approximation of the AUC using fluorescent kinetic data obtained after the addition of glutamic acid to wells.

Statistical analysis

The number of animals used in each experiment was justified by statistical power calculation based on a previous study [60]. Group sizes have been calculated based on a predicted treatment effect of 40%, at a power level of 80–90% and an alpha level of 0.05. Mean percentage infarct volume, behavioural measurements weight gain and neuronal viability data were analysed by analysis of variance (ANOVA), followed by post-hoc Fisher's PLSD test, with $P < 0.05$ values considered statistically significant. All descriptive statistics are presented in Table 3 and Additional file 1: Table S1, Additional file 2: Table S2 and Additional file 3: Table S3.

Results

Infarct volume measurements

Data on infarct volume and representative TTC stained coronal brain slices are presented in Fig. 1a and b. When compared to the saline vehicle control (hereafter referred to as saline), both R18 and R18D significantly reduced infarct volume at all doses examined (30, 100, 300 and 1000 nmol/kg) by between 25.27 and 43.80% ($P = 0.045$ and < 0.001, respectively; refer to Table 3 for descriptive statistics). By comparison, the JNKI-1-TATD peptide (1000 nmol/kg) reduced infarct volume by 25.27% ($P = 0.073$). No single R18, R18D or JNKI-1-TATD dose was significantly more effective than any other dose. To assess infarct development within 2 mm coronal slices, rostral to caudal topographic analysis of infarcts revealed that R18, R18D and JNKI-1-TATD at all doses significantly reduced brain injury in one or more coronal slices 1 to 6 (Fig. 1c; refer to Additional file 1: Table S1 for descriptive statistics).

Behavioural outcomes, weight gain and gender analysis

Data on behavioural outcomes and weight gain is presented in Fig. 2a–h and descriptive statistics presented in Additional file 2: Table S2. All data is transformed to demonstrate the percentage improvement from baseline for each treatment group, 48 h following HI. The sham procedure is taken as equivalent to 100% improvement and saline control to 0% improvement. The results of the righting reflex test demonstrated that R18 (30 and 1000 nmol/kg) and R18D (300 and 1000 nmol/kg) significantly improved the righting reflex time by between 53.95% and 79.88% ($P = 0.008$ and 0.007), respectively, when compared to saline. In comparison, animals treated with JNKI-1-TATD (1000 nmol/kg) showed no

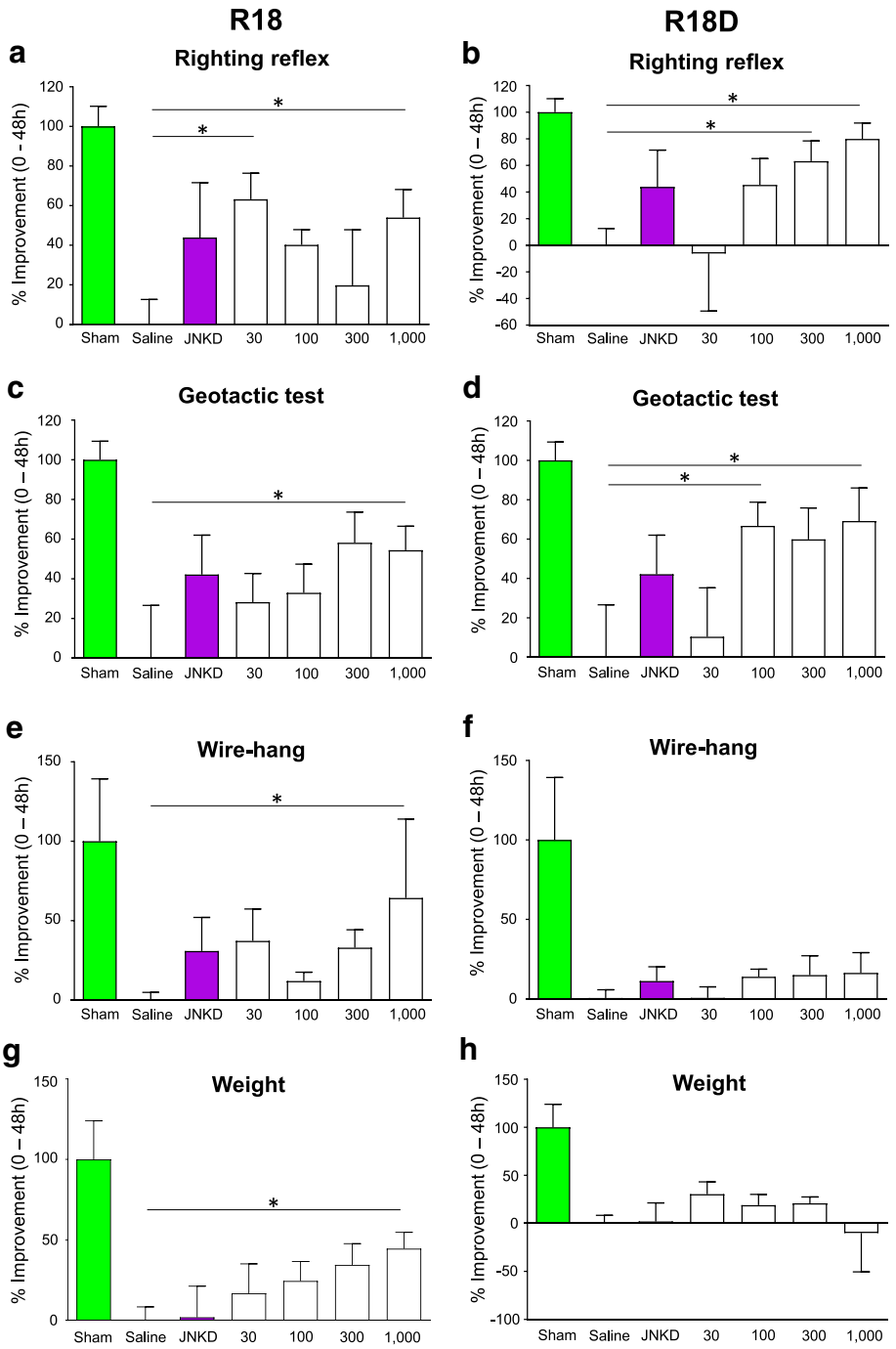

Fig. 2 Behavioural measurements using righting reflex, negative geotactic response, wire-hang test and weight gain 48 h after HI. Treatments were administered intraperitoneally (saline, R18, R18D or JNKI-1-TATD; doses in nmol/kg). The sham procedure group was assessed 48 h following sham-surgery. **a** R18 righting reflex percentage improvement from 0 to 48 h. **b** R18D righting reflex percentage improvement from 0 to 48 h. **c** R18 negative geotactic response percentage improvement from 0 to 48 h. **d** R18D negative geotactic response percentage improvement from 0 to 48 h. **e** R18 wire-hang percentage improvement from 0 to 48 h. **f** R18D wire-hang percentage improvement from 0 to 48 h. **g** R18 weight percentage improvement from 0 to 48 h. **h** R18D weight percentage improvement from 0 to 48 h. Values are mean ± SE. *$P < 0.05$ when compared to saline. JNKD = JNKI-1-TATD

statistically significant improvement, although there was a trend towards improvement (43.87%; $P = 0.063$).

Analysis of the negative geotactic response test revealed that R18 (1000 nmol/kg) and R18D (100 and 1000 nmol/kg) significantly improved the time taken for animals to rotate 150° up the 45° slope when compared to saline by between 54.44% and 69.17% ($P = 0.049$ and 0.036), respectively. All other doses improved the

negative geotactic response time by between 10.40% and 59.87% ($P = 0.738$ and 0.057), respectively. In comparison, JNKI-1-TATD (1000 nmol/kg) resulted in no statistically significant improvement, although there was a trend towards improvement (42.18%; $P = 0.187$).

For the wire-hang test, only R18 at a dose of 1000 nmol/kg resulted in a statistically significant improvement in the time animals held onto the wire, increasing hang-time by 64.29% ($P = 0.033$) when compared to saline. All other doses improved the wire hang time by between 0.59% and 37.26% ($P = 0.997$ and 0.227), respectively. By comparison, JNKI-1-TATD (1000 nmol/kg) resulted in no statistically significant improvement in the wire-hang time (30.93%; $P = 0.374$).

Analysis of weight gain over 48 h revealed that R18 at a dose of 1000 nmol/kg was the only treatment to significantly improve weight gain (44.59%; $P = 0.009$) when compared to saline (see Additional file 3: Table S3 for descriptive statistics), while all other doses of R18 and R18D demonstrated an increase in weight by between 16.83% and 34.49% ($P = 0.327$ and 0.065), respectively. In comparison, JNKI-1-TATD (1000 nmol/kg) treated animals demonstrated a gain in weight (1.94%; $P = 0.935$). The only dose to demonstrate a loss of weight was R18D at 1000 nmol/kg (−10.01%; $P = 0.659$).

Analysis of R18 and R18D neuroprotective efficacy in male and female animals revealed a significant reduction in total infarct volume in both sexes when compared to male and female saline treated animals (Additional file 4: Figure S1; note: for analysis the different doses of R18 and R18D were combined). While intra-group comparisons demonstrated no significant differences in total infarct volumes between male and female animals treated with R18, R18D or saline; there was a trend towards reduced infarcts in female animals treated with R18 and R18D (Additional file 4: Figure S1).

In vitro neuroprotective efficacy and calcium kinetics following glutamic acid excitotoxicity

To provide an insight into the potential mechanism of action of R18 and R18D, in vitro neuroprotective efficacy and excitotoxic neuronal calcium influx kinetics were assessed. In line with previous findings from our laboratory R18 and JNKI-1-TATD [7, 10, 11], as well as R18D displayed dose-dependent neuroprotection following excitotoxicity (Fig. 3). For example, R18 and R18D increased neuronal survival from 5% for the glutamic acid control to 89% and 83% and 96% and 100% at 1 μM and 2 μM, respectively (Fig. 3). By comparison, JNKI-1-TATD increased neuronal survival to 23 and 71% at 1 μM and 2 μM, respectively. As we have previously observed, higher peptide concentrations (i.e. 5 μM) can have a negative impact on neuronal survival [8], this was particularly evident for R18D, a fact which most likely reflects the higher stability of D-isoform peptides in the closed neuronal culture system [9].

Again, in line with our previous findings, R18 and JNKI-1-TATD [7, 10, 11], as well as R18D, reduced glutamic acid induced neuronal intracellular calcium influx in a dose dependent manner (Fig. 4). In addition, the calcium influx data for R18, R18D and JNKI-1-TATD correlated with their neuroprotective effectiveness following glutamic acid excitotoxicity, with JNKI-1-TATD displaying the least neuronal intracellular calcium influx inhibitory effects.

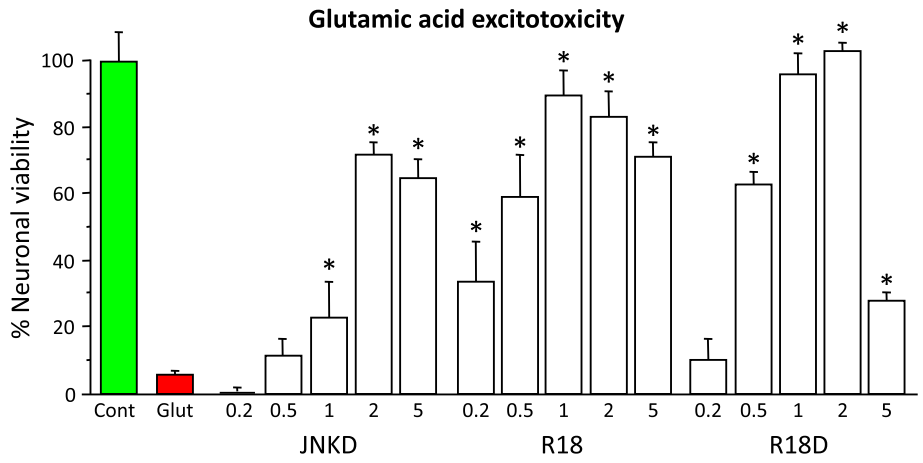

Fig. 3 Glutamic acid excitotoxicity model; R18, R18D and JNKI-1-TATD dose response study. Peptides present in neuronal cultures 10 min before and during 5 min glutamic acid exposure. Neuronal viability measured 24 h after glutamic acid exposure. Concentration of peptide in μmol/L. MTS data were expressed as percentage neuronal viability with no insult (100% viability) and glutamic acid control (5% viability). Values are mean ± SE; $n = 4$; *$P < 0.05$ when compared to no glutamic acid control. Cont = no treatment control. Glut = glutamic acid control. JNKD = JNKI-1-TATD

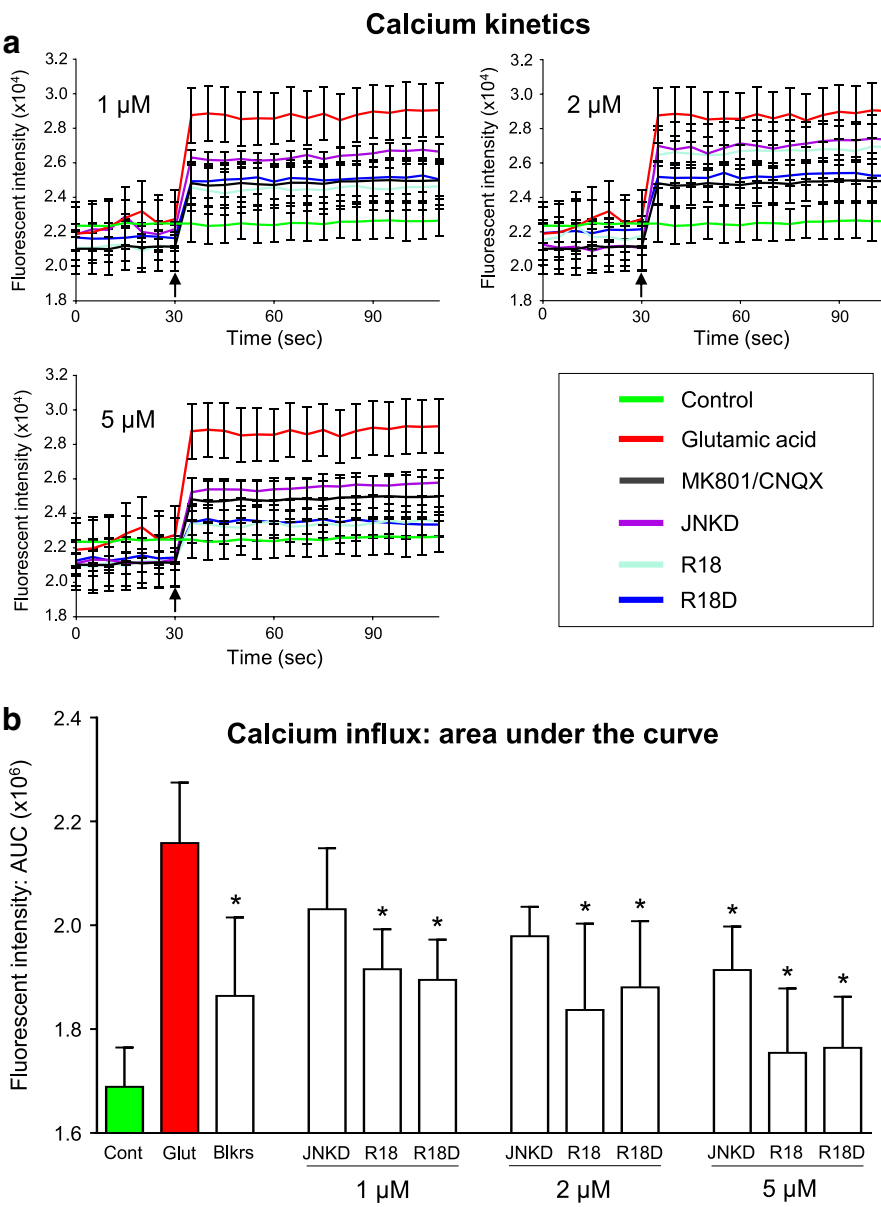

Fig. 4 Intracellular calcium assessment using Fura-2 AM after glutamic acid exposure in primary neuronal cultures. **a** Fluorescent Fura-2 AM tracers; fluorescent intensity (FI) of neuronal cultures 30 s before and after the addition (arrow) of glutamic acid (100 μM final concentration). Peptides (1, 2 and 5 μM) or glutamate receptor blockers (MK801/CNQX; 5 μM/5 μM) were added to neuronal cultures for 10 min and removed (time = 0) before glutamic acid addition (time = 30 s). Values are mean ± SE; $n = 3$. **b** Trapezoidal area under the curve (AUC) approximation of calcium kinetic tracers. AUC is determined at 35 s (point after glutamic acid addition. Values are mean ± SE; $n = 3$; *$P < 0.05$ when compared to glutamic acid control. Cont = no treatment control. Glut = glutamic acid control. Blkrs = glutamate receptor blockers (MK801/CNQX; 5 μM/5 μM). JNKD = JNKI-1-TATD

Discussion

The present study extends our previous findings examining the neuroprotective effectiveness of CARPs in in vitro and animal stroke injury models [7–11, 13–16]. In doing so, the data provides compelling evidence for the neuroprotective action of poly-arginine peptides R18 and R18D, as well as the JNKI-1-TATD peptide, which is also a CARP, in a modified Rice-Vannucci model of HIE. The modified Rice-Vannucci model used in this study leads to the generation of a more reproducible infarct, accompanied with a greater severity of brain injury [60]. The original and modified Rice-Vannucci models are likely to mimic the clinical development of a pattern of brain injury, whereby white matter and cerebral cortex, supplied by the middle cerebral and posterior cerebral arteries, are affected following prolonged birth asphyxia [62]. Importantly, the neuroprotective actions of R18 and R18D, as measured in terms of infarct volume, was

associated with improved behavioural outcomes at a number of the peptide doses with respect to the righting reflex, negative geotactic response and wire-hang tests, while JNKI-1-TATD only demonstrated trends towards improvement in the righting reflex and negative geotactic response tests. In addition, unlike JNKI-1-TATD, some doses of R18 and R18D improved weight gain following HI. This is another indicator for improved behavioural outcomes as it is likely to reflect the animals' increased motor capacity to search and feed from the dam, as well as potential reduced weight loss due to increases in respiratory demand, metabolic rate and cachexia [63]. Furthermore, treatment with R18 and R18D was effective at reducing total infarct volume in both male and female animals following HI.

It is noteworthy that, the R18 and R18D were highly effective at reducing infarct volume at all doses examined without displaying a typical dose response effect. The efficacy of both R18 and R18D over a wide dose range (30–1000 nmol/kg) is highly significant, which ultimately could translate to the peptides being effective at low doses when used clinically following HIE. The effectiveness of JNKI-1-TATD (also referred to as XG-102) in a wide dose range with IP administration has also been demonstrated previously following transient MCAO in adult mice [64] and following permanent MCAO in P14 rats [65].

In the present study, R18 and R18D appeared more effective than JNKI-1-TATD across all the in vivo (infarct volume and behavioural outcomes) and in vitro (neuroprotection and neuronal intracellular calcium influx inhibition) outcomes examined. The lower efficacy of JNKI-1-TATD may reflect its lower arginine content (R = 9) and cationic charge (+ 12) compared to R18 and R18D (R = 18, charge = + 18). On this point, our previous studies have confirmed that CARP neuroprotective efficacy and neuronal excitotoxic influx inhibition increases with increasing peptide arginine content and peptide positive charge [8, 9]. It is also noteworthy that in the present study, no obvious overall differences were uncovered between the R18 peptide and its R18D enantiomer.

As mentioned above, the only currently available treatment known to improve neurological outcomes following HIE is moderate hypothermia (32–34 °C for 72 h). As such there is an urgent need for the development of an effective pharmacological neuroprotective agent that can be readily administered following HIE and that is compatible and synergistic with hypothermia. Therefore, it will be important in future studies to assess whether R18 or R18D treatment is compatible with hypothermia, and whether the combined therapies have an additional effect in reducing brain injury and improving behavioural outcomes. In addition, whilst a 48 h endpoint is commonly used in initial neuroprotective and pathophysiological investigations, it is important that the effectiveness of R18 and R18D at more extended timepoints should also be evaluated. We also recognise that the IP route for peptide administration may not be ideally suited to the clinical situation, and that an intravenous (IV) route would be preferable. Furthermore, due to the potential differences in blood pharmacokinetics following IP or IV administration of R18 and R18D, at present it is not known how the different delivery routes would impact on the neuroprotective efficacy of the peptides. To this end, further assessment of R18 and R18D when administered by the IV route could be more appropriately carried out in a large animal model of HI (i.e. piglet or lamb).

Additional files

Additional file 1: Table S1. Cerebral infarct. Percentage of topographical coronal slices. (DOCX 16 kb)

Additional file 2: Table S2. Behavioural assessment. (DOCX 17 kb)

Additional file 3: Table S3. Weight gain 48 h after hypoxia-ischaemia. (DOCX 16 kb)

Additional file 4: Figure S1. Gender comparison of infarct volume. (PPTX 59 kb)

Abbreviations

ANOVA: Analysis of variance; AUC: Area under the curve; CARPs: Cationic arginine rich peptides; HI: Hypoxia-ischaemia; HIE: Hypoxic ischaemic encephalopathy; HIF1α: Hypoxia-inducible factor 1-α; IP: Intraperitoneal; IV: Intravenous; MCAO: Middle cerebral artery occlusion; MEM: Minimum essential medium; MMPs: Matrix metalloproteinases; MTS: 3-(4,5,dimethyliazol-2-yl)-5-(3-carboxymethoxy-phenyl)-2-(4-sulfophenyl)-2H–tetrazolium salt; NCX3: Sodium calcium exchanger 3; NFκB: Nuclear factor kappa-light-chain enhancer of B cells; NMDA: N-methyl-D-aspartic acid; R12: Poly-arginine-12; R18: Poly-arginine-18; R18D: Poly-arginine-18 D-enantiomer; R9: Poly-arginine-9; ROS: Reactive oxygen species; TTC: 2,3,5-triphenyltetrazolium chloride

Acknowledgments

This study in part was supported by the Department of Neurosurgery, Sir Charles Gairdner Hospital. The authors acknowledge the feedback on the manuscript provided by Professors Frank Mastaglia and Norman Palmer.

Funding

This research was in part funded by the Sir Charles Gardiner Hospital, Department of Neurosurgery. This funding body had no part in the study, collection, analysis and interpretation of data.

Availability of data and materials

Please contact author for data requests.

Authors' contributions

AE and JC contributed to animal procedures, post-surgical monitoring, functional assessment, infarct volume or statistical analysis. AE and BM contributed to in vitro experiments. AE, RA, NK and BM contributed to experimental design and manuscript preparation. All authors read and approved the final manuscript.

Ethics approval and consent to participate

Not applicable

Consent for publication

Not applicable

Competing interests
B.P. Meloni and N.W. Knuckey are named inventors of several patent applications regarding the use of arginine-rich peptides as neuroprotective agents. The other authors declare no conflict of interest.

Publisher's Note
Springer Nature remains neutral with regard to jurisdictional claims in published maps and institutional affiliations.

Author details
[1]Perron Institute for Neurological and Translational Sciences, QEII Medical Centre, RR Block, Ground Floor, 8 Verdun St, Nedlands, WA 6009, Australia. [2]School of Health Sciences and Institute for Health Research, The University of Notre Dame Australia, Fremantle, WA 6160, Australia. [3]Department of Neurosurgery, Sir Charles Gardiner Hospital, QEII Medical Centre, Western Nedlands 6009, Australia. [4]Centre for Neuromuscular and Neurological Disorders, The University of Western Australia, Nedlands, WA 6009, Australia.

Received: 16 January 2018 Accepted: 1 February 2018
Published online: 09 February 2018

References

1. Kurinczuk JJ, White-Koning M, Badawi N. Epidemiology of neonatal encephalopathy and hypoxic-ischaemic encephalopathy. Early Hum Dev. 2010;86(6):329–38.
2. Graham EM, Ruis KA, Hartman AL, Northington FJ, Fox HE. A systematic review of the role of intrapartum hypoxia-ischemia in the causation of neonatal encephalopathy. Am J Obstet Gynecol. 2008;199(6):587–95.
3. Vannucci RC, Perlman JM. Interventions for perinatal hypoxic-ischemic encephalopathy. Pediatrics. 1997;100(6):1004–14.
4. Shankaran S. Therapeutic hypothermia for neonatal encephalopathy. Curr Treat Options Neurol. 2012;14(6):608–19.
5. Ferrer-Montiel AV, et al. Selected peptides targeted to the NMDA receptor channel protect neurons from excitotoxic death. Nat Biotechnol. 1998;16(3):286–91.
6. Marshall J, et al. Inhibition of N-methyl-d-aspartate-induced retinal neuronal death by Polyarginine peptides is linked to the attenuation of stress-induced Hyperpolarization of the inner mitochondrial membrane potential. J Biol Chem. 2015;290(36):22030–48.
7. Meloni BP, et al. Neuroprotective peptides fused to arginine-rich cell penetrating peptides: Neuroprotective mechanism likely mediated by peptide endocytic properties. Pharmacol Ther. 2015;153:36–54.
8. Meloni BP, et al. Poly-arginine and arginine-rich peptides are neuroprotective in stroke models. J Cereb Blood Flow Metab. 2015;35(6):993–1004.
9. Edwards AB, Anderton RS, Knuckey NW, Meloni BP. Characterisation of neuroprotective efficacy of modified poly-arginine-9 (R9) peptides using a neuronal glutamic acid excitotoxicity model. Mol Cell Biochem. 2017;426(1-2):75–85.
10. Meloni BP, Craig AJ, Milech N, Hopkins RM, Watt PM, Knuckey NW. The neuroprotective efficacy of cell-penetrating peptides TAT, penetratin, Arg-9, and Pep-1 in glutamic acid, kainic acid, and in vitro ischemia injury models using primary cortical neuronal cultures. Cell Mol Neurobiol. 2014;34(2):173–81.
11. Meloni BP, et a. Assessment of the Neuroprotective Effects of Arginine-Rich Protamine Peptides, Poly-Arginine Peptides (R12-Cyclic, R22) and Arginine–Tryptophan-Containing Peptides Following In Vitro Excitotoxicity and/or Permanent Middle Cerebral Artery Occlusion in Rats. NeuroMolecular Med. 2017;19(2-3):271–85.
12. McQueen J, et al. Pro-death NMDA receptor signaling is promoted by the GluN2B C-terminus independently of Dapk1. Elife. 2017;6:e17161.
13. Chiu LS, et al. Assessment of R18, COG1410, and APP96-110 in Excitotoxicity and traumatic brain injury. Transl Neurosci. 2017;8:147–57.
14. Milani D, Clark VW, Cross JL, Anderton RS, Knuckey NW, Meloni BP. Poly-arginine peptides reduce infarct volume in a permanent middle cerebral artery rat stroke model. BMC Neurosci. 2016;17(1):19.
15. Milani D, Cross JL, RS, Blacker DJ, Knuckey NW, Meloni BP. Neuroprotective efficacy of poly-arginin Andertone R18 and NA-1 (TAT-NR2B9c) peptides following transient middle cerebral artery occlusion in the rat. Neurosci Res. 2016;114:9–15.
16. Milani D, et al. The R18 Polyarginine peptide is more effective than the TAT-NR2B9c (NA-1) peptide when administered 60 minutes after permanent middle cerebral artery occlusion in the rat. Stroke Res Treat. 2016;2016:1–9.
17. Cook DR, et al. NMDA receptor modulation by the neuropeptide apelin: implications for excitotoxic injury. J Neurochem. 2011;118(6):1113–23.
18. García-Caballero A, et al. The deubiquitinating enzyme USP5 modulates neuropathic and inflammatory pain by enhancing Cav3.2 channel activity. Neuron. 2014;83(5):1144–58.
19. Xie JY, et al. Sustained relief of ongoing experimental neuropathic pain by a CRMP2 peptide aptamer with low abuse potential. Pain. 2016;157(9):2124–40.
20. MacDougall G, Anderton RS, Edwards AB, Knuckey NW, Meloni BP. The Neuroprotective Peptide Poly-Arginine-12 (R12) Reduces Cell Surface Levels of NMDA NR2B Receptor Subunit in Cortical Neurons; Investigation into the Involvement of Endocytic Mechanisms. J Mol Neurosci. 2017;61(2):235–46.
21. Brustovetsky T, Pellman JJ, Yang X-FF, Khanna R, Brustovetsky N. Collapsin response mediator protein 2 (CRMP2) interacts with N-methyl-D-aspartate (NMDA) receptor and Na+/Ca2+ exchanger and regulates their functional activity. J Biol Chem. 2014;289(11):7470–82.
22. Sinai L, Duffy S, Roder JC. Src inhibition reduces NR2B surface expression and synaptic plasticity in the amygdala. Learn Mem. 2010;17(8):364–71.
23. Tu W, et al. DAPK1 interaction with NMDA receptor NR2B subunits mediates brain damage in stroke. Cell. 2010;140(2):222–34.
24. Brittain JM, et al. Neuroprotection against traumatic brain injury by a peptide derived from the collapsin response mediator protein 2 (CRMP2). J Biol Chem. 2011;286(43):37778–92.
25. Feldman P, Khanna R. Challenging the catechism of therapeutics for chronic neuropathic pain: targeting CaV2.2 interactions with CRMP2 peptides. Neurosci Lett. 2013;557 Pt A:27–36.
26. Birk AV, Chao WM, Liu S, Soong Y, Szeto HH. Disruption of cytochrome c heme coordination is responsible for mitochondrial injury during ischemia. Biochim Biophys Acta. 2015;1847(10):1075–84.
27. Ferré CA, et al. Manipulation of the N-terminal sequence of the Borna disease virus X protein improves its mitochondrial targeting and neuroprotective potential. FASEB J. 2016;30(4):1523–33.
28. Rigobello MP, Barzon E, Marin O, Bindoli A. Effect of polycation peptides on mitochondrial permeability transition. Biochem Biophys Res Commun. 1995;217(1):144–9.
29. Szelechowski M, et al. A viral peptide that targets mitochondria protects against neuronal degeneration in models of Parkinson's disease. Nat Commun. 2014;5:5181.
30. Szeto HH, et al. Mitochondria-targeted peptide accelerates ATP recovery and reduces ischemic kidney injury. J Am Soc Nephrol. 2011;22(6):1041–52.
31. Zhao K, et al. Cell-permeable peptide antioxidants targeted to inner mitochondrial membrane inhibit mitochondrial swelling, oxidative cell death, and reperfusion injury. J Biol Chem. 2004;279(33):34682–90.
32. Cerrato CP, Pirisinu M, Vlachos EN, Langel Ü. Novel cell-penetrating peptide targeting mitochondria. FASEB J. 2015;29(11):4589–99.
33. Anbanandam A, Albarado DC, Tirziu DC, Simons M, Veeraraghavan S. Molecular basis for proline- and arginine-rich peptide inhibition of proteasome. J Mol Biol. 2008;384(1):219–27.
34. Gaczynska M, Osmulski PA, Gao Y, Post MJ, Simons M. Proline- and arginine-rich peptides constitute a novel class of allosteric inhibitors of proteasome activity. Biochemistry. 2003;42(29):8663–70.
35. Cameron A, Appel J, Houghten RA, Lindberg I. Polyarginines are potent Furin inhibitors. J Biol Chem. 2000;275(47):36741–9.
36. Fugere M, Appel J, Houghten RA, Lindberg I, Day R. Short polybasic peptide sequences are potent inhibitors of PC5/6 and PC7: use of positional scanning-synthetic peptide combinatorial libraries as a tool for the optimization of inhibitory sequences. Mol Pharmacol. 2007;71(1):323–32.
37. Kacprzak MM, et al. Inhibition of furin by polyarginine-containing peptides: nanomolar inhibition by nona-D-arginine. J Biol Chem. 2004;279(35):36788–94.
38. Tian S, Huang Q, Fang Y, Wu J. FurinDB: a database of 20-residue furin cleavage site motifs, substrates and their associated drugs. Int J Mol Sci. 2011;12(2):1060–5.
39. Doeppner TR, et al. Systemic Proteasome inhibition induces sustained post-stroke neurological recovery and Neuroprotection via mechanisms involving reversal of peripheral Immunosuppression and preservation of blood-brain-barrier integrity. Mol Neurobiol. 2016;53(9):6332–41.
40. Wojcik C, Di Napoli M. Ubiquitin-proteasome system and proteasome inhibition: new strategies in stroke therapy. Stroke. 2004;35(6):1506–18.

41. Yang Y, Zhang X, Cui H, Zhang C, Zhu C, Li L. Apelin-13 protects the brain against ischemia/reperfusion injury through activating PI3K/Akt and ERK1/2 signaling pathways. Neurosci Lett. 2014;568:44–9.
42. Hilchie AL, Wuerth K, Hancock REW. Immune modulation by multifaceted cationic host defense (antimicrobial) peptides. Nat Chem Biol. 2013;9(12):761–8.
43. Kellett DN. On the anti-inflammatory activity of Protamine Sulphate and of Hexadimethrine bromide, inhibitors of plasma Kinin formation. Br J Pharmacol Chemother. 1965;24:705–13.
44. Li L-H, et al. A synthetic cationic antimicrobial peptide inhibits inflammatory response and the NLRP3 inflammasome by neutralizing LPS and ATP. PLoS One. 2017;12(7):e0182057.
45. Courderot-Masuyer C, Dalloz F, Maupoil V, Rochette L. Antioxidant properties of aminoguanidine. Fundam Clin Pharmacol. 1999;13(5):535–40.
46. Yildiz G, Demiryürek AT, Sahin-Erdemli I, Kanzik I. Comparison of antioxidant activities of aminoguanidine, methylguanidine and guanidine by luminol-enhanced chemiluminescence. Br J Pharmacol. 1998;124(5):905–10.
47. Lass A, Suessenbacher A, Wölkart G, Mayer B, Brunner F. Functional and analytical evidence for scavenging of oxygen radicals by L-arginine. Mol Pharmacol. 2002;61(5):1081–8.
48. Mandal SM, et al. Identification of multifunctional peptides from human milk. Peptides. 2014;56:84–93.
49. Marshall J, et al. Inhibition of N-methyl-D-aspartate-induced retinal neuronal death by Polyarginine peptides is linked to the attenuation of stress-induced Hyperpolarization of the inner mitochondrial membrane potential. J Biol Chem. 2015;290(36):22030–48.
50. Nijboer CH, van der Kooij MA, van Bel F, Ohl F, Heijnen CJ, Kavelaars A. Inhibition of the JNK/AP-1 pathway reduces neuronal death and improves behavioral outcome after neonatal hypoxic-ischemic brain injury. Brain Behav Immun. 2010;24(5):812–21.
51. Tan X, et al. The inhibition of Cdk5 activity after hypoxia/ischemia injury reduces infarct size and promotes functional recovery in neonatal rats. Neuroscience. 2015;290:552–60.
52. van der Kooij MA, et al. NF-kappaB inhibition after neonatal cerebral hypoxia-ischemia improves long-term motor and cognitive outcome in rats. Neurobiol Dis. 2010;38(2):266–72.
53. Zhou M, Xu W, Liao G, Bi X, Baudry M. Neuroprotection against neonatal hypoxia/ischemia-induced cerebral cell death by prevention of calpain-mediated mGluR1alpha truncation. Exp Neurol. 2009;218(1):75–82.
54. Bolouri H, et al. Innate defense regulator peptide 1018 protects against perinatal brain injury. Ann Neurol. 2014;75(3):395–410.
55. McAdoo JD, Warner DS, Goldberg RN, Vitek MP, Pearlstein R, Laskowitz DT. Intrathecal administration of a novel apoE-derived therapeutic peptide improves outcome following perinatal hypoxic-ischemic injury. Neurosci Lett. 2005;381(3):305–8.
56. Stalmans S, et al. Cell-penetrating peptides selectively cross the blood-brain barrier in vivo. PLoS One. 2015;10(10):e0139652.
57. Sarko D, et al. The pharmacokinetics of cell-penetrating peptides. Mol Pharm. 2010;7(6):2224–31.
58. Zou L-L, Ma J-L, Wang T, Yang T-B, Liu C-B. Cell-penetrating peptide-mediated therapeutic molecule delivery into the central nervous system. Curr Neuropharmacol. 2013;11(2):197–208.
59. Nijboer CH, Heijnen CJ, Groenendaal F, van Bel F, Kavelaars A. Alternate pathways preserve tumor necrosis factor-alpha production after nuclear factor-kappaB inhibition in neonatal cerebral hypoxia-ischemia. Stroke. 2009; 40(10):3362–8.
60. Edwards AB, et al. Modification to the Rice-Vannucci perinatal hypoxic-ischaemic encephalopathy model in the P7 rat improves the reliability of cerebral infarct development after 48 hours. J Neurosci Methods. 2017;288:62–71.
61. CJ Heyser. Assessment of Developmental Milestones in Rodents. In: Current Protocols in Neuroscience. Hoboken, NJ, USA: John Wiley & Sons, Inc; 2004. vol. Chapter 8. p. Unit 8.18.
62. de Vries LS, Groenendaal F. Patterns of neonatal hypoxic-ischaemic brain injury. Neuroradiology. 2010;52(6):555–66.
63. Roe SY, Rothwell NJ. Whole body metabolic responses to brain trauma in the rat. J Neurotrauma. 1997;14(6):399–408.
64. Wiegler K, Bonny C, Coquoz D, Hirt L. The JNK inhibitor XG-102 protects from ischemic damage with delayed intravenous administration also in the presence of recombinant tissue Plasminogen activator. Cerebrovasc Dis. 2008;26(4):360–6.
65. Vaslin A, Naegele-Tollardo S, Puyal J, Clarke PGH. Excitotoxicity-induced endocytosis mediates neuroprotection by TAT-peptide-linked JNK inhibitor. J Neurochem. 2011;119(6):1243–52.

Supplementary Table 1. Cerebral infarct. Percentage of topographical coronal slices.

Treatment	Slice	N	Mean (%)	SE (%)	Percentage reduction	*P*
Saline	1	19	0.683	0.148	-	-
	2		2.392	0.290	-	-
	3		3.858	0.387	-	-
	4		4.124	0.358	-	-
	5		4.081	0.269	-	-
	6		2.860	0.272	-	-
JNKD 1,000	1	7	0.063	0.041	90.65	**0.031**
	2		1.152	0.345	51.83	**0.008**
	3		2.973	0.805	22.93	0.211
	4		3.529	0.620	14.42	0.376
	5		3.797	0.777	6.95	0.671
	6		2.170	0.536	24.12	0.200
R18 30	1	10	0.233	0.107	65.90	0.074
	2		1.327	0.301	44.52	**0.010**
	3		2.243	0.363	41.86	**0.011**
	4		3.034	0.522	26.43	0.069
	5		2.665	0.359	34.69	**0.019**
	6		1.732	0.182	39.44	**0.030**
R18 100	1	10	0.374	0.103	45.29	0.216
	2		1.488	0.369	37.79	0.227
	3		2.514	0.574	34.83	**0.033**
	4		2.747	0.374	33.38	**0.022**
	5		2.998	0.418	26.53	0.071
	6		1.852	0.309	35.24	0.051
R18 300	1	8	0.623	0.500	8.76	0.823
	2		1.015	0.349	57.56	**0.002**
	3		1.747	0.344	54.71	**0.002**
	4		2.729	0.460	33.82	**0.032**
	5		3.057	0.502	25.09	0.112
	6		2.606	0.535	8.88	0.644
R18 1,000	1	11	0.067	0.038	90.07	**0.013**
	2		0.409	0.131	82.90	**<0.0001**
	3		1.739	0.436	54.92	**<0.001**
	4		2.541	0.476	38.38	**0.007**
	5		3.217	0.621	21.17	0.135
	6		2.275	0.559	20.45	0.239

Supplementary Table 1 continued. Cerebral infarct. Percentage of topographical coronal slices.

R18D 30	1	9	0.383	0.142	43.86	0.122
	2		1.351	0.309	43.52	**0.014**
	3		3.237	0.604	16.09	0.334
	4		3.263	0.575	20.87	0.130
	5		2.950	0.458	27.71	**0.028**
	6		2.634	0.256	7.90	0.591
R18D 100	1	9	0.308	0.128	54.86	0.054
	2		1.135	0.260	52.55	**0.003**
	3		1.702	0.265	55.88	**0.001**
	4		2.597	0.230	37.02	**0.008**
	5		2.580	0.300	36.78	**0.004**
	6		2.008	0.151	29.79	**0.046**
R18D 300	1	9	0.347	0.106	49.12	0.084
	2		1.296	0.359	45.81	**0.010**
	3		2.182	0.418	43.44	**0.011**
	4		2.791	0.333	32.32	**0.021**
	5		3.092	0.378	24.23	0.533
	6		2.358	0.283	17.55	0.234
R18D 1,000	1	8	0.428	0.145	37.38	0.204
	2		1.425	0.217	40.42	**0.028**
	3		2.416	0.498	37.37	**0.034**
	4		2.757	0.424	33.14	**0.023**
	5		2.845	0.188	30.28	0.213
	6		1.964	0.404	31.32	**0.044**

N, number of animals; SEM, standard error of mean; *P*, calculated compared to saline vehicle control. All doses are in nmol/kg. Mean and SE expressed as percentage of total slice volume. JNKD = JNKI-1-TATD. Percentage reduction expressed as percentage reduction from corresponding saline slice. All values $P < 0.05$ are bold.

Supplementary Table 2. Behavioural assessment.

Behavioural assessment	Treatment	Dose	N	Mean* (%)	SE (%)	*P*
Righting reflex	Sham	-	6	100	10.36	**<0.001**
Righting reflex	Saline	-	19	0	13.41	-
Righting reflex	JNKD	1,000	7	43.87	27.69	0.063
Righting reflex	R18	30	10	63.21	13.16	**0.003**
		100	10	40.20	7.70	0.054
		300	8	19.77	28.03	0.375
		1,000	11	53.95	14.22	**0.008**
Righting reflex	R18D	30	9	-6.18	43.28	0.822
		100	9	45.33	19.81	0.104
		300	9	63.14	15.24	**0.025**
		1,000	8	79.88	11.97	**0.007**
Geotactic test	Sham	-	6	100	9.30	**0.004**
Geotactic test	Saline	-	19	0	26.59	-
Geotactic test	JNKD	1,000	7	42.18	19.85	0.187
Geotactic test	R18	30	10	28.23	14.48	0.317
		100	10	32.95	14.46	0.243
		300	8	58.21	15.44	0.058
		1,000	11	54.44	12.11	**0.049**
Geotactic test	R18D	30	9	10.40	24.84	0.738
		100	9	66.71	12.06	**0.035**
		300	9	59.87	15.96	0.057
		1,000	8	69.17	16.83	**0.036**

Supplementary Table 2 continued. Behavioural assessment.

Wire hang	Sham	-	6	100	39.27	**<0.001**
Wire hang	Saline	-	19	0	4.91	-
Wire hang	JNKD	1,000	7	30.93	21.15	0.374
Wire hang	R18	30	10	37.26	20.08	0.227
		100	10	11.99	5.579	0.695
		300	8	32.99	11.25	0.320
		1,000	11	64.29	49.70	**0.033**
Wire hang	R18D	30	9	0.59	6.67	0.997
		100	9	13.9	4.80	0.410
		300	9	14.95	12.15	0.356
		1,000	8	16.36	12.7	0.330

*Mean percentage improvement from baseline to 48 h after HI. N, number of animals; SE, standard error of mean; *P* calculated compared to saline. All doses are in nmol/kg. Mean and SE expressed as percentage improvement in behavioural assessment from baseline to 48 h after HI. All values $P < 0.05$ are in bold.

Supplementary Table 3. Weight gain 48 hours after hypoxia-ischaemia.

Treatment	Dose	N	Mean (g)*	SE (g)	Mean (%)#	SE (%)	*P*
Sham	-	6	4.6	0.841	100	23.95	**<0.001**
Saline	-	19	1.089	0.295	0	8.424	-
JNKD	1,000	7	1.157	0.67	1.941	19.34	0.935
R18	30	10	1.68	0.64	16.83	18.32	0.327
	100	10	1.95	0.42	24.52	12.07	0.155
	300	8	2.30	0.46	34.49	13.20	0.065
	1,000	11	2.65	0.35	44.59	10.17	**0.009**
R18D	30	9	2.15	0.45	30.38	12.87	0.167
	100	9	1.75	0.39	18.98	11.22	0.386
	300	9	1.82	0.23	20.88	6.62	0.340
	1,000	8	0.73	1.42	-10.01	40.50	0.659

*Mean weight gain from P7 (day of injury) to P9 (48 hour endpoint). #Mean percentage weight gain from baseline to 48 h after HI. N, number of animals; g, gram; SE, standard error of mean; *P* calculated compared to saline. All doses are in nmol/kg. Mean and SE are expressed as gram improvement from baseline to 48 h after HI. All values $P < 0.05$ are in bold.

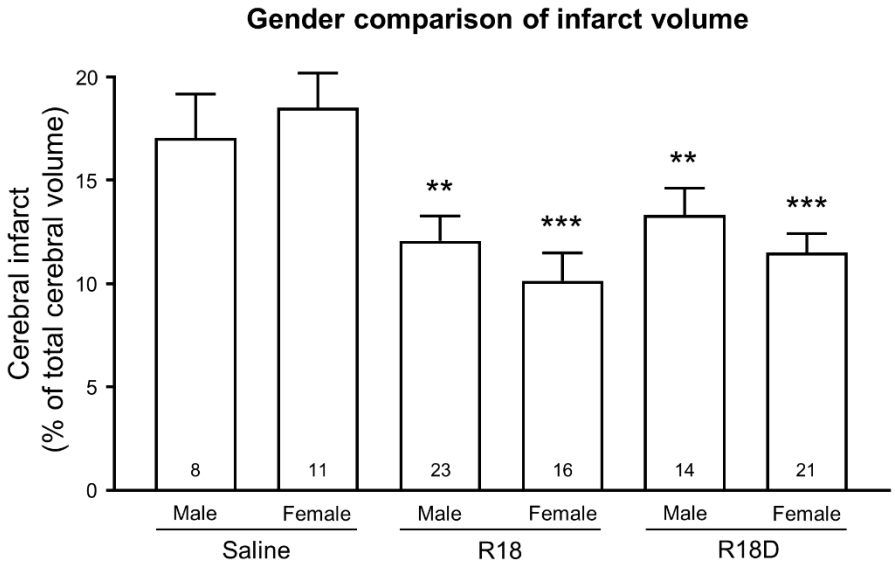

Supplementary Figure 1. Comparison of percentage total infarct volume in male and female animals treated with R18, R18D or saline. Due to the small number of female and male animals within the different peptide treatment groups total infarct volume data for R18 and R18D doses have been pooled. Values are mean ± SE; ** $P < 0.01$ and *** $P < 0.001$ when compared to corresponding male or female saline control. Note: due to small animal numbers the JNKI-1-D peptide was not included in the analysis.

Chapter 6

Assessment of therapeutic window for poly-arginine-18D (D-enantiomer) in a P7 rat model of perinatal hypoxic-ischaemic encephalopathy

Published: Journal of Neuroscience Research

Assessment of therapeutic window for poly-arginine-18D (D-enantiomer) in a P7 rat model of perinatal hypoxic-ischaemic encephalopathy

Adam B. Edwards [1,2,3], Ryan S. Anderton [1,2,4], Neville W. Knuckey [1,3,4], Bruno P. Meloni [1,3,4]

[1] Perron Institute for Neurological and Translational Science, Nedlands, Western Australia

[2] School of Health Sciences, The University of Notre Dame Australia, Fremantle, Western Australia

[3] Department of Neurosurgery, Sir Charles Gardiner Hospital, Nedlands, Western Australia

[4] Centre for Neuromuscular and Neurological Disorders, The University of Western Australia, Nedlands, Western Australia

Author contributions

Adam Edwards: 82%

Ryan Anderton: 5%

Neville Knuckey: 3%

Bruno Meloni: 10%

Signed..... Signed.....

Adam Edwards Bruno Meloni (coordinating supervisor)

Received: 29 April 2018 | Revised: 24 July 2018 | Accepted: 24 July 2018

DOI: 10.1002/jnr.24315

RESEARCH ARTICLE

WILEY

Assessment of therapeutic window for poly-arginine-18D (R18D) in a P7 rat model of perinatal hypoxic-ischaemic encephalopathy

Adam B. Edwards[1,2,3] | Ryan S. Anderton[1,2,4] | Neville W. Knuckey[1,3,4] | Bruno P. Meloni[1,3,4]

[1]Perron Institute for Neurological and Translational Science, QEII Medical Centre, Nedlands, Western Australia, Australia

[2]School of Health Sciences and Institute for Health Research, The University of Notre Dame Australia, Fremantle, Western Australia, Australia

[3]Department of Neurosurgery, Sir Charles Gairdner Hospital, QEII Medical Centre, Nedlands, Western Australia, Australia

[4]Centre for Neuromuscular and Neurological Disorders, The University of Western Australia, Nedlands, Western Australia, Australia

Correspondence
Adam Edwards, Perron Institute for Neurological and Translational Science, First Floor, RR Block, QEII Medical Centre, 8 Verdun Street, Nedlands, Western Australia, 6009, Australia.
Email: adam.edwards1@my.nd.edu.au

Abstract

Hypoxic-ischaemic encephalopathy (HIE) remains the leading cause of mortality and morbidity in neonates, with no available neuroprotective therapeutic agent. In the development of a therapeutic for HIE, we examined the neuroprotective efficacy of the poly-arginine peptide R18D (arginine 18 mer synthesised with D-arginine) in a perinatal model of hypoxia-ischaemia (HI; common carotid and external carotid occlusion + 8%O_2/92%N_2 for 2.5 hr) in the P7 Sprague-Dawley rat. R18D was administered intraperitoneally 30 min (doses 10, 30, 100, 300 and 1,000 nmol/kg), 60 min (doses 30 and 300 nmol/kg) or 120 min (doses 30 and 300 nmol/kg) after HI. Infarct volumes and behavioural outcomes were measured 48 hr after HI. When administered 30 min after HI, R18D at varying doses reduced infarct volume by 23.7% to 35.6% (p = 0.009 to < 0.0001) and resulted in improvements in the negative geotactic response and wire-hang times, at a dose of 30 nmol/kg. When administered 60 min after HI, R18D at the 30 nmol/kg dose reduced total infarct volume by 34.2% (p = 0.002), whilst the 300 nmol/kg dose improved wire-hang time. When administered 120 min after HI, R18D at the 30 and 300 nmol/kg doses had no significant impact on infarct volume, but the 300 nmol/kg dose improved the negative geotactic response. This study further confirms the neuroprotective properties of poly-arginine peptides, demonstrating that R18D can reduce infarct volume and improve behavioural outcomes after HI if administered up to 60 min after HI and improve behavioural outcomes up to 2 hr after HI.

KEYWORDS

hypoxia, hypoxia-ischaemia, neonatal, neuroprotection

1 | INTRODUCTION

Hypoxic-ischaemic encephalopathy (HIE) remains the leading cause of neonatal mortality and morbidity, affecting between 3 and 26 per 1,000 live births in developed and developing countries, respectively (Douglas-Escobar & Weiss, 2015; Logitharajah, Rutherford, & Cowan, 2009; Pierrat et al., 2005). The relatively high prevalence and devastating neurological sequelae of HIE is accompanied with a significant social and economic burden (Kruse et al., 2009). Clinically, moderate hypothermia (33.5°C for 72 hr) within 6 hr of birth is used to treat moderate or severe hypoxia-ischaemia (HI), but is largely restricted for use in tertiary hospitals due to the need for specialised equipment and trained staff to monitor neonates during the procedure. Whilst hypothermia appears to be well tolerated in term infants

Significance

Hypoxic-ischaemic encephalopathy (HIE) remains the leading cause or mortality and morbidity in neonates, with no known clinically appropriate therapeutic agent to treat the ensuing brain injury. This study demonstrates that the poly-arginine peptide R18D is neuroprotective in a P7 rodent model of HIE, following administration up to 60 min after hypoxia-ischaemia (HI), with concomitant improvements in behavioural assessments. This study further confirms the neuroprotective properties of poly-arginine peptides, offering an exciting potential in the prevention of brain injury in infants following HI.

(> 36 weeks gestation) (Azzopardi et al., 2009; Gluckman et al., 2005; Jacobs et al., 2011; Shankaran et al., 2005), most infants do not benefit from the intervention, and its use in preterm infants (≤ 36 weeks gestation) warrants caution due to a high risk of adverse effects (e.g., coagulopathy, hyperglycaemia, hypocalcemia, hyponatremia, hypovolemia and immune suppression) and high mortality rate (Jenkins et al., 2013; Mosalli, 2012; Rao et al., 2016). Hence, there is an urgent need for the development of new and easily applicable neuroprotective therapies that can be used in combination with hypothermia to further improve patient outcomes and/or minimise side-effects associated with hypothermia, or when hypothermia cannot be applied, as a stand-alone therapy to reduce HI-mediated brain injury.

Recently, we have highlighted the potential of cationic arginine-rich peptides (CARPs), which possess inherent cell penetrating properties and can cross the blood brain barrier, as a new class of neuroprotective agent. This class of peptide includes poly-arginine peptides (e.g., R9 and R18) and in terms of mechanism of action, most likely extends to most, if not all, putative neuroprotective peptides fused to cationic cell penetrating peptides (e.g., TAT-NR2B9c, JNKI-1-TATD, TAT-NR2Bct, TAT-CBD3, R9-CBD3, COG112) because of their arginine content and positive charge (Marshall et al., 2015; McQueen et al., 2017; Meloni, Brookes, et al., 2015; Meloni, Milani, et al., 2015). Importantly, we have demonstrated that the poly-arginine peptides R18 and its D-enantiomer R18D, can reduce brain injury in P7 rats when administered immediately after HI (Edwards, Cross, Anderton, Knuckey, & Meloni, 2018). The positive findings with R18 and R18D in HI are in line with previous studies from our laboratory demonstrating efficacy of these peptides in adult rat models of stroke due to middle cerebral artery occlusion (MCAO) and traumatic brain injury (Chiu et al., 2017; Edwards et al., 2018; Milani, Clark, et al., 2016; Milani, Cross, et al., 2016; Milani, Knuckey, et al., 2016; Meloni et al., 2014, 2017).

Whilst the exact mechanisms whereby CARPs exert their neuroprotective effects are still being explored, there is increasing evidence that this class of peptides possess properties that can impart multiple potential beneficial effects following acute brain injuries such HIE and stroke. For example, CARPs have the capacity to mitigate excitotoxicity (Edwards et al., 2018; Edwards, Anderton, Knuckey, & Meloni, 2016; Meloni et al., 2014; Meloni, Milani, et al., 2015), reduce intracellular and mitochondrial calcium influx (Edwards et al., 2016; 2018; Marshall et al., 2015; Meloni, Milani, et al., 2015; Rigobello, Barzon, Marin, & Bindoli, 1995), reduce cell surface levels of ion channels (Brittain et al., 2011; Brustovetsky, Pellman, Yang, Khanna, & Brustovetsky, 2014; MacDougall, Anderton, Edwards, Knuckey, & Meloni, 2016; Sinai, Duffy, & Roder, 2010) and TNF receptors (Fotin-Mleczek et al., 2005), assist in maintaining mitochondrial integrity (Birk, Chao, Liu, Soong, & Szeto, 2015; Cerrato, Pirisinu, Vlachos, & Langel, 2015; Ferré et al., 2016; Marshall et al., 2015; Rigobello et al., 1995; Szelechowski et al., 2014; Szeto et al., 2011; Zhao et al., 2004), inhibit the activity of the proteasome and matrix metalloproteinases (Anbanandam, Albarado, Tirziu, Simons, & Veeraraghavan, 2008; Cameron, Appel, Houghten, & Lindberg, 2000; Fugere, Appel, Houghten, Lindberg, & Day, 2007; Gaczynska, Osmulski, Gao, Post, & Simons, 2003; Kacprzak et al., 2004), reduce lipid peroxidation and oxidative stress and modulate immune responses and activate pro-survival signalling (Cook et al., 2011; Yang et al., 2014).

In a previous study in the P7 rat, we demonstrated that both R18 and R18D peptides reduced infarct volume and improved behavioural outcomes when administrated intraperitoneally (IP) immediately after HI (Edwards et al., 2018). The objective of the present study was to examine the therapeutic time window when R18D could be administered IP in P7 rats and still have a significant impact on infarct volume and/or behavioural outcomes when measured 48 hr after HI. In addition, in view of the increased resistance of peptides synthesised with D-amino acids to proteolytic degradation and hence potentially higher potency, the R18D peptide was used for the therapeutic time window studies.

2 | MATERIALS AND METHODS

2.1 | Peptides used in the study

The R18D peptide (H-rrrrrrrrrrrrrrrrrr-OH; charge +18; *r* = D-arginine) was synthesised by Mimotopes (Melbourne, Australia). R18D was purified using high performance liquid chromatography to at least 98% purity and subjected to hydrolysis and amino acid liquid chromatography analysis to obtain a precise measure of peptide content.

2.2 | Animal ethics and study design

All experimental procedures in this study adhered to the guidelines approved by the Animal Ethics Committee of the University of Western Australia (RA/3/100/1329 and RA/3/100/1569), in accordance with Policies and Guidelines of the National Health and Medical Research Council, Australia. Treatments were randomised and all procedures (e.g., peptide administration, behavioural assessments and measurement of infarct volumes) were performed whilst being blinded to treatments, with an experimental end-point of 48 hr post-HI. A diagrammatic representation of the study design is presented in Figure 1.

2.3 | Surgical procedure for modified Rice-Vannucci model

The modified Rice-Vannucci procedure was performed as previously described (Edwards et al., 2017, 2018). Briefly, unsexed, Sprague-Dawley P7 rat pups (Animal Resource Centre, Murdoch, Australia; P0 = day of birth; RRID: RGD_1566457) with a body weight of 16 ± 1.5 grams were used. Litters were culled to a maximum of 12 pups per litter to facilitate uniform growth without littermate competition. Rat pups were anaesthetised using isoflurane (5% induction, 1%–2% maintenance) in 100% oxygen, whilst on a heating pad (37°C). Through a 1 cm mid-line ventral incision, the right common, internal and external carotid arteries were exposed and isolated from the vagus nerve, venous circulation and carotid body. The right common carotid and external carotid arteries were permanently ligated using 6-0 silk sutures. Occlusion of the external carotid artery is a modification to the original Rice-Vannucci model that we have shown to result in a more reproducible infarct, accompanied by a more severe degree of brain injury (Edwards et al, 2017). The wound was closed using Vetbond (3M, Maplewood, USA), and animals were recovered on 100% oxygen for 5 min on a heating pad. The duration of anaesthesia from induction to beginning of recovery did not exceed 8 min. Sham-operated animals underwent the same operative procedure, except the exposed carotid arteries were not ligated; duration of anaesthesia from induction to recovery did not exceed 5 min.

Pups were returned to their dam for 1 hr before the commencement of hypoxia which consisted of placing 4–6 pups in an airtight container (approximate volume: 4 L) and exposing them to humidified and warmed hypoxic gas (8% O_2/92% N_2; 3 L/min) for 2.5 hr. The container was placed in an incubator with an ambient air temperature of 35°C, ensuring a body temperature of 36.5 ± 0.5°C, which was periodically monitored using an infrared thermometer. Following hypoxia, animals were placed on a heating pad for 5 min in a normoxic environment before being placed back with the dam. Sham-operated animals remained with the dam at all times.

2.4 | Post-surgical analgesia and monitoring

Immediately before the cessation of anaesthesia, pethidine was administered (5 mg/kg; IP). The surface body temperature of the animals was monitored using an infrared thermometer following the cessation of anaesthesia, before and after hypoxia and maintained between 36.5 and 37.5°C. To avoid hypothermia, rat cages were housed in a Ventilated Warming Cabinet (Techniplast; New South Wales, Australia) maintained at 26°C until the end of experiment. Animals that recorded a surface body temperature of >37.5°C within 1 hr after hypoxia were excluded from the study (Supplementary Table 1).

2.5 | Peptide administration

R18D was administered at separate time points of 30, 60 or 120 min after the conclusion of hypoxia. Treatments were administered IP (50 μL bolus) and consisted of either saline vehicle (0.9% sodium chloride for injection) or R18D, at up to five different doses (10, 30, 100, 300 or 1,000 nmol/kg).

2.6 | Animals used and sample size

One-hundred and ninety-five Sprague-Dawley P7 pups (96 female and 99 male), housed with the dam under controlled conditions on a 12 hr light-dark cycle, underwent surgery for HI or the sham procedure (i.e., anaesthesia, neck incision, wound closure and analgesia). Twenty nine animals were excluded from the study based on exclusion criteria provided in Supplementary Table 1. For the 30 min post-HI time point, the saline group consisted of 15 animals and the R18D treatment groups consisted of between 9 and 12 animals (see Figure 2a). For the 60 min post-HI time point, the saline group consisted of 16 animals and the R18D treatment groups consisted of between 10 and 11 animals (see Figure 3a). For the 120 min post-HI time point, the saline group consisted of 14 animals and R18D treatment groups consisted of between 10 and 13 animals (see Figure 4a). Separate sham animals were used for all the time window studies. As sham animals were treated in an identical fashion, functional data from these animals were pooled (N = 25).

2.7 | Infarct volume assessment

Forty-eight hours after HI, animals were euthanised by pentobarbital overdose (50 mg/kg; IP). Infarct volume was determined by preparing 2 mm thick serial coronal brain slices, and incubating in 3% 2,3,5-triphenyltetrazolium chloride (TTC; Sigma Aldrich, St. Louis, USA) at 37°C for 20 min, followed by fixation in 4% formalin at room temperature overnight. Digital images of coronal slices were acquired using a colour scanner and analysed using ImageJ software (3rd edition, NIH, Bethesda, USA; RRID: SCR_003070). Total infarct volume was determined by measuring the area of infarcted tissue on both surfaces of the 2 mm slices. Due to the presence of cerebral oedema, infarct volume measurements were corrected for a degree of hemisphere volume changes (Edwards et al., 2017). Final infarct data was expressed as percentage infarct volume compared to whole brain volume (minus cerebellum).

2.8 | Behavioural assessments

To determine if R18D treatment improved sensorimotor outcomes, three behavioural tests (righting reflex, negative geotactic response and wire-hang) were performed at 48 hr after HI, as previously reported (Edwards et al., 2017, 2018). Briefly, for three consecutive days before surgery (P4 to P6 inclusive), pups were accustomed to behavioural assessments with a target inclusion range of ≤ 2 s for the righting reflex and ≤ 30 s for the negative geotactic response. Each animal was given three attempts to complete each sensorimotor task, with 5 min between each attempt. One animal did not record responses within these parameters at P7 (day of surgery) and was excluded from the study. All of these reflexes are reproducible

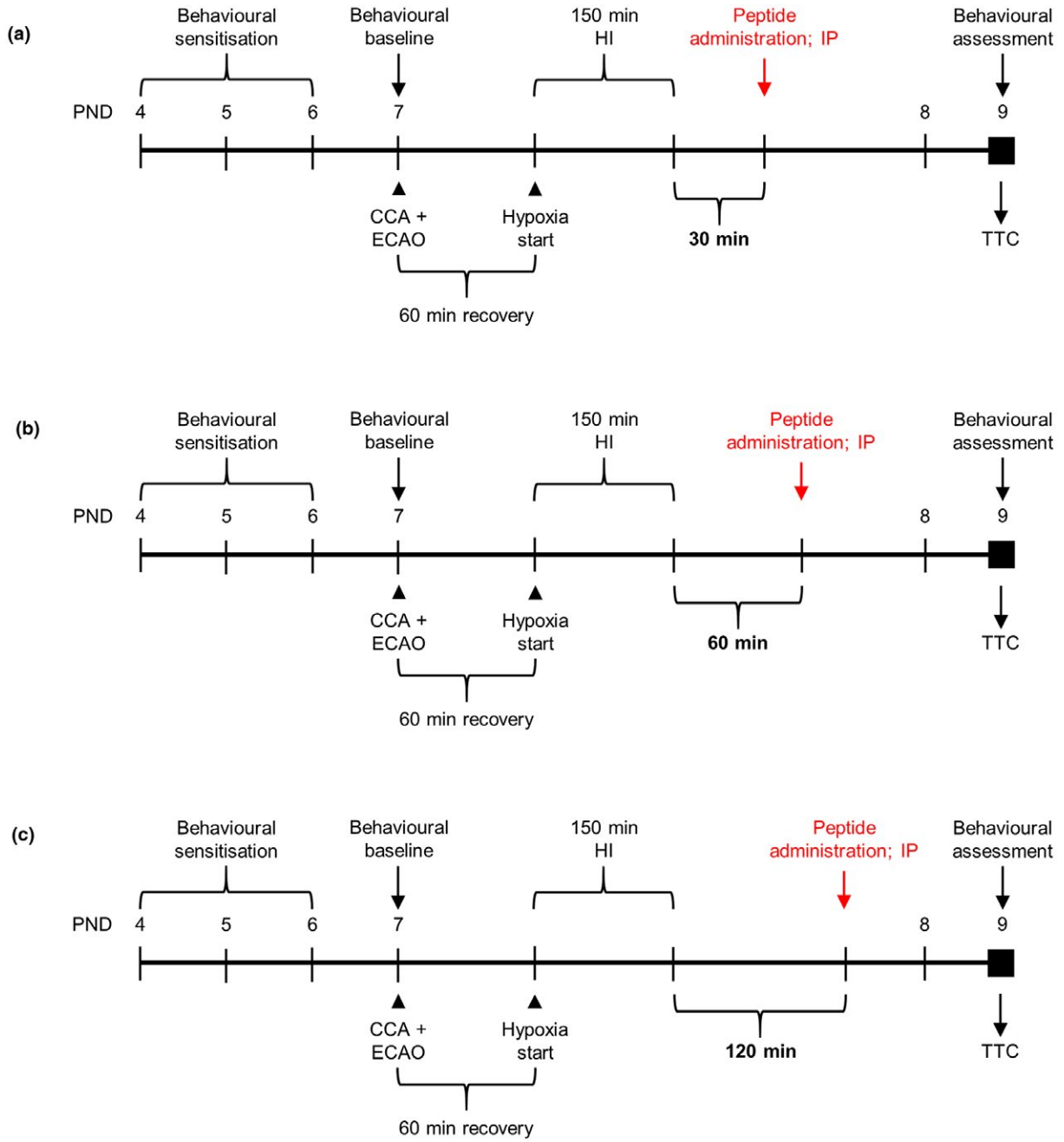

FIGURE 1 Schematic representation followed for R18D neuroprotective study in a perinatal rodent model of HIE. PND = postnatal day of age, CCA + ECAO = common carotid artery and external carotid artery occlusion, HI = hypoxia-ischaemic, min = minutes, TTC = 2,3,5-triphenyltetrazolium chloride. [Color figure can be viewed at wileyonlinelibrary.com]

throughout the murine preweaning period (< P30) and are strain- and gender-independent (Heyser, 2004).

The righting reflex involved placing pups in a supine position, and measuring the time required to rotate to the prone position. The negative geotactic response involved placing pups facing downslope, on a 45° angled surface, and measuring the time required for the animal to turn 150° upslope. Testing of the righting reflex and negative geotactic response was performed on a board covered with a tightly-stretched close knit-fabric, to ensure adequate grip. Wire-hang test was performed by suspending pups by their forelimbs on a 2 mm diameter steel wire suspended 20 cm above a foam surface, and recording the time taken for the animal to fall to the foam surface.

2.9 | Statistical analysis

The number of animals used in each experiment was justified by statistical power calculation based on a previous study (Edwards et al.,

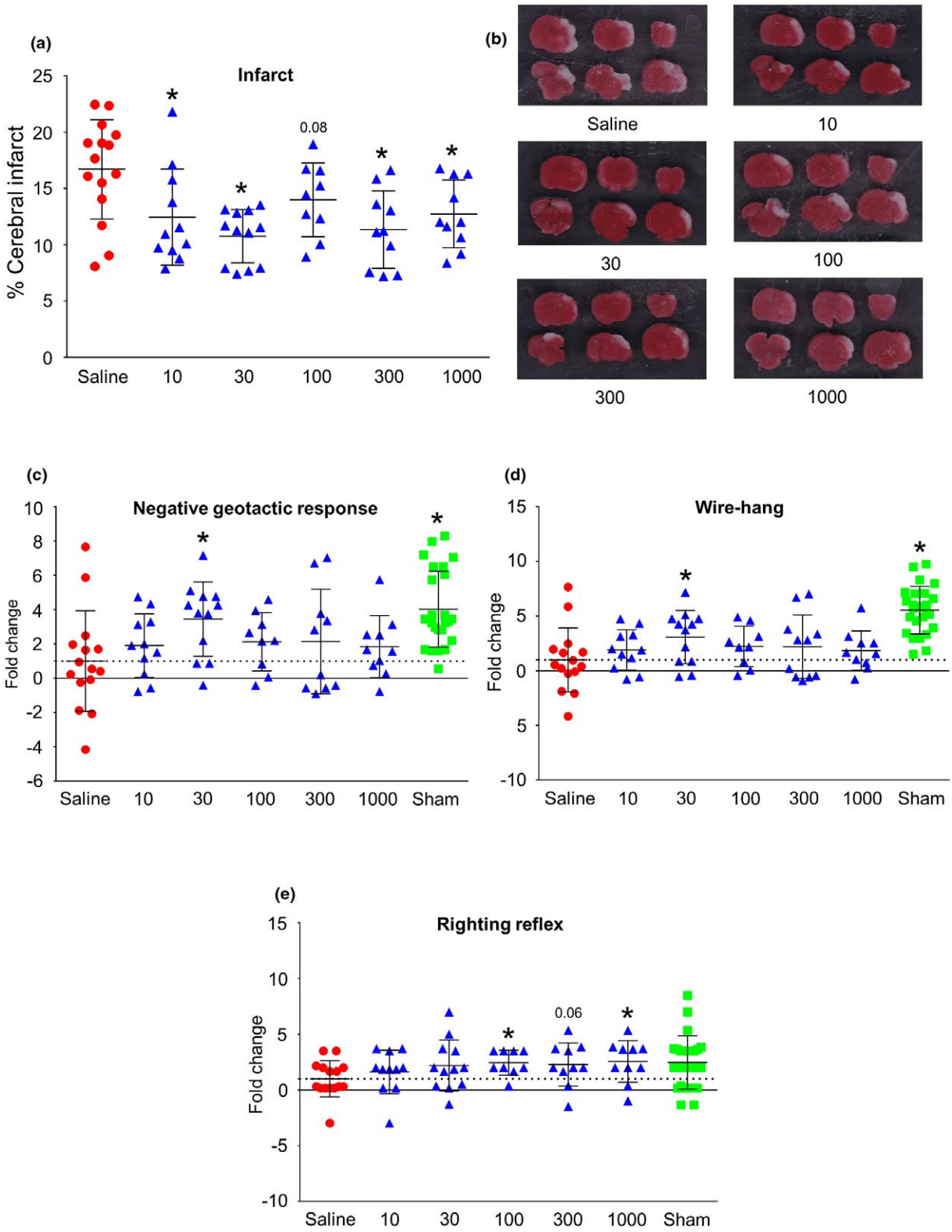

FIGURE 2 Assessment of R18D when administered 30 min after the conclusion of hypoxia. Histological and behavioural assessments for saline, sham and R18D treatment groups determined 48 hr after HI. Treatments were administered IP (saline or R18D; doses in nmol/kg). Behavioural assessments are presented as fold change (baseline vs. 48 hr). (a) Percentage of infarct volume when compared to total brain volume. (b) Representative TTC coronal brain slices from saline and R18D treated animals. (c) Negative geotactic response. (d) Wire-hang test. (e) Righting reflex. Values are mean ± *SD*. $^{*}p < 0.05$ when compared to saline. [Color figure can be viewed at wileyonlinelibrary.com]

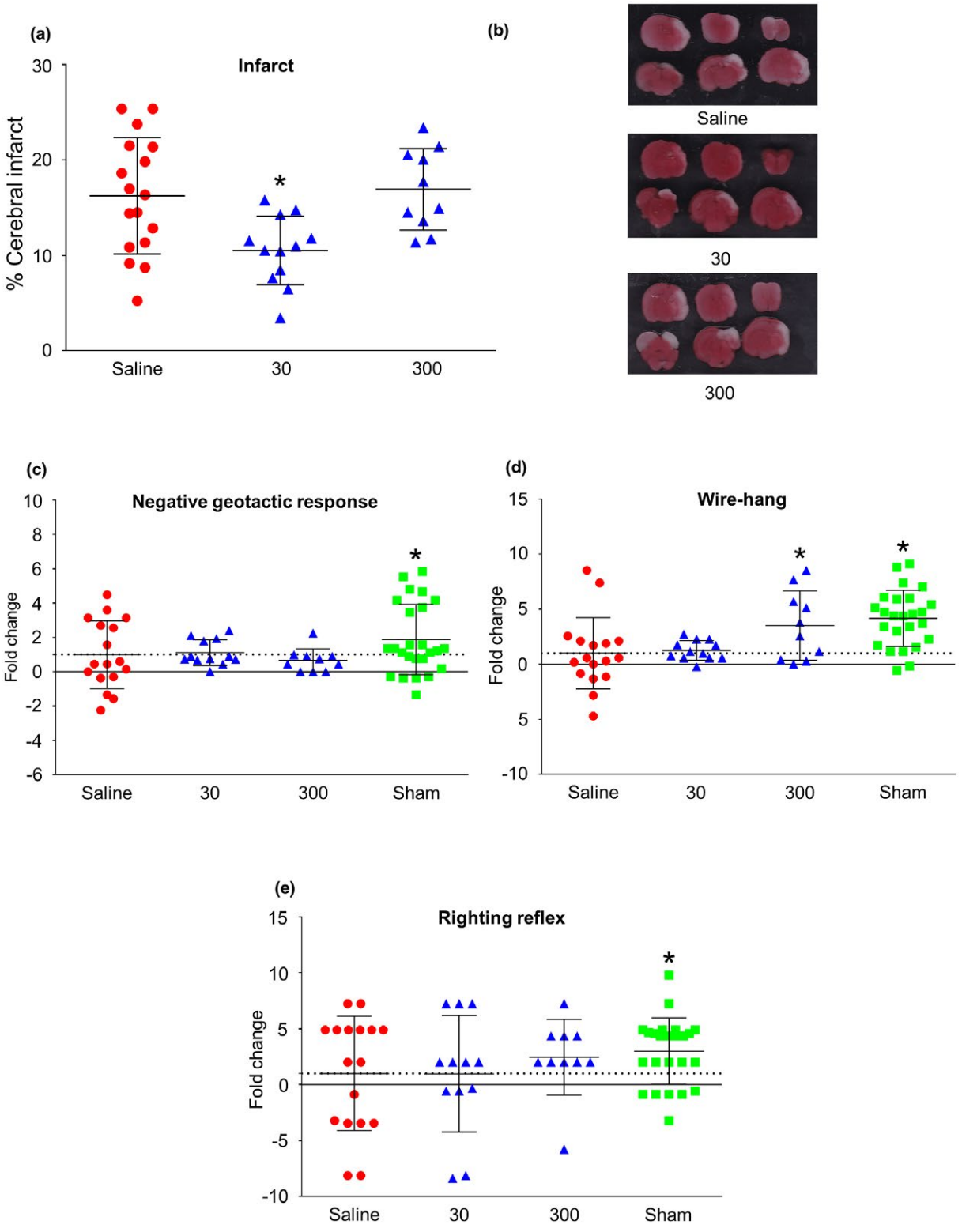

FIGURE 3 Assessment of R18D when administered 60 min after the conclusion of hypoxia. Histological and behavioural assessments for saline, sham and R18D treatment groups determined 48 hr after HI. Treatments were administered IP (saline or R18D; doses in nmol/kg). Behavioural assessments are presented as fold change (baseline vs. 48 hr). (a) Percentage of infarct volume when compared to total brain volume. (b) Representative TTC coronal brain slices from saline and R18D treated animals. (c) Negative geotactic response. (d) Wire-hang test. (e) Righting reflex. Values are mean ± *SD*. $^{*}p < 0.05$ when compared to saline. [†]Brain assigned largest infarct due to liquefactive brain incompatible for sectioning. [Color figure can be viewed at wileyonlinelibrary.com]

2018). Group sizes have been calculated based on a predicted treatment effect of a 33% reduction in infarct volume, at a power level of 90% and an alpha level of 0.05. Mean percentage infarct volume and weight gain were analysed by analysis of variance (ANOVA), followed by post-hoc Fisher's PLSD test, with $p < 0.05$ values considered statistically significant. For behavioural assessment analysis, data has been expressed as a fold change improvement as assessed 48 hr after HI. All values have been transformed to express saline treated as a reference value of 1 and analysed using a one-sample *t*-test, with $p < 0.05$ values considered statistically significant. Cohen's *d* effect size was calculated for mean infarct differences. All statistical analysis was performed using Graphpad Prism (RRID: SCR_0020798).

3 | RESULTS

3.1 | Infarct volume measurements

Data on infarct volume and representative TTC stained coronal brain slices are presented in Figures 2–4a,b. When administered 30 min after hypoxia (i.e., 3 hr after the commencement of HI) R18D at doses of 10, 30, 300 and 1,000 nmol/kg significantly reduced infarct volume by between 23.7 [$F(5, 61) = 0.70$; $n = 10$; $p < 0.01$] and 35.6% [$F(5, 61) = 0.70$; $n = 12$; $p < 0.0001$], whilst at the 100 nmol/kg dose, infarct volume was also reduced by 16.2%, albeit not to a statistically significant extent [$F(5, 61) = 0.70$; $n = 9$; $p = 0.07$] (refer to Supplementary Table 2 for descriptive statistics). To confirm dose efficacy in the 30 min post-hypoxia treatment group, Cohen's *d* effect size calculations determined the 30 and 300 nmol/kg doses provided the largest treatment effects at the 30 min post-hypoxia time point, therefore these doses were assessed at the 60 and 120 min post-hypoxia time points.

When administered 60 min after hypoxia (3.5 hr after the commencement of HI) R18D at a dose of 30 nmol/kg significantly reduced infarct volume by 34.2% [$F(2, 36) = 2.89$; $n = 12$; $p < 0.01$], whilste the 300 nmol/kg dose was ineffective. When administered 120 min after hypoxia (4 hr after the commencement of HI) R18D at a dose of 30 nmol/kg decreased infarct volume by 8% [$F(2, 35) = 0.09$; $n = 13$; p 0.52], albeit not to a statistically significant level. The R18D 300 nmol/kg dose did not influence infarct volume with a 12.8% increase in cerebral infarct [$F(2, 35) = 0.09$; $n = 10$; $p = 0.26$]. For all treatment groups, gender had no significant effect on infarct volume (data not shown).

3.2 | Behavioural outcomes following R18D administration

Data on behavioural outcomes is presented in Figures 2c–e, 3c–e, 4c–e and Supplementary Tables 3–5. Data on weight gain is presented in Supplementary Table 6. For all treatment groups, gender had no significant effect on behavioural outcomes (data not shown).

3.2.1 | 30 min post-HI

R18D, at a dose of 30 nmol/kg, significantly improved the negative geotactic response (3.45-fold; $p < 0.01$) and wire-hang (3.11-fold; $p = 0.01$). Similarly, R18D at doses of 100 and 1,000 nmol/kg significantly improved righting reflex (2.44 and 2.55-fold; $p < 0.01$ and 0.02, respectively). All other R18D treated groups did not improve performance in behavioural assessments (Figure 2).

3.2.2 | 60 min post-HI

R18D, at a dose of 300 nmol/kg, significantly improved wire-hang time (3.51-fold; $p = 0.03$). All other R18D treated groups did not improve performance in behavioural assessments (Figure 3).

3.2.3 | 120 min post-HI

R18D, at a dose of 300 nmol/kg, significantly improved the negative geotactic response (2.32-fold; $p < 0.01$). All other R18D treated groups did not improve performance in behavioural assessments (Figure 4).

4 | DISCUSSION

The present study adds to our previous findings which demonstrate the neuroprotective effectiveness of R18 and R18D in a P7 rat model of perinatal HIE (Edwards et al., 2018), and other acute neuronal injury models (Chiu et al., 2017; Edwards et al., 2016; Meloni et al., 2017; Meloni, Brookes, et al., 2015; Meloni, Milani, et al., 2015; Milani et al., 2018; Milani, Clark, et al., 2016; Milani, Cross, et al., 2016; Milani, Knuckey, et al., 2016). Importantly, the present study examined the neuroprotective efficacy of R18D when administered 30, 60 or 120 min after HI. The 30 min post-HI treatment time window study examined the dose response effectiveness of R18D and revealed that at all doses (10, 30, 100, 300 and 1,000 nmol/kg) resulted in a reduction in infarct volume by between 16.2% and 35.6%. In addition, R18D treatment was associated with animals displaying significantly improved, or positive trends for improved, negative geotactic response, wire-hang and righting reflex times.

The reduction in infarct volume and improved behavioural outcomes at the 30 min treatment time point are similar to our previous findings for R18D and R18 when administered immediately after HI at doses of 30, 100, 300 and 1,000 nmol/kg in the same experimental HIE model and 48 hr endpoint (Edwards et al., 2017). In addition, as previously observed when R18D and R18 were administered immediately after HI (Edwards et al., 2017), treatment with R18D at 30 min after HI at the doses used did not generate a typical dose response effect in terms of infarct volume reduction. These findings suggest that when administered early after HI, R18D is effective over a wide dose range from 10 to 1,000 nmol/kg, however, we cannot exclude the possibility that there may be a typical dose response effect with doses outside of this range. Interestingly, the JNKI-1-TATD peptide (also referred to as XG-102), which is also a

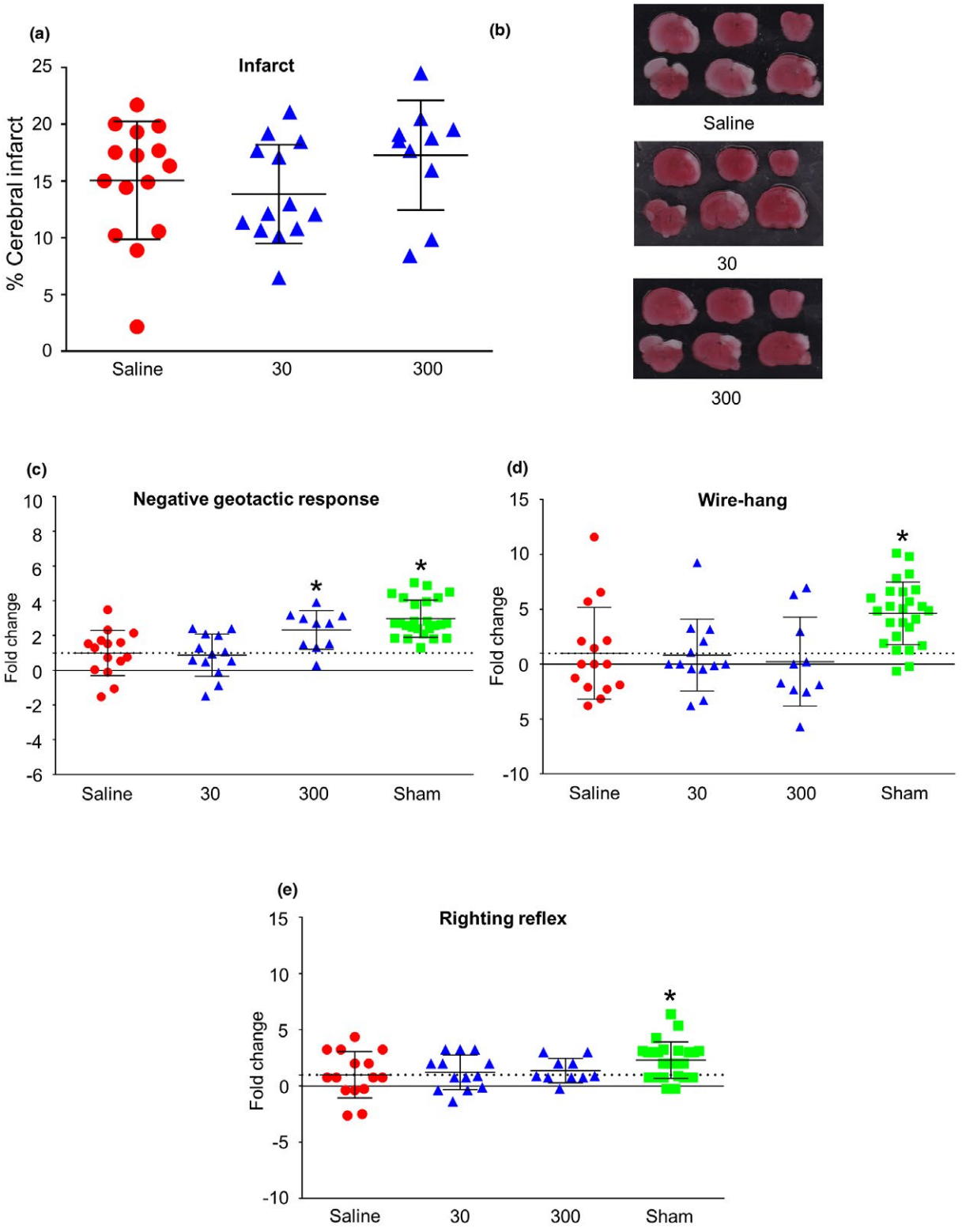

FIGURE 4 Assessment of R18D when administered 120 min after the conclusion of hypoxia. Histological and behavioural assessments for saline, sham and R18D treatment groups determined 48 hr after HI. Treatments were administered IP (saline or R18D; doses in nmol/kg). Behavioural assessments are presented as fold change (baseline vs. 48 hr). (a) Percentage of infarct volume when compared to total brain volume. (b) Representative TTC coronal brain slices from saline and R18D treated animals. (c) Negative geotactic response. (d) Wire-hang test. (e) Righting reflex. Values are mean ± *SD*. $^{*}p < 0.05$ when compared to saline. [Color figure can be viewed at wileyonlinelibrary.com]

CARP (arginine residues = 9 and net charge +12), displayed a non-dose response reduction in infarct volume over a wide dose range (0.076 to 760 nmol/kg), when administered intravenously 6 hr after a 30 min duration of MCAO in mice (Wiegler, Bonny, Coquoz, & Hirt, 2008).

When R18D was administered 60 min after HI, the 30 nmol/kg, but not the 300 nmol/kg dose significantly reduced infarct volume. Animals treated with the 30 nmol/kg dose, but not the 300 nmol/kg dose, 120 min after HI, displayed a nonsignificant reduction in infarct volume, but animals treated with the higher peptide dose displayed better negative geotactic response. At present, the reason for the lack of efficacy of R18D in reducing infarct volume at the 300 nmol/kg dose when administered 60 min after HI is not known. One possible explanation is that over time after HI, vulnerable, but potentially salvageable brain tissue becomes more sensitive to the adverse effects of higher peptide concentrations. In support of this, we have observed that following *in vitro* glutamic acid neuronal excitotoxicity, higher R18D concentrations (e.g., 5 μM) result in reduced neuroprotective efficacy (30% neuronal survival) compared to lower peptide concentrations (e.g., 2 μM; 100% neuronal survival). In addition, any adverse effects of R18D would likely to be exacerbated by the increased stability of the peptide due its D-arginine configuration. Notwithstanding the lack of efficacy of the 300 nmol/kg dose in reducing infarct volume, this dose did provide beneficial effects in terms of functional outcomes. This suggests that the R18D peptide may be having additional beneficial effects independent of reducing the infarct, possibly by improving synaptic function in noninfarcted areas, as observed with other CARPs (e.g., TAT-NR2B9c) (Srejic, Hutchison, & Aarts, 2013).

4.1 | Limitations of study

Whilst we have confirmed the effectiveness of R18D when administered after HI, there are several limitations associated with the study. Whilst the 48 hr endpoint was used to replicate our initial neuroprotection study, it is important that the efficacy of R18D also be evaluated at more extended time points after HI (e.g., 1–4 weeks). In addition, behavioural outcomes were quite variable when measured at 48 hr after HI, and therefore may not have provided an accurate reflection of the beneficial effects of R18D treatment. It will therefore be important that in longer-term studies, suitable behavioural tests with high sensitivity and low variability are used to detect potential treatment effects (e.g., gait analysis, rotarod, Barnes maze). Due to the current clinical application of therapeutic hypothermia to treat HIE, the assessment of CARP-mediated neuroprotection adjunctly to therapeutic hypothermia is required. We also acknowledge that an intravenous rather than intraperitoneal route of administration would be favoured in a clinical setting and would be more appropriately assessed in a larger animal model of HIE such as the piglet or lamb. Finally, a typical R18D dose response pattern in infarct volume reduction and behavioural outcomes was not observed in the study, and therefore it would be worthwhile examining a wider dose range of the peptide in future studies.

5 | CONCLUSION

Whilst hypothermia is currently the only available treatment known to improve neurological outcomes following HIE, the use of R18/R18D peptides as neuroprotective therapies offers exciting potential in the prevention of brain injury in infants following HI. This study demonstrates R18D efficacy when administered up to 60 min after HI in the rat, with concomitant improvements in behavioural assessments. Following on from these positive results, it will be important for future preclinical studies to assess R18D or R18 in other pre-term and term HIE models using larger animals (foetal sheep or piglet), and when combined with hypothermia.

ACKNOWLEDGEMENTS

The authors acknowledge the feedback on the manuscript provided by Professor Frank Mastaglia.

COMPETING INTERESTS

B.M. and N.K. are named inventors of several patent applications regarding the use of arginine-rich peptides as neuroprotective agents. The other authors declare no conflict of interest.

AUTHOR CONTRIBUTIONS

All authors had full access to all the data in the study and take responsibility of the integrity of the data and the accuracy of the data analysis. *Conceptualisation*, A.E. and B.M.; *Methodology*, A.E. and B.M.; *Investigation*, A.E.; *Formal Analysis*, A.B. and R.A., *Resources*, A.E., R.A., N.K. and B.M.; *Writing—Original Draft*, A.E. and B.M.; *Writing—Review & Editing*, A.E., R.A., N.K., B.M.; *Visualisation*, A.E. and B.M.; *Supervision*, R.A., N.K., and B.M.; *Funding Acquisition*, N.K. and B.M.

DATA ACCESSIBILITY

All supplementary information available at https://onlinelibrary.wiley.com/journal/10974547.

ORCID

Adam B. Edwards http://orcid.org/0000-0002-7503-3232

REFERENCES

Anbanandam, A., Albarado, D. C., Tirziu, D. C., Simons, M., & Veeraraghavan, S. (2008). Molecular basis for proline- and arginine-rich peptide inhibition of proteasome. *Journal of Molecular Biology*, *384*(1), 219–227. https://doi.org/10.1016/j.jmb.2008.09.021

Azzopardi, D. V., Strohm, B., Edwards, A. D., Dyet, L., Halliday, H. L., Juszczak, E., … Brocklehurst, P. (2009). Moderate hypothermia to treat perinatal asphyxial encephalopathy. *New England Journal of Medicine*, *361*(14), 1349–1358. https://doi.org/10.1056/NEJMoa0900854

Birk, A. V., Chao, W. M., Liu, S., Soong, Y., & Szeto, H. H. (2015). Disruption of cytochrome c heme coordination is responsible for mitochondrial

injury during ischemia. *Biochimica Et Biophysica Acta*, *1847*(10), 1075–1084. https://doi.org/10.1016/j.bbabio.2015.06.006

Brittain, J. M., Chen, L., Wilson, S. M., Brustovetsky, T., Gao, X., Ashpole, N. M., … Khanna, R. (2011). Neuroprotection against traumatic brain injury by a peptide derived from the collapsin response mediator protein 2 (CRMP2). *Journal of Biological Chemistry*, *286*(43), 37778–37792. https://doi.org/10.1074/jbc.M111.255455

Brustovetsky, T., Pellman, J. J., Yang, X. F. F., Khanna, R., & Brustovetsky, N. (2014). Collapsin response mediator protein 2 (CRMP2) interacts with N-methyl-D-aspartate (NMDA) receptor and Na^+/Ca^{2+} exchanger and regulates their functional activity. *Journal of Biological Chemistry*, *289*(11), 7470–7482. https://doi.org/10.1074/jbc.M113.518472

Cameron, A., Appel, J., Houghten, R. A., & Lindberg, I. (2000). Polyarginines are potent furin inhibitors. *Journal of Biological Chemistry*, *275*(47), 36741–36749. https://doi.org/10.1074/jbc.M003848200

Cerrato, C. P., Pirisinu, M., Vlachos, E. N., & Langel, Ü. (2015). Novel cell-penetrating peptide targeting mitochondria. *The FASEB Journal*, *29*(11), 4589–4599. https://doi.org/10.1096/fj.14-269225

Chiu, L. S., Anderton, R. S., Cross, J. L., Clark, V. W., Edwards, A. B., Knuckey, N. W., & Meloni, B. P. (2017). Assessment of R18, COG1410, and APP96-110 in excitotoxicity and traumatic Brain Injury. *Translational Neuroscience*, *8*(1), 147–157. https://doi.org/10.1515/tnsci-2017-0021

Cook, D. R., Gleichman, A. J., Cross, S. A., Doshi, S., Ho, W., Jordan-Sciutto, K. L., … Kolson, D. L. (2011). NMDA receptor modulation by the neuropeptide apelin: Implications for excitotoxic injury. *Journal of Neurochemistry*, *118*(6), 1113–1123. https://doi.org/10.1111/j.1471-4159.2011.07383.x

Douglas-Escobar, M., & Weiss, M. D. (2015). Hypoxic-ischemic encephalopathy: A review for the clinician. *JAMA Pediatrics*, *169*(4), 397–403. https://doi.org/10.1001/jamapediatrics.2014.3269

Edwards, A. B., Anderton, R. S., Knuckey, N. W., & Meloni, B. P. (2016). Characterisation of neuroprotective efficacy of modified poly-arginine-9 (R9) peptides using a neuronal glutamic acid excitotoxicity model. *Molecular and Cellular Biochemistry*, *426*(1-2), 75–85. https://doi.org/10.1007/s11010-016-2882-z

Edwards, A. B., Cross, J. L., Anderton, R. S., Knuckey, N. W., & Meloni, B. P. (2018). Poly-arginine R18 and R18D (D-enantiomer) peptides reduce infarct volume and improves behavioural outcomes following perinatal hypoxic-ischaemic encephalopathy in the P7 rat. *Molecular Brain*, *11*(1), 8. https://doi.org/10.1186/s13041-018-0352-0

Edwards, A. B., Feindel, K. W., Cross, J. L., Anderton, R. S., Clark, V. W., Knuckey, N. W., & Meloni, B. P. (2017). Modification to the Rice-Vannucci perinatal hypoxic-ischaemic encephalopathy model in the P7 rat improves the reliability of cerebral infarct development after 48 hours. *Journal of Neuroscience Methods*, *288*, 62–71. https://doi.org/10.1016/j.jneumeth.2017.06.016

Ferré, C. A., Davezac, N., Thouard, A., Peyrin, J.-M., Belenguer, P., Miquel, M.-C., … Szelechowski, M. (2016). Manipulation of the N-terminal sequence of the Borna disease virus X protein improves its mitochondrial targeting and neuroprotective potential. *The FASEB Journal*, *30*(4), 1523–1533. https://doi.org/10.1096/fj.15-279620

Fotin-Mleczek, M., Welte, S., Mader, O., Duchardt, F., Fischer, R., Hufnagel, H., … Brock, R. (2005). Cationic cell-penetrating peptides interfere with TNF signalling by induction of TNF receptor internalization. *Journal of Cell Science*, *118*(15), 3339–3351. https://doi.org/10.1242/jcs.02460

Fugere, M., Appel, J., Houghten, R. A., Lindberg, I., & Day, R. (2007). Short polybasic peptide sequences are potent inhibitors of PC5/6 and PC7: Use of positional scanning-synthetic peptide combinatorial libraries as a tool for the optimization of inhibitory sequences. *Molecular Pharmacology*, *71*(1), 323–332. https://doi.org/10.1124/mol.106.027946

Gaczynska, M., Osmulski, P. A., Gao, Y., Post, M. J., & Simons, M. (2003). Proline- and arginine-rich peptides constitute a novel class of allosteric inhibitors of proteasome activity. *Biochemistry*, *42*(29), 8663–8670. https://doi.org/10.1021/bi034784f

Gluckman, P. D., Wyatt, J. S., Azzopardi, D., Ballard, R., Edwards, A. D., Ferriero, D. M., … Gunn, A. J. (2005). Selective head cooling with mild systemic hypothermia after neonatal encephalopathy: Multicentre randomised trial. *The Lancet*, *365*(9460), 663–670. https://doi.org/10.1016/S0140-6736(05)17946-X

Heyser, C. J. (2004). Assessment of developmental milestones in rodents. In *Current protocols in neuroscience* (Vol. Chapter 8, p. Unit 8.18). Hoboken, NJ: John Wiley & Sons, Inc. https://doi.org/10.1002/0471142301.ns0818s25

Jacobs, S. E., Morley, C. J., Inder, T. E., Stewart, M. J., Smith, K. R., McNamara, P. J., … Collaboration, I. C. E. (2011). Whole-body hypothermia for term and near-term newborns with hypoxic-ischemic encephalopathy. *Archives of Pediatrics & Adolescent Medicine*, *165*(8), 692. https://doi.org/10.1001/archpediatrics.2011.43

Jenkins, D. D., Lee, T., Chiuzan, C., Perkel, J. K., Rollins, L. G., Wagner, C. L., … Martin, R. (2013). Altered circulating leukocytes and their chemokines in a clinical trial of therapeutic hypothermia for neonatal hypoxic ischemic encephalopathy. *Pediatric Critical Care Medicine*, *14*(8), 786–795. https://doi.org/10.1097/PCC.0b013e3182975cc9

Kacprzak, M. M., Peinado, J. R., Than, M. E., Appel, J., Henrich, S., Lipkind, G., … Lindberg, I. (2004). Inhibition of furin by polyarginine-containing peptides: Nanomolar inhibition by nona-D-arginine. *The Journal of Biological Chemistry*, *279*(35), 36788–36794. https://doi.org/10.1074/jbc.M400484200

Kruse, M., Michelsen, S. I., Flachs, E. M., Bronnum-Hansen, H., Madsen, M., & Uldall, P. (2009). Lifetime costs of cerebral palsy. *Developmental Medicine & Child Neurology*, *51*(8), 622–628. https://doi.org/10.1111/j.1469-8749.2008.03190.x

Logitharajah, P., Rutherford, M. A., & Cowan, F. M. (2009). Hypoxic-ischemic encephalopathy in preterm infants: Antecedent factors, brain imaging, and outcome. *Pediatric Research*, *66*(2), 222–229. https://doi.org/10.1203/PDR.0b013e3181a9ef34

MacDougall, G., Anderton, R. S., Edwards, A. B., Knuckey, N. W., & Meloni, B. P. (2016). The neuroprotective peptide poly-arginine-12 (R12) reduces cell surface levels of NMDA NR2B receptor subunit in cortical neurons; Investigation into the involvement of endocytic mechanisms. *Journal of Molecular Neuroscience*. *61*(2), 235–246. https://doi.org/10.1007/s12031-016-0861-1

Marshall, J., Wong, K. Y., Rupasinghe, C. N., Tiwari, R., Zhao, X., Berberoglu, E. D., … Goebel, D. J. (2015). Inhibition of N-methyl-D-aspartate-induced retinal neuronal death by polyarginine peptides is linked to the attenuation of stress-induced hyperpolarization of the inner mitochondrial membrane potential. *The Journal of Biological Chemistry*, *290*(36), 22030–22048. https://doi.org/10.1074/jbc.M115.662791

McQueen, J., Ryan, T. J., McKay, S., Marwick, K., Baxter, P., Carpanini, S. M., … Hardingham, G. M. (2017). Pro-death NMDA receptor signaling is promoted by the GluN2B C-terminus independently of Dapk1. *Elife*, *6*, e17161. https://doi.org/10.7554/eLife.17161

Meloni, B. P., Brookes, L. M., Clark, V. W., Cross, J. L., Edwards, A. B., Anderton, R. S., … Knuckey, N. W. (2015). Poly-arginine and arginine-rich peptides are neuroprotective in stroke models. *Journal of Cerebral Blood Flow & Metabolism*, *35*(6), 993–1004. https://doi.org/10.1038/jcbfm.2015.11

Meloni, B. P., Craig, A. J., Milech, N., Hopkins, R. M., Watt, P. M., & Knuckey, N. W. (2014). The neuroprotective efficacy of cell-penetrating peptides TAT, penetratin, Arg-9, and Pep-1 in glutamic acid, kainic acid, and in vitro ischemia injury models using primary cortical neuronal cultures. *Cellular & Molecular Neurobiology*, *34*(2), 173–181. https://doi.org/10.1007/s10571-013-9999-3

Meloni, B. P., Milani, D., Cross, J. L., Clark, V. W., Edwards, A. B., Anderton, R. S., … Knuckey, N. W. (2017). Assessment of the neuroprotective effects of arginine-rich protamine peptides, poly-arginine peptides (R12-Cyclic, R22) and arginine–tryptophan-containing peptides following in vitro excitotoxicity and/or permanent middle cerebral artery occlusion in rats. *NeuroMolecular Medicine*, *19*(2-3), 271–285. https://doi.org/10.1007/s12017-017-8441-2

Meloni, B. P., Milani, D., Edwards, A. B., Anderton, R. S., O'Hare Doig, R. L., Fitzgerald, M., … Knuckey, N. W. (2015). Neuroprotective peptides fused to arginine-rich cell penetrating peptides: Neuroprotective mechanism likely mediated by peptide endocytic properties. *Pharmacology & Therapeutics*, *153*, 36–54. https://doi.org/10.1016/j.pharmthera.2015.06.002

Milani, D., Bakeberg, M. C., Cross, J. L., Clark, V. W., Anderton, R. S., Blacker, D. J., … Meloni, B. P. (2018). Comparison of neuroprotective efficacy of poly-arginine R18 and R18D (D-enantiomer) peptides following permanent middle cerebral artery occlusion in the Wistar rat and in vitro toxicity studies. *PLoS One*, *13*(3), e0193884. https://doi.org/10.1371/journal.pone.0193884

Milani, D., Clark, V. W., Cross, J. L., Anderton, R. S., Knuckey, N. W., & Meloni, B. P. (2016). Poly-arginine peptides reduce infarct volume in a permanent middle cerebral artery rat stroke model. *BMC Neuroscience*, *17*(1), 19. https://doi.org/10.1186/s12868-016-0253-z

Milani, D., Cross, J. L., Anderton, R. S., Blacker, D. J., Knuckey, N. W., & Meloni, B. P. (2016). Neuroprotective efficacy of poly-arginine R18 and NA-1 (TAT-NR2B9c) peptides following transient middle cerebral artery occlusion in the rat. *Neuroscience Research*, *114*, 9–15. https://doi.org/10.1016/j.neures.2016.09.002

Milani, D., Knuckey, N. W., Anderton, R. S., Cross, J. L., Meloni, B. P., Milani, D., … Meloni, B. P. (2016). The R18 Polyarginine peptide is more effective than the TAT-NR2B9c (NA-1) peptide when administered 60 minutes after permanent middle cerebral artery occlusion in the rat. *Stroke Research and Treatment*, *2016*, 1–9. https://doi.org/10.1155/2016/2372710

Mosalli, R. (2012). Whole body cooling for infants with hypoxic-ischemic encephalopathy. *Journal of Clinical Neonatology*, *1*(2), 101–106. https://doi.org/10.4103/2249-4847.96777

Pierrat, V., Haouari, N., Liska, A., Thomas, D., Subtil, D., & Truffert, P., & Groupe d'Etudes en Epidémiologie Périnatale. (2005). Prevalence, causes, and outcome at 2 years of age of newborn encephalopathy: Population based study. *Archives of Disease in Childhood - Fetal and Neonatal Edition*, *90*(3), F257–F261. https://doi.org/10.1136/adc.2003.047985

Rao, R., Trivedi, S., Vesoulis, Z., Liao, S. M., Smyser, C. D., & Mathur, A. M. (2016). Safety and short-term outcomes of therapeutic hypothermia in preterm neonates 34–35 weeks gestational age with hypoxic-ischemic encephalopathy. *The Journal of Pediatrics*, *183*, 37–42. https://doi.org/10.1016/j.jpeds.2016.11.019

Rigobello, M. P., Barzon, E., Marin, O., & Bindoli, A. (1995). Effect of polycation peptides on mitochondrial permeability transition. *Biochemical and Biophysical Research Communications*, *217*(1), 144–149. https://doi.org/10.1006/bbrc.1995.2756

Shankaran, S., Laptook, A. R., Ehrenkranz, R. A., Tyson, J. E., McDonald, S. A., Donovan, E. F., … Jobe, A. H. (2005). Whole-body hypothermia for neonates with hypoxic-ischemic encephalopathy. *The New England Journal of Medicine*, *353*(15), 1574–1584. https://doi.org/10.1056/NEJMcps050929

Sinai, L., Duffy, S., & Roder, J. C. (2010). Src inhibition reduces NR2B surface expression and synaptic plasticity in the amygdala. *Learning & Memory*, *17*(8), 364–371. https://doi.org/10.1101/lm.1765710

Srejic, L. R., Hutchison, W. D., & Aarts, M. M. (2013). Uncoupling PSD-95 interactions leads to rapid recovery of cortical function after focal stroke. *Journal of Cerebral Blood Flow and Metabolism: Official Journal of the International Society of Cerebral Blood Flow and Metabolism*, *33*(12), 1937–1943. https://doi.org/10.1038/jcbfm.2013.153

Szelechowski, M., Bétourné, A., Monnet, Y., Ferré, C. A., Thouard, A., Foret, C., … Gonzalez-Dunia, D. (2014). A viral peptide that targets mitochondria protects against neuronal degeneration in models of Parkinson's disease. *Nature Communications*, *5*(1), 5181. https://doi.org/10.1038/ncomms6181

Szeto, H. H., Liu, S., Soong, Y., Wu, D., Darrah, S. F., Cheng, F. Y., … Seshan, S. V. (2011). Mitochondria-targeted peptide accelerates ATP recovery and reduces ischemic kidney injury. *Journal of the American Society of Nephrology*, *22*(6), 1041–1052. https://doi.org/10.1681/ASN.2010080808

Wiegler, K., Bonny, C., Coquoz, D., & Hirt, L. (2008). The JNK inhibitor XG-102 protects from ischemic damage with delayed intravenous administration also in the presence of recombinant tissue plasminogen activator. *Cerebrovascular Diseases*, *26*(4), 360–366. https://doi.org/10.1159/000151639

Yang, Y., Zhang, X., Cui, H., Zhang, C., Zhu, C., & Li, L. (2014). Apelin-13 protects the brain against ischemia/reperfusion injury through activating PI3K/Akt and ERK1/2 signaling pathways. *Neuroscience Letters*, *568*, 44–49. https://doi.org/10.1016/j.neulet.2014.03.037

Zhao, K., Zhao, G.-M., Wu, D., Soong, Y., Birk, A. V., Schiller, P. W., & Szeto, H. H. (2004). Cell-permeable peptide antioxidants targeted to inner mitochondrial membrane inhibit mitochondrial swelling, oxidative cell death, and reperfusion injury. *The Journal of Biological Chemistry*, *279*(33), 34682–34690. https://doi.org/10.1074/jbc.M402999200

SUPPORTING INFORMATION

Additional Supporting Information may be found online in the supporting information tab for this article.

How to cite this article: Edwards AB, Anderton RS, Knuckey NW, Meloni BP. Assessment of therapeutic window for poly-arginine-18D (R18D) in a P7 rat model of perinatal hypoxic-ischaemic encephalopathy. *J Neuro Res*. 2018;96:1816–1826. https://doi.org/10.1002/jnr.24315

Supplementary Table 1. Animals excluded in the study.

Exclusion rationale	Number of exclusions	R18D peptide treatment time after HI (min)	R18D peptide dose (nmol/kg)	Total number of exclusions
No detectable infarct	6	30	30	11
	1	60	30	
	1	60	Saline	
	1	120	30	
	2	120	Saline	
Hyperthermia*	1	30	100	7
	4	60	30	
	2	60	300	
Failure to complete behavioural assessment	1	-	-	1
Surgical haemorrhage[#]	4	-	-	4
Premature death[†]	3	-	-	3

*Hyperthermia is a recorded body temperature >37.5 immediately after hypoxia. [#]Surgical haemorrhage is defined as any animal which had an abnormal bleed (arterial rupture) during the surgical procedure. [†]Premature deaths occurred during hypoxia.

Supplementary Table 2. Cerebral infarct. Percentage of total cerebral volume

Peptide administration time after HI (min)	Dose	N	Mean of total infarct volume (SD) (%)	Reduction in cerebral infarct (%)	*P*	*d*
30	Saline	15	16.7 (4.41)	-	-	-
	10	11	12.4 (4.25)	25.4	**<0.01**	0.99
	30	12	10.7 (2.36)	35.6	**<0.0001**	1.70
	100	9	14.0 (3.27)	16.2	0.08	0.70
	300	10	11.3 (3.43)	32.0	**<0.01**	1.37
	1,000	10	12.7 (3.01)	23.7	**<0.01**	1.06
60	Saline	17	16.2 (6.01)	-	-	-
	30	12	10.5 (3.60)	34.2	**<0.01**	1.15
	300	10	16.9 (4.27)	0.06	0.73	0.13
120	Saline	15	15.0 (5.20)	-	-	-
	30	13	13.8 (4.35)	8.0	0.52	0.25
	300	10	17.2 (4.83)	-14.6	0.26	0.44

N, number of animals; SE, standard error of mean; *P*, calculated compared to saline vehicle control. All doses are in nmol/kg. Mean and SE expressed as percentage of total cerebral volume. Percentage reduction is mean percentage reduction compared to saline. All values $P < 0.05$ are in bold. Cohen's *d* is compared to the saline within each peptide administration group (30, 60 or 120 min).

Supplementary Table 3. Behavioural assessment; treatment 30 min post-HI.

Behavioural assessment	Treatment	Dose	N	Mean (SD)* (seconds)	*P* when compared to hypothetical mean of 1
Negative geotactic response	Saline	-	15	2.06 (6.04)	1
	R18D	10	11	0.20 (3.81)	0.13
		30	12	-3.00 (4.45)	**<0.01**
		100	9	-0.26 (3.50)	0.08
		300	10	-0.30 (6.30)	0.26
		1000	10	0.32 (3.71)	0.17
	Sham	-	25	-4.20 (4.56)	**<0.0001**
Wire hang	Saline	-	15	-2.06 (6.04)	1
	R18	10	11	-0.20 (3.81)	0.15
		30	12	2.24 (5.03)	**0.01**
		100	9	0.48 (3.82)	0.08
		300	10	0.41 (6.00)	0.19
		1000	10	-0.32 (3.71)	0.17
	Sham	-	25	7.32 (4.50)	**<0.0001**
Righting reflex	Saline	-	15	0.20 (0.32)	1
	R18D	10	11	0.07 (0.40)	0.34
		30	12	-0.04 (0.46)	0.09
		100	9	-0.11 (0.22)	**<0.01**
		100	10	-0.06 (0.40)	0.06
		1000	10	-0.11 (0.37)	**0.02**
	Sham	-	25	-0.10 (0.50)	**<0.01**

*Mean time difference to perform behavioural assessment from baseline to 48 h after HI; negative integer indicates a reduction in time taken to perform task. N, number of animals; SD, standard deviation; *P* calculated compared to hypothetical mean of 1. All doses are in nmol/kg. All values $P < 0.05$ are bold.

Supplementary Table 4. Behavioural assessment; treatment 60 min post-HI.

Behavioural assessment	Treatment	Dose	N	Mean (SD)* (fold change)	*P* when compared to hypothetical mean of 1
Negative geotactic response	Saline	-	17	-2.23 (4.40)	1
	R18D	30	12	-2.48 (1.66)	0.61
		300	10	-1.50 (1.51)	0.15
	Sham	-	25	-4.20 (4.56)	**0.04**
Wire hang	Saline	-	17	1.76 (5.70)	1
	R18	30	12	2.20 (1.55)	0.34
		300	10	6.20 (5.53)	**0.03**
	Sham	-	25	7.32 (4.50)	**<0.0001**
Righting reflex	Saline	-	17	0.13 (0.65)	1
	R18D	30	12	0.13 (0.67)	0.98
		300	10	-0.50 (0.43)	0.21
	Sham	-	25	-0.10 (0.50)	**<0.01**

*Mean time difference to perform behavioural assessment from baseline to 48 h after HI; negative integer indicates a reduction in time taken to perform task. N, number of animals; SD, standard deviation; *P* calculated compared to hypothetical mean of 1. All doses are in nmol/kg. All values $P < 0.05$ are bold.

Supplementary Table 5. Behavioural assessment; treatment 120 min post-HI

Behavioural assessment	Treatment	Dose	N	Mean (SD)* (fold change)	*P* when compared to hypothetical mean of 1
Negative geotactic response	Saline	-	15	4.27 (5.60)	**1**
	R18D	30	13	4.82 (5.20)	0.71
		300	10	-1.40 (4.74)	**<0.01**
	Sham	-	25	-4.20 (4.56)	**<0.0001**
Wire hang	Saline	-	15	1.60 (6.60)	**1**
	R18	30	13	1.31 (5.16)	0.85
		300	10	0.36 (6.40)	**0.56**
	Sham	-	25	7.32 (4.50)	**<0.0001**
Righting reflex	Saline	-	15	0.30 (0.61)	**1**
	R18D	30	13	0.23 (0.45)	0.61
		300	10	0.20 (0.32)	0.30
	Sham	-	25	-0.10 (0.50)	**<0.01**

*Mean time difference to perform behavioural assessment from baseline to 48 h after HI; negative integer indicates a reduction in time taken to perform task. N, number of animals; SD, standard deviation; *P* calculated compared to hypothetical mean of 1. All doses are in nmol/kg. All values $P < 0.05$ are bold.

Supplementary Table 6. Weight gain from baseline to 48 h post HI.

Peptide administration time after HI (min)	Dose	N	Mean of total weight gain (SD) (g)	*P* when compared to saline
30	Saline	15	-0.07 (1.94)	-
	10	11	0.62 (1.88)	0.29
	30	12	1.02 (1.57)	0.09
	100	9	0.14 (1.60)	0.75
	300	10	1.01 (1.94)	0.09
	1,000	10	0.68 (2.24)	0.28
60	Saline	17	1.63 (1.32)	-
	30	12	1.30 (2.20)	0.54
	300	10	1.37 (1.30)	0.64
120	Saline	15	1.21 (1.70)	-
	30	13	1.77 (1.57)	0.26
	300	10	1.16 (1.83)	0.93
Sham	-	25	5.10 (0.80)	**<0.0001**

N, number of animals; SE, standard error of mean; *P*, calculated compared to saline vehicle control or sham animals. All doses are in nmol/kg. Mean, SD and SE expressed as grams. All values $P < 0.05$ are in bold.

Chapter 7

General Discussion

7.1 INTRODUCTION

Perinatal HIE occurs when there is a reduction in fetal CBF and/or cerebral oxygen supply, resulting in neuronal and glial cell loss and brain injury. Currently, the most effective clinical therapy to minimise cerebral injury is moderate hypothermia (33.5°C for 72 hours); to be effective, hypothermia needs to be administered within 6 hours of HIE onset. In infants who suffer moderate or severe encephalopathy, hypothermia has been shown to decrease mortality from 40% to 28%, while in surviving infants, neurological morbidity (e.g. cerebral palsy, epilepsy, intellectual disability and autism spectrum disorders) is reduced from 31% to 19% (Jacobs et al., 2013).

Despite the clinical benefits of hypothermia in HIE, its application can be associated with low risk levels of adverse effects such as haemorrhage, infection, impairment of oxygen retention and an increased risk of drug related side-effects (van den Broek, Groenendaal, Egberts, & Rademaker, 2010). Importantly, whilst hypothermia is safe in pre-term infants with necrotising enterocolitis (Hall et al., 2010), it has not been adequately evaluated for use in pre-term infants suffering HIE. Information regarding the safety and efficacy of hypothermia to treat pre-term infants suffering HIE is lacking. In one study, hypothermia in pre-term infants was associated with higher mortality and increased clinical complications when compared to term infants (Rao et al., 2016); and for these reasons it is not routinely used in these patients. In addition, the induction of hypothermia requires specialised equipment, intensive care monitoring and trained staff, which limits its use to centres that have the facilities and medical personnel to undertake the procedure. The transfer of infants to a centre equipped to deliver hypothermia, delays cooling induction, or if induced during

transfer, creates uncertainty regarding the safety and effectiveness of the cooling provided (Committee on Fetus and Newborn et al., 2014). In light of this, the application of a neuroprotective therapeutic agent to HIE patients (e.g. a neuroprotective cationic arginine-rich peptide) prior to transfer to a tertiary hospital may extend the therapeutic time window and effectiveness of hypothermia. In addition, as HIE infant mortality and morbidity are still relatively high following hypothermia treatment (discussed in Chapter 2), there is an urgent need for the development of additional therapeutic agents, which can be used in combination with hypothermia, to further improve outcomes in infants suffering HI. Furthermore, in situations when hypothermia is not available or contra-indicated, an alternative neuroprotective therapy would be highly advantageous.

Recent studies in A/Prof Meloni's laboratory have demonstrated that cationic arginine-rich peptides (CARPs), such as R18, are highly neuroprotective agents both in *in vitro* neuronal and animal models of stroke (Edwards, Anderton, Knuckey, & Meloni, 2016; MacDougall, Anderton, Edwards, Knuckey, & Meloni, 2016; Meloni, Brookes, et al., 2015; Meloni et al., 2017; Meloni, Milani, et al., 2015; Milani, Clark, et al., 2016; Milani et al., 2017; Milani, Knuckey, Anderton, Cross, & Meloni, 2016). As such, previous studies in A/Prof Meloni's laboratory have provided the rationale for this thesis to investigate the application of CARPs as a potential neuroprotective therapy for HIE.

7.2 KEY FINDINGS ARISING FROM THIS THESIS

7.2.1 Cerebral collateral circulation and infarct volume variability

The application of the HIE model using the 7-day-old (P7) rat was first described by Rice et al. (1981), and is often referred to as the Rice-Vannucci model. This is the most commonly used animal model for perinatal HIE neuroprotective and neurodegenerative pre-clinical studies. The model involves the permanent occlusion of the common carotid artery (CCAO) followed by a transient period of hypoxia (e.g. 8% O_2/92% N_2; for 2.5 h). Since its inception, the Rice-Vannucci model is widely reported to be associated with variable outcomes with respect to infarct presence, infarct volume size and by extension, functional outcomes (Ashwal, Tone, Tian, Chong, & Obenaus, 2007; Barks et al., 2017; Hagberg, Gilland, Diemer, & Andiné, 1994; Okusa et al., 2014; Ota, Ikeda, Ikenoue, & Toshimori, 1997; Palmer, Towfighi, Roberts, & Heitjan, 1993; Palmer, Vannucci, & Towfighi, 1990; Rice et al., 1981).

Whilst several sources of variability in the Rice-Vannucci model have been described (see Table 1, Chapter 4), an additional source of variability in both perinatal and adult ischaemic brain injury models can be attributed to the presence of cerebral collateral circulation via the circle of Willis and/or cerebral anastomoses; stabilising CBF following vessel occlusion and/or haemodynamic compromise. However, prior to this thesis the impact of collateral circulation as a source of variability in the Rice-Vannucci model had not been investigated.

In an attempt to minimise the known variability associated with the Rice-Vannucci model of HIE, a modified Rice-Vannucci model was developed (Chapter 4). The surgical procedure involves the permanent ligation of both the right common carotid artery (CCA) and external carotid artery (ECA) followed by hypoxia (8% O_2/92% N_2; for 2.5 h). The modified Rice-Vannucci model demonstrated a more reproducible cerebral infarct (infarct presence and reduced standard deviation), a larger infarct lesion, and more severe behavioural deficits when compared to the original Rice-Vannucci model.

In addition, magnetic resonance angiography phase-contrast velocity encoding and pulsed arterial spin labelling analysis in animals subjected to the original Rice-Vannucci model (right CCA occlusion only) demonstrated residual blood flow in the right internal carotid artery; an effect that would help preserve CBF to tissue affected by the CCA occlusion. In contrast, animals subjected to the modified Rice-Vannucci model (right ECA/CCA occlusion) demonstrated complete cessation of blood flow within the right internal, external and common carotid arteries, and a significant overall reduction in CBF to the right hemisphere. The source of cerebral collateral and anastomotic circulation is detailed diagrammatically in Figure 1, Chapter 4.

As a consequence of the modification to the original Rice-Vannucci surgical procedure, the model now offers a more reliable and reproducible cerebral infarct and was used for all animal experimental studies in this thesis (Chapters 5 & 6).

7.2.2 Effectiveness of R18 and R18D in a perinatal HIE model

One of the primary aims of this study was to identify a potential lead neuroprotective poly-arginine peptide and an effective peptide dose. Based on previous *in vitro* (Meloni, Brookes, et al., 2015) and adult animal studies in stroke related brain injury models (Milani, Clark, et al., 2016; Milani et al., 2017; Milani, Knuckey, et al., 2016), two peptides were selected; R18 ($_{L}$-enantiomer) and R18D ($_{D}$-enantiomer). The initial study examined the dose response effectiveness of R18 and R18D when administered immediately after HI in the modified Rice-Vannucci model. The CARP, JNKI-1-TATD (also referred to as XG-102) at the 1000 nmol/kg dose (equivalent to the highest dose of R18 and R18D examined), was used as a positive control and benchmark (Nijboer et al., 2010).

This thesis demonstrated that both R18 and R18D at all doses examined reduced cerebral infarct volume, and at several doses improved functional outcome measures, as well as improving weight gain in animals. In contrast, JNKI-1-TATD treatment resulted in a non-significant reduction in cerebral infarct volume and did not significantly improve any functional outcomes or weight gain. The efficacy of both R18 and R18D over a wide dose range (30 – 1000 nmol/kg) is highly significant and could ultimately translate to clinical efficacy at low doses, which would have the advantage of reducing the risk of side effects due to the peptide. Interestingly, a wide neuroprotective dose-response range has been observed previously for JKNI-1-TATD following intraperitoneal administration in adult mice (Wiegler, Bonny, Coquoz, & Hirt, 2008) and P14 rats (Vaslin, Naegele-Tollardo, Puyal, & Clarke, 2011) subjected to a middle cerebral artery occlusion.

However, the inferior efficacy observed with JNKI-1-TATD in HIE may reflect its lower arginine content (R = 9) and cationic charge (+12), compared to R18 and R18D (R = 18, net charge +18). In support of this, previous studies from our laboratory have confirmed that the neuroprotective efficacy of CARPs increases with increasing peptide arginine content and peptide positive charge (Edwards et al., 2016; Meloni, Brookes, et al., 2015).

One of the key principals to developing a therapeutic intervention for HIE is the concept of a delayed secondary phase of brain injury. In infants suffering from a cerebral HI event, the development of secondary brain injury is associated with mitochondrial energy failure, cytotoxic oedema, cell death and the presence of clinical seizures. The secondary injury phase typically occurs 6 – 15 hours following HI onset, and thus provides a therapeutic window for intervention to reduce further brain injury. Therefore, a subsequent aim of this thesis was to determine if the R18 peptide was effective when administered at delayed time points following hypoxia in the modified Rice-Vannucci model. While R18 and R18D demonstrated similar efficacy when administered immediately after hypoxia, the R18D peptide was selected for the delayed administration studies in view of the known resistance of D-enantiomer peptides to enzymatic degradation (Weinstock, Francis, Redman, & Kay, 2012), which would potentially extend peptide half-life and tissue bioavailability. Furthermore, due to the acute and ongoing nature of brain injury following HI, delayed administration would expose the peptide to increasing levels of proteolytic enzymes activated in the extracellular matrix and released from dead and dying cells in the brain. Hence, the use of a D-enantiomer peptide (R18D), as opposed to a L-enantiomer peptide (R18) is potentially likely to be more effective in this situation.

The therapeutic window study revealed that R18D at all the doses examined significantly reduced cerebral infarct volume when administered 30 or 60 minutes after hypoxia (3 and 3.5 h after the commencement of HI, respectively), and at several doses improved functional outcomes. As with the dose response study, the efficacy of R18D over a wider dose range (10 – 1000 nmol/kg) when administered after HI was shown to be highly significant and demonstrated neuroprotective efficacy at even lower doses down to 10 nmol/kg.

7.3 LIMITATIONS OF THIS THESIS

While this thesis has confirmed the neuroprotective efficacy of R18 and R18D in a rat model of HI, and the potential application of the peptides as a novel therapeutic to treat HIE, there are several limitations associated with the study. A 48-hour endpoint was used in the HI studies (Chapters 5 and 6), however, to confirm that neuroprotection provided by R18 and R18D is maintained longer-term, extended time points after HI (e.g. 4 – 7 weeks) need to be assessed. In addition, the use of an extended study endpoint would allow for the assessment of R18 and R18D neuroprotective effects following cell death that occurs beyond 48 hour time point, as well as examine additional behavioural assessments (e.g. gait analysis, rotarod and Barnes maze) to provide a more comprehensive and sensitive measure of functional outcomes and therapeutic benefit.

Whilst the R18D peptide was chosen for the delayed treatment studies due to its potentially greater resistance to proteolytic degradation, it remains to be determined if the R18 peptide is less, more or equally effective than R18D. The efficacy of delayed

administration of R18 will be important to determine, as the use of an L-enantiomer peptide may be more suitable for repetitive dosing due to less likelihood of the accumulation of the peptide in affected brain tissue, which at high concentrations may be toxic to already vulnerable neurons and glial cells.

Histologically, the P7 rat brain corresponds with a late pre-term human (34 weeks gestation), while growth/proliferation, persistence of a periventricular germinal matrix, neurochemical and metabolic data, EEG pattern, synapse formation and patency of the blood brain barrier of the P7 rat correspond well with the full term human (37 weeks gestation) (Hagberg, Bona, Gilland, & Puka-Sundvall, 1997). Despite the physiological similarities, to confirm R18 and R18D neuroprotective efficacy in term humans, pre-clinical efficacy in P10 rodents would need to be assessed.

The current clinical 'gold standard' to treat HIE is hypothermia. Consequently, in the event that a R18 peptide progresses to clinical trials, it would have to be assessed alongside or in combination with hypothermia. Therefore, it will be essential for pre-clinical studies to determine if the addition of R18 has synergistic effects or can extend the therapeutic time window of hypothermia. Initial preclinical studies could be examined in the rodent HI model, and if positive, could then be extended to the fetal sheep or piglet HI models. To this end, previous studies have been performed examining adjunct therapies with hypothermia in rodent, sheep and piglet animal models of HI (Davidson et al., 2015; Faulkner et al., 2011; Liu, Dingley, Scull-Brown, & Thoresen, 2015).

It is acknowledged that an intravenous, rather than intraperitoneal, route of administration would be favoured in a clinical setting. Owing to the difficulty for intravenous administration of rodent pups due to their small size, assessment of the intravenous route for peptide delivery would be more appropriately assessed in a larger animal model of HIE, such as the piglet or lamb. It should also be noted that following intraperitoneal injection, the first circulatory pass of the peptide would be through the hepatic portal vein, which would likely reduce the concentration of the peptide available reaching the brain. An additional benefit of using a larger animal model is the assessment of R18 efficacy in an animal with a gyrencephalic brain, which more closely resembles the human brain.

It is widely accepted that temperature maintenance in rodent neuroprotective studies is paramount. Despite surface temperatures of the animals routinely examined until the end of experiment and animals being house in a ventilated warming cabinet (26°C ± 1°C) throughout the experimental period, it is possible animal temperatures can vary. Alternative telemetric rectal probes are inappropriate for long-term temperature monitoring in this model as the leads cannot be incorporated into the sealed hypoxic chamber and maternal grooming would result in the removal of the probes. Additional implantable wireless temperature probes are not appropriate for the current studies as this would require extended surgical times and isoflurane exposure to allow for intraperitoneal implantation.

Finally, as a typical dose-response pattern of cerebral infarct volume reduction was not observed in this thesis, it would be worthwhile examining a wider dose range of

both R18 and R18D in future pre-clinical studies. The assessment and identification of an R18 peptide dose, lower than the lowest dose used this thesis may prove beneficial in terms of reducing potential side effects of the treatment.

7.4 SUMMARY OF IMPORTANT FINDINGS OF STUDIES

The findings presented in this thesis have for the first time confirmed the neuroprotective properties of the poly-arginine peptide R18 and its $_{D}$-enantiomer R18D in a modified and more consistent rat model of perinatal HIE. Although additional studies are required to elucidate the full neuroprotective potential of the R18 peptides as a neuroprotective therapy in this model of HIE, the present findings do suggest that CARPs are an exciting and promising new class of neuroprotective agents. Further evaluation of CARP neuroprotective mechanisms of actions are warranted, as well as the assessment of neuroprotective efficacy in other animal models of HIE.

Although the present studies have provided clear evidence of neuroprotective efficacy of the R18 peptides in a rodent model of HIE, a number of crucial questions will need to be resolved before consideration is given to their evaluation in a human clinical trial. Firstly, their efficacy will next need to be demonstrated in a larger gyrencephalic animal model (e.g. the piglet or lamb), which have longer but clearly defined gestation times and whose brain and cerebrovascular anatomy is closer to that of the human. Furthermore, as therapeutic hypothermia is considered ‘standard care’ for infants suffering from HIE, it is paramount that R18 peptides are assessed as an adjunct to hypothermia in a larger animal model of HIE, to ensure safety and to identify any synergistic effects associated with hypothermia. Moreover, as there is currently no

available therapeutic agent to reduce the severity of brain injury in the pre-term infants with HIE, and as HIE in pre-term and term infants share pathophysiological similarities relating to the mechanism of action of R18, it is important that R18 peptides are also assessed in pre-clinical animal models of pre-term HIE, both to ensure safety and the capacity to reduce brain injury and functional impairment.

7.5 REFERENCES

Ashwal, S., Tone, B., Tian, H. R., Chong, S., & Obenaus, A. (2007). Comparison of Two Neonatal Ischemic Injury Models Using Magnetic Resonance Imaging. *Pediatric Research*, *61*(1), 9–14. https://doi.org/10.1203/01.pdr.0000251612.16069.4b

Barks, J. D., Liu, Y., Shangguan, Y., Djuric, Z., Ren, J., & Silverstein, F. S. (2017). Maternal high-fat diet influences outcomes after neonatal hypoxic-ischemic brain injury in rodents. *Journal of Cerebral Blood Flow & Metabolism*, *37*(1), 307–318. https://doi.org/10.1177/0271678X15624934

Committee on Fetus and Newborn, C. O. F. A., Papile, L.-A., Baley, J. E., Benitz, W., Cummings, J., Carlo, W. A., … Wang, K. S. (2014). Hypothermia and neonatal encephalopathy. *Pediatrics*, *133*(6), 1146–1150. https://doi.org/10.1542/peds.2014-0899

Davidson, J. O., Rout, A. L., Wassink, G., Yuill, C. A., Zhang, F. G., Green, C. R., … Gunn, A. J. (2015). Non-Additive Effects of Delayed Connexin Hemichannel Blockade and Hypothermia after Cerebral Ischemia in Near-Term Fetal Sheep. *Journal of Cerebral Blood Flow & Metabolism*, *35*(12), 2052–2061. https://doi.org/10.1038/jcbfm.2015.171

Edwards, A. B., Anderton, R. S., Knuckey, N. W., & Meloni, B. P. (2016). Characterisation of neuroprotective efficacy of modified poly-arginine-9 (R9) peptides using a neuronal glutamic acid excitotoxicity model. *Molecular and Cellular Biochemistry*. https://doi.org/10.1007/s11010-016-2882-z

Faulkner, S., Bainbridge, A., Kato, T., Chandrasekaran, M., Kapetanakis, A. B.,

Hristova, M., … Robertson, N. J. (2011). Xenon augmented hypothermia reduces early lactate/N-acetylaspartate and cell death in perinatal asphyxia. *Annals of Neurology*, *70*(1), 133–150. https://doi.org/10.1002/ana.22387

Hagberg, H., Bona, E., Gilland, E., & Puka-Sundvall, M. (1997). Hypoxia-ischaemia model in the 7-day-old rat: possibilities and shortcomings. *Acta Paediatrica*, *86*(S422), 85–88. https://doi.org/10.1111/j.1651-2227.1997.tb18353.x

Hagberg, H., Gilland, E., Diemer, N. H., & Andiné, P. (1994). Hypoxia-ischemia in the neonatal rat brain: histopathology after post-treatment with NMDA and non-NMDA receptor antagonists. *Biology of the Neonate*, *66*(4), 205–213. Retrieved from http://www.ncbi.nlm.nih.gov/pubmed/7865635

Hall, N. J., Eaton, S., Peters, M. J., Hiorns, M. P., Alexander, N., Azzopardi, D. V, & Pierro, A. (2010). Mild controlled hypothermia in preterm neonates with advanced necrotizing enterocolitis. *Pediatrics*, *125*(2), e300-8. https://doi.org/10.1542/peds.2008-3211

Jacobs, S. E., Berg, M., Hunt, R., Tarnow-Mordi, W. O., Inder, T. E., & Davis, P. G. (2013). Cooling for newborns with hypoxic ischaemic encephalopathy. *Cochrane Database of Systematic Reviews*. https://doi.org/10.1002/14651858.CD003311.pub3

Liu, X., Dingley, J., Scull-Brown, E., & Thoresen, M. (2015). Adding 5 h delayed xenon to delayed hypothermia treatment improves long-term function in neonatal rats surviving to adulthood. *Pediatric Research*, *77*(6), 779–783. https://doi.org/10.1038/pr.2015.49

MacDougall, G., Anderton, R. S., Edwards, A. B., Knuckey, N. W., & Meloni, B. P. (2016). The Neuroprotective Peptide Poly-Arginine-12 (R12) Reduces Cell

Surface Levels of NMDA NR2B Receptor Subunit in Cortical Neurons; Investigation into the Involvement of Endocytic Mechanisms. *Journal of Molecular Neuroscience : MN*. https://doi.org/10.1007/s12031-016-0861-1

Meloni, B., Brookes, L., Clark, V., Cross, J., Edwards, A., Anderton, R., … Knuckey, N. (2015). Poly-arginine and arginine-rich peptides are neuroprotective in stroke models. *J Cereb Blood Flow Metab*. https://doi.org/10.1038/jcbfm.2015.11

Meloni, B., Milani, D., Cross, J., Clark, V., Edwards, A., Anderton, R., … Knuckey, N. (2017). Assessment of the Neuroprotective Effects of Arginine-Rich Protamine Peptides, Poly-Arginine Peptides (R12-Cyclic, R22) and Arginine–Tryptophan-Containing Peptides Following In Vitro Excitotoxicity and/or Permanent Middle Cerebral Artery Occlusion in Rats. *NeuroMolecular Medicine, 19*(2–3), 271–285. https://doi.org/10.1007/s12017-017-8441-2

Meloni, B., Milani, D., Edwards, A., Anderton, R., O'Hare Doig, R., Fitzgerald, M., … Knuckey, N. (2015). Neuroprotective peptides fused to arginine-rich cell penetrating peptides: Neuroprotective mechanism likely mediated by peptide endocytic properties. *Pharmacology & Therapeutics, 153,* 36–54. https://doi.org/10.1016/j.pharmthera.2015.06.002

Milani, D., Clark, V., Cross, J., Anderton, R., Knuckey, N., & Meloni, B. (2016). Poly-arginine peptides reduce infarct volume in a permanent middle cerebral artery rat stroke model. *BMC Neuroscience, 17*(1), 19. https://doi.org/10.1186/s12868-016-0253-z

Milani, D., Cross, J., Anderton, R., Blacker, D., Knuckey, N., & Meloni, B. (2017). Neuroprotective efficacy of poly-arginine R18 and NA-1 (TAT-NR2B9c) peptides following transient middle cerebral artery occlusion in the rat.

Neuroscience Research, *114*, 9–15. https://doi.org/10.1016/j.neures.2016.09.002

Milani, D., Knuckey, N., Anderton, R., Cross, J., & Meloni, B. (2016). The R18 Polyarginine Peptide Is More Effective Than the TAT-NR2B9c (NA-1) Peptide When Administered 60 Minutes after Permanent Middle Cerebral Artery Occlusion in the Rat. *Stroke Research and Treatment*, *2016*, 1–9. https://doi.org/10.1155/2016/2372710

Nijboer, C. H., van der Kooij, M. A., van Bel, F., Ohl, F., Heijnen, C. J., & Kavelaars, A. (2010). Inhibition of the JNK/AP-1 pathway reduces neuronal death and improves behavioral outcome after neonatal hypoxic-ischemic brain injury. *Brain, Behavior, and Immunity*, *24*(5), 812–821. https://doi.org/10.1016/j.bbi.2009.09.008

Okusa, C., Oeschger, F., Ginet, V., Wang, W.-Z., Hoerder-Suabedissen, A., Matsuyama, T., … Molnár, Z. (2014). Subplate in a rat model of preterm hypoxia-ischemia. *Annals of Clinical and Translational Neurology*, *1*(9), 679–691. https://doi.org/10.1002/acn3.97

Ota, A., Ikeda, T., Ikenoue, T., & Toshimori, K. (1997). Sequence of neuronal responses assessed by immunohistochemistry in the newborn rat brain after hypoxia-ischemia. *American Journal of Obstetrics and Gynecology*, *177*(3), 519–526. https://doi.org/10.1016/S0002-9378(97)70139-X

Palmer, C., Towfighi, J., Roberts, R. L., & Heitjan, D. F. (1993). Allopurinol administered after inducing hypoxia-ischemia reduces brain injury in 7-day-old rats. *Pediatric Research*, *33*(4 Pt 1), 405–411. https://doi.org/10.1203/00006450-199304000-00018

Palmer, C., Vannucci, R. C., & Towfighi, J. (1990). Reduction of perinatal hypoxic-

ischemic brain damage with allopurinol. *Pediatric Research*, *27*(4 Pt 1), 332–336. https://doi.org/10.1203/00006450-199004000-00003

Rao, R., Trivedi, S., Vesoulis, Z., Liao, S. M., Smyser, C. D., & Mathur, A. M. (2016). Safety and Short-Term Outcomes of Therapeutic Hypothermia in Preterm Neonates 34-35 Weeks Gestational Age with Hypoxic-Ischemic Encephalopathy. *The Journal of Pediatrics*. https://doi.org/10.1016/j.jpeds.2016.11.019

Rice, J. E., Vannucci, R. C., & Brierley, J. B. (1981). The influence of immaturity on hypoxic-ischemic brain damage in the rat. *Annals of Neurology*, *9*(2), 131–141. https://doi.org/10.1002/ana.410090206

van den Broek, M. P. H., Groenendaal, F., Egberts, A. C. G., & Rademaker, C. M. A. (2010). Effects of Hypothermia on Pharmacokinetics and Pharmacodynamics. *Clinical Pharmacokinetics*, *49*(5), 277–294. https://doi.org/10.2165/11319360-000000000-00000

Vaslin, A., Naegele-Tollardo, S., Puyal, J., & Clarke, P. G. H. (2011). Excitotoxicity-induced endocytosis mediates neuroprotection by TAT-peptide-linked JNK inhibitor. *J Neurochem*, *119*(6), 1243–1252. https://doi.org/10.1111/j.1471-4159.2011.07535.x

Weinstock, M. T., Francis, J. N., Redman, J. S., & Kay, M. S. (2012). Protease-resistant peptide design-empowering nature's fragile warriors against HIV. *Biopolymers*, *98*(5), 431–442. https://doi.org/10.1002/bip.22073

Wiegler, K., Bonny, C., Coquoz, D., & Hirt, L. (2008). The JNK Inhibitor XG-102 Protects from Ischemic Damage with Delayed Intravenous Administration Also in the Presence of Recombinant Tissue Plasminogen Activator. *Cerebrovascular Diseases*, *26*(4), 360–366. https://doi.org/10.1159/000151639